

Field Evaluation of the Error Arising from Inadequate Time Averaging in the Standard Use of Depth-Integrating Suspended-Sediment Samplers

Professional Paper 1774



U.S. Department of the Interior
U.S. Geological Survey

FRONT COVER:

Collection of suspended-sediment data from the measurement cableway at the U.S. Geological Survey Colorado River near Grand Canyon, Arizona, gaging station during April 1996 using a P-61 point-integrating suspended-sediment sampler. View looking upstream from the Kaibab Trail Bridge (see fig. 2B).

Field Evaluation of the Error Arising from Inadequate Time Averaging in the Standard Use of Depth-Integrating Suspended-Sediment Samplers

By David J. Topping, David M. Rubin, Scott A. Wright, and Theodore S. Melis

Professional Paper 1774

**U.S. Department of the Interior
U.S. Geological Survey**

U.S. Department of the Interior
KEN SALAZAR, Secretary

U.S. Geological Survey
Marcia K. McNutt, Director

U.S. Geological Survey, Reston, Virginia: 2011

This report and any updates to it are available online at:
<http://pubs.usgs.gov/pp/1774/>

For more information on the USGS—the Federal source for science about the Earth, its natural and living resources, natural hazards, and the environment, visit <http://www.usgs.gov> or call 1-888-ASK-USGS

For an overview of USGS information products, including maps, imagery, and publications, visit <http://www.usgs.gov/pubprod>

To order this and other USGS information products, visit <http://store.usgs.gov>

Any use of trade, product, or firm names is for descriptive purposes only and does not imply endorsement by the U.S. Government.

Although this report is in the public domain, permission must be secured from the individual copyright owners to reproduce any copyrighted materials contained within this report.

Suggested citation:

Topping, D.J., Rubin, D.M., Wright, S.A., and Melis, T.S., 2011, Field evaluation of the error arising from inadequate time averaging in the standard use of depth-integrating suspended-sediment samplers: U.S. Geological Survey Professional Paper 1774, 95 p.

Contents

Abstract	1
Introduction.....	1
Purpose and Scope.....	3
Acknowledgments.....	3
Study Sites.....	3
Theoretical Framework	5
Data.....	10
Analysis	14
At-a-Point Error.....	14
Effect of Changing Flow Conditions on the Mean At-a-Point Error	15
Depth-Integrated Error	25
Effect of Different Durations of Time Averaging on Suspended-Sediment-Concentration Errors.....	26
Evaluation of Spatial Correlations Between Verticals and Temporal Correlations at Verticals in a Cross Section.....	35
Combination of Temporal and Spatial Errors into an Estimate of the Total Uncertainty in the Time-Averaged Velocity-Weighted Suspended-Sediment Concentration in a Cross Section	38
Conclusions.....	48
References Cited.....	49
Appendix A. Suspended-Sediment Data	53
Appendix B. Cross-Stream Spatial Structures in Depth-Integrated Suspended-Sediment Concentration in Noncomposited Nine-Vertical Measurements at the River-mile 30 Sediment Station and Lower Marble Canyon Gaging Station	87

Figures

1. Map of the Colorado River drainage basin showing the locations of the study sites	4
2. Sampling locations at the four study sites	6
3. Time-averaged sand flux, absolute value of the fluctuating component of the sand flux, minimum sand flux, and maximum sand flux among point samples.....	9
4. Depiction of different equal-width-increment sampling designs in a trapezoidal cross section.....	13
5. At-a-point error in the flux of each size class of sediment at different elevations above the bed.....	16
6. Combined mean at-a-point error as a function of grain size for the five datasets.....	25
7. Combined mean at-a-point error as a function of Rouse number for the five datasets.....	25
8. Comparison of the mean depth-integrated error in the velocity-weighted depth-integrated suspended-sediment concentration in each size class and the mean at-a-point error in the flux of each size class of sediment.....	27
9. Likely range in the ratio of mean depth-integrated error to mean at-a-point error as a function of grain size in 10 cases	29

10. Likely range in mean value among all 10 cases in figure 9 of the ratio of mean depth-integrated error to mean at-a-point error plotted as a function of grain size.....	30
11. Mean value of the mean at-a-point error among the five point-sample datasets, and mean values of the mean number-of-transits errors calculated for the one-way, two-way, and the various synthetic multitransit depth-integrated data plotted as a function of grain size	32
12. Ratios between the mean values of the mean number-of-transits-errors in figure 11 associated with different numbers of transits plotted as a function of grain size.....	34
13. Examples of stable cross-stream spatial structures in depth-integrated suspended-sand concentration.....	37
14. Examples of unstable cross-stream spatial structures in depth-integrated suspended-silt-and-clay concentration.....	39
15. Comparison of number-of-verticals relative standard error, mean number-of-transits relative standard error, and relative total uncertainty in equal-discharge-increment- or equal-width-increment-measured suspended-sand concentration in a simple trapezoidal channel.....	45
16. Examples of equal-width-increment-measured suspended-sand concentrations, with error bars, for four different equal-width-increment sampling designs, showing key steps in analysis of behaviors of total uncertainty and number-of-verticals error	46
17. Comparison of empirical and theoretical relations between $n_{SE, best}$ and cumulative probability or confidence interval for total uncertainty and number-of-verticals error	47
18. Evaluation of the dependence of $n_{SE, best}$ associated with total uncertainty and number-of-verticals error on the “optimal concentration of agreement”	48
B1–B8. Cross-stream spatial structures in depth-integrated suspended-sediment concentration.....	88

Tables

1. Flow and sediment-supply conditions during the collection of point suspended-sediment samples.....	11
2. Levels of statistical significance at which the at-a-point error in each size class of sediment depends on elevation above the bed.....	20
3. Levels of statistical significance at which the at-a-point error at each elevation above the bed depends on grain size.....	22
4. Combined mean at-a-point error in each size class ± 1 standard error.....	23
5. Combined mean at-a-point error in each Rouse-number class ± 1 standard error	24
6. Levels of statistical significance at which the mean depth-integrated error depends on grain size	26
7. Levels of statistical significance at which groupings of the mean value of the mean at-a-point error and various mean number-of-transits-errors plotted in figure 11 are different in each sediment size class	33
8. Levels of statistical significance associated with correlations (1) in suspended-sediment concentration between adjacent verticals in one measurement and (2) in cross-stream spatial structures in suspended-sediment concentration between two noncomposited nine-vertical measurements made hours apart on the same day.....	36
9. Results from random-number simulations to determine the behavior of the standard-error form of the multivertical mean number-of-transits error	42

Conversion Factors and Datums

Inch/Pound to SI

Multiply	By	To obtain
Length		
foot (ft)	0.3048	meter (m)
mile (mi)	1.609	kilometer (km)
Volume		
ounce, fluid (fl. oz)	0.02957	liter (L)
pint (pt)	0.4732	liter (L)
quart (qt)	0.9464	liter (L)
gallon (gal)	3.785	liter (L)
Flow rate		
foot per second (ft/s)	0.3048	meter per second (m/s)
cubic foot per second (ft ³ /s)	0.02832	cubic meter per second (m ³ /s)
Mass		
ounce, avoirdupois (oz)	28.35	gram (g)

SI to Inch/Pound

Multiply	By	To obtain
Length		
meter (m)	3.281	foot (ft)
kilometer (km)	0.6214	mile (mi)
Volume		
liter (L)	33.82	ounce, fluid (fl oz)
liter (L)	2.113	pint (pt)
liter (L)	1.057	quart (qt)
liter (L)	0.2642	gallon (gal)
Flow rate		
meter per second (m/s)	3.281	foot per second (ft/s)
cubic meter per second (m ³ /s)	35.31	cubic foot per second (ft ³ /s)
Mass		
gram (g)	0.03527	ounce, avoirdupois (oz)

Horizontal coordinate information is referenced to the North American Datum of 1983 (NAD 83).

Notation

\bar{x}	Time-averaged value of x
$\langle x \rangle$	Depth-averaged value of x
$ x $	Absolute value of x
$ d\bar{z}/dt $	Scalar magnitude of $d\bar{z}/dt$
\hat{x}	Unit vector in the x -direction
C_m	Instantaneous concentration of suspended sediment in size class m at a point
C_{mDI}	Velocity-weighted concentration of sediment in size class m measured at a vertical with a depth-integrating sampler
C_{sand}	Instantaneous concentration of all sand-size suspended sediment at a point
\bar{C}_m	Time-averaged component of concentration of suspended sediment in size class m at a point averaged over a time scale longer than that of fluctuations in concentration as a result of turbulence
\bar{C}_{sand}	Time-averaged component of concentration of all sand-size suspended sediment at a point averaged over a time scale longer than that of fluctuations in concentration as a result of turbulence
C'_m	Component of concentration of suspended sediment in size class m at a point that fluctuates over time as a result of turbulence
C'_{sand}	Component of concentration of all sand-size suspended sediment at a point that fluctuates over time as a result of turbulence
C_1	Depth-integrated concentration in a given size class of suspended sediment at a vertical during the first of two sequential measurements
C_2	Depth-integrated concentration in a given size class of suspended sediment at a vertical during the second of two sequential measurements
D	Grain size
D_{50}	Median grain size
DI	Path taken by a depth-integrating sampler
k	von Karman's constant
m	Suspended-sediment size class
n	Number of measurements or observations
n_{SE}	Number of standard errors
n_{trans}	Number of transits at each vertical
n_{verts}	Number of verticals in an equal-discharge-increment (EDI) or equal-width-increment (EWI) measurement
P	Probability (confidence interval)
p	Level of statistical significance
p_m	Rouse number for suspended-sediment size class m

Q	Discharge of water
SE	Standard error of the mean
s	Arc length along a given path in the complex plane
T	Total time the sampler nozzle is open in the water
t	Time
\vec{U}	Instantaneous velocity of water (vector)
u	Scalar magnitude of downstream velocity in right-handed Cartesian coordinates (positive downstream)
\bar{u}	Reynold's averaged magnitude of downstream velocity averaged over a time scale longer than that of fluctuations in velocity as a result of turbulence
u'	Component of downstream velocity that fluctuates over time as a result of turbulence
u_*	Shear velocity
v	Scalar magnitude of cross-stream velocity in right-handed Cartesian coordinates (positive from right to left bank)
w	Scalar magnitude of vertical velocity in right-handed Cartesian coordinates (positive from bed to water surface)
w_m	Settling velocity for each sediment size class m
x	Downstream position in a river in a right-handed Cartesian coordinate system (positive downstream)
y	Cross-stream position in a river cross section in a right-handed Cartesian coordinate system (positive from right to left bank)
z	Elevation above bed in a river cross section in a right-handed Cartesian coordinate system (positive from the bed to the water surface)
z_0	Nikuradse roughness parameter
$z(t)$	Scalar value of z at time t
$\vec{z}(t)$	Vector value of z at time t
ϕ	Unit of grain size equal to $-\log_2 D$, where D is the grain size in millimeters
γ	Exponent in the denominator of equations relating the MNOTE to the number of transits and the MNOTE _{SE} to the number of verticals
ρ	Density of water
σ	Standard deviation
τ_b	Boundary shear stress
ζ	Nondimensionalized elevation above the bed
ψ	Optimal concentration of agreement among EWI sampling designs composed of different numbers of verticals
ψ_{\max}	Maximum concentration among EWI sampling designs composed of different numbers of verticals
ψ_{\min}	Minimum concentration among EWI sampling designs composed of different numbers of verticals

Field Evaluation of the Error Arising from Inadequate Time Averaging in the Standard Use of Depth-Integrating Suspended-Sediment Samplers

By David J. Topping, David M. Rubin, Scott A. Wright, and Theodore S. Melis

Abstract

Several common methods for measuring suspended-sediment concentration in rivers in the United States use depth-integrating samplers to collect a velocity-weighted suspended-sediment sample in a subsample of a river cross section. Because depth-integrating samplers are always moving through the water column as they collect a sample, and can collect only a limited volume of water and suspended sediment, they collect only minimally time averaged data. Four sources of error exist in the field use of these samplers: (1) bed contamination, (2) pressure-driven inrush, (3) inadequate sampling of the cross-stream spatial structure in suspended-sediment concentration, and (4) inadequate time averaging. The first two of these errors arise from misuse of suspended-sediment samplers, and the third has been the subject of previous study using data collected in the sand-bedded Middle Loup River in Nebraska. Of these four sources of error, the least understood source of error arises from the fact that depth-integrating samplers collect only minimally time-averaged data.

To evaluate this fourth source of error, we collected suspended-sediment data between 1995 and 2007 at four sites on the Colorado River in Utah and Arizona, using a P-61 suspended-sediment sampler deployed in both point- and one-way depth-integrating modes, and D-96-A1 and D-77 bag-type depth-integrating suspended-sediment samplers. These data indicate that the minimal duration of time averaging during standard field operation of depth-integrating samplers leads to an error that is comparable in magnitude to that arising from inadequate sampling of the cross-stream spatial structure in suspended-sediment concentration. This random error arising from inadequate time averaging is positively correlated with grain size and does not largely depend on flow conditions or, for a given size class of suspended sediment, on elevation above the bed. Averaging over time scales >1 minute is the likely minimum duration required to result in substantial decreases in this error. During standard two-way depth integration, a depth-integrating suspended-sediment sampler collects a sample of the water-sediment mixture during two transits at each vertical in a cross section: one transit while moving from

the water surface to the bed, and another transit while moving from the bed to the water surface. As the number of transits is doubled at an individual vertical, this error is reduced by ~ 30 percent in each size class of suspended sediment.

For a given size class of suspended sediment, the error arising from inadequate sampling of the cross-stream spatial structure in suspended-sediment concentration depends only on the number of verticals collected, whereas the error arising from inadequate time averaging depends on both the number of verticals collected and the number of transits collected at each vertical. Summing these two errors in quadrature yields a total uncertainty in an equal-discharge-increment (EDI) or equal-width-increment (EWI) measurement of the time-averaged velocity-weighted suspended-sediment concentration in a river cross section (exclusive of any laboratory-processing errors). By virtue of how the number of verticals and transits influences the two individual errors within this total uncertainty, the error arising from inadequate time averaging slightly dominates that arising from inadequate sampling of the cross-stream spatial structure in suspended-sediment concentration. Adding verticals to an EDI or EWI measurement is slightly more effective in reducing the total uncertainty than adding transits only at each vertical, because a new vertical contributes both temporal and spatial information. However, because collection of depth-integrated samples at more transits at each vertical is generally easier and faster than at more verticals, addition of a combination of verticals and transits is likely a more practical approach to reducing the total uncertainty in most field situations. Therefore, the most practical, best EDI or EWI sampling design to minimize the total uncertainty in time-averaged velocity-weighted suspended-sediment concentration is to double the number of transits collected during standard two-way depth integration and thus collect four transits at as many verticals as is practical for a given field situation.

Introduction

Depth-integrating samplers are the standard devices used by the U.S. Geological Survey (USGS) and other workers to

2 Field Evaluation of Error from Inadequate Time Averaging in Depth-Integrating Suspended-Sediment Samplers

measure suspended-sediment concentration in rivers (Edwards and Glysson, 1999; Nolan and others, 2005). These devices are deployed in a subsample of a river cross section by using either the equal-discharge-increment (EDI) or the equal-width-increment (EWI) method. In the EDI method, a river cross section is divided into multiple increments of equal discharge, whereas in the EWI method, a river cross section is divided into multiple increments of equal width. The center of each increment in either method is termed a “vertical.” These verticals together compose the subsample of the river cross section that is assumed to be representative of the flow and suspended-sediment conditions in the entire cross section. An insufficient number or incorrect location of verticals will therefore result in an error arising from inadequate sampling of the cross-stream spatial structure in suspended-sediment concentration. It is important to recognize, however, that, because a finite amount of time is required to complete EDI and EWI measurements (possibly a minimum of 15 minutes to >1 hour), the data obtained by either method are not a true spatial average because flow and sediment-supply conditions may change over the time interval required to complete a single measurement (resulting in substantial changes in the cross-stream spatial structure in suspended-sediment concentration).

Correct deployment of a depth-integrating sampler using either the EDI or EWI method results in a measurement of the velocity-weighted concentration of each size class of suspended sediment in a cross section (over the finite time interval of the measurement). In both these methods, the mixture of water and suspended sediment is sampled at each vertical by lowering the depth-integrating sampler to the bed and then immediately raising the sampler to the surface at a constant transit rate. Depth-integrating samplers have isokinetic nozzles that remain open and sample at the local instantaneous flow velocity. Therefore, these samplers collect a velocity-weighted sample of the water-sediment mixture as they move through the water column. In the EWI method, the goal is to hold the sampler transit rate constant among all the verticals. Depending on the cross-stream distribution of discharge, the volumes of water collected at various verticals may differ substantially when this method is used. In the EDI method, the transit rates at various verticals may differ from one another, depending on the cross-stream distribution of discharge. If a sample collected by using the EDI method is to be composited before laboratory analysis, an equal volume of water must be collected at each vertical; otherwise the sample collected at each vertical must be analyzed separately for suspended-sediment concentration and grain size. In both the EWI and composited-EDI methods, the velocity-weighted suspended-sediment concentration in the cross section is calculated by summing the mass of suspended sediment collected at all the verticals and then dividing by the total volume of water-sediment mixture collected at all the verticals. No averaging of observations among the different verticals occurs in either of these methods.

Because depth-integrating samplers are continuously moving through the water column when deployed in either method, and pass through any given elevation in each vertical only twice

(once on the downward transit¹ and once on the upward transit), these samplers collect only minimally time-averaged data. Thus, the velocity-weighted suspended-sediment concentration measured by depth-integrating samplers is actually a composite of the instantaneous fluxes of suspended sediment encountered as the sampler passes through each elevation in each vertical. Owing to turbulent velocity fluctuations (as reviewed by Tennekes and Lumley, 1972; McLean, 1992) and boils shed from dunes on the bed (as reviewed by Best, 2005), the suspended-sediment flux at any point in a river cross section may vary considerably over time scales of seconds to minutes. Therefore, because the instantaneous fluxes of suspended sediment can differ substantially from the time-averaged fluxes of suspended sediment at each elevation in each vertical, the suspended-sediment concentration in a cross section as measured by using a depth-integrating sampler does not necessarily equal the average velocity-weighted suspended-sediment concentration over the time scale required to complete an EDI or EWI measurement. Thus, minimal time averaging of the instantaneous fluxes of suspended sediment may lead to considerable errors in the velocity-weighted suspended-sediment concentration as measured by using depth-integrating samplers.

Suspended-sediment concentration and water discharge can be poorly correlated. In rivers, the concentration of some grain-size fraction of suspended sediment is typically controlled by changes in the upstream supply of this fraction. These supply-driven changes in suspended-sediment concentration can vary somewhat independently of the water discharge (Colby, 1963; Guy, 1970; Dinehart, 1998; Topping and others, 2000a, b; Rubin and Topping, 2001, 2008). In addition, the occurrence of a progressive lag between suspended-sediment concentration and the kinematic discharge wave during a flood may also result in poor correlation between suspended-sediment concentration and water discharge (Heidel, 1956; Dinehart, 1998). Therefore, many measurements of suspended-sediment concentration may be required over time to accurately calculate suspended-sediment loads (Porterfield, 1972). Because of this requirement and the labor intensity and cost of EDI or EWI measurements of suspended-sediment concentration, other approaches, such as automatic pump samplers (for example, Edwards and Glysson, 1999), optical backscatter (for example, Webster and others, 2000; Schoellhamer, 2001), laser diffraction (for example, Melis and others, 2003; Topping and others, 2004, 2006), or acoustic attenuation and backscatter (for example, Topping and others, 2004, 2006, 2007a; Wall and others, 2006), have been used to collect data at a much higher temporal resolution than is practical with EDI or EWI measurements. Measurements of suspended-sediment concentration using these other approaches are typically calibrated to the velocity-weighted suspended-sediment concentration in a cross section on the basis of EDI or EWI

¹ “One transit” is defined herein as the path a depth-integrating suspended-sediment sampler takes either from the water surface to the bed or from the bed to the water surface. Therefore, standard deployment of a depth-integrating sampler at a vertical, where the nozzle is open as the sampler is lowered to the bed and subsequently raised to the surface, consists of two transits.

measurements made using depth-integrating samplers. Thus, the errors arising from the use of depth-integrating samplers are additive to those associated with these other approaches to measuring suspended-sediment concentration. These other approaches, in turn, may have errors comparable to those associated with the field use of depth-integrating samplers (Topping and others, 2006). Thus, accurate calibration of any of these other approaches requires a detailed understanding of the sources, styles (that is, systematic bias or random), and magnitudes of the various errors associated with the field use of depth-integrating samplers.

Of all these errors, the best understood are those that arise from bed contamination (Allen and Petersen, 1981), pressure-driven inrush on the downward transit (Edwards and Glysson, 1999), and inadequate sampling of the cross-stream spatial structure in suspended-sediment concentration (Guy and Norman, 1970; Edwards and Glysson, 1999). Although bed contamination and pressure-driven inrush may lead to large positive and negative systematic errors (biases), respectively, these two errors should be negligible if a depth-integrating sampler is deployed properly, that is, if the sampler nozzle does not gouge the bed and the sampler is not operated at too high a transit rate. Because we took great care to deploy suspended-sediment samplers properly in this study, these two errors are assumed to be negligible in the analyses herein and are therefore disregarded. Inadequate sampling of the cross-stream spatial structure in suspended-silt-and-clay concentration has been estimated to result in negligible errors because these grain sizes are generally transported as washload and so are fairly uniformly distributed in many river cross sections (Guy and Norman, 1970; Edwards and Glysson, 1999). However, inadequate sampling of the cross-stream spatial structure in suspended-sand concentration may lead to large positive or negative errors, depending on channel geometry and the distribution of sand on the bed upstream from the measurement cross section. Although this error is expressed as a relative standard error by Guy and Norman (1970) and Edwards and Glysson (1999), thus implying that it is random, it may be systematic over time scales longer than those required to complete an EDI or EWI measurement because the spatial cross-stream structure in suspended-sand concentration in a cross section is controlled by features that either are constant or change relatively slowly (for example, interaction between the flow and channel geometry, distribution of sand on the bed upstream from the measurement cross section, and the geometry and positions of dunes on the bed upstream from the measurement cross section). In this report, this error is therefore referred to as “quasi-systematic.” Although the error in suspended-sand concentration arising from subsampling a cross section with too few verticals may be as great as ± 40 percent for highly nonuniform cross sections, it is likely less than or equal to ± 4 percent in trapezoidal cross sections when five or more verticals are used (Guy and Norman, 1970, fig. 25; Edwards and Glysson, 1999, fig. 38). Among the least understood errors associated with the field use of depth-integrating samplers is the random error arising from the fact that these samplers collect only minimally time-averaged data.

Purpose and Scope

The purpose and scope of this report are (1) to report on data collected to evaluate the error that arises from depth-integrating suspended-sediment samplers collecting minimally time-averaged data when deployed according to the standard methods described by Edwards and Glysson (1999) and (2) to analyze these data to evaluate the importance of this error and possible methods to reduce this error. We collected suspended-sediment data at four sites on the Colorado River in Utah and Arizona between 1995 and 2007, which we analyzed to determine the magnitude of the error arising from the minimal time averaging that occurs under standard field operation of depth-integrating samplers. We then compared the magnitude of this error with estimates of the error arising from inadequate sampling of the cross-stream spatial structure in suspended-sediment concentration. Finally, we suggest sampling protocols to reduce the error arising from inadequate time averaging.

Acknowledgments

This research was funded by the U.S. Department of the Interior’s Glen Canyon Dam Adaptive Management Program through the USGS Grand Canyon Monitoring and Research Center, USGS Water Resources Discipline, the National Research Program of the USGS Water Resources Discipline, and the Federal Interagency Sedimentation Project. Jonathan Nelson (USGS), Randy Parker (USGS), Dallas Childers (USGS), David Schoellhamer (USGS), Johnny McGregor (U.S. Army Corps of Engineers), Rich McDonald (USGS), and the first author all participated in the collection of suspended-sediment data in 1995, Joe Lyons (Bureau of Reclamation) in 1996, Les Vierra in 1998, Ron Griffiths, Robert Tusso, Nicholas Voichick, David Mueller, and Stuart Reeder in 2006, and Ron Griffiths, Tom Sabol, Nicholas Voichick, and Stuart Reeder in 2007. John Gray (USGS Office of Surface Water), Doug Glysson (USGS Office of Water Quality), Roger Kuhnle (U.S. Department of Agriculture’s Agricultural Research Service), and David Schoellhamer (USGS California Water Science Center) provided insightful reviews of the manuscript.

Study Sites

The study sites for this report (fig. 1) are the USGS “Colorado River near Cisco, Utah,” gaging station (herein referred to as the Cisco gaging station); a location on the Colorado River at river mile 30 in Grand Canyon National Park (herein referred to as the River-mile 30 sediment station); the USGS “Colorado River above Little Colorado River near Desert View, Arizona,” gaging station (herein referred to as the Lower Marble Canyon gaging station); and the USGS “Colorado River near Grand Canyon, Arizona,” gaging station (herein referred to as the Grand Canyon gaging station). The geometries of the sampled cross sections at these study sites are similar to the simple, trapezoidal cross section geometry

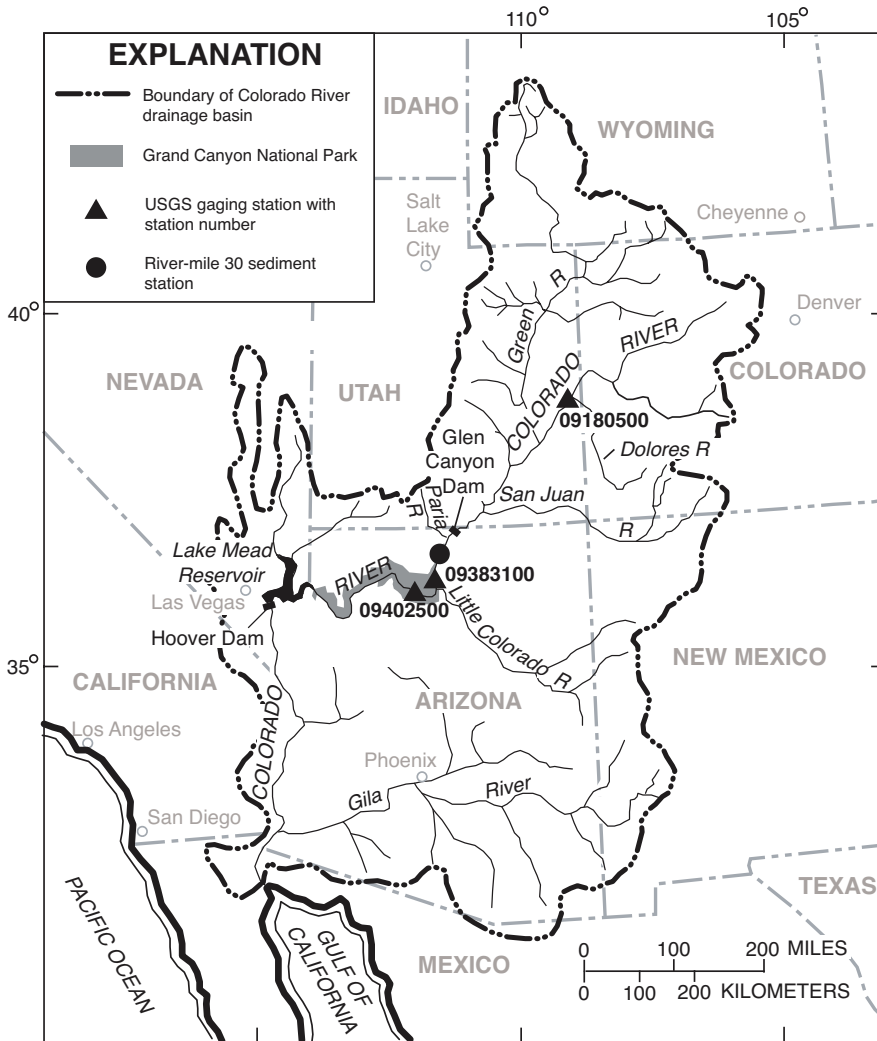


Figure 1. Colorado River drainage basin showing locations of study sites on the Colorado River at the Cisco gaging station (USGS Colorado River near Cisco, Utah gaging station, sta. number 09180500); at the River-mile 30 sediment station; at the Lower Marble Canyon gaging station (USGS Colorado River above Little Colorado River near Desert View, Arizona, gaging station, sta. number 09383100); and at the Grand Canyon gaging station (USGS Colorado River near Grand Canyon, Arizona, gaging station, sta. number 09402500). Base modified from figure 1 of Smith and others (1960).

preferred by the USGS for the geometry of the measurement cross section at gaging stations (Rantz and others, 1982). Mean velocities, suspended-silt-and-clay concentrations, and suspended-sand concentrations measured in these cross sections cover most of the normal range in rivers at USGS gaging stations. During collection of the suspended-sediment samples analyzed in this study, depth-averaged flow velocities ranged from ~ 0.1 to 3 m/s, depth-integrated suspended-silt-and clay concentrations from ~ 10 to $10,000$ mg/L, and depth-integrated suspended-sand concentrations from ~ 20 to $4,000$ mg/L. Finally, the bed sediment at the sampled cross sections ranged in composition from all sand to mostly gravel, with intermediate compositions of various mixtures of sand and gravel. Therefore, the results from this study should be generally applicable.

During the initial phase of this study in May 1995, we measured suspended-sediment concentrations from the upstream side of the historic wooden Dewey Bridge (destroyed by fire in April 2008), located 800 m downstream from the Cisco gaging station (figs. 1, 2A). The reach between the gaging

station and the bridge is relatively straight, with a riffle located ~ 100 to 200 m upstream from the bridge serving as hydraulic control for the gaging station and a second riffle located ~ 500 m downstream from the bridge serving as hydraulic control for the pool under the bridge. The cross section at the bridge is approximately trapezoidal to triangular, with the deepest part of the cross section on the right (north) side. Dunes were present on the bed under the bridge during measurements.

In March 1996, fieldwork shifted to the Grand Canyon gaging station (figs. 1, 2B). The reach at the Grand Canyon gaging station is relatively straight, with the debris fan formed at the mouth of Bright Angel Creek serving as hydraulic control for the gaging station. Two gages are present in the reach, one located on the right bank (constructed in 1922) and one located 200 m upstream on the left bank (constructed in 1933). Downstream from the left-bank gage, the water depth decreases, the high-velocity core broadens, and velocities become more uniform across the channel. The measurement cableway is located 190 m downstream from the left-bank gage in this region of more uniform flow; the herein-reported

suspended-sediment concentrations were measured from this cableway. The cross section at this cableway is trapezoidal, with the right (north) half tending to be slightly deeper than the left half. Dunes were present on the bed upstream from and under the cableway (Rubin and others, 2001; R. Anima, written commun., 2006; Topping and others, 2007b); scour and fill of the bed in this reach were described in detail by Topping and others (2000a, b). Suspended-sediment data were collected from the measurement cableway at this gaging station during March–April 1996, September 1998, and August 2007.

The Lower Marble Canyon gaging station is located 123 km downstream from Glen Canyon Dam and 41 km upstream from the Grand Canyon gaging station (figs. 1, 2C). We measured suspended-sediment concentrations at this study site in September 1998, February 2006, August 2006, February 2007, and August 2007. In 1998, measurements were made from the measurement cableway (removed in June 2003), located ~100 m upstream from the now-removed right-bank gage; and in 2006 and 2007, measurements were made from a boat positioned under a tagline located at the former site of the measurement cableway. This measurement cross section is herein referred to as cross section C. The reach at the site is relatively straight, and the measurement cross section is also trapezoidal, with the right (west) half slightly deeper than the left half. Rotating-side-scan-sonar data (Rubin and others, 2001; Rubin and others, 2006) collected in 1998 indicated that starved dunes composed of sand were present on the gravel bed at the measurement cross section. During February 2006, August 2006, February 2007, and August 2007, pipe dredging indicated that the bed consisted of sand patches on gravel (confirmed by subsequent underwater video transects). Additional measurements were made during February and August 2007 from a boat positioned under taglines at two other cross sections, A and B, located upstream from cross section C (fig. 2C). Cross section A is approximately triangular, with the right (west) half deeper than the left half; and cross section B is trapezoidal, with a narrow, much deeper section located adjacent to the left (east) bank. Underwater video transects indicated that the bed at these two upstream cross sections was composed of much more gravel than was the bed at cross section C; the bed at cross section A was composed almost entirely of boulders, whereas the bed at cross section B was composed largely of gravel with relatively small sand patches (mostly located in the deeper, left part of the cross section). Hydraulic controls for cross sections A, B, and C are formed by debris fans A, B, and C, respectively, deposited at the mouths of unnamed small tributaries (fig. 2C).

The River-mile 30 sediment station is located 73 km downstream from Glen Canyon Dam and 91 km upstream from the Grand Canyon gaging station (figs. 1, 2D). We measured suspended-sediment concentrations at this study site in February 2006, August 2006, February 2007, and August 2007 from a boat positioned under a tagline. This measurement cross section is herein referred to as cross

section B. The reach at this site is also straight, and the measurement cross section is trapezoidal, with the right (west) half slightly deeper than the left half. During February 2006, August 2006, February 2007, and August 2007, pipe dredging indicated that sand covered the bed under the tagline and that dunes were present (confirmed by subsequent underwater video transects). We measured suspended-sediment concentrations during February and August 2007 from a boat positioned under an additional tagline located at cross section A, 450 m upstream from cross section B (fig. 2D). Cross section A is trapezoidal, with the left (east) half slightly deeper than the right half. Underwater video transects indicated that the bed at this upstream cross section was composed of much more gravel than was the bed at cross section B; the bed at cross section A was composed of sand patches on gravel, whereas the bed at cross section B was composed almost entirely of sand. Hydraulic controls for cross sections A and B are formed by debris fans A and B, respectively, deposited at the mouths of unnamed small tributaries (fig. 2D).

Theoretical Framework

The instantaneous velocity of water, \vec{U} , is a vector quantity (that is, it has both magnitude and direction). In a standard right-handed Cartesian coordinate system,

$$\vec{U} = u\hat{x} + v\hat{y} + w\hat{z}, \quad (1)$$

where \hat{x} is the unit vector in the x -direction, \hat{y} is the unit vector in the y -direction, \hat{z} is the unit vector in the z -direction, u is the scalar magnitude of the velocity in the downstream direction, v is the scalar magnitude of the velocity in the cross-stream direction, and w is the scalar magnitude of the velocity in the vertical direction. In a right-handed Cartesian coordinate system in a river cross section, x is positive in the downstream direction, y is positive moving from the right bank to the left bank (left and right banks defined when facing downstream), and z is positive moving from the bed to the water surface. To simplify the mathematics in this report as much as possible, we assume v and w to be zero, with u therefore becoming equal to the scalar magnitude of the velocity in the direction parallel to the nozzle orientation of a suspended-sediment sampler. We note that in real field settings, this simplification may not hold because the nozzle (that is, intake) of a suspended-sediment sampler may not point directly into the flow direction, especially when w is locally large. In such situations, the velocity of water entering the sampler intake may be less than the local flow velocity described by vector algebra.

Given the above simplification, the instantaneous velocity of water at a point in time in the direction pointing into the nozzle of a suspended-sediment sampler can be defined as

$$u = \bar{u} + u', \quad (2)$$

where \bar{u} is the Reynold's averaged magnitude of the velocity averaged over a time scale longer than that of the fluctuations in velocity as a result of turbulence and u' is the component of the velocity that fluctuates over time as a result of turbulence.

6 Field Evaluation of Error from Inadequate Time Averaging in Depth-Integrating Suspended-Sediment Samplers

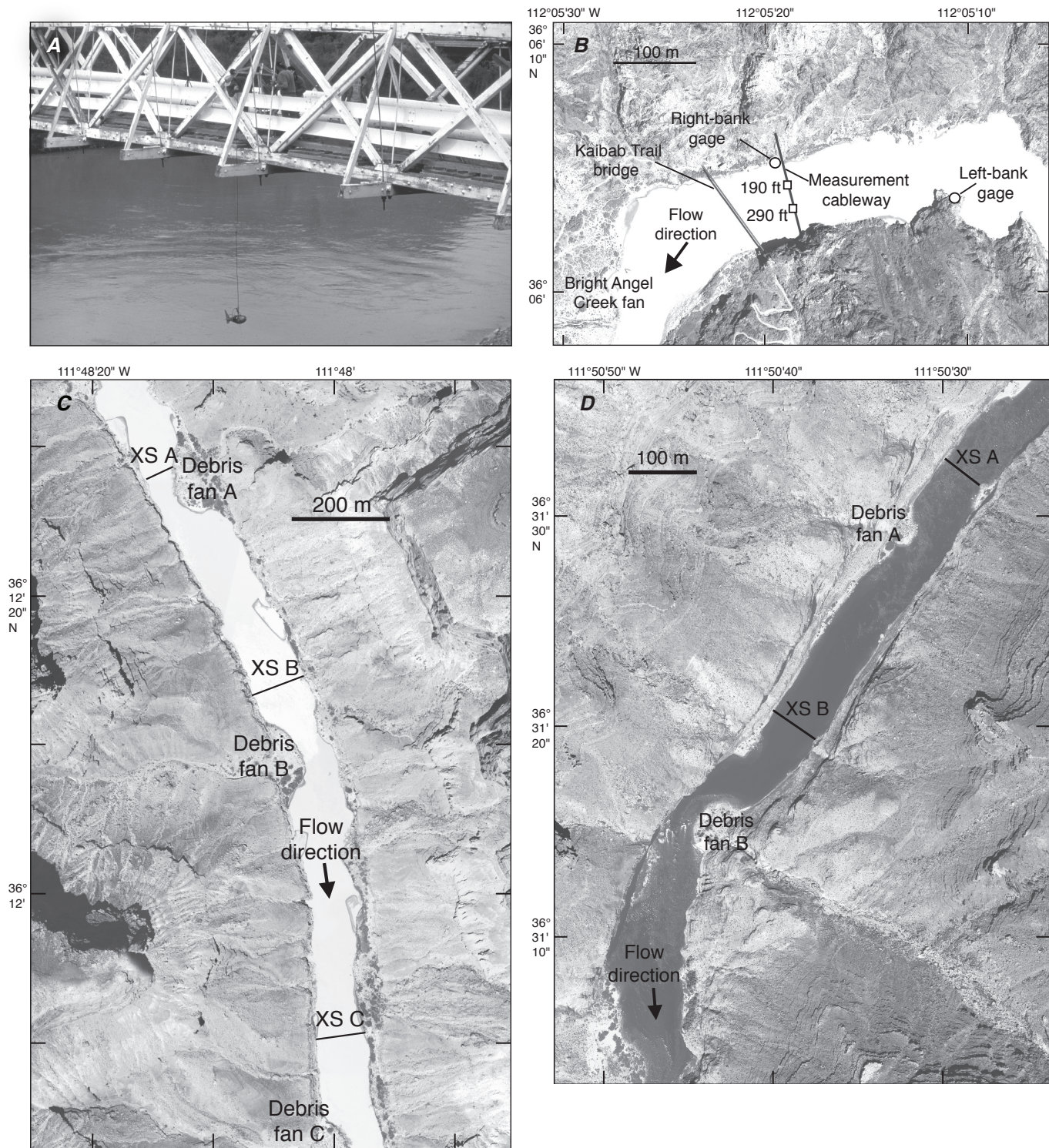


Figure 2. Sampling locations at the four study sites in the Colorado River drainage basin (fig. 1). Coordinate system in NAD 1983. *A*, P-61 point-integrating suspended-sediment sampler deployed from upstream side of the Dewey Bridge near the Cisco gaging station. *B*, Orthorectified aerial photograph of study site near the Grand Canyon gaging station, showing locations of the debris fan formed by Bright Angel Creek, the Kaibab Trail Bridge, left-bank (upper) gage, right-bank (lower) gage, measurement cableway, and stations at 190 ft and 290 ft along cableway where principal two verticals described in this report were located. *C*, Orthorectified aerial photograph of study site near the Lower Marble Canyon gaging station, showing locations of three measurement cross sections (XS A, XS B, XS C) where suspended-sediment data were collected. Hydraulic controls for these three cross sections are identified as debris fans A, B, and C, respectively. Measurement cross section C is the site of former measurement cableway. *D*, Orthorectified aerial photograph of study site near the River-mile 30 sediment station, showing locations of two measurement cross sections (XS A, XS B) where suspended-sediment data were collected. The hydraulic controls for these two cross sections are identified as debris fans A and B, respectively.

Likewise, the instantaneous concentration of suspended sediment in size class m at a point in time can be defined as

$$C_m = \bar{C}_m + C'_m, \quad (3)$$

where \bar{C}_m is the component of concentration averaged over a time scale longer than that of the fluctuations in concentration as a result of turbulence and C'_m is the component of concentration that fluctuates over time as a result of turbulence. Using the convention in equations 2 and 3, the instantaneous flux of suspended sediment in size class m at a point in time is defined as

$$uC_m = \overline{uC}_m + (uC_m)', \quad (4)$$

where \overline{uC}_m is the component of the flux averaged over a time scale longer than that of the fluctuations in velocity and concentration as a result of turbulence and $(uC_m)'$ is the component of the flux that fluctuates over time as a result of turbulence. The instantaneous flux of suspended sediment in all M size classes at a point in time is therefore

$$u \sum_{m=1}^M C_m = \overline{u \sum_{m=1}^M C_m} + \left(u \sum_{m=1}^M C_m \right)'. \quad (5)$$

Suspended-sediment samplers cannot collect data at an instant in time because a finite amount of sample (that is, water-sediment mixture) is required for laboratory analysis. For the purposes of this report, therefore, the time scale associated with time-averaged components is greater than several minutes, and the time scale associated with fluctuating components is much less than 1 minute (that is, the minimum time required to collect a suspended-sediment sample at a point).

Depth-integrating samplers can sample uC_m at each elevation (that is, point) in each vertical² only as they move through the water column. Because uC_m varies over time at each elevation and depth-integrating samplers are always moving through the water column as they collect the water-sediment mixture, the mathematical expression of C_{mDI} , the velocity-weighted concentration of sediment in each size class m measured at a vertical with a depth-integrating sampler, is complicated. C_{mDI} is not a depth- or time-averaged quantity. To be a depth-averaged quantity, C_{mDI} would have to be the velocity-weighted concentration of suspended sediment in size class m averaged over the entire flow depth at an instant in time, whereas to be a time-averaged quantity, C_{mDI} would have to be the velocity-weighted concentration of suspended sediment in size class m averaged over a suitably long time scale, that is, longer than that of turbulent fluctuations.

The best approach to mathematically describe C_{mDI} may be to use path integration, a type of line integration (Press and others, 1992; Weisstein, 2004), where DI is defined as the path taken by the depth-integrating sampler. There are two styles of depth integration: (1) one-way depth integration, where DI is either from the water surface to the bed (with the nozzle

closed when the sampler reaches the bed) or from the bed to the water surface (with the nozzle opened at the bed before the sampler is raised to the water surface); and (2) two-way depth integration, where DI is from the water surface to the bed and then back to the water surface. In one-way depth integration, DI consists of a single transit, and no time averaging occurs because the water-sediment mixture is sampled at each elevation only once. In two-way depth integration, DI consists of two transits, and only minimal time averaging occurs because the water-sediment mixture is sampled at each elevation twice. This minimal time averaging at each elevation occurs over different time intervals because it takes a finite amount of time for the sampler to move through the water column. Although time averaging occurs in two-way depth integration, C_{mDI} is not necessarily an adequately time-averaged quantity because (1) even though an average can be calculated from only two values, such an average is not necessarily a physically meaningful time average, (2) the time scale of the average differs at each elevation because the sampler collects different volumes of water from each elevation (owing to the sampler encountering different water velocities as it moves at a constant transit rate through the water column), and (3) the time scale of the average is not necessarily longer than that of turbulent fluctuations.

Regardless of the style of depth integration, C_{mDI} can be defined by using path integration as follows:

$$C_{mDI} = \int_{DI} (uC_m) ds / \int_{DI} u ds, \quad (6)$$

where s denotes the arc length along DI . Rearranging, making the appropriate substitutions into equation 6 for s to be a complex number, and defining $DI : s = z(t)$ as the path in the complex plane parameterized by time t from 0 to T yields

$$C_{mDI} = \int_0^T (uC_m) \left(\frac{dz}{dt} \right) dt / \int_0^T u \left(\frac{dz}{dt} \right) dt, \quad (7)$$

where T is the total time the sampler nozzle is open in the water along DI .³ z depends on time t because the elevation of the sampler nozzle in the flow changes over time.

Two key assumptions are implicit in the standard field use of depth-integrating samplers. The first assumption is that the velocity-weighted concentration of each size class of suspended sediment in an entire cross section can be calculated from the velocity-weighted concentration of each size class of suspended sediment measured at the verticals composing the EDI or EWI subsample of the cross section. This assumption was the focus of a 1968 analysis by P.R. Jordan that led to the technique adopted by the USGS for determining the number of verticals needed to achieve a specified error (Guy and Norman, 1970; Edwards and Glysson, 1999). Jordan analyzed the suspended-sediment data that Hubbell and others

² "Vertical" in this usage and as used throughout this report refers to the station at which a suspended-sediment sampler is deployed, not the z -direction.

³ Note that $z(t)$ in equation 7 is a scalar quantity only because the sampler is moving up and (or) down along a transit path that is parallel to the z -direction. In the general form of path integration, $\vec{z}(t)$ would be a vector quantity, and dz/dt in equation 7 would be replaced by $|d\vec{z}/dt|$, the scalar magnitude of $d\vec{z}/dt$.

(1956) collected in the sand-bedded Middle Loup River near Dunning, Nebraska. Jordan's analysis was based on Colby's (1964) theoretical distribution of $\overline{uC_m}$ in a steady, uniform flow with an effectively infinite upstream supply of sediment. Therefore, his analysis may not hold for the field use of depth-integrating samplers because, as these samplers collect only minimally time-averaged data under standard field operation, $\overline{uC_m}$ is never truly measured. This limitation leads to the second assumption that over the time interval required to complete an EDI or EWI measurement, the velocity-weighted suspended-sediment concentration measured with a depth-integrating sampler in an EDI or EWI subsample of a cross section approximately equals the true time-averaged velocity-weighted suspended-sediment concentration in this subsample. Basically, the error in an EDI or EWI measurement arising from minimal time averaging is generally assumed to be much smaller than the error arising from inadequate sampling of the cross-stream spatial structure in suspended-sediment concentration.

This second assumption, however, may not be valid. For a given sediment size class m , the absolute value of the fluctuating component of the suspended-sediment flux, $\left| (uC_m)' \right|$, at individual points in the verticals in an EDI or EWI subsample of a cross section may, in fact, be large relative to the time-averaged suspended-sediment flux, $\overline{uC_m}$, at these points. This effect may lead to large errors, as illustrated by the following two cases where the size class m is set equal to all sand-size sediment (and the subscript m is replaced by "sand").

In the first case, $\left| (uC_{\text{sand}})' \right| \ll \overline{uC_{\text{sand}}}$ at all points in a vertical (thus satisfying the condition required for the second assumption to be true), the error in the velocity-weighted suspended-sand concentration measured by a depth-integrating sampler relative to the true depth- and time-averaged velocity-weighted suspended-sand concentration is, in fact, minimal, as illustrated by point samples collected by using a P-61 point-integrating suspended-sediment sampler (Edwards and Glysson, 1999) at the Grand Canyon gaging station on March 28, 1996 (fig. 3A). In this case, the depth-averaged velocity-weighted suspended-sand concentration calculated from the minimum values of uC_{sand} measured at each elevation is only 5.3 percent⁴ less than the time- and depth-averaged velocity-weighted suspended-sand concentration calculated from $\overline{uC_{\text{sand}}}$ at each elevation. Likewise, the depth-averaged velocity-weighted suspended-sand concentration calculated from the maximum values of uC_{sand} measured at each elevation is only 6.4 percent greater than the time- and depth-averaged velocity-weighted suspended-sand concentration calculated from $\overline{uC_{\text{sand}}}$ at each elevation. Thus, in this first case, the

⁴ Because a finite amount of time is required to collect point suspended-sediment samples, the "instantaneous" values of uC_{sand} and $(uC_{\text{sand}})'$ calculated from point samples are, in fact, averaged over seconds. Thus, the amplitudes of the fluctuations in fluxes calculated from the point samples are damped, leading to errors that are likely to be somewhat smaller than those that would be calculated if true instantaneous fluxes could be measured.

velocity-weighted depth-averaged suspended-sand concentration measured by a depth-integrating sampler would be within ~5 to 6 percent of the true depth- and time-averaged velocity-weighted suspended-sand concentration at this vertical.

In contrast, in a case where $\left| (uC_{\text{sand}})' \right|$ approaches or is greater than $\overline{uC_{\text{sand}}}$ at one or more points in a vertical, the error in the velocity-weighted suspended-sand concentration measured by a depth-integrating sampler relative to the true depth- and time-averaged velocity-weighted suspended-sediment concentration can be substantial, as illustrated by P-61 point samples collected at the Cisco gaging station on May 10, 1995 (fig. 3B). In this case, the depth-averaged velocity-weighted suspended-sand concentration calculated from the minimum values of uC_{sand} measured at each elevation is 54 percent less than the time- and depth-averaged velocity-weighted suspended-sand concentration calculated from $\overline{uC_{\text{sand}}}$ at each elevation. Similarly, the depth-averaged velocity-weighted suspended-sand concentration calculated from the maximum values of uC_{sand} measured at each elevation is 104 percent greater than the time- and depth-averaged velocity-weighted suspended-sand concentration calculated from $\overline{uC_{\text{sand}}}$ at each elevation. Therefore, in this second case, the velocity-weighted suspended-sand concentration measured by a depth-integrating sampler would be within only 54 to 104 percent of the true depth- and time-averaged velocity-weighted suspended-sand concentration, an error potentially 8 to 20 times larger than in the first case.

As illustrated by these two cases, an instantaneous vertical profile (similar to that sampled by a depth-integrating sampler) may differ considerably from a time-averaged profile of suspended-sediment concentration. To further illustrate this point, substituting the time-averaged and fluctuating-component terms from equation 4 into equation 7 yields

$$C_{mDf} = \left(\int_0^T \overline{uC_m} \left(\frac{dz}{dt} \right) dt + \int_0^T (uC_m)' \left(\frac{dz}{dt} \right) dt \right) / \int_0^T u \left(\frac{dz}{dt} \right) dt. \quad (8)$$

Here, for the second assumption to hold (that is, for the net error associated with any EDI or EWI measurement to be dominated by the quasi-systematic error evaluated by P.R. Jordan [Guy and Norman, 1970; Edwards and Glysson, 1999]),

$$\int_0^T \overline{uC_m} \left(\frac{dz}{dt} \right) dt \gg \int_0^T (uC_m)' \left(\frac{dz}{dt} \right) dt$$

over the verticals sampled in a full EDI or EWI measurement. Because $(uC_m)'$ fluctuates about zero over time, repeated sequential sampling of the same vertical would lead to

$$\int_0^T (uC_m)' \left(\frac{dz}{dt} \right) dt \ll \int_0^T \overline{uC_m} \left(\frac{dz}{dt} \right) dt$$

by time averaging over progressively longer durations. However, $\int_0^T (uC_m)' \left(\frac{dz}{dt} \right) dt$

may not be substantially smaller than $\int_0^T \overline{uC_m} \left(\frac{dz}{dt} \right) dt$ when all elevations in a vertical are sampled only once (during one-way depth integration) or twice (during standard two-way depth integration).

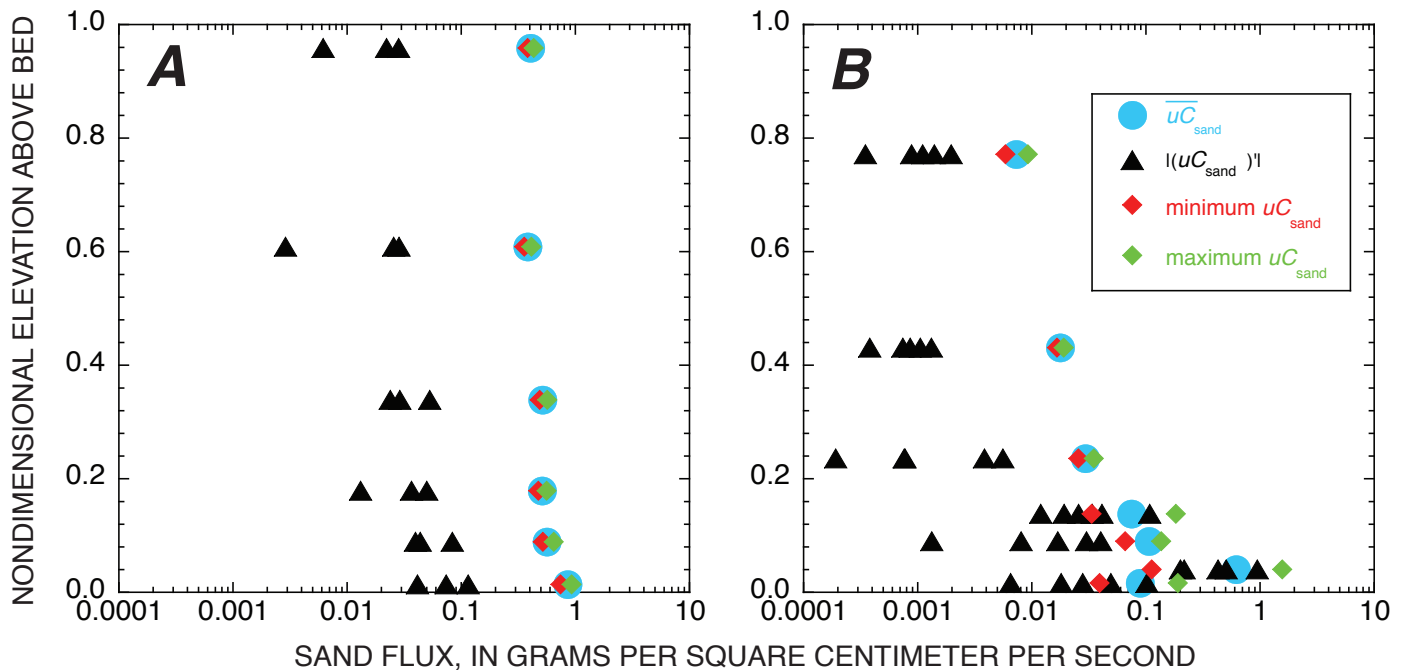


Figure 3. Time-averaged sand flux $\overline{uC}_{\text{sand}}$, absolute value of the fluctuating component of the sand flux $|(\overline{uC}_{\text{sand}})'|$, and minimum and maximum sand flux measured using a P-61 point-integrating suspended-sediment sampler at (A) the Grand Canyon gaging station (figs. 1, 2B) at six elevations above bed at the vertical located at the station 190 ft from the right endpoint of the measurement cableway on March 28, 1996, and at (B) the Cisco gaging station (figs. 1, 2A) at seven elevations above bed at the vertical located at the station 385 ft from the left-bank bridge abutment on May 10, 1995. Nondimensionalized elevation above bed is calculated by dividing measured elevation of each sample above bed by mean water depth at vertical. Values of $\overline{uC}_{\text{sand}}$ at the Grand Canyon gaging station were calculated using three individual point samples, and those at the Cisco gaging station were calculated using five to six individual point samples, at each elevation.

Generally, there is no reason to assume identical sediment-transport conditions at different verticals in a cross section, especially in cross sections with complex bed topography or irregular distributions of sand and gravel on the bed. The more complex the cross section, the more verticals that are required to obtain an EDI or EWI measurement with an acceptably low error arising from inadequate sampling of the cross-stream spatial structure in suspended-sediment concentration, as determined by P.R. Jordan's 1968 analysis as presented by Guy and Norman (1970) and Edwards and Glysson (1999). Thus, the standard procedure in conducting either an EDI or an EWI measurement is to collect depth-integrated data at the minimum number of verticals (each with potentially different sediment-transport conditions) to sample the cross-stream spatial structure in the time-averaged velocity-weighted suspended-sediment concentration at an acceptable level of error. No previous work has been done to evaluate the relative magnitudes of this "spatial structure" error and the random error arising from the minimal time averaging that occurs during standard deployment of depth-integrating samplers in an EDI or EWI measurement, nor to determine whether the "time averaging" error is reduced as additional verticals are sampled or whether additional transits at each vertical are required to reduce this error to an acceptably low

level. The only guaranteed way to reduce a random error is to conduct repeated measurements under the same conditions (for example, Taylor, 1997; Bevington and Robinson, 2003). In the case of an EDI or EWI measurement, reduction of the random "time averaging" error could require repeated depth-integrated measurements at each of the verticals sampled (that is, adding transits at each vertical). Repeated measurements at the same vertical would result in a reduction of the standard error of the mean velocity-weighted concentration at each vertical, and if these repeated measurements are uncorrelated (by not being collected too closely spaced in time), this error would decrease as $1/\sqrt{n}$, where n is the number of repeated depth-integrated measurements at each vertical. Additionally, reduction in the "time averaging" error is also possible as additional verticals are sampled. The rate at which adding verticals reduces this random error likely depends on the spatial and temporal correlations between adjacent verticals. This study will therefore evaluate (1) the relative magnitudes of "spatial structure" and "time averaging" errors, (2) whether the greatest decrease in the "time averaging" error occurs as transits or verticals are added to an EDI or EWI measurement, and (3) the behavior of the total uncertainty (composed of these two errors) in an EDI or EWI measurement as transits and (or) verticals are added.

Data

To evaluate the error arising from depth-integrating samplers collecting minimally time-averaged data, we collected suspended-sediment samples by using a P-61 point-integrating suspended-sediment sampler and D-96-A1 and D-77 bag-type depth-integrating suspended-sediment samplers. The P-61 suspended-sediment sampler is described by Edwards and Glysson (1999), the D-96-A1 suspended-sediment sampler is described by the Federal Interagency Sedimentation Project (2003), and the D-77 bag-type suspended-sediment sampler is described by Szalona (1982). The P-61 sampler was operated in both point-integrating and one-way depth-integrating modes, and the D-96-A1 and D-77 bag-type samplers were operated in the standard two-way depth-integrating mode.

Data were collected by using a P-61 suspended-sediment sampler between 1995 and 2006. P-61 point data were collected from the Dewey Bridge near the Cisco gaging station (figs. 1, 2A) during May 10–12, 1995, at water discharges ranging from 342 to 374 m³/s. Additional P-61 depth-integrated data were collected at this site on May 13–14, 1995, at water discharges ranging from 464 to 504 m³/s. P-61 point and depth-integrated data were collected from the measurement cableway at the Grand Canyon gaging station (figs. 1, 2B) on March 28, March 30, and April 2, 1996, at a steady water discharge of 1,280 m³/s, and on September 26, 1998, at a water discharge of ~589 m³/s. Additional P-61 depth-integrated data were collected at this site on March 27, March 29, March 31, and April 1, 1996, at a steady water discharge of 1,280 m³/s and on April 3, 1996, at a water discharge of ~905 m³/s. P-61 point and depth-integrated data were collected from the measurement cableway at the Lower Marble Canyon gaging station (figs. 1, 2C) on September 22, 1998, at a water discharge of ~550 m³/s. Additional P-61 point data were collected at the former location of the measurement cableway on February 8, 2006, at a water discharge of ~376 m³/s and on August 11, 2006, at a water discharge of ~474 m³/s. P-61 point data were collected under a tagline along cross section B at the River-mile 30 sediment station (figs 1, 2D) on February 5, 2006, at a water discharge of ~345 m³/s and on August 7, 2006, at a water discharge of ~300 m³/s. The mean discharge of water, depth- and time-averaged suspended-silt-and-clay concentration, and depth- and time-averaged suspended-sand concentration during the collection of the point samples at each vertical at these four study sites are listed in table 1.

In addition to the P-61 data, suspended-sediment data were also collected by using depth-integrating samplers. Single-vertical D-96-A1 depth-integrated data were collected under a tagline along cross section B at the River-mile 30 sediment station (XS B, fig. 2D) on August 25, 2007 (at a water discharge of 309 m³/s), under a tagline along cross section C at the Lower Marble Canyon gaging station (XS C, fig. 2C) on August 30, 2007 (at a water discharge of 482 m³/s), and from the measurement cableway at the Grand Canyon gaging station (fig. 2B) on August 31, 2007 (at a water discharge

of 481 m³/s). Noncomposited⁵ nine-vertical EWI data were collected by using D-96-A1 and D-77 bag-type suspended-sediment samplers along cross sections A and B at the River-mile 30 sediment station (XS A, XS B, fig. 2D) on February 24 and 25, 2007, at water discharges ranging from ~261 to 294 m³/s, and on August 24 and 25, 2007, at water discharges ranging from ~276 to 364 m³/s. Noncomposited nine-vertical EWI data were collected by using D-96-A1 and D-77 bag-type suspended-sediment samplers along cross sections A, B, and C at the Lower Marble Canyon gaging station (XS A, XS B, XS C, fig. 2C) on February 27 and 28, 2007, at water discharges ranging from ~297 to 357 m³/s, and on August 28 and 29, 2007, at water discharges ranging from ~376 to 469 m³/s. The two different types of depth-integrating samplers were used in this data-collection program to meet the needs of another study investigating systematic differences in measurements of suspended-sediment concentration and grain size made using D-77 bag-type and D-96-A1 depth-integrating samplers. Removal of biases in the measurements of suspended-sediment concentration made using the D-77 bag-type sampler (described below) was thus required before the D-77 bag-type sampler data could be used in this study.

The details (that is, time, flow depth, sample depth, sample duration, intake velocity, sediment concentration, and grain-size distribution) associated with all the suspended-sediment samples described and analyzed in this report are presented in appendix A. For each sample, the point or depth-integrated intake velocity was calculated by using the sample duration, sampled water volume, and nozzle diameter.

The point-sample data-collection program was designed to allow an estimation of the error associated with no time averaging in the flux of each size class of suspended sediment. This error was estimated on the basis of multiple sequential (back-to-back) point suspended-sediment samples collected at various elevations above the bed. The sampling protocol was such that a complete set of back-to-back point samples were collected at one elevation before moving to the next elevation in the flow. These samples were collected at each elevation over the shortest time scale required to obtain a sample large enough to be analyzed in the laboratory (ranging from 5 to 49 seconds), and so some minimal time averaging occurred during sample collection. Errors in flux arising from collecting non-time-averaged data could thus be calculated by comparing the minimally time-averaged data from individual samples with the time-averaged data from the entire set of sequential samples at each elevation. Because these samples were collected at different sites and under different flow conditions, this point-sample data-collection program also allowed an evaluation of the dependence of these errors on flow conditions.

On each of the 3 days at the Cisco gaging station (fig. 1), sequential point samples were collected at various elevations at individual verticals (fig. 2A). The sampled vertical was located on May 10 at the station marked 385 ft

⁵ That is, the samples collected at each vertical in the cross section were processed separately in the laboratory.

Table 1. Flow and sediment-supply conditions during collection of point suspended-sediment samples at the Cisco, Grand Canyon (GC), and Lower Marble Canyon (LMC) gaging stations and the River-mile 30 (RM30) sediment station.

Flow and sediment-supply conditions	Study site, month-day, year, and station of vertical										
	Cisco	Cisco	Cisco	GC	GC	GC	GC	GC	GC	GC	GC
	5-10 1995 385 ft	5-11 1995 411 ft	5-12 1995 340 ft	3-28 1996 190 ft	3-28 1996 290 ft	3-30 1996 190 ft	3-30 1996 290 ft	4-2 1996 190 ft	4-2 1996 290 ft	9-26 1998 190 ft	9-26 1998 290 ft
Mean discharge of water (m ³ /s)	351	342	374	1,280	1,280	1,280	1,280	1,280	1,280	583	595
Mean silt and clay concentration (mg/L)	618	458	525	358	363	206	211	260	176	160	179
Mean sand concentration (mg/L)	1,230	243	406	2,260	1,940	1,390	1,690	1,380	1,460	154	230

Flow and sediment-supply conditions	Study site, month-day, year, and station of vertical									
	LMC	LMC	LMC	LMC	LMC	LMC	RM30	RM30	RM30	RM30
	9-22 1998 180 ft	9-22 1998 280 ft	2-8 2006 165 ft	2-8 2006 295 ft	8-11 2006 165 ft	8-11 2006 295 ft	2-5 2006 92 ft	2-5 2006 188 ft	8-7 2006 92 ft	8-7 2006 188 ft
Mean discharge of water (m ³ /s)	563	533	372	380	469	479	353	337	304	296
Mean silt and clay concentration (mg/L)	232	241	17.1	13.7	50.1	46.9	15.5	12.7	16.5	16.1
Mean sand concentration (mg/L)	211	156	36.1	21.7	94.0	86.2	19.3	19.2	19.8	21.0

from the left-bank bridge abutment, on May 11 at the station marked 411 ft from the left-bank bridge abutment, and on May 12 at the station marked 340 ft from the left-bank bridge abutment. The left and right edges of water were located at the stations marked 246 and 480 ft, respectively, from the left-bank bridge abutment. On May 10, five to six sequential point samples were collected at seven elevations above the bed; each point sample was collected for 16 seconds and each set of sequential point samples at each elevation required an average of 16 minutes to complete. On May 11, four to seven sequential point samples were collected at nine elevations above the bed; each point sample was collected for 14 to 23 seconds (most were collected for 16 seconds), and each set of sequential point samples at each elevation required an average of 13 minutes to complete. On May 12, five to eight sequential point samples were collected at six elevations above the bed; each point sample was collected for 12 to 20 seconds (depending on height above the bed, with sampling time consistent at each elevation), and each set of sequential point samples at each elevation required an average of 12 minutes to complete.

At the Grand Canyon gaging station (fig. 1), three sequential point samples were collected on March 28 and 30, 1996, April 2, 1996, and September 26, 1998, at six elevations at each of two verticals (fig. 2B) located at approximately one-third and two-thirds of the channel width at the stations marked 190 and 290 ft from the right-bank end point of the

cableway (fig. 2B). In 1996, each point sample was collected for 5 to 15 seconds (depending on height above the bed, with sampling time consistent at each elevation) and each set of three sequential point samples at each of the six elevations required an average of 6 minutes to complete; in 1998, each point sample was collected for 12 to 20 seconds and each set of three sequential point samples at each of the six elevations also required an average of 6 minutes to complete.

At the Lower Marble Canyon gaging station (fig. 1), three sequential point samples were collected on September 22, 1998, at six elevations at each of two verticals located at approximately one-third and two-thirds of the channel width at the stations marked 180 and 280 ft from the right-bank end point of the cableway; each point sample was collected for 8 to 20 seconds and each set of three sequential point samples at each of the six elevations required an average of 7 minutes to complete. On February 8, 2006, three sequential point samples were collected at four elevations at a vertical located 165 ft from the former right-bank end point of the cableway, and three sequential point samples were collected at five elevations at a vertical located 295 ft from the former right-bank end point of the cableway; each point sample was collected for 25 to 43 seconds and each set of three sequential point samples at each of the six elevations required an average of 6 minutes to complete. On August 11, 2006, three sequential point samples were collected at four elevations at these two verticals; each

point sample was collected for 20 to 30 seconds and each set of three sequential point samples at each of the six elevations required an average of 6 minutes to complete.

At the River-mile 30 sediment station (fig. 1), three sequential point samples were collected on February 5, 2006, at five elevations at each of two verticals located at approximately one-third and two-thirds of the channel width at the stations marked 92 and 188 ft from the left-bank endpoint of the tagline; each point sample was collected for 25 to 49 seconds and each set of three sequential point samples at each of the six elevations required an average of 7 minutes to complete. On August 8, 2006, three sequential point samples were collected at five elevations at each of these two verticals; each point sample was collected for 40 to 46 seconds, and each set of three sequential point samples at each of the six elevations required an average of 8 minutes to complete.

The at-a-point values of uC_m and $(uC_m)'$ measured during each period at the Cisco, Grand Canyon, and Lower Marble Canyon gaging stations and at the River-mile 30 sediment station (fig. 1) were therefore averaged over 5 to 49 seconds, the time required to collect each point sample; and the at-a-point values of $\overline{uC_m}$ were averaged over 6 to 16 minutes, the time required to collect each set of sequential point samples at a given elevation. Thus, the values of $\overline{uC_m}$ are likely time averaged over time scales longer than most of the turbulent fluctuations, and the values of uC_m and $(uC_m)'$ are minimally time averaged over time scales less than most of the turbulent fluctuations. As mentioned previously, because a short, but finite, amount of time is required to collect a point sample containing amounts of water and suspended sediment sufficient for laboratory analysis, the amplitudes of fluctuations in the fluxes are damped. Therefore, errors calculated from these point-sample data likely are somewhat smaller than the errors that would be calculated if true instantaneous fluxes could actually be measured.

The depth-integrated-sample data-collection program was designed to allow (1) comparison of the errors calculated from non-time-averaged depth-integrated data with those computed from the minimally time-averaged point-sample data described above; (2) evaluation of the errors associated with different durations of time averaging on the depth-integrated velocity-weighted concentration of each size class of suspended sediment; (3) evaluations of the temporal correlations at individual verticals in EWI measurements spaced hours apart and of the spatial correlations between adjacent verticals in the same EWI measurement; and (4) comparison of P.R. Jordan's "spatial structure" error, the "time averaging" error, and the total uncertainty (composed of these two errors) when different numbers of transits and verticals are present in an EWI measurement. The first objective was accomplished by collecting one-way (upward) depth-integrated suspended-sediment samples bracketing point samples; the second objective was accomplished by comparing the errors calculated from the single-vertical collection of sequential (back-to-back) one-way depth-integrated suspended-sediment samples (no time averaging) and sequential two-way depth-integrated

suspended-sediment samples (minimal time averaging); the third objective was accomplished by collecting noncomposed EWI data over two multiday periods at multiple cross sections; and the fourth objective was accomplished by comparing the data collected to address objectives 2 and 3.

One-way depth-integrated samples were collected before and after each complete set of 18 point samples (that is, bracketing the point samples) at the Grand Canyon gaging station (fig. 2B) in 1996 and 1998 and at the Lower Marble Canyon gaging station (fig. 2C) in 1998. These one-way depth-integrated samples were collected with a P-61 sampler by opening the nozzle above the bed and then raising the sampler to the surface at a uniform transit rate. Collection of these samples allowed a direct comparison of the errors estimated for non-time-averaged depth-integrated data with the errors estimated for point-sample data collected at the same vertical. At the Grand Canyon gaging station, these bracketing one-way depth-integrated samples were collected over 6 to 8 seconds in 1996 and over 10 to 19 seconds in 1998; in both years, the samples were spaced ~1 hour apart (the time required to collect the 18 point samples). At the Lower Marble Canyon gaging station, these bracketing one-way depth-integrated samples were collected over 11 to 17 seconds and also spaced ~1 hour apart. Additional one-way, upward depth-integrated samples (see appendix A) were also collected as part of this study at the Grand Canyon gaging station on March 27, 29, and 31 and April 1 and 3, 1996, and on September 26, 1998.

Sequential one-way, upward depth-integrated samples were collected with a P-61 sampler at the Cisco gaging station (fig. 2A) in 1995. On May 13, 1995, four sets of five sequential samples were collected at the vertical located at the station 340 ft from the left-bank bridge abutment; and on May 14, 1995, three sets of five sequential samples were collected at the vertical located at the station 403 ft from the left-bank bridge abutment. Each depth-integrated sample was collected for 10 to 13 seconds, and the samples within each set were spaced ~2 minutes apart.

In 2007, sequential single-vertical two-way depth-integrated samples were collected with a D-96-A1 sampler at the River-mile 30 sediment station and at the Lower Marble Canyon and Grand Canyon gaging stations (fig. 1). On August 25, 2007, 15 sequential depth-integrated samples were collected at the River-mile 30 sediment station in the middle of the river, at the vertical located at the station 138 ft from the left-bank end point of the tagline; each sample was collected for 64 to 68 seconds, and the samples within each set were spaced ~4 minutes apart. On August 30, 2007, 15 sequential depth-integrated samples were collected at the Lower Marble Canyon gaging station in the middle of the river, at the vertical located at the station 230 ft from the former right-bank end point of the cableway; each sample was collected for 33 to 35 seconds, and the samples within each set were spaced ~3 minutes apart. On August 31, 2007, 14 sequential depth-integrated samples were collected at the Grand Canyon gaging station in the middle of the river, at the vertical located at the station 258 ft from the right-bank end point of the cableway; each sample was

collected for 37 to 40 seconds, and the samples within each set were spaced ~2 minutes apart.

In February and August 2007, noncomposited multitransit, multivertical data were collected with D-96-A1 and D-77 bag-type samplers along two cross sections (XS A and XS B, fig. 2D) at the River-mile 30 sediment station and along three cross sections (XS A, XS B, and XS C, fig. 2C) at the Lower Marble Canyon gaging station. To accomplish objectives 3 and 4 of the depth-integrated-sample data-collection program, it was desirable to collect noncomposited EWI data that could be analyzed by using as many different numbers of verticals as possible.

On the basis of P.R. Jordan's analysis (Guy and Norman, 1970; Edwards and Glysson, 1999), five equal-width increments are reasonably sufficient to sample the cross-stream spatial structure in suspended-sand concentration in a simple trapezoidal channel like the Colorado River. For convenience in the analyses, it was preferable to design a sampling program that would allow new verticals to be added while keeping the positions of the verticals in the middle of these original five equal-width increments fixed. However, the EWI measurement with the next-highest cross-stream spatial resolution that keeps the positions of the original five verticals fixed is one composed of 15 equal-width increments (fig. 4), which would require adding two new verticals between each of the original five verticals and adding one vertical between each bank and the first and last of the original five verticals (with these two verticals located very close to the banks). This addition of 10 new verticals was impractical in the field for several reasons (for example, the length of time required to collect 15 noncomposited verticals, the large volume of water that would have to be collected in a 15-vertical measurement, and the shallow flow depths and extremely low velocities at the new near-bank verticals that would make deployment of depth-integrating samplers difficult). As a compromise design, one new vertical was added between each of the original five verticals, resulting in the ability to compare the five-vertical EWI measurement with nine- and three-vertical quasi-EWI measurements (figs. 4C–D). The spacing between verticals in the nine-vertical measurements approximately equaled the mean flow depth in each cross section, resulting in only two small triangular regions near the banks in the three- and nine-vertical quasi-EWI measurements that were “ignored.” Ultimately, EWI measurements composed of one, three, five, and nine verticals were compared under this sampling design.

To allow mathematical compositing⁶ of the multivertical data as EWI measurements with different numbers of verticals, the sampler transit rate was held constant among the verticals in each cross section. The sampler transit rate in each cross section was highly constrained on the basis of conditions at the verticals near the middle of the cross section, where velocities and flow depths were largest, and conditions near the sides of the cross section, where velocities and flow depths were smallest. That is, the transit rate for the cross section had to be set at a rate fast enough so that the sampler did not overflow upon

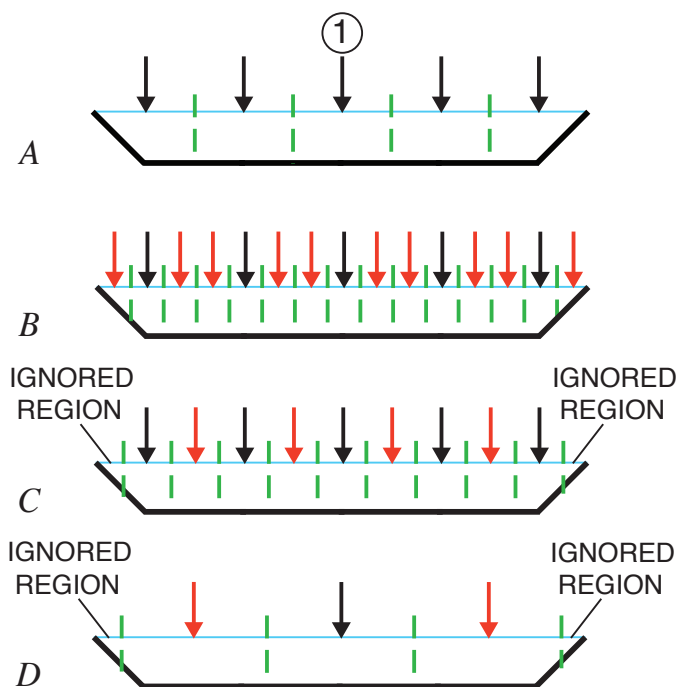


Figure 4. Trapezoidal cross sections showing edges (green dashed lines) of equal-width increments and positions of verticals (arrows) in different equal-width-increment (EWI) sampling designs. Water surface in each cross section indicated by thin blue line. *A*, Five-vertical EWI measurement. Circled number 1 denotes position of vertical in center of cross section used to construct a one-vertical EWI measurement. *B*, 15-vertical EWI measurement. Black arrows denote positions of original five verticals in figure 4A; red arrows denote positions of added verticals. *C*, Nine-vertical quasi-EWI measurement. Black arrows denote positions of original five verticals in figure 4A; red arrows denote positions of added verticals. Note presence of two triangular “ignored regions” adjacent to the banks in this compromise sampling design. *D*, Three-vertical quasi-EWI measurement. Black and red arrows denote positions of three of nine verticals in figure 4C retained in construction of this measurement. Ignored regions adjacent to the banks in this compromise sampling design are the same as in figure 4C.

two transits (one downward and one upward) at the verticals in the middle of the cross section, and slow enough that it did not exceed ~40 percent of the flow velocity (to avoid large entrance angles between the direction of flow and the nozzle; see Federal Interagency Sedimentation Project, 1952; Edwards and Glysson, 1999) at the verticals near the sides of the cross section. Because flow depths and velocities were small in the “ignored regions” adjacent to the banks in figures 4C–D, not sampling these regions had a negligible effect on the three- and nine-vertical quasi-EWI measurements.

On February 24, 2007, noncomposited nine-vertical data were collected under this sampling design with the D-77 bag-type sampler at cross sections A and B and with the D-96-A1 sampler at cross section A at the River-mile 30

⁶ These EWI measurements were mathematically composited by using the raw laboratory sample masses, sediment masses, and grain-size distributions.

sediment station (fig. 2D). On February 25, 2007, noncomposited nine-vertical data were collected with the D-96-A1 sampler at cross section B at the River-mile 30 sediment station. During the afternoon of August 24, 2007, and again during the morning of August 25, 2007, noncomposited nine-vertical data were collected with both the D-77 bag-type and D-96-A1 samplers at the two cross sections at the River-mile 30 sediment station. On February 27, 2007, noncomposited nine-vertical data were collected with the D-96-A1 sampler, and on February 28, 2007, noncomposited nine-vertical data were collected with the D-77 bag-type sampler, at cross sections A, B, and C at the Lower Marble Canyon gaging station (fig. 2C). On August 28, 2007, and again on August 29, 2007, noncomposited nine-vertical data were collected with both the D-77 bag-type and D-96-A1 samplers at the three cross sections at the Lower Marble Canyon gaging station. Samplers with $\frac{5}{16}$ -in. nozzles were used during February 2007 and with $\frac{1}{4}$ -in. nozzles during August 2007. From two to eight transits were collected at each vertical. Depending on the nozzle diameter, number of transits, flow velocity, and flow depth, the depth-integrated sample at each vertical was collected over durations between 1 and 8 minutes; and depending on the conditions at each cross section, each noncomposited nine-vertical measurement took 17 to 94 minutes to complete.

Recent measurements at multiple sites along the Colorado River in Grand Canyon (fig. 1) indicate that relative to the D-96-A1 sampler, the D-77 bag-type sampler on average oversamples suspended silt and clay by ~5 percent and suspended sand by ~20 percent (Sabot and others, 2010) because the D-77 bag-type sampler is not as isokinetic as the D-96-A1 sampler and samples at a rate slightly lower than the instantaneous flow velocity.⁷ The noncomposited nine-vertical EWI data were therefore processed in such a way as to prevent this D-77 bag-type sampler bias from affecting the analyses in this report. This result was achieved by normalizing the concentrations of suspended silt and clay or sand measured at each individual vertical in an EWI measurement by the mean concentration of suspended silt and clay or sand measured among the nine verticals in that EWI measurement. In this way, the biases between data collected with the D-77 bag-type and D-96-A1 samplers were removed, and the noncomposited EWI data collected using the two depth-integrating suspended-sediment samplers could be directly compared.

All the data collected in this study were processed for suspended-sediment concentration by using standard USGS methods, with sand-size material separated from silt- and clay-sized material by wet sieving through a 0.0625-mm stainless-steel sieve (Guy, 1969; Knott and others, 1992, 1993). For the 1996 and 1998 data, grain-size distributions of the material retained on this sieve were measured at $\frac{1}{4}$ - ϕ increments by using a visual accumulation tube (Federal Interagency Sedimentation Project, 1957, 1958) calibrated to give results identical to those obtained by dry sieving. For the 2006 and 2007 data, grain-size

distributions of the material retained on the 0.0625-mm sieve were measured at $\frac{1}{4}$ - ϕ increments by using a Beckman Coulter LS-100Q Laser Diffraction Particle Size Analyzer calibrated to give results identical to those obtained by dry sieving. Wet-sieving results in some silt and clay adhering to the sand retained on the 0.0625-mm sieve. This effect, which has been observed by using electron microscopy (Gordon and others, 2001), was observed in our laboratory by comparing the results from wet and dry sieving. In this study, the amount of silt and clay retained with the sand during wet sieving was measured by using either the visual accumulation tube or the LS-100Q Laser Diffraction Particle Size Analyzer. The suspended-silt-and-clay concentrations reported in appendix A were calculated by adding the weight of silt and clay retained on the 0.0625-mm sieve during the wet-sieving process to the weight of sediment passing through this sieve. Likewise, the suspended-sand concentrations reported in appendix A were calculated by subtracting the weight of silt and clay retained on the 0.0625-mm sieve from the weight of material retained on this sieve. This approach removes the negative bias in suspended-silt-and-clay concentration and the positive bias in suspended-sand concentration observed by Gordon and others (2001). Owing to the type of the analyses in this study (that use field data processed through a laboratory), laboratory-processing errors (typically well within 5 percent) are embedded within the errors calculated in the analyses presented here. These laboratory-processing errors are likely random and of similar small magnitude (that is, generally much less than about ± 5 percent) and so are assumed to cancel out within each of the analyses conducted in this study.

Analysis

At-a-Point Error

Before quantifying the error associated with assuming that $\int_0^r \overline{u C_m} \left(\frac{dz}{dt} \right) dt \gg \int_0^r (u C_m)' \left(\frac{dz}{dt} \right) dt$ over either a single-vertical, EDI, or EWI measurement, the relative mean absolute error (that is, relative mean unsigned error) arising from this assumption must first be calculated at each point in each vertical. This random error in sediment flux, herein termed the at-a-point error (APE, in percent), is defined as

$$\text{APE} = 100 \frac{\left| u \sum_{m=1}^M C_m - \overline{u \sum_{m=1}^M C_m} \right|}{\overline{u \sum_{m=1}^M C_m}}, \quad (9)$$

which simplifies for each size class m to

$$\text{APE} = 100 \frac{\left| (u C_m)' \right|}{\overline{u C_m}}, \quad (10)$$

where $\left| (u C_m)' \right|$ is the time-averaged absolute value of the fluctuating component of the flux of suspended sediment in size class m at a given elevation above the bed and $\overline{u C_m}$ is

⁷ See Federal Interagency Sedimentation Project (1941) for analyses of the effect of non-isokinetic sampling on measurements of suspended-sediment concentration for various size classes of sediment.

the time-averaged flux of suspended sediment in size class m at that same elevation. Statistical analyses were conducted on the 1995 Cisco, 1996 and 1998 Grand Canyon, 1998 and 2006 Lower Marble Canyon, and 2006 River-mile 30 P-61 point-sample data to evaluate whether the APE depends on either elevation above the bed or grain size. APEs calculated from these point-sample data are plotted in figure 5. As previously noted, because a finite amount of time is required to collect point suspended-sediment samples, the APEs calculated from these point-sample data are not true instantaneous errors (for example, the type of error expected in a one-way depth-integrated sample with zero time averaging) and so likely are somewhat smaller than the errors that would be calculated if true instantaneous fluxes were measurable.

The APE in each size class of sediment does not systematically depend on elevation above the bed. In some places, the point samples collected closest to the bed exhibited the largest values of this error, for example, at the Cisco vertical at station 385 ft on May 10, 1995, and at the Grand Canyon vertical at station 190 ft on March 28, 1996; in other places, the point samples collected near the surface exhibited the largest values of this error, for example, at the Cisco vertical at station 340 ft on May 12, 1995, and at the Grand Canyon vertical at station 290 ft on September 26, 1998. Analysis of variance using a standard F -test indicates that in 84.4 percent of the 301 cases for which data were available to calculate this error, no significant relation existed at the $p=0.05$ level between the elevation above the bed and the APE in each size class (table 2). In only 14.3 percent of cases the APE increased, and in just 1.3 percent of the cases decreased, with distance above the bed. Although the APE does not systematically depend on elevation above the bed, it does ordinarily depend on grain size. Analysis of variance using a standard F -test indicates that at the $p=0.05$ level of significance, the APE was positively correlated with grain size in 84.7 percent of the 118 cases for which data were available to calculate this error (table 3). No significant relation between grain size and APE was observed in the remaining 15.3 percent of these 118 cases. In no case was the APE negatively correlated with grain size.

Similarity in the behavior of the APE at different elevations above the bed and at different verticals under similar flow conditions allows for some simplification. Because the APE does not systematically depend on elevation above the bed but does depend on grain size, the APEs in each size class can therefore be depth-averaged (among all sampled elevations above the bed) to result in a mean APE, hereafter referred to as the mean at-a-point error (MAPE). This depth averaging effectively reduces the number of datasets from 121 (that is, the total number of sampled elevations in all verticals) to 21 (that is, the total number of verticals sampled at the four study sites). Furthermore, because of the similar behavior of the APE at each of the verticals sampled under similar flow conditions, the MAPEs associated with similar flow conditions at each of the study sites were combined, this further reducing the number of datasets from 21 to 5: (1)

the 1995 Cisco gaging-station dataset (with water discharge ranging from 342 to 374 m^3/s), (2) the 1996 Grand Canyon gaging-station dataset (with a steady water discharge of 1,280 m^3/s), (3) the 1998 Grand Canyon gaging-station dataset (with water discharge ranging from 583 to 595 m^3/s), (4) the 1998–2006 Lower Marble Canyon gaging-station dataset (with water discharge ranging from 372 to 563 m^3/s), and (5) the 2006 River-mile 30 sediment-station dataset (with water discharge ranging from 296 to 353 m^3/s).

The combined MAPEs at the four study sites, which are similar in magnitude and behavior (fig. 6; table 4), were calculated from the APEs at all elevations in all verticals except at the Grand Canyon gaging station (fig. 1), where the combined MAPEs for 1996 and 1998 data were computed separately because of the relatively large difference in flow conditions between these two datasets. The average of the combined MAPEs for silt and clay among the five datasets is 10 ± 2 percent (mean ± 1 standard error). For sand-size material, the average of the combined MAPEs among the five datasets is the smallest at 15 ± 3 percent for the 0.105- to 0.125-mm size class (generally the median size of suspended sand in the Colorado River in Grand Canyon). For the size classes that typically dominate suspended sand in the Colorado River in Grand Canyon (that is, the size classes between 0.088 and 0.177 mm), the average of the combined MAPEs among the five datasets ranges from ~ 15 to 20 percent, whereas for the coarser size classes of sand, the average of the combined MAPEs among the five datasets exceeds 100 percent.

Effect of Changing Flow Conditions on the Mean At-a-Point Error

In addition to the general positive correlation between grain size and combined MAPEs, the combined MAPEs in each size class of sand tend to be negatively correlated with flow conditions, likely as a result of the reduction in the z -direction gradient in the concentration of suspended sediment of each size class as the flow strength increases. An increase in the discharge of water through a cross section or in the flow strength at any given vertical in a cross section will generally result in an increase in the boundary shear stress, τ_b , and therefore an increase in the shear velocity, u_* (because $u_* = \sqrt{\tau_b/\rho}$). This increase, in turn, will result in a decrease in the z -direction gradient (away from the bed) in the concentration of suspended sediment in each size class, through a reduction in the Rouse number (for example, McLean, 1992). By standard convention, the Rouse number is defined as $p_m = w_m/ku_*$, where w_m is the settling velocity for each size class m and k is von Karman's constant, equal to 0.408 (Long and others, 1993). Vertical mixing (arising from turbulent velocity fluctuations or boils being shed from dunes on the bed) across larger z -direction concentration gradients gives rise to greater temporal variation in suspended-sediment concentration through relatively infrequent larger events transporting coarser grains higher into the flow

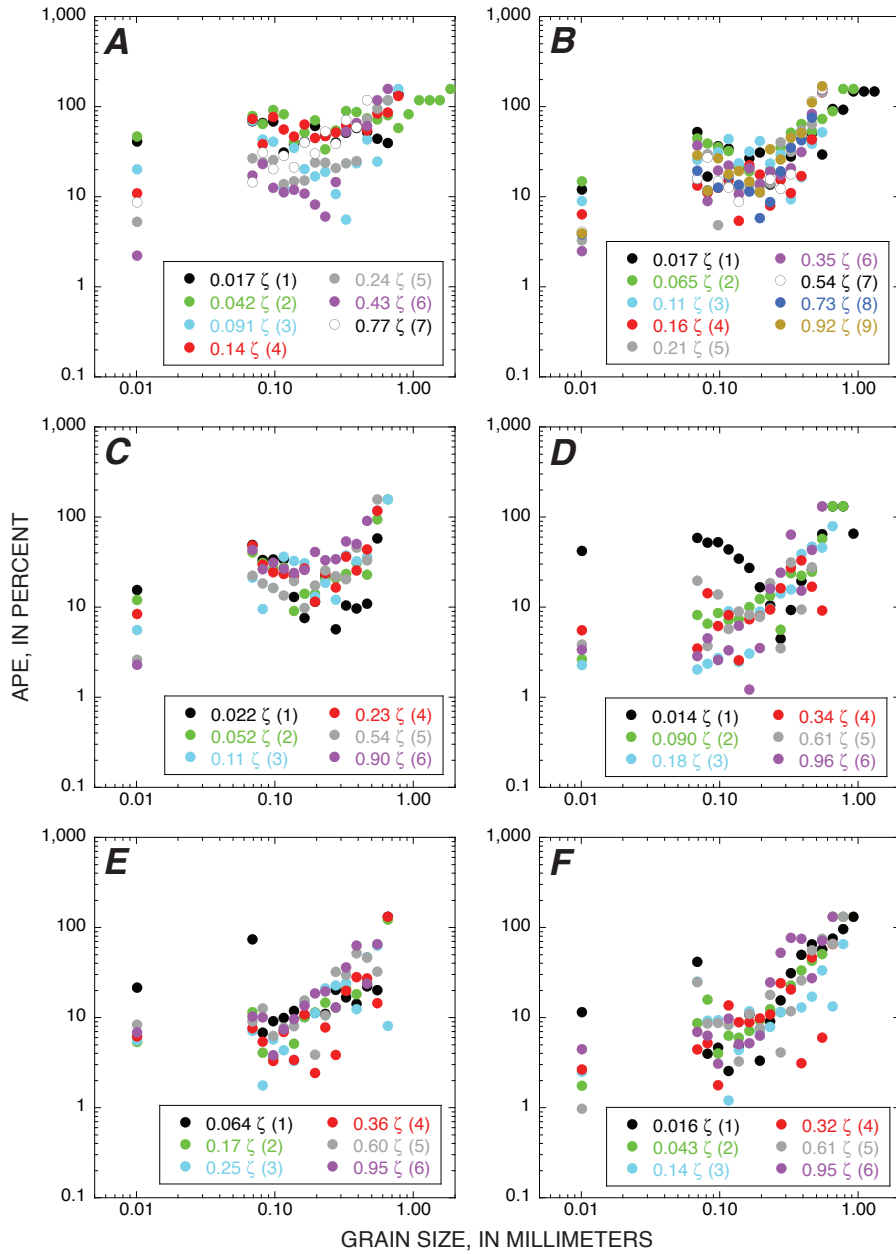


Figure 5. At-a-point error (APE) in flux of each size class of suspended sediment at six to nine elevations above the bed at the Dewey Bridge near the Cisco gaging station (figs. 1, 2A) at vertical located at station 385 ft on May 10, 1995 (A), at station 411 ft on May 11, 1995 (B), at station 340 ft on May 12, 1995 (C); at six elevations above the bed along measurement cableway at the Grand Canyon gaging station (fig. 2B) at vertical located at station 190 ft on March 28, 1996 (D), at station 290 ft on March 28, 1996 (E), at station 190 ft on March 30, 1996 (F), at station 290 ft on March 30, 1996 (G), at station 190 ft on April 2, 1996 (H), at station 290 ft on April 2, 1996 (I), at station 190 ft on September 26, 1998 (J), and at station 290 ft on September 26, 1998 (K); at six elevations above the bed along former measurement cableway at the Lower Marble Canyon gaging station (XS C, fig. 2C) at vertical located at station 180 ft on September 22, 1998 (L), at station 280 ft on September 22, 1998 (M); at four to five elevations above the bed along tagline at cross section C at the Lower Marble Canyon gaging station (XS C, fig. 2C) at vertical located at station 165 ft on February 8, 2006 (N), at station 295 ft on February 8, 2006 (O), at station 165 ft on August 11, 2006 (P), and at station 295 ft on August 11, 2006 (Q); and at five elevations above the bed along tagline at cross section B at the River-mile 30 sediment station (XS B, fig. 2D) at vertical located at station 92 ft on February 5, 2006 (R), at station 188 ft on February 5, 2006 (S), at station 92 ft on August 8, 2006 (T), and at station 188 ft on August 8, 2006 (U). ζ indicates nondimensionalized elevation above the bed and, as in figure 3, is calculated by dividing measured elevation of each sample above the bed by the mean water depth at the vertical. Numbers in parentheses next to each ζ elevation indicate its relative position above the bed (see table 3), where relative position 1 is closest to the bed. All silt-and-clay-sized sediment was assigned to the 0.01-mm size class; all sediment in each $\frac{1}{4}$ - ϕ size class of sand was assigned to the grain size at the logarithmic midpoint of each $\frac{1}{4}$ - ϕ size class.

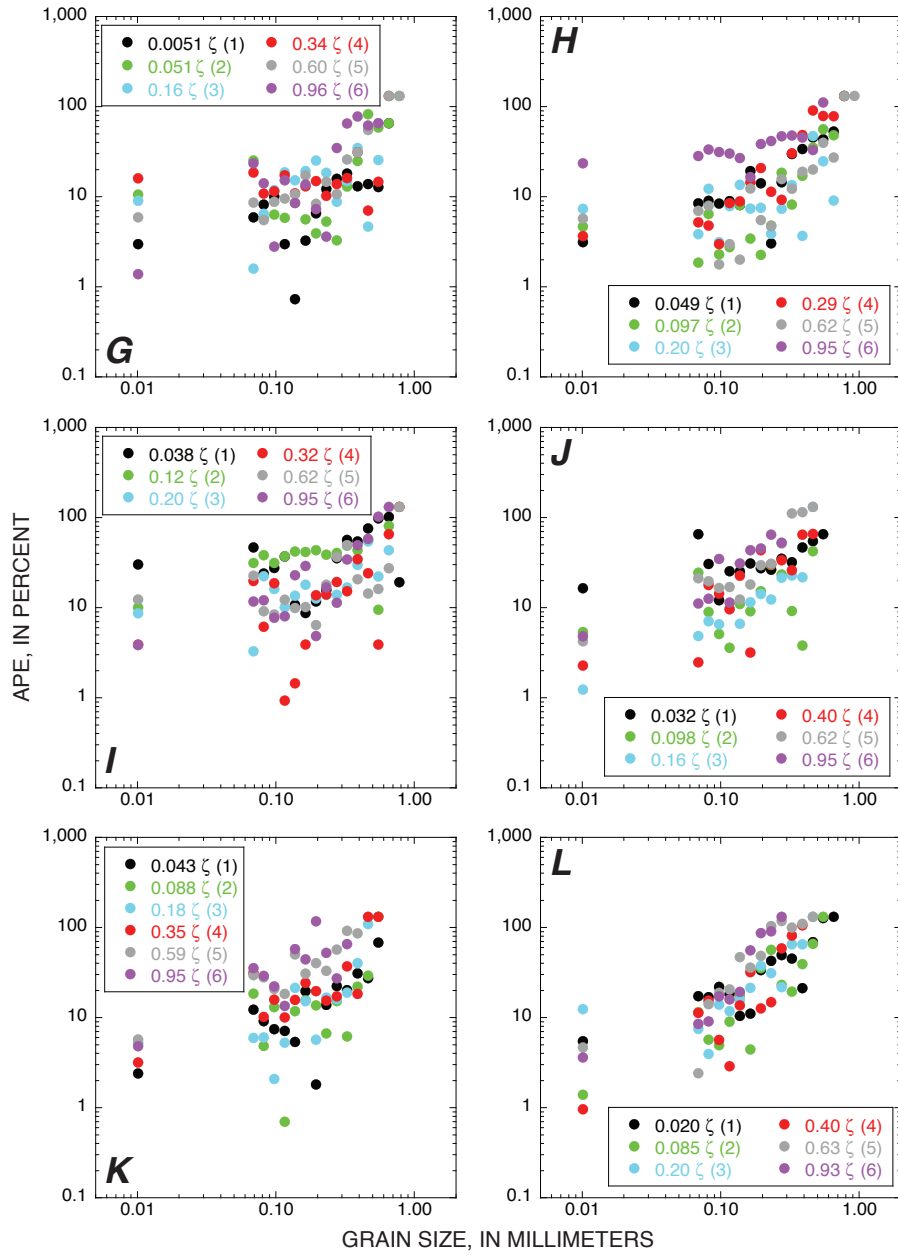


Figure 5.—Continued

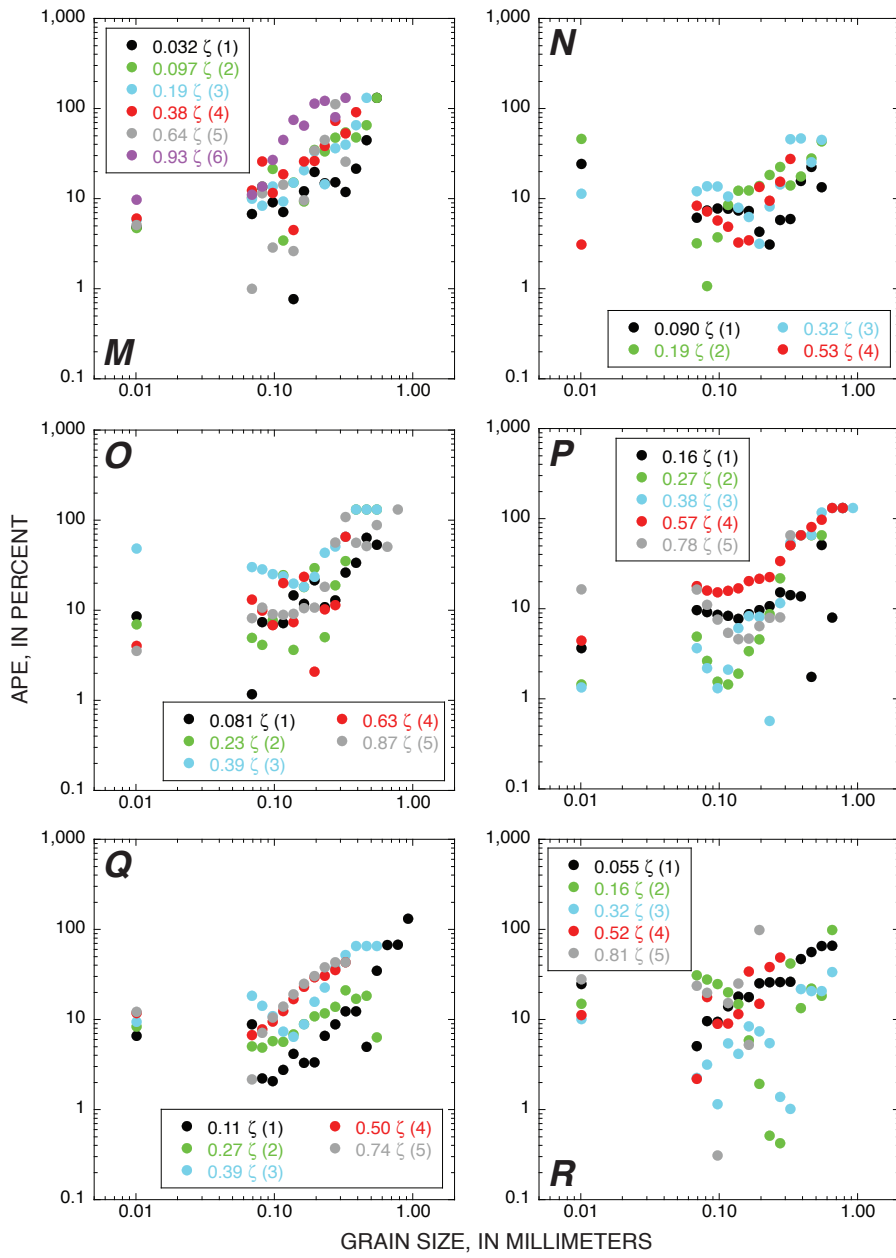


Figure 5.—Continued

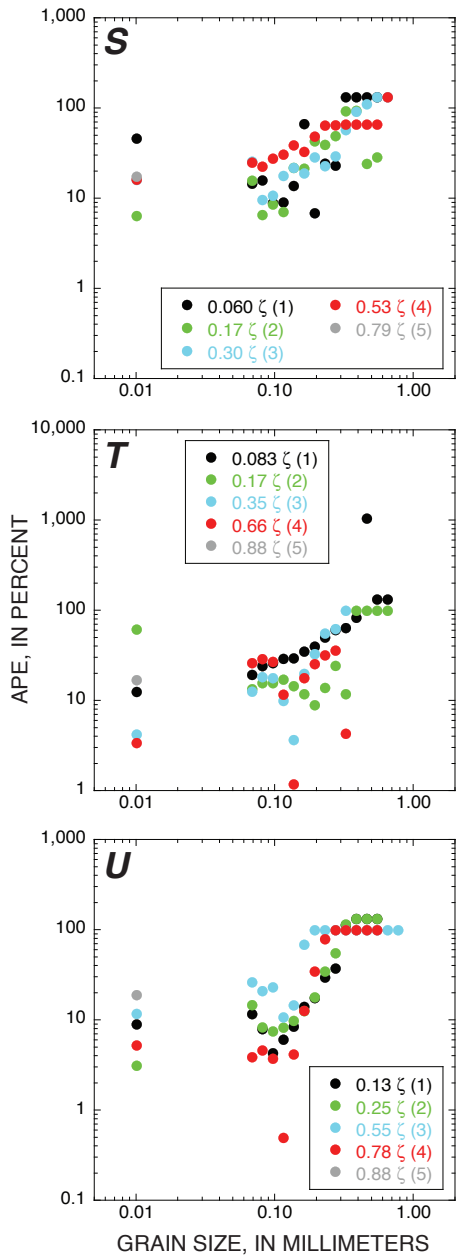


Figure 5.—Continued

(Schmeeckle and others, 1999). A reduction in the z -direction suspended-sediment concentration gradient in any given size class will therefore result in less temporal variation in the suspended-sediment concentration at each elevation above the bed and likely cause a reduction in the MAPE.

To further evaluate the effect of flow conditions on the combined MAPEs in each of the five datasets, each size class of sediment was converted to a Rouse-number class (fig. 7; table 5). To compute the Rouse number for each sediment size class in each of the five datasets, the settling velocity for each $1/4\text{-}\phi$ size class m was calculated, using the method of Dietrich (1982), for sediment with a Powers index of 3.0 and a Corey shape factor of 0.7 (typical values for Colorado River sediment; Topping, 1997) and a water temperature of 15°C (an average value close to the water temperatures measured during collection of suspended-sediment data at the three gaging stations). The mean shear velocity for each of the five datasets was calculated by regressing the best-fit velocity profiles (using the two-part eddy viscosity of Rattray and Mitsuda, 1974) to the intake velocities measured with a P-61 sampler at each elevation in each vertical, and then averaging the shear velocities calculated from these regressions at all the verticals in each dataset. Each regression was conducted such that the shear velocity and the Nikuradse roughness parameter, z_0 , were free to vary independently of each other until a best fit was obtained. Because z_0 values smaller than about 0.2 cm are physically unrealistic in the Colorado River (Topping and others, 2007b), regressed shear velocities that required z_0 values <0.2 cm were precluded during this procedure.

When all five datasets are treated as a single dataset, inclusion of the effects of flow conditions in this analysis through conversion of grain size to Rouse number results in a decrease of only ~ 11 percent in the variance of the MAPE about the best-fit linear regression in figure 7 relative to that in figure 6. Although grain size is a reasonably good predictor of MAPE, Rouse number is only slightly better. Changes in flow conditions, at least over the range investigated in this study, therefore result in only minor changes in the MAPE. Grain size thus dominates over all other likely influences on the MAPE (that is, elevation above the bed and flow conditions).

22 Field Evaluation of Error from Inadequate Time Averaging in Depth-Integrating Suspended-Sediment Samplers

Table 3. Levels of statistical significance at which the at-a-point error at each elevation above the bed depends on grain size.

[Relative positions of each sampled elevation are numbered, where position 1 is the sampled elevation closest to the bed; see figure 3 for actual elevations associated with these relative positions. Critical level of significance is set equal to 0.05; values ≤ 0.05 are shown in bold; (+) indicates significant positive correlation and (-) significant negative correlation between grain size and at-a-point error. Cisco, Cisco gaging station; GC, Grand Canyon gaging station; LMC, Lower Marble Canyon gaging station; RM30, River-mile 30 sediment station. n/a indicates analysis not applicable because data were not collected at this relative position above the bed]

Relative position above the bed	Study site, month-day-year, and station of vertical							
	Cisco 5-10-1995 385 ft	Cisco 5-11-1995 411 ft	Cisco 5-12-1995 340 ft	GC 3-28-1996 190 ft	GC 3-28-1996 290 ft	GC 3-30-1996 190 ft	GC 3-30-1996 290 ft	GC 4-2-1996 190 ft
1	0.099	0.30	0.99	0.023(+)	0.076	<0.00001(+)	0.0015(+)	<0.00001(+)
2	0.55	0.0027(+)	0.050(+)	<0.00001(+)	0.00010(+)	<0.00001(+)	0.00043(+)	0.00001(+)
3	0.0084(+)	0.16	0.0062(+)	<0.00001(+)	0.012(+)	0.0016(+)	0.0078(+)	0.080
4	0.00084(+)	0.0050(+)	0.018(+)	0.040(+)	0.0026(+)	0.0035(+)	0.021(+)	<0.00001(+)
5	0.00002(+)	0.00009(+)	0.0042(+)	0.0071(+)	0.00028(+)	<0.00001(+)	0.00001(+)	0.00035(+)
6	<0.00001(+)	0.0011(+)	0.00066(+)	0.00044(+)	0.00019(+)	0.00002(+)	0.00008(+)	0.00261(+)
7	0.00002(+)	0.00030(+)	n/a	n/a	n/a	n/a	n/a	n/a
8	n/a	0.00035(+)	n/a	n/a	n/a	n/a	n/a	n/a
9	n/a	0.00005(+)	n/a	n/a	n/a	n/a	n/a	n/a

Relative position above the bed	Study site, month-day-year, and station of vertical						
	GC 4-2-1996 290 ft	GC 9-26-1998 190 ft	GC 9-26-1998 290 ft	LMC 9-22-1998 180 ft	LMC 9-22-1998 280 ft	LMC 2-8-2006 165 ft	LMC 2-8-2006 295 ft
1	0.026(+)	0.13	0.00009(+)	0.0013(+)	0.0011(+)	0.40	0.00001(+)
2	0.0023(+)	0.099	0.0066(+)	0.0013(+)	<0.00001(+)	0.11	0.00003(+)
3	0.0011(+)	0.0040(+)	0.0014(+)	0.00004(+)	0.00008(+)	0.0019(+)	0.00005(+)
4	0.00051(+)	0.00008(+)	0.00066(+)	0.00008(+)	0.00006(+)	0.0026(+)	0.054
5	0.0056(+)	<0.00001(+)	0.00006(+)	<0.00001(+)	0.027(+)	n/a	0.00033(+)
6	<0.00001(+)	0.00044(+)	0.11	0.00005(+)	0.00021(+)	n/a	n/a

Relative position above the bed	Study site, month-day-year, and station of vertical					
	LMC 8-11-2006 165 ft	LMC 8-11-2006 295 ft	RM30 2-5-2006 92 ft	RM30 2-5-2006 188 ft	RM30 8-8-2006 92 ft	RM30 8-8-2006 188 ft
1	0.0046(+)	<0.00001(+)	<0.00001(+)	0.00036(+)	0.10	<0.00001(+)
2	<0.00001(+)	0.029(+)	0.057	0.044(+)	0.0012(+)	<0.00001(+)
3	<0.00001(+)	<0.00001(+)	0.0023(+)	<0.00001(+)	0.00012(+)	0.0011(+)
4	<0.00001(+)	0.00001(+)	0.0046(+)	<0.00001(+)	0.65	0.00002(+)
5	0.15	0.00003(+)	0.28	n/a	n/a	n/a

Table 4. Combined mean at-a-point error in each size class ± 1 standard error.

[Cisco, Cisco gaging station; GC, Grand Canyon gaging station; LMC, Lower Marble Canyon gaging station; RM30, River-mile 30 sediment station. n/a indicates analysis not applicable because of insufficient data in size class]

Size class (mm)	Study site, year, and range in water discharge (Q)					Mean of five datasets
	Cisco 1995 $Q=342-374$ m ³ /s	GC 1996 $Q=1,280$ m ³ /s	GC 1998 $Q=583-595$ m ³ /s	LMC 1998-2006 $Q=372-563$ m ³ /s	RM30 2006 $Q=296-353$ m ³ /s	
<0.0625	11.1 \pm 2.5	8.5 \pm 1.5	5.2 \pm 1.1	9.7 \pm 2.0	17.1 \pm 3.3	10.3\pm2.0
0.0625–0.074	38.1 \pm 4.5	16.9 \pm 2.8	22.3 \pm 5.2	9.5 \pm 1.1	16.2 \pm 2.3	20.6\pm4.8
0.074–0.088	27.9 \pm 3.4	11.6 \pm 1.8	15.6 \pm 2.8	10.4 \pm 1.2	15.5 \pm 2.0	16.2\pm3.1
0.088–0.105	31.3 \pm 4.7	10.2 \pm 1.8	14.5 \pm 2.6	10.7 \pm 1.2	13.4 \pm 2.3	16.0\pm3.9
0.105–0.125	27.9 \pm 3.7	11.3 \pm 1.7	11.2 \pm 2.0	12.0 \pm 1.6	13.2 \pm 2.0	15.1\pm3.2
0.125–0.149	21.4 \pm 2.4	10.1 \pm 1.5	22.9 \pm 4.9	13.5 \pm 2.6	15.2 \pm 2.5	16.6\pm2.4
0.149–0.177	24.4 \pm 3.1	12.5 \pm 1.4	22.5 \pm 3.8	17.3 \pm 2.6	23.9 \pm 4.6	20.1\pm2.3
0.177–0.210	24.1 \pm 3.8	11.5 \pm 1.5	31.6 \pm 9.0	25.5 \pm 4.3	32.7 \pm 7.0	25.1\pm3.8
0.210–0.250	24.4 \pm 2.8	14.0 \pm 1.4	28.1 \pm 5.0	29.3 \pm 5.4	38.8 \pm 6.6	26.9\pm4.0
0.250–0.297	25.6 \pm 2.9	18.3 \pm 2.1	31.6 \pm 4.4	39.5 \pm 6.1	45.2 \pm 7.3	32.0\pm4.8
0.297–0.354	36.3 \pm 4.7	28.7 \pm 2.9	40.7 \pm 10.6	48.4 \pm 5.5	68.8 \pm 11.3	44.6\pm6.8
0.354–0.420	43.6 \pm 4.2	32.1 \pm 3.1	45.7 \pm 11.1	57.7 \pm 7.8	86.1 \pm 10.9	53.0\pm9.2
0.420–0.500	62.2 \pm 6.3	39.8 \pm 3.6	81.6 \pm 15.3	67.5 \pm 9.6	158.3 \pm 75.6	81.9\pm20.2
0.500–0.595	102.0 \pm 10.9	52.0 \pm 5.8	100.6 \pm 8.9	82.7 \pm 10.6	89.9 \pm 12.5	85.4\pm9.1
0.595–0.707	111.4 \pm 12.7	84.4 \pm 8.2	n/a	88.0 \pm 21.8	100.1 \pm 12.5	95.9\pm6.1
0.707–0.841	124.2 \pm 16.4	119.8 \pm 8.1	n/a	120.4 \pm 12.9	100.0	116.1\pm5.5
0.841–1.00	131.3 \pm 23.9	111.1 \pm 22.2	n/a	133.3 \pm 0.0	n/a	125.3\pm7.1
1.00–1.19	135.0 \pm 15.0	n/a	n/a	n/a	n/a	135.0
1.19–1.41	135.0 \pm 15.0	n/a	n/a	n/a	n/a	135.0
1.41–1.68	120	n/a	n/a	n/a	n/a	120.0
1.68–2.00	160	n/a	n/a	n/a	n/a	160.0

Table 5. Combined mean at-a-point error in each Rouse-number class ± 1 standard error.

[Cisco, Cisco gaging station; GC, Grand Canyon gaging station; LMC, Lower Marble Canyon gaging station; RM30, River-mile 30 sediment station. n/a indicates analysis not applicable because of insufficient data in Rouse-number class]

Rouse-number class	Study site, year, range in water discharge (Q), and mean shear velocity (u_*)					Mean of five datasets
	Cisco 1995 $Q=342\text{--}374\text{ m}^3/\text{s}$ $u_*=9.15\pm 0.25$	GC 1996 $Q=1,280\text{ m}^3/\text{s}$ $u_*=12.49\pm 0.46$	GC 1998 $Q=583\text{--}595\text{ m}^3/\text{s}$ $u_*=6.46\pm 0.18$	LMC 1998-2006 $Q=372\text{--}563\text{ m}^3/\text{s}$ $u_*=6.98\pm 0.38$	RM30 2006 $Q=296\text{--}353\text{ m}^3/\text{s}$ $u_*=4.15\pm 0.11$	
<0.01	11.1 \pm 2.5	8.5 \pm 1.5	5.2 \pm 1.1	9.7 \pm 2.0	17.1 \pm 3.3	10.3\pm2.0
0.05–0.07	n/a	16.9 \pm 2.8	n/a	n/a	n/a	16.9
0.07–0.09	38.1 \pm 4.5	11.6 \pm 1.8	n/a	n/a	n/a	24.9\pm13.3
0.09–0.13	27.9 \pm 3.4	10.2 \pm 1.8	22.3 \pm 5.2	9.5 \pm 1.1	n/a	17.5\pm4.6
0.13–0.17	31.3 \pm 4.7	11.3 \pm 1.7	15.6 \pm 2.8	10.4 \pm 1.2	n/a	17.1\pm4.9
0.17–0.23	27.9 \pm 3.4	10.1 \pm 1.5	14.5 \pm 2.6	10.7 \pm 1.2	16.2 \pm 2.3	15.9\pm3.2
0.23–0.32	21.4 \pm 2.4	12.5 \pm 1.4	11.2 \pm 2.0	12.0 \pm 1.6	15.5 \pm 2.0	14.5\pm1.9
0.32–0.40	24.4 \pm 3.1	11.5 \pm 1.5	22.9 \pm 4.9	13.5 \pm 2.6	13.4 \pm 2.3	17.1\pm2.7
0.40–0.52	24.1 \pm 3.8	14.0 \pm 1.4	22.5 \pm 3.8	17.3 \pm 2.6	13.2 \pm 2.0	18.2\pm2.2
0.52–0.70	24.4 \pm 2.8	18.3 \pm 2.1	31.6 \pm 9.0	25.5 \pm 4.3	15.2 \pm 2.5	23.0\pm2.9
0.70–0.82	25.6 \pm 2.9	28.7 \pm 2.9	n/a	29.3 \pm 5.4	23.9 \pm 4.6	26.9\pm1.3
0.82–1.05	36.3 \pm 4.7	32.1 \pm 3.1	28.1 \pm 5.0	39.5 \pm 6.1	32.7 \pm 7.0	33.8\pm1.9
1.05–1.28	43.6 \pm 4.2	39.8 \pm 3.6	31.6 \pm 4.4	n/a	n/a	38.3\pm3.5
1.28–1.6	62.2 \pm 6.3	52.0 \pm 5.8	40.7 \pm 10.6	48.4 \pm 5.5	38.8 \pm 6.6	48.4\pm4.2
1.6–2.0	102.0 \pm 10.9	84.4 \pm 8.2	45.7 \pm 11.1	57.7 \pm 7.8	45.2 \pm 7.3	67.0\pm11.3
2.0–2.5	111.4 \pm 12.7	119.8 \pm 8.1	81.6 \pm 15.3	67.5 \pm 9.6	68.8 \pm 11.3	89.8\pm10.9
2.5–3.0	124.2 \pm 16.4	111.1 \pm 22.2	100.6 \pm 8.9	82.7 \pm 10.6	86.1 \pm 10.9	100.9\pm7.7
3.0–3.6	131.3 \pm 23.9	n/a	n/a	88.0 \pm 21.8	158.3 \pm 75.6	125.9\pm20.5
3.6–4.4	135.0 \pm 15.0	n/a	n/a	120.4 \pm 12.9	89.9 \pm 12.5	115.1\pm13.3
4.4–5.0	135.0 \pm 15.0	n/a	n/a	133.3 \pm 0.0	100.1 \pm 12.5	122.8\pm11.4
5.0–6.0	120	n/a	n/a	n/a	n/a	120
6.0–7.0	160	n/a	n/a	n/a	100.0	130.0\pm30.0

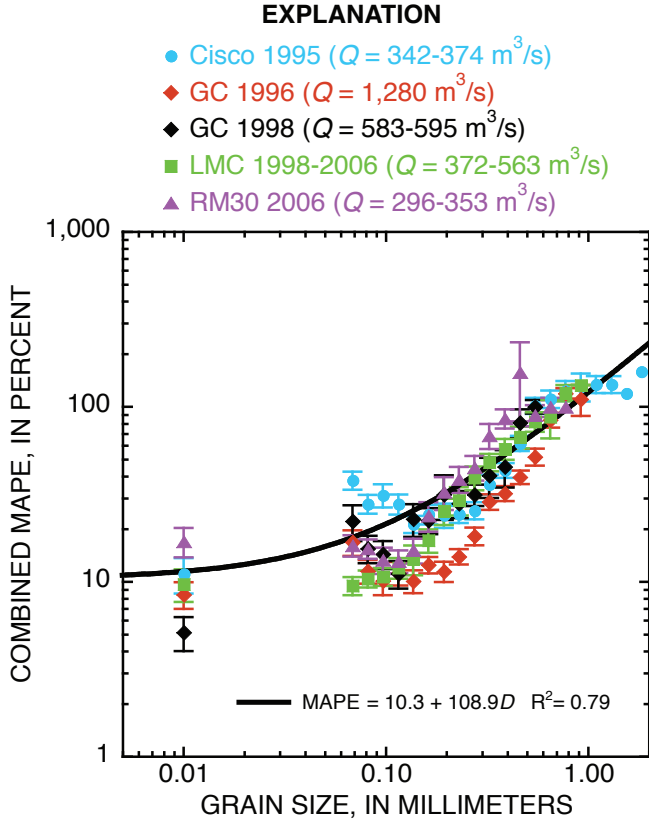


Figure 6. Combined mean at-a-point error (MAPE) as a function of grain size for the five point-sample datasets, showing ranges in discharge (Q) during collection of each dataset and linear-regression fit to the combined data in all five datasets. Error bars are 1 standard error. Cisco, Cisco gaging station; GC, Grand Canyon gaging station; LMC, Lower Marble Canyon gaging station; RM30, River-mile 30 sediment station (see figure 1 for locations).

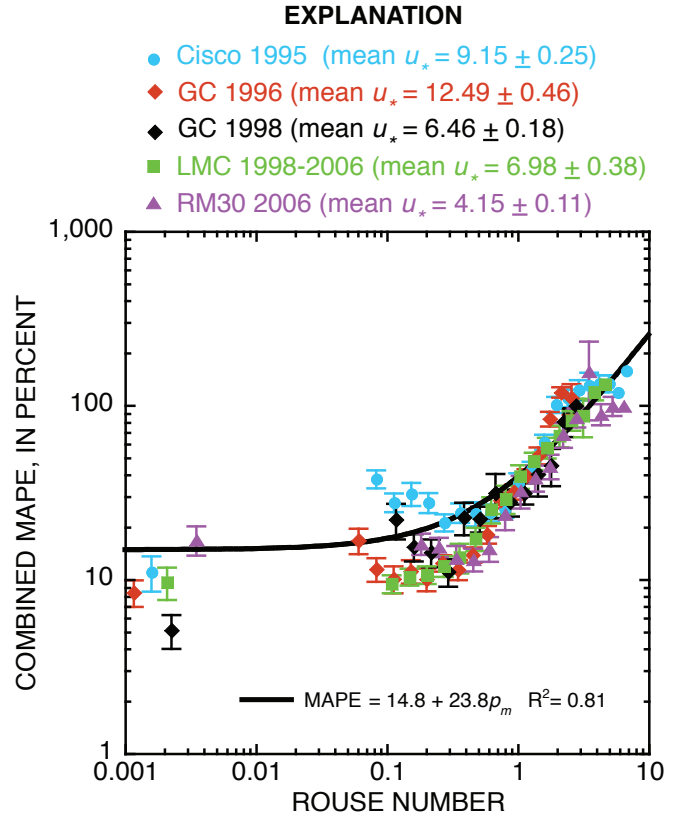


Figure 7. Combined mean at-a-point error (MAPE) as a function of Rouse number for the five point-sample datasets, showing the mean shear velocity (u_*) ± 1 standard error during collection of each dataset and linear-regression fit to the combined data in all five datasets. Error bars are 1 standard error. Cisco, Cisco gaging station; GC, Grand Canyon gaging station; LMC, Lower Marble Canyon gaging station; RM30, River-mile 30 sediment station (see figure 1 for locations).

Depth-Integrated Error

The depth-integrated relative mean absolute error (DIE, in percent) in the velocity-weighted depth-integrated suspended-sediment concentration, arising from assuming that

$\int_0^T \overline{u} C_m \left(\frac{dz}{dt} \right) dt \gg \int_0^T (u C_m)' \left(\frac{dz}{dt} \right) dt$ in a one-way depth-

integrated suspended-sediment measurement at a single vertical, is defined for each size class m as

$$\text{DIE} = 100 \left(\frac{\left| \int_0^T \overline{u} C_m \left(\frac{dz}{dt} \right) dt / \int_0^T u \left(\frac{dz}{dt} \right) dt - \int_0^h \overline{u} C_m dz / \langle \overline{u} \rangle h \right|}{\int_0^h \overline{u} C_m dz / \langle \overline{u} \rangle h} \right), \quad (11)$$

where $\int_0^T \overline{u} C_m \left(\frac{dz}{dt} \right) dt / \int_0^T u \left(\frac{dz}{dt} \right) dt$ is the velocity-weighted concentration in size class m measured by a depth-integrating

sampler at a given vertical and $\int_0^h \overline{u} C_m dz / \langle \overline{u} \rangle h$ is the

depth- and time-averaged velocity-weighted concentration in size class m calculated from point samples at that same vertical. To determine whether the DIE behaves similarly to the APE in the previous analysis, equation 11 was calculated as a function of grain size, using the 1996 and 1998 point-sample and one-way depth-integrated P-61 data collected at the Grand Canyon and Lower Marble Canyon gaging stations (figs. 1, 2B, 2C). To calculate this error, $\int_0^h \overline{u} C_m dz / \langle \overline{u} \rangle h$

for each vertical sampled in 1996 and 1998 was determined by using the 18 point samples collected at each vertical, and

$\int_0^T \overline{u} C_m \left(\frac{dz}{dt} \right) dt / \int_0^T u \left(\frac{dz}{dt} \right) dt$ was determined by using the

one-way depth-integrated sample collected before or after each set of 18 point samples. The mean depth-integrated error (MDIE, in percent) was then calculated by averaging the DIEs

associated with the one-way depth-integrated samples collected before and after each set of 18 point samples. Mathematically, the MDIE is expressed as

$$MDIE = 100 \left(\frac{\int_0^T u C_m \left(\frac{dz}{dt} \right) dt / \int_0^T u \left(\frac{dz}{dt} \right) dt - \int_0^h \overline{u C_m} dz / \langle \bar{u} \rangle h}{\int_0^h \overline{u C_m} dz / \langle \bar{u} \rangle h} \right) \quad (12)$$

The results of this analysis indicate that as with the MAPE, the MDIE also depends on grain size. Analysis of variance using a standard *F*-test indicates that at the *p*=0.05 level of significance, the MDIE was positively correlated with grain size in all 10 cases for which data were available to calculate this error (table 6).

Comparison of the MDIE and MAPE indicates that these two errors are somewhat similar at each vertical but that the MDIEs are generally larger than the MAPEs (figs. 8, 9). This difference could partly arise from the fact that the MAPEs are not true instantaneous errors, whereas the MDIEs are the instantaneous errors arising from a complete lack of time averaging (since a depth-integrating sampler passes through each elevation only once during a single transit). MAPEs include some time averaging (over time scales of seconds to <1 minute) because they are calculated by comparing the fluxes from individual point samples with time-averaged fluxes, whereas MDIEs are calculated by comparing non-time-averaged suspended-sediment concentrations collected by using one-way depth integration with depth- and time-averaged suspended-sediment concentrations calculated from point samples.

At both the Grand Canyon and Lower Marble Canyon gaging stations (figs. 1, 2B, 2C), the MDIEs ranged from being equivalent to the MAPEs to being about a factor of 3 larger than the MAPEs for all size classes of sediment (fig. 10). On average, the MDIEs were therefore a factor of ~2 larger

than the MAPEs. In addition to the above-described effects of differing durations of time averaging on the MDIEs and MAPEs, part of this factor-of-2 difference between MDIEs and MAPEs could also arise from changes in sediment-supply conditions over the 1 hour required to collect the 18 point samples and two bracketing one-way depth-integrated samples at each vertical. The importance of the effect of changing sediment-supply conditions on suspended-sediment-concentration errors calculated over hourly time scales is evaluated in more detail below.

Effect of Different Durations of Time Averaging on Suspended-Sediment-Concentration Errors

To further evaluate the effect of different durations of time averaging on the error in the time- and depth-averaged velocity-weighted concentration of suspended sediment in any size class *m*, sequential one-way (non-time-averaged, with only one “measurement” at each elevation in the flow) depth-integrated samples and sequential two-way (minimally time-averaged, with two “measurements” at each elevation in the flow) depth-integrated samples were analyzed to determine whether this error decreases as the number of repeated transits at the same vertical increases. As above, “one transit” in this usage is defined as the path the sampler takes either from the bed to the water surface or from the water surface to the bed. For example, a standard two-way depth-integrated sample collected with a D-96-A1 sampler at a single vertical consists of two transits, and a one-way depth-integrated sample collected with a P-61 sampler at a single vertical consists of one transit. This analysis was accomplished by mathematically combining sequential depth-integrated samples into single samples (using laboratory-determined masses and grain-size distributions, not simply suspended-sediment concentrations) and then

Table 6. Levels of statistical significance at which the mean depth-integrated error depends on grain size.

[Critical level of significance is set equal to 0.05; values ≤0.05 (in this table, all) are shown in bold; (+) indicates significant positive correlation and (-) significant negative correlation between grain size and mean depth-integrated error. GC, Grand Canyon gaging station; LMC, Lower Marble Canyon gaging station]

Study site, month-day-year, and cableway station of vertical				
GC 3-28-1996 190 ft	GC 3-28-1996 290 ft	GC 3-30-1996 190 ft	GC 3-30-1996 290 ft	GC 4-2-1996 190 ft
0.042(+)	0.00007(+)	0.013(+)	0.016(+)	0.00001(+)
Study site, month-day-year, and station of vertical				
GC 4-2-1996 290 ft	GC 9-26-1998 190 ft	GC 9-26-1998 290 ft	LMC 9-22-1998 180 ft	LMC 9-22-1998 280 ft
0.00005(+)	0.00008(+)	0.00001(+)	0.00017(+)	0.038(+)

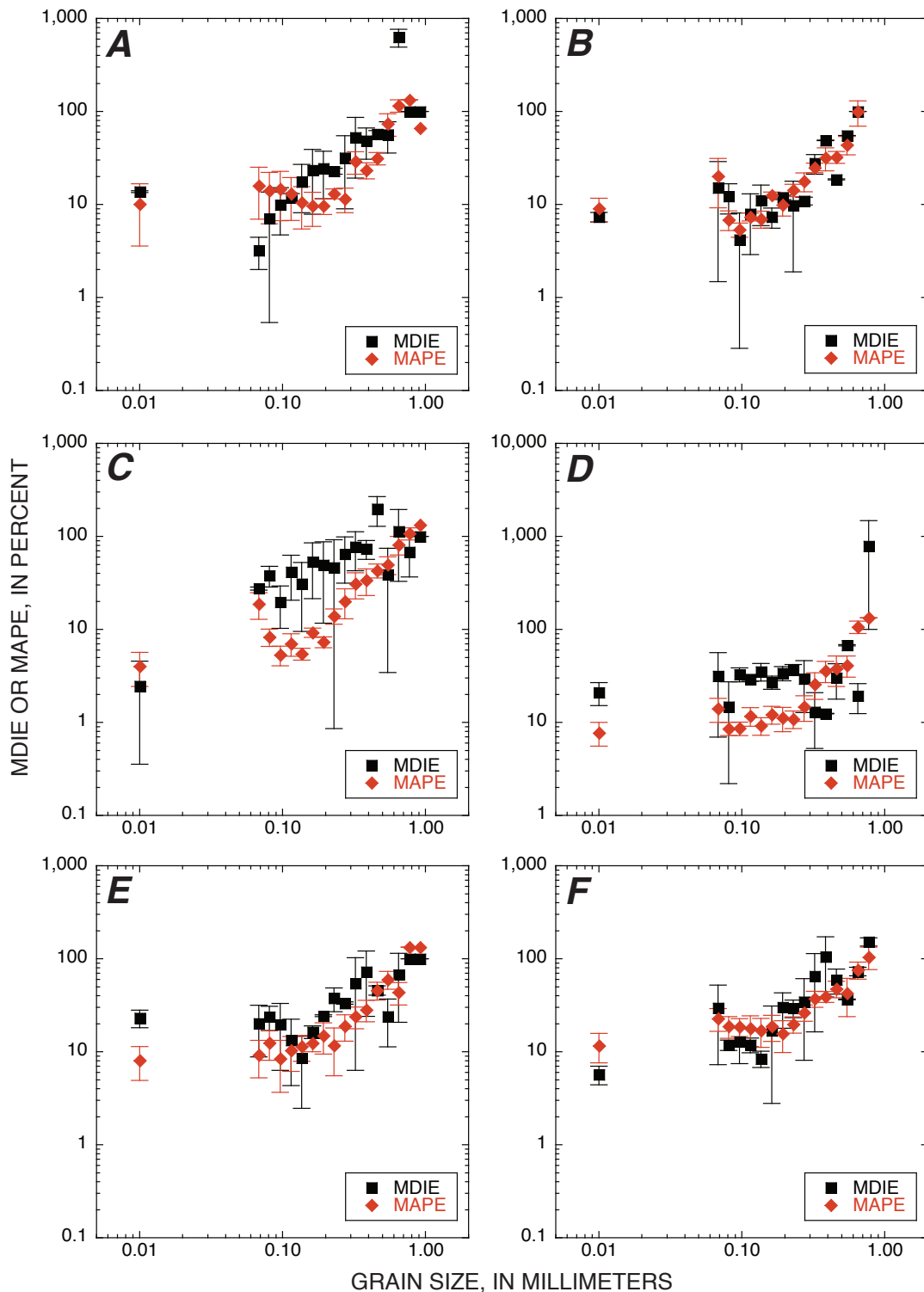


Figure 8. Comparison of the mean depth-integrated error (MDIE) in velocity-weighted one-way depth-integrated concentration of suspended sediment in each size class and mean at-a-point error (MAPE) in flux of sediment in each size class at the Grand Canyon gaging station (figs. 1, 2*B*) at vertical located along measurement cableway at station 190 ft on March 28, 1996 (A), at station 290 ft on March 28, 1996 (B), at station 190 ft on March 30, 1996 (C), at station 290 ft on March 30, 1996 (D), at station 190 ft on April 2, 1996 (E), at station 290 ft on April 2, 1996 (F), at station 190 ft on September 26, 1998 (G), and at station 290 ft on September 26, 1998 (H); and at the Lower Marble Canyon gaging station (fig. 2*C*) at vertical located along former measurement cableway at station 180 ft on September 22, 1998 (I), and at station 280 ft on September 22, 1998 (J). Error bars are 1 standard error.

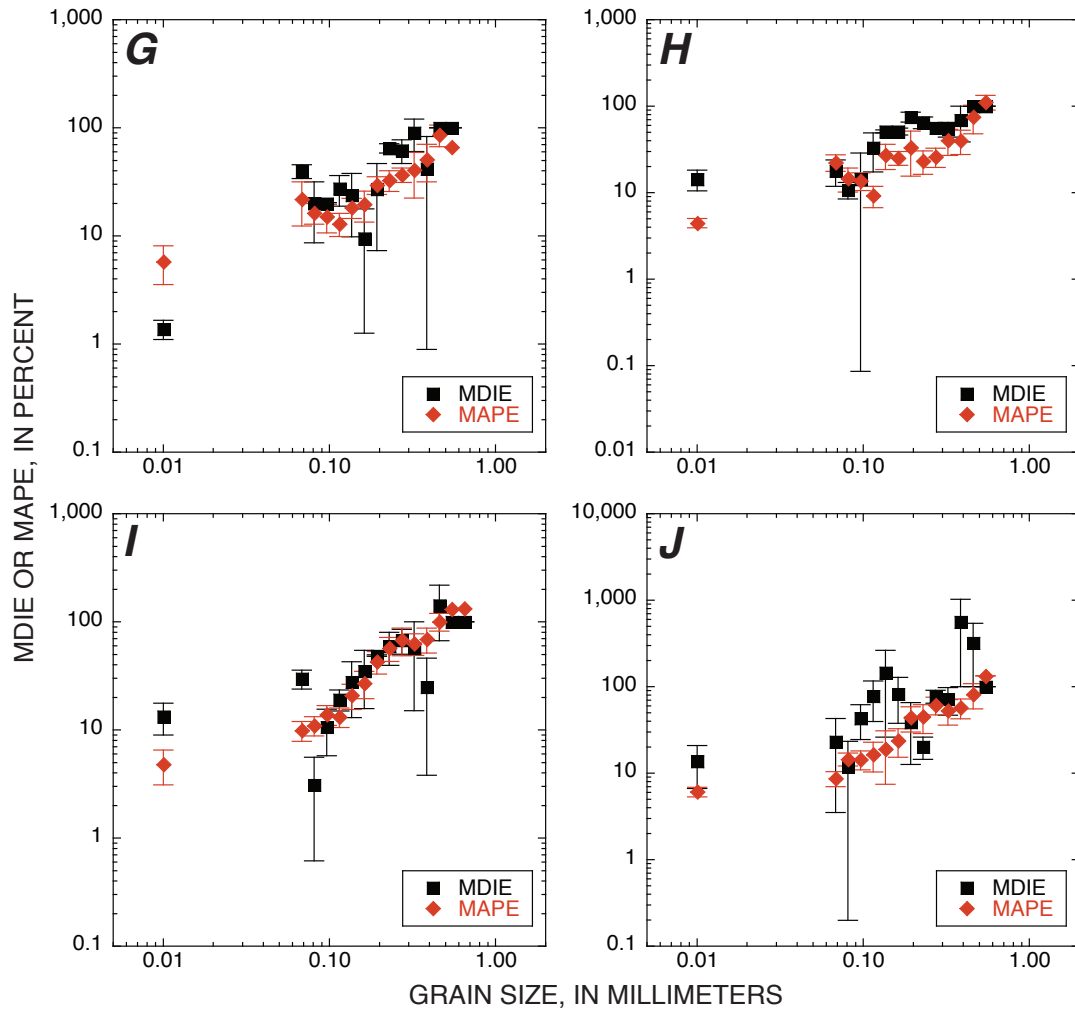


Figure 8.—Continued

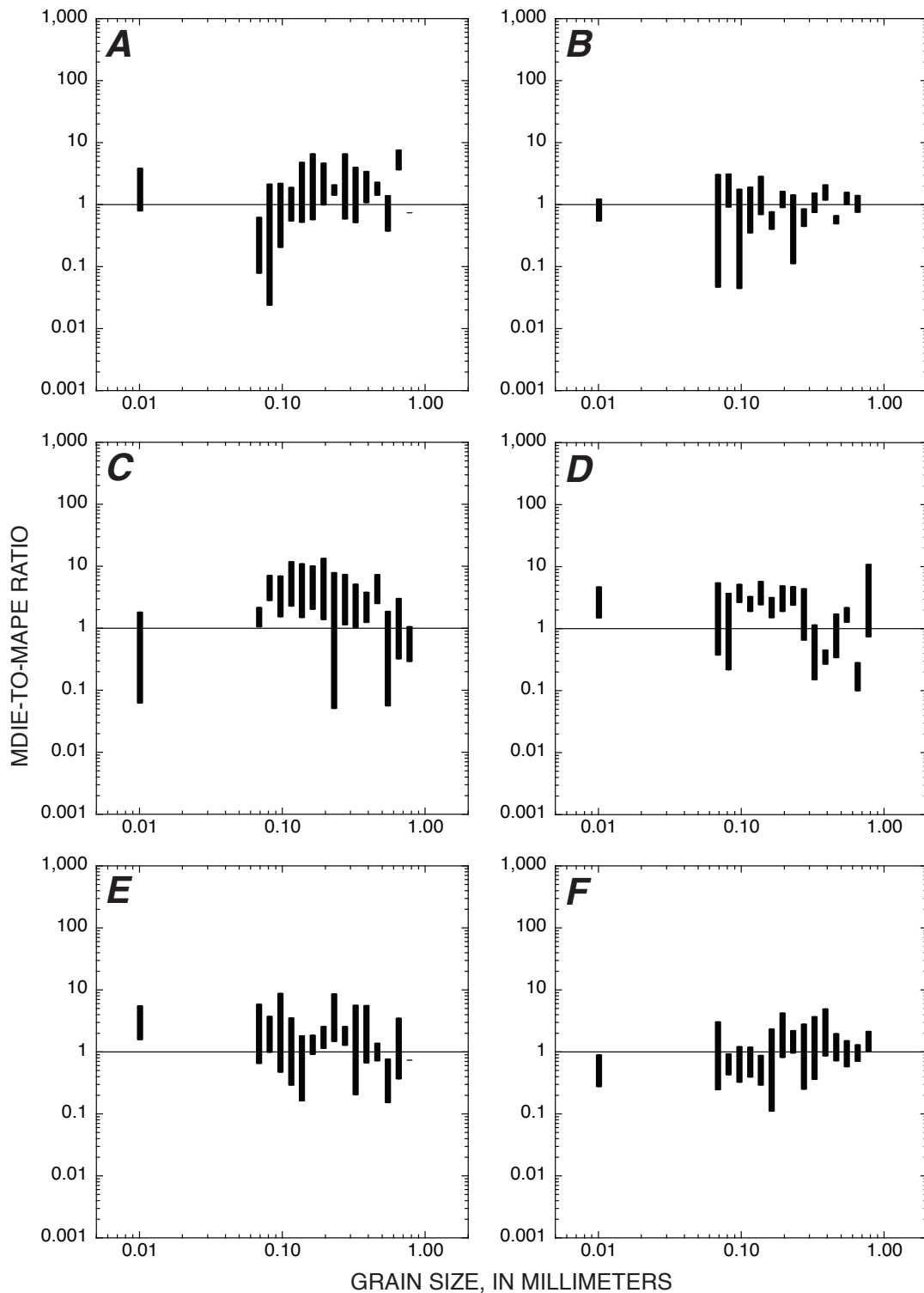


Figure 9. Likely range in the ratio of mean depth-integrated error (MDIE) to mean at-a-point error (MAPE) as a function of grain size at the Grand Canyon gaging station (figs. 1, 2B) at vertical located along measurement cableway at station 190 ft on March 28, 1996 (A), at station 290 ft on March 28, 1996 (B), at station 190 ft on March 30, 1996 (C), at station 290 ft on March 30, 1996 (D), at station 190 ft on April 2, 1996 (E), at station 290 ft on April 2, 1996 (F), at station 190 ft on September 26, 1998 (G), and at station 290 ft on September 26, 1998 (H); and at the Lower Marble Canyon gaging station (fig. 2C) at vertical located along former measurement cableway at station 180 ft on September 22, 1998 (I), and at station 280 ft on September 22, 1998 (J). For each sediment size class, maximum value of this ratio was calculated as $(MDIE+1SE)/(MAPE-1SE)$, and minimum value of this ratio as $(MDIE-1SE)/(MAPE+1SE)$, where SE is standard error.

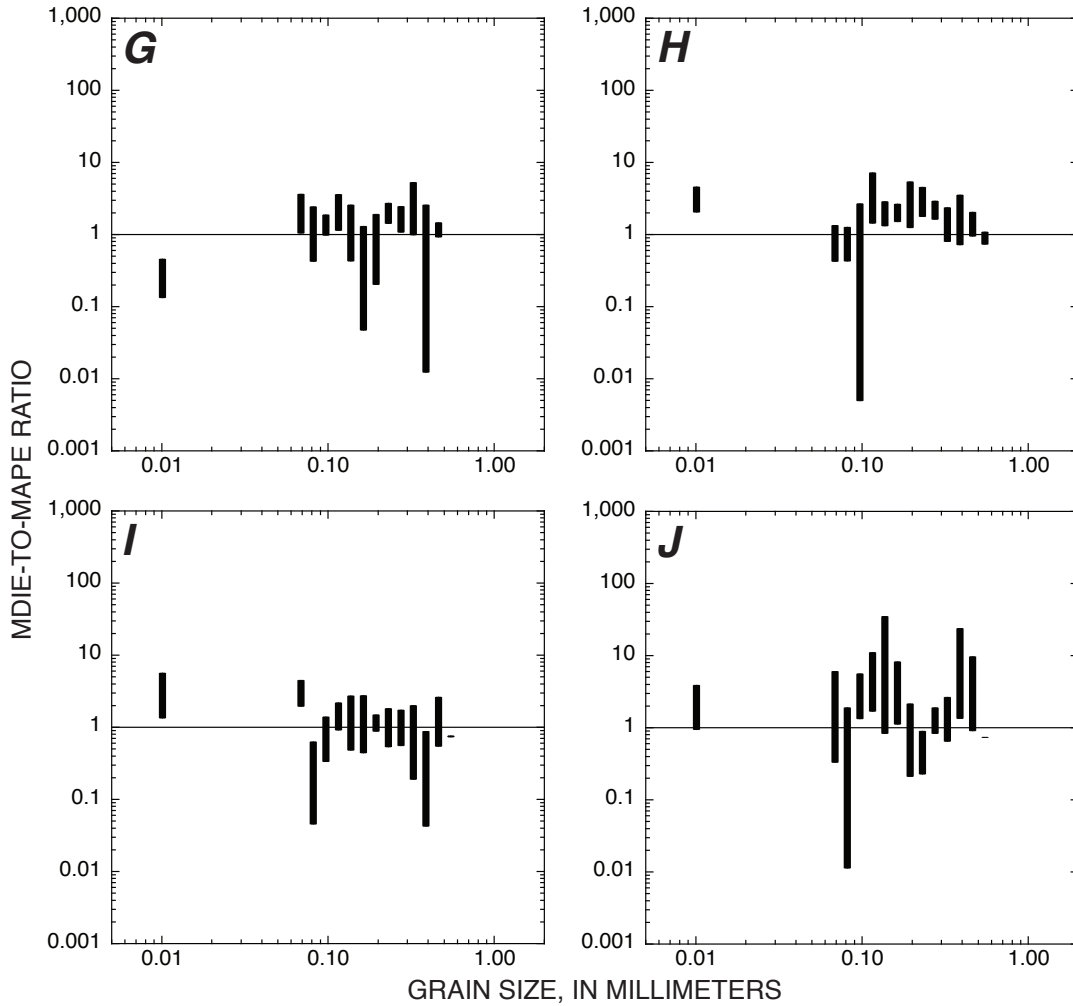


Figure 9.—Continued

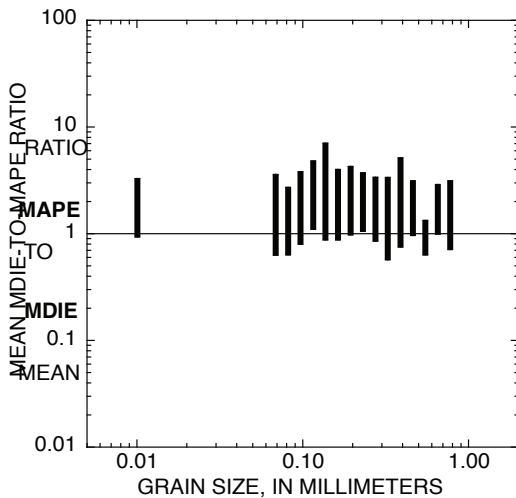


Figure 10. Likely range in mean value among all 10 cases in figure 9 of the ratio of mean depth-integrated error (MDIE) to mean at-a-point error (MAPE) plotted as a function of grain size. For each sediment size class, maximum value of this mean ratio was calculated by averaging maximum values of the MDIE-to-MAPE ratio among all 10 cases, calculated as $(MDIE+1SE)/(MAPE-1SE)$, and minimum values of this mean ratio among all 10 cases, calculated as $(MDIE-1SE)/(MAPE+1SE)$, where SE is standard error.

evaluating the effect of increasing the duration of time averaging on a modified version of the MDIE.

The error evaluated in these analyses, which is a modified version of the MDIE in equation 12, is referred to as the mean number-of-transits error (MNOTE, in percent):

$$\text{MNOTE} = 100 \left(\frac{\int_0^T u C_m \left(\frac{dz}{dt} \right) dt / \int_0^T u \left(\frac{dz}{dt} \right) dt - \overline{\int_0^T u C_m \left(\frac{dz}{dt} \right) dt / \int_0^T u \left(\frac{dz}{dt} \right) dt}}{\int_0^T u C_m \left(\frac{dz}{dt} \right) dt / \int_0^T u \left(\frac{dz}{dt} \right) dt} \right) \quad (13)$$

where the depth- and time-averaged velocity-weighted concentration in sediment size class m , that is, the term $\int_0^h \overline{u C_m} dz / \langle \bar{u} \rangle h$ in equation 12 evaluated with the point-sample data, is replaced by the “time-averaged velocity-weighted concentration in sediment size class m ,” calculated by averaging the velocity-weighted concentration in sediment size class m among each set of sequential depth-integrated

samples, $\int_0^T u C_m \left(\frac{dz}{dt} \right) dt / \int_0^T u \left(\frac{dz}{dt} \right) dt$.

The first step in this analysis was to determine whether a demonstrable net change in suspended-sediment concentration occurred over the time scale of each of these sets of sequential depth-integrated samples. Analyses of the sequential depth-integrated data using F -tests indicate that at the $p=0.05$ level of significance: (1) no changes in suspended-sand concentration occurred during data collection at any of the four study sites, (2) no changes in suspended-silt-and-clay concentration occurred during data collection at the River-mile 30 sediment station (fig. 2D) or at the Cisco and Lower Marble Canyon gaging stations (figs. 2A, 2C), and (3) an ~6 percent increase in suspended-silt-and-clay concentration occurred during data collection at the Grand Canyon gaging station (fig. 2B). Thus, the MNOTEs calculated with equation 13 cannot be demonstrated to include the effects of real changes in sand-supply conditions during the periods of time averaging in these analyses, nor to include the effects of substantial changes in silt- and clay-supply conditions during the periods of time averaging in these analyses. As stated above, the MDIEs calculated in the analysis in the previous section likely include the effect of larger changes in sediment-supply conditions over the hour required to collect the 18 point samples and bracketing depth-integrated samples. Therefore, the MNOTEs calculated with equation 13 in this analysis are likely to be smaller and more accurate (that is, essentially devoid of the effects of changes in sediment supply) than those calculated with equation 12 in the previous section.

An even number of sequential samples that could be combined multiple times was required for this operation. For example, 12 sequential samples could first be combined into 6 samples and then subsequently combined into 3 samples. Therefore, the odd number of samples (seven sets of 5 samples at the Cisco gaging station, and one set of 15 samples at both the River-mile 30 sediment station and the Lower Marble Canyon gaging station) and the 14 samples at the Grand Canyon gaging

station that could be combined only once (into 7 samples) were analyzed in two different configurations of combinations.

Analysis of the data from the Cisco gaging station (figs. 1, 2A) was conducted such that the first four samples of each set of five sequential samples were analyzed as four samples and then as two synthetically combined samples, and then the last four of each set of five sequential samples were analyzed in the same manner. Flow conditions have been shown to play only a minor role in the MAPE; the MDIE has been shown to be similar to the MAPE; and flow conditions were, in any case, similar during the 2 days of depth-integrated-sample data collection at the Cisco gaging station. Thus, the MNOTEs calculated for each grouping of samples were analyzed together. For each sediment size class m , this procedure resulted in 14 observations of the one-transit MNOTE with no time averaging (that is, the one-transit MNOTE among each set of four sequential one-way depth-integrated samples) and in 14 observations of the MNOTE with minimal time averaging (that is, the MNOTE among each set of two sequential synthetic “two-transit” depth-integrated samples constructed from the one-way depth-integrated samples). The mean MNOTEs for each sediment size class m for these 14 observations of the MNOTE with no and minimal time averaging are plotted in figure 11.

Data from the River-mile 30 sediment station and the Lower Marble Canyon gaging station (figs. 1, 2C, 2D) were analyzed such that the first 12 samples of each set of 15 sequential samples were analyzed as 12 samples and then as 3 synthetically combined samples, and then the last 12 of each set of 15 sequential samples were analyzed in the same manner. The first and last 12 of the 14 sequential samples collected at the Grand Canyon gaging station were then also analyzed in this same manner. Because flow conditions play only a minor role in this error and, as at the Cisco gaging station (fig. 2A), flow conditions were similar during collection of the two-way depth-integrated data at the River-mile 30 sediment station and the Lower Marble Canyon and Grand Canyon gaging stations, the MNOTEs calculated for each grouping of samples at these three sites were also analyzed together, resulting in six observations of the MNOTE with minimal time averaging (that is, the MNOTE among each set of 12 two-way depth-integrated samples) and two distributions of six observations of the MNOTEs with greater durations of time averaging (that is, the MNOTEs among each set of six sequential “synthetic four-transit” depth-integrated samples and each set of four sequential “synthetic eight-transit” depth-integrated samples constructed from the two-way depth-integrated samples). The mean MNOTEs for each sediment size class m for these three distributions of six observations of the MNOTE with different durations of time averaging are also plotted in figure 11.

Large increases in the duration of time averaging result in a substantial and significant decrease in the MNOTEs, especially in the sand size classes (fig. 11; table 7). To determine the relative significance of the effect on the MDIE in each sediment size class of increasing the duration of time averaging, Student’s t -tests were conducted on appropriate groupings of

EXPLANATION

- Mean MAPE among the five point-sample datasets
- ◆ Cisco mean single-transit MNOTE
- ◆ Cisco mean "synthetic two-transit" MNOTE
- RM30, LMC, GC mean two-transit MNOTE
- ▲ RM30, LMC, GC mean "synthetic four-transit" MNOTE
- ▲ RM30, LMC, GC mean "synthetic eight-transit" MNOTE

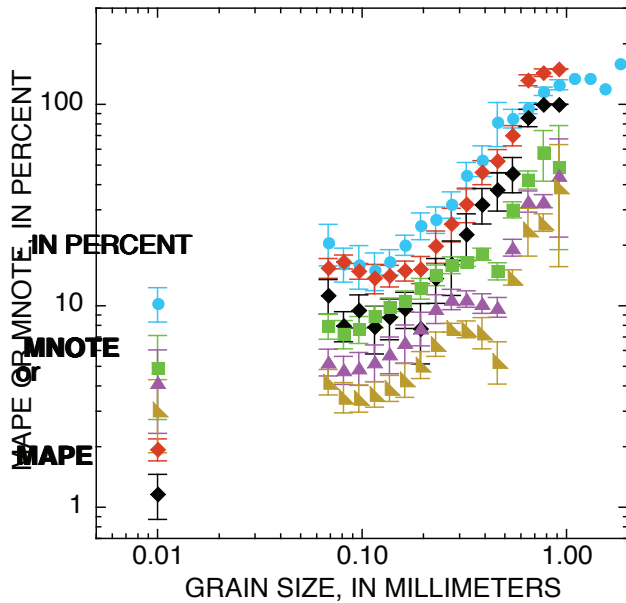


Figure 11. Mean value of mean at-a-point error (MAPE) among the five point-sample datasets, and mean values of mean number-of-transits errors (MNOTEs) calculated for one-way, two-way, and the various synthetic multitransit depth-integrated data plotted as a function of grain size. Error bars are 1 standard error. Increase in duration of time averaging (as more transits are added) generally leads to a progressive decrease in mean value of MNOTE, especially in sand size classes. Cisco, Cisco gaging station; RM30, River-mile 30 sediment station (see figure 1 for locations).

the mean MAPE calculated from the five point-sample datasets (fig. 6; table 4) and the MNOTEs calculated with equation 13 for the one-way, two-way, and various synthetic multitransit depth-integrated-sample data. For these t -tests, a Student's t -test comparing the means of two groups with equal variance was used when an F -test indicated that the variances of the two groups could not be determined to differ at the $p=0.05$ level of significance, and a Student's t -test comparing the means of two groups with unequal variance was used when an F -test indicated that the variances of the two groups differed at the $p=0.05$ level of significance. The only difference between these two tests was in degrees of freedom: the t -test comparing two groups with unequal variance had fewer degrees of freedom than the t -test comparing two groups of equal variance. Results from the t -tests listed in table 7 indicate that the most similar errors are (1) the MAPEs and one-transit MNOTEs and (2) the Cisco

"synthetic two-transit" MNOTEs and two-transit MNOTEs calculated using the data collected at the River-mile 30 sediment station (fig. 2D) and at the Lower Marble Canyon and Grand Canyon gaging stations (figs. 2B, 2C). Because the differences between MAPEs (arising from minimal time averaging over time scales of seconds to <1 minute in the point samples) and the one-transit MNOTEs (arising from zero time averaging in the one-way depth-integrated samples) are minimal, averaging over time scales in excess of 1 minute is likely required to result in substantial reductions in the MNOTE. The similarity between the MNOTEs in the "synthetic two-transit" Cisco P-61 data and the two-transit D-96-A1 data collected at the other three study sites indicates that differences in study-site geometry, flow and sediment-supply conditions, and the type of isokinetic suspended-sediment sampler used do not greatly influence the MNOTE, thus providing further support for the approach used in this study of analyzing data from all four study sites together.

Although an increase in the number of transits reduces the MNOTE in each sediment size class, as well as the level of significance at which different-transit MNOTEs can be distinguished, the number of transits must be quadrupled before different-transit MNOTEs can be demonstrated to generally differ at the $p=0.05$ level of significance because the large variance in the "number-of-transits error" in each sediment size class makes it difficult to statistically distinguish between MNOTEs associated with different numbers of transits unless either the sample size is relatively large (that is, larger than the sample sizes of 6 to 14 in table 7) or the difference in the number of transits exceeds a factor of ~4. On the basis of the median (among all size classes) level of significance in the difference between the various errors, the most different of the various cases compared in table 7 are (1) the one-transit and "synthetic four-transit" MNOTEs and (2) the two-transit and "synthetic eight-transit" MNOTEs. The two cases in table 7 that border on being significantly different are (1) the one-transit and "synthetic two-transit" MNOTEs and (2) the two-transit and "synthetic four-transit" MNOTEs. Therefore, the most significant difference exists between the errors associated with the greatest increase (that is, a quadrupling) in the number of transits. This result makes sense in that an increase from zero time averaging in the one-transit depth-integrated data (with each elevation in the flow sampled only once) to finite time averaging in the "four-transit" depth-integrated data (with each elevation in the flow sampled four times) is effectively an infinite increase in the duration of time averaging (that is, the duration of time averaging increases from zero to a small positive number). Thus, the greatest significant difference between MNOTEs should be associated with this "infinite" increase in the duration of time averaging.

Although quadrupling the number of transits is required to result in a significant decrease in the MNOTE, doubling the number of transits does result in a fairly consistent, ~30-percent reduction in the MNOTE in any given sediment size class, as illustrated by the ratios between the MNOTEs associated with different numbers of transits (fig. 12). Among all size classes of sediment in the analyses (silt and clay plus 16 size classes of sand), the mean ± 1 standard-error ratio between the MNOTE

Table 7. Levels of statistical significance at which groupings of the mean value of the mean at-a-point error (MAPE) and various mean number-of-transits errors (MNOTEs) plotted in figure 11 are different in each sediment size class.

[Critical level of significance is set equal to 0.05; values ≤ 0.05 are shown in bold; (=) indicates Student's *t*-test comparing the means of two groups with equal variance utilized based on *F*-test level of significance > 0.05 ; (\neq) indicates Student's *t*-test comparing the means of two groups with unequal variance utilized based on *F*-test level of significance ≤ 0.05 . Cisco, Cisco gaging station; GC, Grand Canyon gaging station; LMC, Lower Marble Canyon gaging station; RM30, River-mile 30 sediment station. n/a indicates analysis not applicable because of insufficient data in size class]

Size class (mm)	Groups compared													
	MAPE among five datasets (n=5)	MNOTE Cisco 1-transit (n=14)	MNOTE Cisco 1-transit (n=14)	MNOTE Cisco synthetic 2-transit (n=14)	MNOTE Cisco synthetic 2-transit (n=14)	MNOTE RM30, LMC, GC 2-transit (n=6)	MNOTE RM30, LMC, GC 2-transit (n=6)	MNOTE RM30, LMC, GC synthetic 4-transit (n=6)	MNOTE RM30, LMC, GC synthetic 4-transit (n=6)	MNOTE RM30, LMC, GC synthetic 8-transit (n=6)	MNOTE Cisco 1-transit (n=14)	MNOTE RM30, LMC, GC synthetic 4-transit	MNOTE RM30, LMC, GC 2-transit (n=6)	MNOTE RM30, LMC, GC synthetic 8-transit (n=6)
< 0.0625	0.012 (\neq)		0.051 (=)		0.15 (\neq)		0.80 (=)		0.50 (=)		0.28 (\neq)		0.48 (=)	
0.0625–0.074	0.22 (=)		0.15 (=)		0.20 (\neq)		0.083 (=)		0.31 (=)		<0.0001 (\neq)		0.015 (=)	
0.074–0.088	0.13 (=)		0.00010 (=)		0.76 (=)		0.11 (=)		0.22 (=)		<0.0001 (\neq)		0.018 (=)	
0.088–0.105	0.72 (=)		0.024 (=)		0.52 (=)		0.097 (=)		0.21 (=)		0.00019 (=)		0.0089 (=)	
0.105–0.125	0.76 (=)		0.069 (=)		0.68 (\neq)		0.045 (=)		0.21 (=)		0.0038 (\neq)		0.0018 (=)	
0.125–0.149	0.46 (=)		0.056 (=)		0.64 (\neq)		0.029 (=)		0.19 (=)		0.0080 (=)		0.00060 (=)	
0.149–0.177	0.12 (=)		0.054 (=)		0.78 (=)		0.059 (=)		0.19 (=)		0.0075 (=)		0.0017 (=)	
0.177–0.210	0.045 (=)		0.040 (=)		0.14 (\neq)		0.057 (=)		0.14 (=)		0.064 (=)		0.0015 (=)	
0.210–0.250	0.30 (=)		0.23 (=)		0.89 (\neq)		0.080 (=)		0.11 (=)		0.021 (\neq)		0.0022 (=)	
0.250–0.297	0.47 (=)		0.18 (=)		0.98 (\neq)		0.027 (=)		0.061 (\neq)		0.0099 (\neq)		0.0026 (\neq)	
0.297–0.354	0.29 (=)		0.28 (=)		0.32 (\neq)		0.0015 (=)		0.029 (=)		0.0047 (\neq)		<0.0001 (=)	
0.354–0.420	0.58 (=)		0.12 (=)		0.052 (\neq)		0.0010 (=)		0.13 (=)		<0.0001 (\neq)		0.00014 (=)	
0.420–0.500	0.096 (=)		0.18 (=)		0.015 (\neq)		0.021 (=)		0.023 (=)		<0.0001 (\neq)		0.00060 (=)	
0.500–0.595	0.32 (=)		0.050 (=)		0.12 (\neq)		0.010 (=)		0.031 (=)		<0.0001 (\neq)		0.00033 (=)	
0.595–0.707	0.035 (=)		0.00073 (=)		0.00031 (\neq)		0.15 (=)		0.25 (=)		<0.0001 (\neq)		0.040 (=)	
0.707–0.841	0.018 (=)		0.00021 (\neq)		0.049 (\neq)		0.19 (\neq)		0.075 (=)		<0.0001 (\neq)		0.11 (\neq)	
0.841–1.00	0.073 (\neq)		<0.0001 (=)		0.16 (\neq)		0.11 (=)		0.88 (=)		0.0098 (\neq)		0.81 (=)	
1.00–1.19	n/a		n/a		n/a		n/a		n/a		n/a		n/a	
1.19–1.41	n/a		n/a		n/a		n/a		n/a		n/a		n/a	
1.41–1.68	n/a		n/a		n/a		n/a		n/a		n/a		n/a	
1.68–2.00	n/a		n/a		n/a		n/a		n/a		n/a		n/a	
Median level of significant difference among all size classes	0.27		0.087		0.20		0.059		0.19		0.0038		0.0022	

associated with two transits and the MNOTE associated with one transit is 0.64 ± 0.02 . Similarly, the mean ratio between the MNOTE associated with four transits and the MNOTE associated with two transits is 0.67 ± 0.02 , and the mean ratio between the MNOTE associated with eight transits and the MNOTE associated with four transits is 0.71 ± 0.02 . For the silt-and-clay size class only, the ratio between the MNOTE associated with two transits and the MNOTE associated with one transit is 0.60, the ratio between the MNOTE associated with four transits to the MNOTE associated with two transits is 0.74, and the ratio between the MNOTE associated with eight transits and the MNOTE associated with four transits is 0.85. For sand analyzed as a single size class, the ratio between the MNOTE associated with two transits and the MNOTE associated with one transit is 0.71, the ratio between the MNOTE associated with four transits and the MNOTE associated with two transits is 0.70, and, the ratio between the MNOTE associated with eight transits and the MNOTE associated with four transits is 0.63. Associated with this reduction in the MNOTE is a reduction in the relative mean absolute error in the median grain size of suspended sand, herein referred to as the D_{50} MNOTE. The ratio between the D_{50} MNOTE associated with two transits and the D_{50} MNOTE associated with one transit is 0.79, the ratio between the D_{50} MNOTE associated with four transits and the D_{50} MNOTE associated with two transits is 0.64, and the ratio between the D_{50} MNOTE associated with eight transits and the D_{50} MNOTE associated with four transits is 0.65.

The previous analysis indicates that with a fair amount of variation, doubling the duration of time averaging through doubling the number of transits decreases the MNOTE or D_{50} MNOTE by ~ 30 percent. To understand the reason for this style of error reduction, it is informative to compare the behavior of the MNOTE⁸ and D_{50} MNOTE with the behavior of the standard error (SE) of the mean, as given by

$$SE = \frac{\sigma}{\sqrt{n}}, \quad (14)$$

where σ is the sample standard deviation and n is the number of uncorrelated observations in the sample (as reviewed by Davis, 1986). Here, an increase in the number of repeated, uncorrelated observations will reduce the SE by a factor of exactly $1/n^{0.5}$. In a form identical to the form of equation 14, a general equation to describe the observed behavior of the single-vertical MNOTE is

$$MNOTE = \frac{MNOTE_1}{n_{trans}^\gamma}, \quad (15)$$

where $MNOTE_1$ is the single-vertical MNOTE in a given sediment size class when only one transit is collected, n_{trans} is the number of transits at this vertical, and γ is the exponent describing the behavior of the MNOTE as transits are added. Rearranging equation 15 into the form

⁸ For review, the mean absolute error (in this case, MNOTE) is 0.8σ (calculated for n degrees of freedom) in a Gaussian normal distribution, and the standard error of the mean is σ/\sqrt{n} .

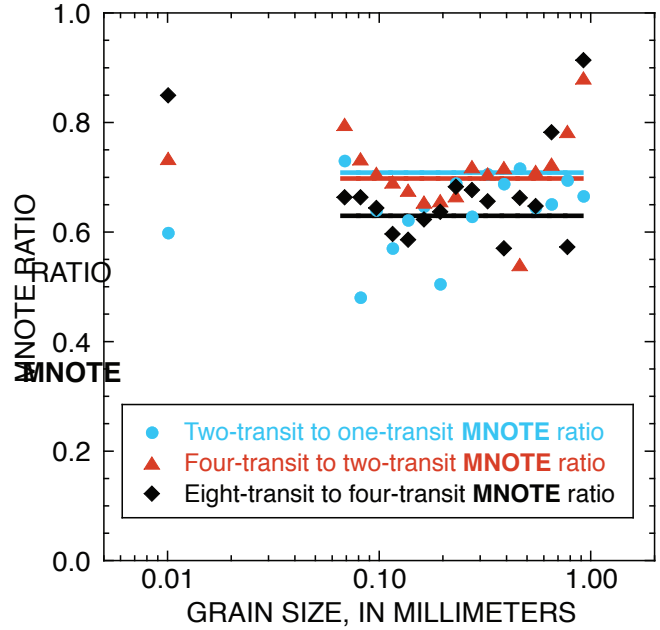


Figure 12. Ratios between the mean values of the mean number-of-transits-errors (MNOTEs) in figure 11 associated with different numbers of transits plotted as a function of grain size. Ratios of two-transit to one-transit MNOTEs (blue dots) are from data collected at the Cisco gaging station (fig. 1), and ratios of four-transit to two-transit MNOTEs (red triangles) and of eight-transit to four-transit MNOTEs (black diamonds) are from data collected at the River-mile 30 sediment station and at the Lower Marble Canyon and Grand Canyon gaging stations. Light-blue line indicates ratio of two-transit to one-transit mean MNOTEs in total suspended-sand concentration at the Cisco gaging station; red line indicates ratio of four-transit to two-transit mean MNOTEs in total suspended-sand concentration at the River-mile 30 sediment station and at the Lower Marble Canyon and Grand Canyon gaging stations; black line indicates ratio of eight-transit to four-transit mean MNOTEs in total suspended-sand concentration at the River-mile 30 sediment station and at the Lower Marble Canyon and Grand Canyon gaging stations.

$$\frac{MNOTE_1}{MNOTE} = n_{trans}^\gamma, \quad (16)$$

using values of the $MNOTE_1$ -to- $MNOTE$ ratios given in the previous paragraph, and solving for γ by logarithmically transforming the data and using least-squares linear regression⁹ yields the following γ values. Use of the mean

⁹ γ can also be solved for explicitly by $\gamma = \log_{n_{TRANS}}(MNOTE_1/MNOTE)$ and then computing the average γ value for the $MNOTE_1$ -to- $MNOTE$ ratios associated with measurements with (1 transit)/(2 transits), (1 transit)/(4 transits), and (1 transit)/(8 transits). This approach assumes equivalent certainty at which each of these three ratios is known. Use of least-squares linear regression on the log-transformed data was deemed a more accurate estimator of γ because (1) it deemphasized the certainty associated with any one of the three empirically determined values of the $MNOTE_1$ -to- $MNOTE$ ratios and (2) it allowed inclusion of four values, with the addition of the $MNOTE_1$ -to- $MNOTE$ ratio of 1 associated with measurements of (1 transit)/(1 transit), instead of only three values in the calculation of γ .

MNOTE₁-to-MNOTE ratios among all sediment size classes results in $\gamma=0.566$, use of the MNOTE₁-to-MNOTE ratios for the silt and clay size class results in $\gamma=0.468$, and use of the MNOTE₁-to-MNOTE ratios for sand analyzed as a single size class results in $\gamma=0.563$. Use of the D_{50} MNOTE₁-to- D_{50} MNOTE ratios results in $\gamma=0.546$. Given the variation, relatively small number of observations, and uncertainty in the data used to calculate the γ values, it is probably best to conclude that $\gamma \approx 0.5$. Thus, the observed reduction in the MNOTE and D_{50} MNOTE as transits are added is identical to the behavior of error reduction arising from an increase in the number of repeated, uncorrelated observations.

The identical behavior of the MNOTE and the SE indicates that the same level of error reduction can be achieved at any one vertical in an EDI or EWI measurement by (1) simply adding more transits or (2) conducting separate, repeated depth-integrated measurements. Error reduction by simply adding more transits to each vertical comes at the modest cost of only a few minutes of additional field time at each vertical. Error reduction through adding repeated, but separate, uncorrelated depth-integrated measurements, however, takes slightly longer in the field (through the addition of more bottles to a measurement) and results in additional laboratory sample-processing time (because each depth-integrated measurement at each vertical needs to be processed separately in the laboratory). Thus, doubling the number of transits reduces the MNOTE by ~ 30 percent and does not increase the amount of laboratory work, whereas doubling the number of repeated separate depth-integrated measurements reduces the standard error of the mean of these measurements by 29 percent, while slightly increasing the field work and doubling the required laboratory work. Therefore, reduction in the error arising from inadequate time averaging is more efficiently achieved by adding more transits to each vertical than by conducting repeated, separate measurements at each vertical.

Evaluation of Spatial Correlations Between Verticals and Temporal Correlations at Verticals in a Cross Section

The best way to reduce random error in a measurement is through increasing the sample size of uncorrelated observations known to come from the same population (for example, Taylor, 1997; Bevington and Robinson, 2003). In the case of the random error at a single vertical arising from inadequate time averaging of turbulent and other short-term fluctuations in sediment flux, the only ways to reduce this error are to make repeated or, as shown above, longer-duration observations. In a multivertical EDI or EWI measurement, this “time averaging” error also can likely be reduced through the addition of verticals, especially if the correlation in depth-integrated concentration between adjacent verticals is small. In any given cross section, the maximum spacing at which the depth-integrated concentration is correlated between adjacent verticals depends on the sediment size class and flow conditions. This spacing

is likely negatively correlated with grain size because the cross-stream spatial structure in suspended-silt-and-clay concentration is generally more uniform than that in suspended-sand concentration. Furthermore, this spacing also is likely negatively correlated with flow conditions because increases in depth, velocity, or turbulence generally reduce the cross-stream spatial structure in the concentration of a given size class of sediment.

This analysis was conducted by evaluating (1) whether the depth-integrated concentration of sediment in a given size class at adjacent verticals in a single EWI measurement was correlated at the $p=0.05$ level of significance and (2) whether the depth-integrated concentration of sediment in a given size class at different verticals exhibited a cross-stream spatial structure that persisted over time scales much longer than those associated with turbulent and other short-term fluctuations in sediment flux (for example, boil shedding from dunes) that operate over seconds to minutes. The data used in this analysis were the 11 total cases at cross sections A and B at the River-mile 30 sediment station (fig. 2D) and cross sections A, B, and C at the Lower Marble Canyon gaging station (fig. 2C), where two noncomposited nine-vertical depth-integrated suspended-sediment measurements were collected ~ 1.5 –6 hours apart on the same day. This analysis was conducted on two size classes of sediment: sand, and silt and clay. As described previously, to remove the effects of changes in the upstream sediment supply or stream flow conditions between measurements, and to remove the small biases between the data collected with the D-77 bag-type and D-96-A1 depth-integrating samplers, the depth-integrated concentration of suspended sediment in a given size class was normalized at each vertical in a measurement through division by the mean depth-integrated suspended-sediment concentration in that size class among the nine verticals in that measurement. *F*-tests were then conducted to determine whether a statistically significant (at the $p=0.05$ level) correlation existed (1) in the suspended-sediment concentration between adjacent verticals in the same EWI measurement and (2) in the suspended-sediment concentration at each vertical between the two EWI measurements made hours apart on the same day.

Results from these analyses indicate that generally no significant correlation exists between the depth-integrated suspended-sand concentrations at adjacent verticals in the same EWI measurement, and correlation is only slightly more significant between the suspended-silt-and-clay concentrations at adjacent verticals in the same EWI measurement. Despite this absence of significant spatial correlation, significant cross-stream spatial structures in suspended-sand and suspended-silt-and-clay concentrations can persist over hours (table 8; see appendix B), that is, over time scales much longer than those required to complete an EDI or EWI measurement. Thus, temporal correlations (over time scales of >1 hour) in suspended-sediment concentration at individual verticals tend to dominate over spatial correlations in suspended-sediment concentration, at least at the approximate one-flow-depth spacing between verticals in the nine-vertical measurements. The absence of

Table 8. Levels of statistical significance associated with correlations (1) in suspended-sediment concentration between adjacent verticals in one measurement and (2) in cross-stream spatial structures in suspended-sediment concentration between two noncomposited nine-vertical measurements made hours apart on the same day at the River-mile 30 (RM30) sediment station and Lower Marble Canyon (LMC) gaging station.

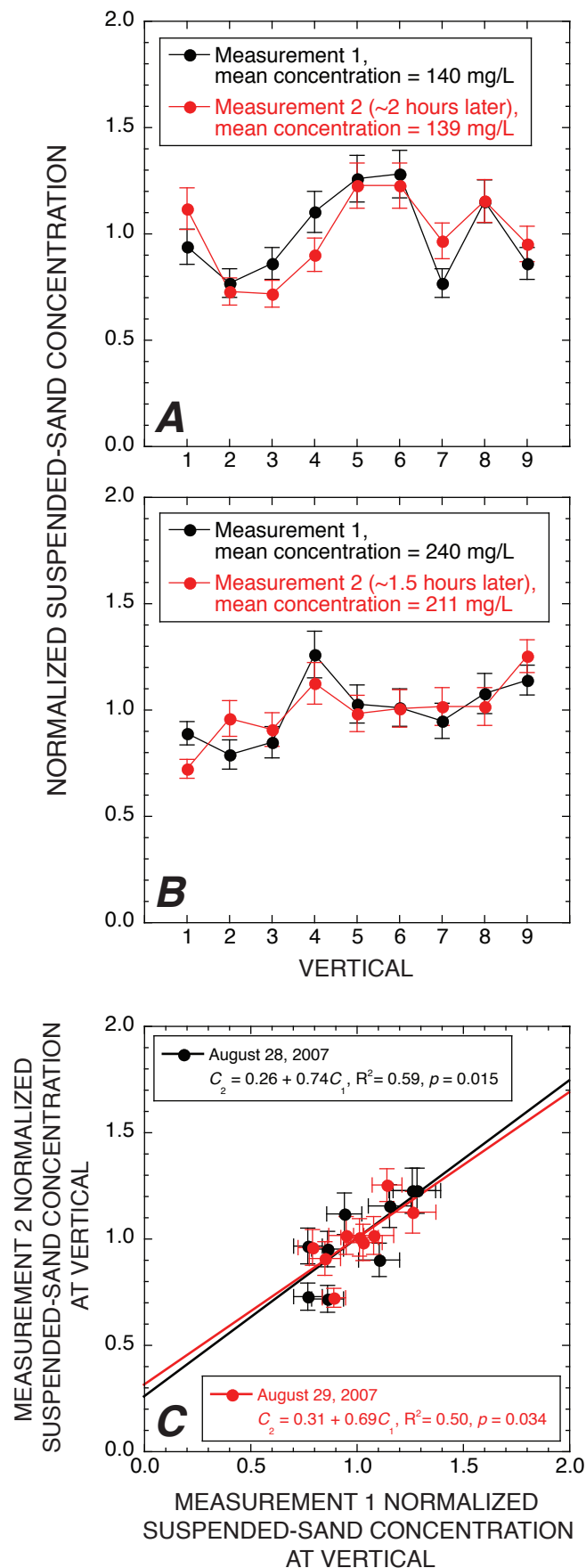
[Critical level of significance is set equal to 0.05; values ≤ 0.05 are shown in bold. Cross sections (XS), dates, times, mean discharges (Q), mean suspended-sand concentrations, and mean suspended-silt-and-clay concentrations are indicated]

Cross section	Date (month-day-year)	Time (MST)	Daily measurement number	Mean Q (m ³ /s)	Mean suspended-sand concentration among nine verticals (mg/L)	Level of significance (p) at which suspended-sand concentration between adjacent verticals is correlated	Level of significance (p) at which cross-stream spatial structure in sand concentration is correlated between two measurements	Mean suspended-silt-and-clay concentration among nine verticals (mg/L)	Level of significance (p) at which suspended-silt-and-clay concentration between adjacent verticals is correlated	Level of significance (p) at which cross-stream spatial structure in suspended-silt-and-clay concentration is correlated between two measurements
RM30 XS A	2-24-2007	11:33–12:43	1	268	55.2	0.42	0.76	16.8	0.63	0.77
RM30 XS A	2-24-2007	17:10–18:41	2	286	68.9	0.0074		17.2	0.23	
RM30 XS A	8-24-2007	14:02–14:37	1	276	64.5	0.26	0.013	31.2	0.22	0.34
RM30 XS A	8-24-2007	15:44–16:18	2	290	87.9	0.20		34.7	0.59	
RM30 XS A	8-25-2007	8:42–9:19	1	348	128	0.69	0.086	47.7	0.12	0.0087
RM30 XS A	8-25-2007	10:27–11:06	2	313	67.3	0.27		27.7	0.49	
RM30 XS B	8-24-2007	14:48–15:25	1	279	51.1	0.62	0.37	32.8	0.65	0.69
RM30 XS B	8-24-2007	16:23–16:55	2	305	92.8	0.48		33.6	0.34	
RM30 XS B	8-25-2007	8:03–8:37	1	364	121	0.35	0.19	47.5	0.36	0.23
RM30 XS B	8-25-2007	9:38–10:19	2	326	65.7	0.82		27.4	0.32	
LMC XS A	8-28-2007	13:50–14:10	1	418	101	0.71	0.022	1,150	0.92	0.030
LMC XS A	8-28-2007	15:51–16:24	2	384	109	0.14		793	0.11	
LMC XS A	8-29-2007	8:26–8:46	1	472	239	0.44	0.015	6,590	0.00004	0.21
LMC XS A	8-29-2007	10:03–10:23	2	457	218	0.14		9,710	0.74	
LMC XS B	8-28-2007	14:18–14:42	1	410	126	0.38	0.84	1,110	0.22	0.48
LMC XS B	8-28-2007	16:32–16:56	2	376	107	0.35		747	0.55	
LMC XS B	8-29-2007	8:04–8:21	1	476	255	0.25	0.51	5,950	0.054	0.077
LMC XS B	8-29-2007	9:41–9:59	2	461	235	0.55		8,090	0.028	
LMC XS C	8-28-2007	13:02–13:24	1	430	140	0.92	0.015	1,490	0.62	0.87
LMC XS C	8-28-2007	14:56–15:32	2	396	139	0.31		1,020	0.077	
LMC XS C	8-29-2007	8:56–9:17	1	469	240	0.50	0.034	6,560	0.013	0.16
LMC XS C	8-29-2007	10:31–10:52	2	450	211	0.83		9,630	0.077	

significant spatial correlation between adjacent verticals suggests that reductions in the “time averaging” error in EDI- or EWI-measured suspended-sediment concentration will occur as verticals are added to an EDI or EWI measurement.

Stable cross-stream spatial structures in suspended-sand concentration were observed at three of the five cross sections and in 5 of the 11 total cases of paired nine-vertical measurements (fig. 13; table 8; see appendix B), and stable cross-stream structures in suspended-silt-and-clay concentration were observed at two of the five cross sections and in 2 of the 11 total cases (table 8; see appendix B). Although these cross-stream spatial structures in suspended-sediment concentration can be stable between measurements spaced hours apart, they either evolve into different stable spatial structures or become unstable over longer time scales (that is, >12 hours). Thus, between measurements made hours apart on subsequent days at these cross sections, either a different stable cross-stream spatial structure or no stable cross-stream spatial structure may exist. At other cross sections, no stable cross-stream spatial structures in suspended-sand or suspended-silt-and-clay

Figure 13. Examples of stable cross-stream spatial structures in depth-integrated suspended-sand concentration along cross section C at the Lower Marble Canyon gaging station (figs. 1, 2C). Error bars indicate mean number-of-transits error (MNOTE) at each vertical; see appendix A for data. Suspended-sand data from other cross sections are plotted in appendix B. *A*, Suspended-sand concentration at each of nine verticals sampled during two measurements on August 28, 2007; concentration at each vertical in each measurement normalized by mean concentration among all nine verticals in each measurement. Note that spatial cross-stream structure in suspended-sand concentration appears to be similar between two measurements spaced ~2 hours apart. *B*, Suspended-sand concentration at each of nine verticals sampled during two measurements made on August 29, 2007; concentration at each vertical in each measurement normalized by mean concentration among all nine verticals in each measurement. Note that spatial cross-stream structure in suspended-sand concentration appears to be similar between the two measurements spaced ~1.5 hours apart but differs significantly from stable spatial structure observed the previous day. *C*, Relations between normalized suspended-sand concentrations at each vertical sampled in measurements 1 (C_1) and 2 (C_2) on August 28 and 29, 2007. Relations are significant at $p=0.05$ level, indicating significant temporal correlation in suspended-sand concentration at each vertical over time scales of hours on each day. Note similarity of relations on the 2 days, even though cross-stream spatial structures in suspended-sand concentration differ significantly between the 2 days.



concentration were observed to persist between measurements spaced hours apart (table 8; see appendix B). This observation of an absence of stable structures at these other cross sections is limited by a small number of observations. Therefore, (1) the result that cross-stream spatial structures in suspended-sediment concentration can be stable for hours and then either change overnight to a different stable structure or disappear altogether and (2) the fact that data were collected in this study only on no more than 2 subsequent days and no more than 3 different days total (that is, the sample size is small) together suggest that stable cross-stream spatial structures in suspended-sediment concentration could exist at these other cross sections when observations were not made. The cases of cross-stream spatial structures in suspended-sediment concentration that were stable over hours but not days are assumed to result from the distribution of dunes or patches of sand on the bed upstream from the measurement cross section. The relatively slow rates of dune migration (for example, Rubin and others, 2001) or change in sand-patch geometry (processes that operate over many hours) could allow stable cross-stream structures in suspended-sediment concentration to persist over hours but not days.

Despite the result that stable cross-stream spatial structures in suspended-sediment concentration may be detectable over hours, the correlation in depth-integrated suspended-sediment concentration is generally insignificant between adjacent verticals in the same measurement. At the $p=0.05$ level of significance, suspended-sand concentration was correlated between adjacent verticals in only 1 of the 22 nine-vertical measurements at the five cross sections, whereas suspended-silt-and-clay concentration was correlated between adjacent verticals in 3 of the 22 nine-vertical measurements at the five cross sections. No change is detectable in the significance of the correlation in suspended-sand concentration between adjacent verticals as suspended-sand concentration increases. The significance of the correlation in suspended-silt-and-clay concentration between adjacent verticals, however, appears to improve (that is, the silt and clay becomes more uniformly distributed in the cross section) as suspended-silt-and-clay concentration increases. Especially at lower concentrations (fig. 14, see appendix B), the cross-stream variation in suspended-silt-and-clay concentration between adjacent verticals greatly exceeds the near-zero cross-stream variation in suspended-silt-and-clay concentration suggested by P.R. Jordan's analysis in the report by Guy and Norman (1970) and Edwards and Glysson (1999). The observed persistence of stable cross-stream structures in suspended-silt-and-clay concentration between measurements spaced hours apart indicates that the greater-than-zero cross-stream variation in suspended-silt-and-clay concentration between adjacent verticals is real, and so laboratory-processing errors cannot entirely explain the cross-stream variation in suspended-silt-and-clay concentration. These observations together suggest that either (1) P.R. Jordan's estimate of the near-zero error in suspended-silt-and-clay concentration arising from inadequate sampling of the cross-stream spatial

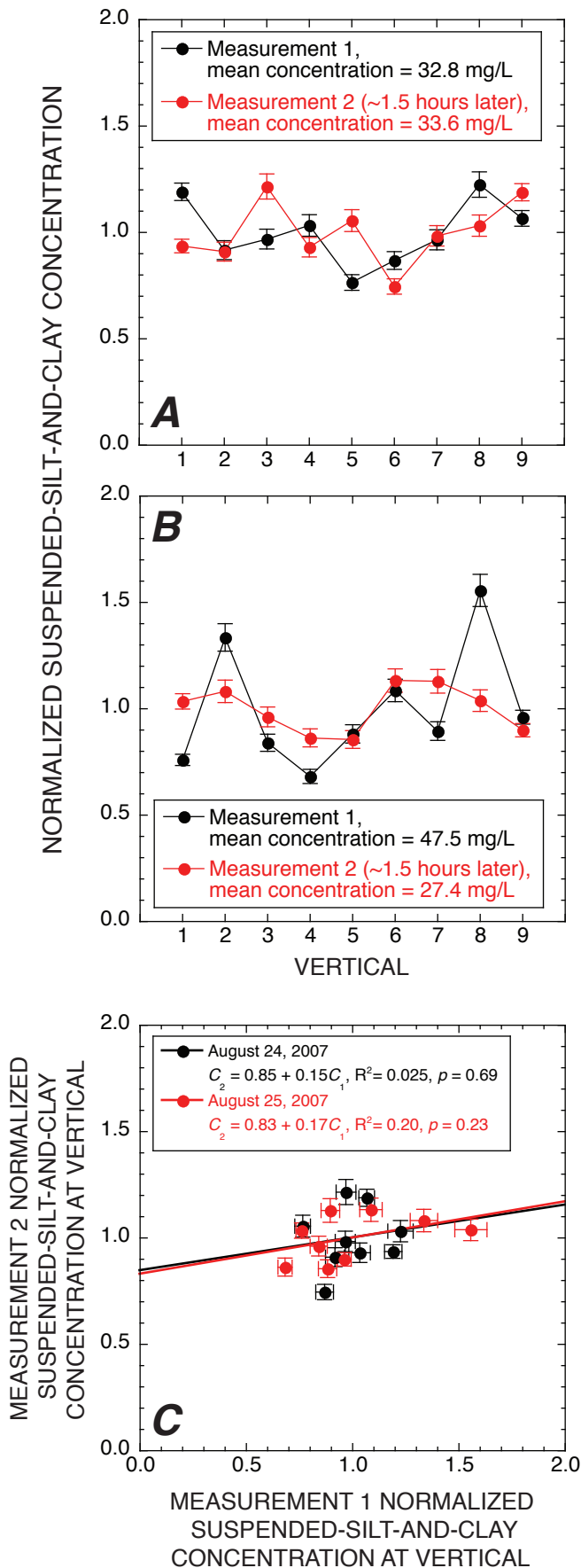
structure in suspended-sediment concentration is incorrect, or (2) the variation in suspended-silt-and-clay concentration between adjacent verticals is dominated by the error arising from inadequate time averaging at each vertical. As shown in the next section of this report, the first of these possibilities is the more likely reason for the large variation in suspended-silt-and-clay concentration between adjacent verticals in the nine-vertical measurements when the mean suspended-silt-and-clay concentration in the cross section is relatively low.

Combination of Temporal and Spatial Errors into an Estimate of the Total Uncertainty in the Time-Averaged Velocity-Weighted Suspended-Sediment Concentration in a Cross Section

As stated previously, much of the focus of previous investigations has been on the quasi-systematic error arising from inadequate sampling of the cross-stream spatial structure in the time-averaged velocity-weighted suspended-sediment concentration in a river cross section. As shown by P.R. Jordan's analysis in the report by Edwards and Glysson (1999, fig. 38), this relative standard error for sand-size sediment is likely about ± 7 percent in simple trapezoidal cross sections when 2 verticals are sampled, about ± 3.9 percent when 5 verticals are sampled, and about ± 2.4 percent when 10 verticals are sampled. In these simple channels, this quasi-systematic "spatial structure" error (herein referred to as the "number-of-verticals error" or NOVE [in percent]) decreases by a factor of $\sim 1/n_{\text{vert}}^{0.7}$ as the number of verticals, n_{vert} , increases. In more complex channels, this error for sand-size sediment can be almost 10 times larger. Depending on the geometric details of the cross section, the spatial distribution of sand on the bed upstream from the measurement cross section, and the use of either the EDI or EWI method, this quasi-systematic error can be either positive or negative. Depending on the number and location of verticals, the sign of the NOVE at a cross section can therefore change as cross-stream spatial structures in depth-integrated suspended-sand concentration change over time (fig. 13; see appendix B). P.R. Jordan's analysis suggests, on the basis that the suspended-silt-and-clay is uniformly distributed in a cross section, that the NOVE for silt and clay is negligible (essentially zero) regardless of the number of verticals sampled. As shown below, this assumption is not necessarily valid, and so the NOVE for silt and clay is not negligible, at least at low suspended-silt-and-clay concentrations, and appears to decrease as verticals are added. Using the results obtained by Edwards and Glysson (1999, fig. 38), generalization of the NOVE in the velocity-weighted suspended-sand concentration in a simple trapezoidal channel for different numbers of verticals yields

$$\text{NOVE} = \frac{12.0}{n_{\text{vert}}^{0.7}} \quad (17)$$

As the complexity in the channel cross section increases, the exponent in the denominator in equation 17 remains



constant at 0.7, and only the numerator increases. Similarly, generalization of the NOVE in the velocity-weighted suspended-silt-and-clay concentration in a simple trapezoidal channel for different numbers of verticals yields

$$\text{NOVE} = 0. \tag{18}$$

The fact that the exponent in the denominator in equation 17 is 0.7 and not 0.5 is important because it means that in the EDI or EWI methods, verticals are sampled in such a way that sequential observations in the resulting series are negatively correlated. The interaction of (1) the nonrandom sampling protocol for how verticals are added to an EDI or EWI measurement with (2) the nonrandom cross-stream structure in the time-averaged velocity-weighted suspended-sand concentration under steady, uniform flow conditions is likely responsible for the nonrandom sequence of values that determines the value of this exponent. As discussed previously, if the depth-integrated suspended-sand concentrations measured at different verticals were completely uncorrelated

Figure 14. Examples of unstable cross-stream spatial structures in depth-integrated suspended-silt-and-clay concentration along cross section B at the River-mile 30 sediment station (figs. 1, 2D). Error bars indicate mean number-of-transits error (MNOTE) at each vertical; see appendix A for data. Suspended-silt-and-clay data from other cross sections are plotted in appendix B. *A*, Suspended-silt-and-clay concentration at each of nine verticals sampled during two measurements on August 24, 2007; concentration at each vertical in each measurement normalized by mean concentration among all nine verticals in each measurement. Note that spatial cross-stream structure in suspended-silt-and-clay concentration is dissimilar between two measurements spaced ~1.5 hours apart and that variation in concentration between adjacent verticals is much larger than expected near-zero cross-stream variation based on P.R. Jordan’s analysis. *B*, Suspended-silt-and-clay concentration at each of nine verticals sampled during two measurements on August 25, 2007; concentration at each vertical in each measurement normalized by mean concentration among all nine verticals in each measurement. Note that spatial cross-stream structure in suspended-silt-and-clay concentration is dissimilar between two measurements spaced ~1.5 hours apart and that both spatial cross-stream structures appear to differ from those observed the previous day. Also note that variation in concentration between adjacent verticals is much larger than expected near-zero cross-stream variation based on P.R. Jordan’s analysis. *C*, Relations between normalized suspended-silt-and-clay concentrations at each vertical sampled in measurements 1 (C_1) and 2 (C_2) on August 24 and 25, 2007. Relations are not significant at $p=0.05$ level, indicating no significant temporal correlation in suspended-silt-and-clay concentration at each vertical over time scales of hours.

with the following value in the sequence, then the exponent in the denominator in equation 17 would be exactly 0.5 by the equation for the SE (equation 14). For situations where correlation exists between sequential observations, however, SE computed by using equation 14 is biased. By the central-limit theorem, the distribution of sample means about a population mean approaches a Gaussian normal distribution as the sample size increases, regardless of the shapes of these individual sample distributions, unless the individual sample distributions do not have finite means and variances (as reviewed by Davis, 1986). The SE defined in equation 14 is the standard deviation of the sample means in this normal distribution. In general, by using equation 14, positive correlations between sequential observations will lead to SEs that are too low, and negative correlations between sequential observations will lead to SEs that are too high (Dunlop, 1994; Quinn and Keough, 2003).

Analysis of simulated EDI and EWI measurements in a hypothetical trapezoidal river cross section, using the same approach as that used by P.R. Jordan (Guy and Norman, 1970; Edwards and Glysson, 1999), confirms that the exponent 0.7 in the denominator in equation 17 in fact arises from the combination of the nonrandom theoretical distribution of $\overline{uC_{sand}}$ in a steady, uniform flow used in P.R. Jordan's analysis, and from the nonrandom protocol stipulating how verticals are added to an EDI or EWI measurement. In a single-vertical EDI measurement, the single vertical would be located in the discharge centroid; and in a single-vertical EWI measurement, the single vertical would be located in the center of the cross section (fig. 4). Under assumed steady, uniform flow conditions, the positions of these single verticals would tend to be where the highest velocities and largest suspended-sand concentrations would occur in a river cross section. As verticals are added to either an EDI or EWI measurement, the previous locations of verticals are not fixed in space but are repositioned as the cross section is divided into more increments of equal discharge or width (fig. 4; Edwards and Glysson, 1999). Thus, in comparison with an EDI or EWI measurement with relatively few verticals, an EDI or EWI measurement with many verticals is likely to have more verticals in regions near the sides of P.R. Jordan's steady, uniform flow cross section, where velocities and suspended-sand concentrations are lower. This method of adding and repositioning verticals in a cross section leads to a relatively rapid decrease in the NOVE in the time-averaged velocity-weighted suspended-sand concentration as the number of verticals increases from one to about three, and then to a much more gradual decrease in the NOVE as the number of verticals exceeds about five. The details of how the NOVE in the time-averaged velocity-weighted suspended-sand concentration is reduced as verticals are added depend on whether the measurement is made using the EDI or EWI method. When fewer than about three verticals are sampled, the NOVE associated with an EWI measurement greatly exceeds that associated with an EDI measurement, whereas when more than about three verticals are sampled, the NOVE associated with an EWI measurement is generally equal to or less than that associated with an EDI measurement. Under steady, uniform flow conditions, the NOVE associated with

an EDI measurement should be positive, whereas the NOVE associated with an EWI measurement may be either positive or negative when fewer than ~ 10 verticals are sampled.

Further analysis of simulated EDI and EWI measurements in a hypothetical trapezoidal river cross section with cross-stream structures in suspended-sand concentration much different from those expected under steady, uniform flow over a full sand bed suggests that the exponent in the denominator of equation 17 may also differ from 0.7 where the flow is strongly nonuniform (that is, that the flow may be accelerating or decelerating, with potentially poor correlation between depth and velocity). The exponents derived from this exploratory analysis ranged from slightly greater than 0 in the cases where the cross-stream structure in the depth- and time-averaged suspended-sand concentration was far less peaked (but with a small positive amplitude) than that expected under steady, uniform flow conditions to almost 2 in the cases where the cross-stream structure in the depth- and time-averaged suspended-sand concentration was far more peaked than that expected under steady, uniform flow conditions. Thus, the interaction of the nonrandom sampling protocols in EDI and EWI measurements with different nonrandom spatial structures in the depth- and time-averaged suspended-sand concentration results in sequential observations that may be either positively or negatively correlated.

The cross-stream structure in the depth- and time-averaged suspended-sand concentration also affects the numerator in equation 17. When the cross-stream structure has a small, broad peak, this numerator can be substantially smaller than 12.0. Conversely, when the cross-stream structure has a large, narrow peak, this numerator can exceed 100, that is, be about an order of magnitude larger. Where the depth- and time-averaged suspended-sand concentration is either uniform across the cross section or varies linearly across the cross section, this numerator is 0.

Therefore, in a river cross section where the flow is strongly nonuniform, the magnitude of the NOVE in the time-averaged velocity-weighted suspended-sand concentration may differ greatly from that in equation 17, and the reduction in the NOVE as verticals are added may be more rapid or more gradual than that expected by equation 17. Because of these complexities, future studies are justified to improve understanding of the NOVE under a wider range of conditions than those studied by P.R. Jordan (Guy and Norman, 1970; Edwards and Glysson, 1999) using Hubbell and others' (1956) data from the Middle Loup River near Dunning, Nebraska. However, because the flow is generally uniform in the types of trapezoidal cross sections preferred as measurement sites by the USGS, the NOVE in the time-averaged velocity-weighted suspended-sand concentration described by equation 17 is probably reasonable for most field situations.

In simple, trapezoidal cross sections like those sampled in this study and preferred as the geometry of the measurement cross section at USGS gaging stations, the random error arising from inadequate time averaging, MNOTE, is comparable to the NOVE when only a single vertical is sampled. Among

the single-vertical two-way depth-integrated data collected at the River-mile 30 sediment station (figs. 1, 2D), and at the Lower Marble Canyon and Grand Canyon gaging stations (figs. 2B, 2C), the mean ± 1 SE MNOTE in velocity-weighted suspended-sand concentration is 8.7 ± 1.2 percent when a standard two-way (that is, two-transit) depth-integrated sample is collected at an individual vertical. Because the NOVE is expressed as a relative SE, direct comparison between the MNOTE and NOVE requires conversion of the MNOTE from a mean absolute error to a relative SE. As reviewed above, this conversion is done by dividing the MNOTE by $0.8\sqrt{n}$, where $n = n_{\text{vert}} = 1$ is the number of repeated, but separate, uncorrelated measurements at an individual vertical.¹⁰ This conversion yields a single-vertical MNOTE_{SE} (where the subscript “SE” denotes the standard-error form of the MNOTE) in the velocity-weighted suspended-sand concentration of 10.9 ± 1.5 percent when a standard two-transit depth-integrated sample is collected at an individual vertical. Among the two-way depth-integrated data collected at the River-mile 30 sediment station and at the Lower Marble Canyon and Grand Canyon gaging stations, the mean ± 1 SE MNOTE in the velocity-weighted suspended-silt and clay concentration is 4.9 ± 2.2 percent when a standard two-transit depth-integrated sample is collected at an individual vertical, equivalent to a single-vertical MNOTE_{SE} of 6.1 ± 2.8 percent. Among the two-way depth-integrated data collected at the River-mile 30 sediment station and at the Lower Marble Canyon and Grand Canyon gaging stations, the mean ± 1 SE D_{50} MNOTE in the velocity-weighted median grain size of the suspended sand is 1.4 ± 0.1 percent when a standard two-transit depth-integrated sample is collected at an individual vertical, equivalent to a single-vertical $D_{50}\text{MNOTE}_{\text{SE}}$ of 1.8 ± 0.1 percent. These MNOTE_{SE} and $D_{50}\text{MNOTE}_{\text{SE}}$ values are used in equation 15 to solve for the $\text{MNOTE}_{1,\text{SE}}$ and $D_{50}\text{MNOTE}_{1,\text{SE}}$.¹¹ Generalization of the single-vertical MNOTE_{SE} in the velocity-weighted suspended-sand concentration for different numbers of transits then yields

$$\text{MNOTE}_{\text{SE}} = \frac{15.4}{n_{\text{trans}}^{0.5}} \quad (19)$$

Likewise, generalization of the single-vertical MNOTE_{SE} in the velocity-weighted suspended-silt-and-clay concentration for different numbers of transits yields

$$\text{MNOTE}_{\text{SE}} = \frac{8.6}{n_{\text{trans}}^{0.5}} \quad (20)$$

and generalization of the single-vertical $D_{50}\text{MNOTE}_{\text{SE}}$ in the velocity-weighted median grain size of suspended sand for different numbers of transits yields

$$D_{50}\text{MNOTE}_{\text{SE}} = \frac{2.5}{n_{\text{trans}}^{0.5}} \quad (21)$$

¹⁰ A measurement at a vertical with two or eight transits is still only one single-vertical measurement; setting n equal to the number of transits at each vertical would be an overcorrection because the MNOTE already includes the effect of adding transits through its decrease by a factor of $1/n_{\text{trans}}^{0.5}$.

¹¹ These terms are the standard-error forms of the MNOTE_1 and $D_{50}\text{MNOTE}_1$.

An estimate of the total uncertainty associated with an EDI or EWI measurement (excluding laboratory-processing errors) requires (1) determining the behavior of the MNOTE_{SE} as verticals are added to a measurement and (2) combining the quasi-systematic NOVE and the random multivertical MNOTE_{SE} . Step 1 was accomplished by using random-number simulations of suspended-sediment concentration in a hypothetical river cross section conducted separately for sand and for silt and clay. For these two sediment size classes, random-number simulations were conducted as follows. First, the time-averaged depth-integrated suspended-sediment concentrations at 15 verticals were evaluated by using a random-number generator.¹² These values were used to construct 15 cases where the time-averaged velocity-weighted suspended-sediment concentration in hypothetical river cross sections could be accurately determined from the time-averaged depth-integrated suspended-sediment concentrations measured at a progressively increasing number of verticals (from 1 to 15). For example, in the first case, time-averaged depth-integrated suspended-sediment measurements at only a single vertical would accurately measure the time-averaged velocity-weighted suspended-sediment concentration in the cross section, whereas in the 15th case, time-averaged depth-integrated suspended-sediment concentrations averaged among all 15 verticals would be required to accurately measure the time-averaged velocity-weighted suspended-sediment concentration in the cross section. For each of these 15 cases, the time-averaged velocity-weighted suspended-sediment concentration in the cross section was calculated by averaging the time-averaged velocity-weighted suspended-sediment concentrations among the required number of verticals. These concentrations are the “true” values used in calculating the multivertical $\text{MNOTE}_{\text{SE}}\text{s}$ in the fourth step in this analysis (described below). Second, 2,500 random numbers were generated at each vertical to describe 2,500 probable suspended-sediment concentrations measured by a depth-integrating sampler at each vertical in an EDI or EWI measurement. These random numbers were generated by assuming a Gaussian normal distribution of depth-integrated concentrations at each vertical, with a mean value equal to the imposed time-averaged suspended-sediment concentration at that vertical and a standard deviation equal to the single-vertical MNOTE_{SE} associated with the appropriate number of transits at that vertical. This procedure was done for measurements with two, four, and eight transits at each vertical, using the appropriate MNOTE_{SE} . Third, for the 1- to 15-vertical cases with two, four, and eight transits at each vertical, 2,500 values of the velocity-weighted suspended-sediment concentration were calculated by averaging the random-number-generated suspended-sediment concentrations among the different verticals. Fourth, for each scenario consisting of a given number of verticals and transits, these 2,500 velocity-weighted suspended-sediment concentrations were used with the previously described true time-averaged

¹² Because the multivertical MNOTE_{SE} is a relative SE, the multivertical $\text{MNOTE}_{\text{SE}}\text{s}$ calculated from the random-number simulations do not depend on the values of the concentrations at these 15 verticals.

velocity-weighted suspended-sediment concentrations to calculate a relative mean absolute error in the time-averaged velocity-weighted suspended-sediment concentration in an EDI or EWI measurement consisting of 1 through 15 verticals, with two, four, and eight transits at each vertical. Each relative mean absolute error was then converted to a relative standard error by dividing by $0.8\sqrt{n}$, where $n=1$ for one EDI or EWI measurement. Results from these random-number simulations for 1- to 15-vertical EDI or EWI measurements with two, four, and eight transits at each vertical are listed in table 9.

Simplification of the results listed in table 9 can be obtained through use of an equation similar in form to equation 15, where the multivertical $MNOTE_{SE}$ is given by

$$MNOTE_{SE} = \frac{MNOTE_{1,SE} / n_{trans}^{0.5}}{n_{vert}^{\gamma}}, \quad (22)$$

where γ is now the exponent describing the behavior of the $MNOTE_{SE}$ as verticals are added. Use of the appropriate values of the $MNOTE_{1,SE}$ from the numerators in equations 19 and 20 and then solving for γ by log-transforming the data and using least-squares linear regression yields the following results. For the suspended-sand cases, $\gamma=0.475$ with two transits at each vertical, $\gamma=0.458$ with four transits at each vertical, and $\gamma=0.469$ with eight transits at each vertical. Similarly, for the suspended-silt-and-clay cases, $\gamma=0.464$ with two transits at each vertical, $\gamma=0.480$ with four transits at each vertical, and $\gamma=0.466$ with eight transits at each vertical. Thus, for all cases, $\gamma \approx 0.5$, indicating that the behavior of the $MNOTE_{SE}$ as verticals are added is identical to the behavior of an SE as uncorrelated observations are added. As in the case of additional transits at a vertical, additional verticals also behave as uncorrelated observations in their influence on the multivertical $MNOTE_{SE}$. The general form of the multivertical $MNOTE_{SE}$ to be used in estimating the total uncertainty in the EDI- or EWI-measured time-averaged velocity-weighted suspended-sediment concentration therefore becomes

$$MNOTE_{SE} = \frac{MNOTE_{1,SE}}{\sqrt{n_{trans} n_{vert}}}. \quad (23)$$

As reviewed by Taylor (1997), the most conservative, and safest, way to combine systematic and (or) random errors into an estimate of the total uncertainty in a measurement is to keep the individual errors separate. If the individual errors are strongly correlated, then this conservative approach is also likely the only valid approach. By this conservative approach, the EDI- or EWI-measured time-averaged velocity-weighted concentration of sediment in size class m , excluding laboratory-processing errors, would be reported as

$$c_m \pm NOVE \left(\frac{c_m}{100} \right) \pm MNOTE_{SE} \left(\frac{c_m}{100} \right). \quad (24)$$

The $c_m/100$ terms in equation 24 are required to convert the relative standard errors NOVE and $MNOTE_{SE}$ (expressed as percentages) into standard errors expressed in the same units as c_m . In this form, the EDI- or EWI-measured time-averaged

Table 9. Results from random-number simulations to determine the behavior of the standard-error form of the multivertical mean number-of-transits error ($MNOTE_{SE}$).

Sediment size class	Number of verticals required to accurately measure time-averaged velocity-weighted suspended-sediment concentration in cross section	Number of transits at each vertical	$MNOTE_{SE}$ (%)
sand	1	2	11.00*
sand	1	4	7.80*
sand	1	8	5.42*
sand	2	2	7.75
sand	2	4	5.48
sand	2	8	3.77
sand	3	2	6.36
sand	3	4	4.61
sand	3	8	3.06
sand	4	2	5.51
sand	4	4	3.98
sand	4	8	2.68
sand	5	2	4.95
sand	5	4	3.58
sand	5	8	2.47
sand	6	2	4.55
sand	6	4	3.29
sand	6	8	2.25
sand	7	2	4.24
sand	7	4	3.05
sand	7	8	2.17
sand	8	2	3.96
sand	8	4	2.85
sand	8	8	2.02
sand	9	2	3.83
sand	9	4	2.81
sand	9	8	1.90
sand	10	2	3.61
sand	10	4	2.65
sand	10	8	1.79
sand	11	2	3.45
sand	11	4	2.50
sand	11	8	1.71
sand	12	2	3.32
sand	12	4	2.39
sand	12	8	1.65
sand	13	2	3.17
sand	13	4	2.27
sand	13	8	1.57
sand	14	2	3.13
sand	14	4	2.40
sand	14	8	1.52
sand	15	2	3.02

Table 9. Results from random-number simulations to determine the behavior of the standard-error form of the multivertical mean number-of-transits error (MNOTE_{SE}).—Continued

Sediment size class	Number of verticals required to accurately measure time-averaged velocity-weighted suspended-sediment concentration in cross section	Number of transits at each vertical	MNOTE _{SE} (%)
sand	15	4	2.28
sand	15	8	1.48
silt and clay	1	2	6.03*
silt and clay	1	4	4.39*
silt and clay	1	8	2.96*
silt and clay	2	2	4.22
silt and clay	2	4	3.05
silt and clay	2	8	2.12
silt and clay	3	2	3.41
silt and clay	3	4	2.47
silt and clay	3	8	1.74
silt and clay	4	2	2.99
silt and clay	4	4	2.16
silt and clay	4	8	1.51
silt and clay	5	2	2.64
silt and clay	5	4	1.89
silt and clay	5	8	1.35
silt and clay	6	2	2.42
silt and clay	6	4	1.72
silt and clay	6	8	1.23
silt and clay	7	2	2.30
silt and clay	7	4	1.66
silt and clay	7	8	1.17
silt and clay	8	2	2.20
silt and clay	8	4	1.55
silt and clay	8	8	1.10
silt and clay	9	2	2.12
silt and clay	9	4	1.53
silt and clay	9	8	1.07
silt and clay	10	2	2.01
silt and clay	10	4	1.43
silt and clay	10	8	1.01
silt and clay	11	2	1.91
silt and clay	11	4	1.36
silt and clay	11	8	0.96
silt and clay	12	2	1.84
silt and clay	12	4	1.30
silt and clay	12	8	0.91
silt and clay	13	2	1.76
silt and clay	13	4	1.24
silt and clay	13	8	0.88
silt and clay	14	2	1.73
silt and clay	14	4	1.21

Table 9. Results from random-number simulations to determine the behavior of the standard-error form of the multivertical mean number-of-transits error (MNOTE_{SE}).—Continued

Sediment size class	Number of verticals required to accurately measure time-averaged velocity-weighted suspended-sediment concentration in cross section	Number of transits at each vertical	MNOTE _{SE} (%)
silt and clay	14	8	0.86
silt and clay	15	2	1.69
silt and clay	15	4	1.15
silt and clay	15	8	0.83

* These values are only slightly different from the values for the single-vertical MNOTE_{SE}s computed using equations 19 and 20 that are used as input to the random-number simulations, indicating that the number of random numbers generated to describe probable concentrations at each vertical in these simulations is sufficient.

velocity-weighted suspended-sand concentration in a simple trapezoidal channel, after making the appropriate substitutions, is expressed as

$$c_{\text{sand}} \pm \left(\frac{12.0}{n_{\text{vert}}^{0.7}} \right) \left(\frac{c_{\text{sand}}}{100} \right) \pm \left(\frac{15.4}{\sqrt{n_{\text{trans}} n_{\text{vert}}}} \right) \left(\frac{c_{\text{sand}}}{100} \right), \quad (25)$$

and the EDI or EWI-measured time-averaged velocity-weighted concentration of silt and clay in a simple trapezoidal channel, after making the appropriate substitutions, is expressed as

$$c_{\text{silt-clay}} \pm \left(\frac{0}{n_{\text{vert}}^{0.7}} \right) \left(\frac{c_{\text{silt-clay}}}{100} \right) \pm \left(\frac{8.6}{\sqrt{n_{\text{trans}} n_{\text{vert}}}} \right) \left(\frac{c_{\text{silt-clay}}}{100} \right). \quad (26)$$

Another, slightly more liberal approach is to actually sum the individual errors in quadrature, where the relative total uncertainty (TU), excluding laboratory-processing errors, is given by

$$\text{TU} = \sqrt{(\text{NOVE})^2 + (\text{MNOTE}_{\text{SE}})^2}. \quad (27)$$

This approach to combining systematic and random errors into a single TU is especially justified in situations where (1) the individual errors are not strongly correlated, (2) the sign associated with the systematic error cannot be known before a measurement, or (3) the systematic error is really random over much longer time scales than the random error, as in an EDI or EWI measurement (that is, the systematic error is really quasi-systematic). As shown in this study, stable spatial cross-stream structures in suspended-sand and suspended-silt-and-clay concentration can persist for hours and then change overnight into different stable spatial structures or disappear altogether. Therefore, an identical number and position of verticals used to sample a cross section may lead to a positive NOVE on the first day and a negative NOVE on the next day.

The approach to combining the NOVE and $MNOTE_{SE}$ into a single TU is mathematically advantageous and leads to the following form of reporting the EDI- or EWI-measured time-averaged velocity-weighted concentration of sediment in size class m :

$$c_m \pm TU \left(\frac{c_m}{100} \right) \text{ or } c_m \pm \sqrt{(\text{NOVE})^2 + (MNOTE_{SE})^2} \left(\frac{c_m}{100} \right). \quad (28)$$

In this form, the EDI- or EWI-measured time-averaged velocity-weighted suspended-sand concentration in a simple trapezoidal channel, after making the appropriate substitutions, is expressed as

$$c_{\text{sand}} \pm \sqrt{\left(\frac{12.0}{n_{\text{vert}}^{0.7}} \right)^2 + \left(\frac{15.4}{\sqrt{n_{\text{trans}} n_{\text{vert}}}} \right)^2} \left(\frac{c_{\text{sand}}}{100} \right), \quad (29)$$

and the EDI- or EWI-measured time-averaged velocity-weighted concentration of silt and clay in a simple trapezoidal channel, after making the appropriate substitutions, is expressed as

$$c_{\text{silt-clay}} \pm \sqrt{\left(\frac{0}{n_{\text{vert}}^{0.7}} \right)^2 + \left(\frac{8.6}{\sqrt{n_{\text{trans}} n_{\text{vert}}}} \right)^2} \left(\frac{c_{\text{silt-clay}}}{100} \right). \quad (30)$$

The relative total uncertainty (equation 27), NOVE, and $MNOTE_{SE}$ in suspended-sand concentration for EDI and EWI measurements composed of different numbers of verticals are plotted in figure 15, which indicates that (1) adding verticals is slightly more effective in reducing the TU than is only adding transits at each vertical, and (2) doubling the number of transits at each vertical from two to four is more effective in reducing the TU than is doubling the number of transits at each vertical from four to eight. For example, the TU with four transits at five verticals is approximately the same as that with two transits at seven verticals, whereas the TU with eight transits at five verticals is approximately the same as that with four transits at six verticals. In many field situations, transits may be easier to add than verticals. However, the amount of reduction in the TU decreases progressively less rapidly as the number of transits increases, thus making the addition of verticals more desirable than the addition of many more transits at each vertical. As shown in the data tables for noncomposited nine-vertical measurements in appendix A, it typically takes more time to move from one vertical to the next in a cross section and begin sampling at that new vertical than to simply add transits at a vertical. Thus, adding verticals has the negative effect of increasing the total time required to complete an EDI or EWI measurement at a higher rate than does increasing the number of transits at each vertical. Therefore, the best EDI or EWI sampling design to minimize the TU in time-averaged velocity-weighted suspended-sand concentration is to collect four transits at as many verticals as is practical.

To determine whether the TU formulated in equations 29 and 30 was consistent with field observations, and whether the TU was better at explaining field observations than the NOVE (the only formulation of EDI- or EWI-measurement error currently used by the USGS), we conducted a final

analysis using noncomposited EWI measurements configured into different sampling designs. As described previously, these sampling designs consisted of EWI measurements at one, three, five, and nine verticals (fig. 4). The data used to calculate the velocity-weighted suspended-sediment concentration under these different EWI sampling designs were the 30 noncomposited nine-vertical depth-integrated measurements made at the five cross sections at the River-mile 30 sediment station (figs. 1, 2D) and the Lower Marble Canyon gaging station (fig. 2C).¹³ The 30 noncomposited nine-vertical depth-integrated measurements were not used in any way to calculate $MNOTE_{SE}$ values, nor were these data used to place constraints on the NOVE. Therefore, this analysis is an independent evaluation of whether the behaviors of the TU and (or) NOVE are consistent with field observations.

Because the $MNOTE_{SE}$ and NOVE are derived as relative SEs, and the TU calculated by summing these two errors in quadrature is therefore also a relative SE, the confidence intervals associated with each of these three errors must behave in the same way as do those associated with any SE. Therefore, because of the normal distribution of sample means about the population mean by the central-limit theorem, the probability that the population mean falls within an interval defined by the SE (that is, the confidence interval), is

$$P = \text{erf} \left(\frac{n_{SE}}{\sqrt{2}} \right), \quad (31)$$

where P is the cumulative probability, or confidence interval, and n_{SE} is the number of SEs defining the width of this interval (after Zelen and Severo, 1964). In the general case, if we can measure the same quantity ψ (that is, the population mean) with m different sampling designs, if the formulation of the SE associated with these sampling designs is accurate, and if the number of times n (that is, sample size) all of these m different sampling designs are used to measure ψ is sufficiently large, then the empirically determined cumulative probability within this sufficiently large sample size n that the number of SEs at which all m sampling designs measure the same value of ψ must behave similarly to that in equation 31. In this specific case, 30 noncomposited nine-vertical EWI measurements were made that could be mathematically combined into four different sampling designs, with one, three, five, and nine verticals. These 30 noncomposited EWI measurements were analyzed by using these different sampling designs to evaluate whether the TU derived in this study and (or) NOVE behaved consistently with that expected by equation 31. For the purposes of this analysis, in each of the 30 cases the population mean, ψ , was set equal to the concentration among the four EWI sampling designs that agreed at the minimum SE; this concentration is referred to below as the "optimal concentration of agreement."

The analysis of the 30 noncomposited nine-vertical depth-integrated measurements was conducted as follows. For each of the 30 measurements, (1) the velocity-weighted

¹³ These 30 noncomposited nine-vertical measurements include the above analyzed 22 measurements made hours apart on the same day.

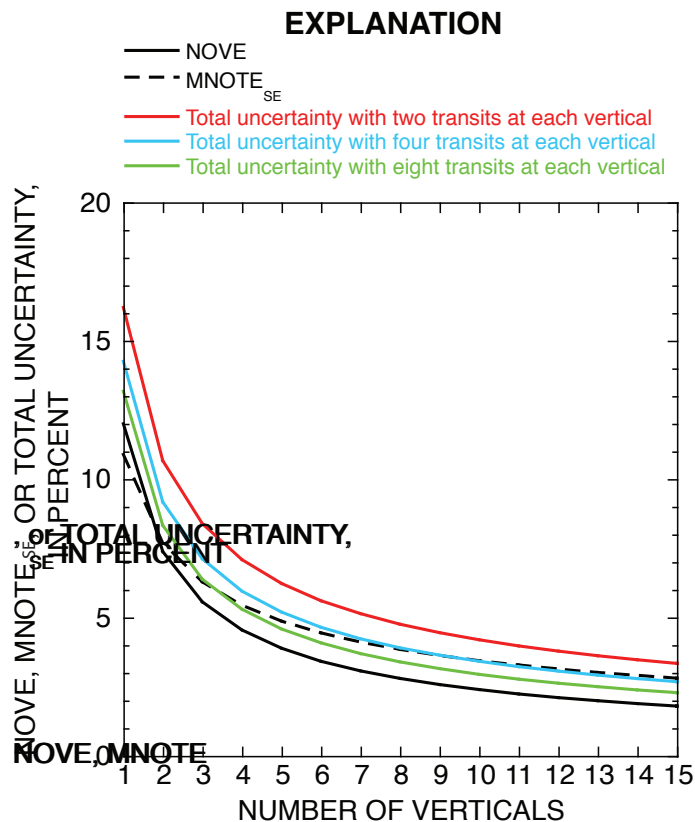


Figure 15. Comparison of number-of-verticals relative standard error (NOVE), mean number-of-transits relative standard error ($MNOTE_{SE}$), and relative total uncertainty in equal-discharge-increment (EDI)- or equal-width-increment (EWI)-measured suspended-sand concentration in a simple trapezoidal channel. Relative total uncertainties were calculated by using equation 27 for EDI or EWI measurements with two, four, and eight transits at each vertical; $MNOTE_{SE}$ was calculated only for an EDI or EWI measurement with two transits at each vertical.

concentration of suspended-sediment in two size classes (sand, and silt and clay) was calculated for EWI measurements composed of one, three, five, and nine verticals (figs. 4, 16A, 16B); (2) the TU in concentration for each of these four EWI sampling designs was calculated by using equation 27 (fig. 16A); (3) the NOVE in concentration for each of these four EWI sampling designs was calculated by using equation 17¹⁴ (fig. 16B); (4) the optimal concentration of agreement ψ (that is, the assumed population mean) among the four EWI sampling designs was defined to fall within the search domain bounded by the minimum and maximum concentrations (ψ_{min} and ψ_{max} , respectively) calculated among the four EWI sampling designs

¹⁴ Because P.R. Jordan assumed that suspended silt and clay was uniformly distributed in a cross section, the NOVE in suspended-silt-and-clay concentration is always zero (equation 18) and so this analysis could not be conducted for silt and clay.

(figs. 16A, 16B); (5) within this search domain, a ψ value was obtained that minimized the number of SEs,¹⁵ $n_{SE, best}$, at which the concentrations measured among all four EWI sampling designs agreed (fig. 16C); (6) the cumulative probability associated with $n_{SE, best}$ within the sample size of 30 measurements was calculated; and finally, (7) this empirical cumulative probability was compared with the theoretical cumulative probability expected by equation 31 for a given $n_{SE, best}$ (fig. 17). The most complicated part of this analysis was the determination of ψ in step 5, which was itself a four-step process: (1) the search domain bounded by ψ_{min} and ψ_{max} was divided into a continuum of extremely small increments, (2) for each of these small increments in concentration, the maximum n_{SE} (that is, $n_{SE, max}$) was determined at which the concentrations measured among all four EWI sampling designs agreed (figs. 16A, 16B), (3) $n_{SE, best}$ was then evaluated as the minimum $n_{SE, max}$ over the search domain (fig. 16C), and (4) the optimal concentration of agreement ψ was thus determined as the concentration associated with $n_{SE, best}$ (figs. 16A, 16B). By this approach, $n_{SE, best}$ was thus the minimum number of SEs at which the concentration measured among all four EWI sampling designs agreed.

Results from this analysis indicate that over the entire range of suspended-sand concentrations in this analysis, the TU (equation 27) provides a substantially better characterization of the error in an EWI measurement of the time-averaged velocity-weighted suspended-sand concentration in a cross section than does the NOVE (equation 17). As shown in figure 17A, the empirical cumulative probability associated with the TU behaves much more like the theoretical cumulative probability expected by equation 31 than does the empirical cumulative probability associated with the NOVE. Furthermore, analysis of variance using a standard F -test indicates that at the $p=0.05$ level of significance, for neither the TU nor the NOVE is there significant dependence of the $n_{SE, best}$ values on suspended-sand concentration (fig. 18A). Use of the TU instead of the NOVE results in a mean 28-percent reduction in $n_{SE, best}$ among the 30 measurements.

The results of this analysis indicate that at moderate to high suspended-silt-and-clay concentrations, the TU (equation 27) reasonably captures the behavior of the error in an EWI measurement of the time-averaged velocity-weighted suspended-silt-and-clay concentration in a cross section, whereas the behavior of the NOVE (equation 18) is inconsistent with the behavior of this error. As derived by P.R. Jordan, the NOVE in suspended-silt-and-clay concentration is zero because he assumed that suspended silt and clay is uniformly distributed in a cross section (Guy and Norman, 1970; Edwards and Glysson, 1999). However, suspended silt and clay was not uniformly distributed across any of the five cross sections at the River-mile 30 sediment station (figs. 1, 2D) and the Lower Marble Canyon gaging station (fig. 2C) when the mean suspended-silt-and-clay concentration in the cross section was less than about 50 mg/L (fig. 14; see

¹⁵ The number of intervals of TU calculated by equation 27 or NOVE calculated by equation 17.

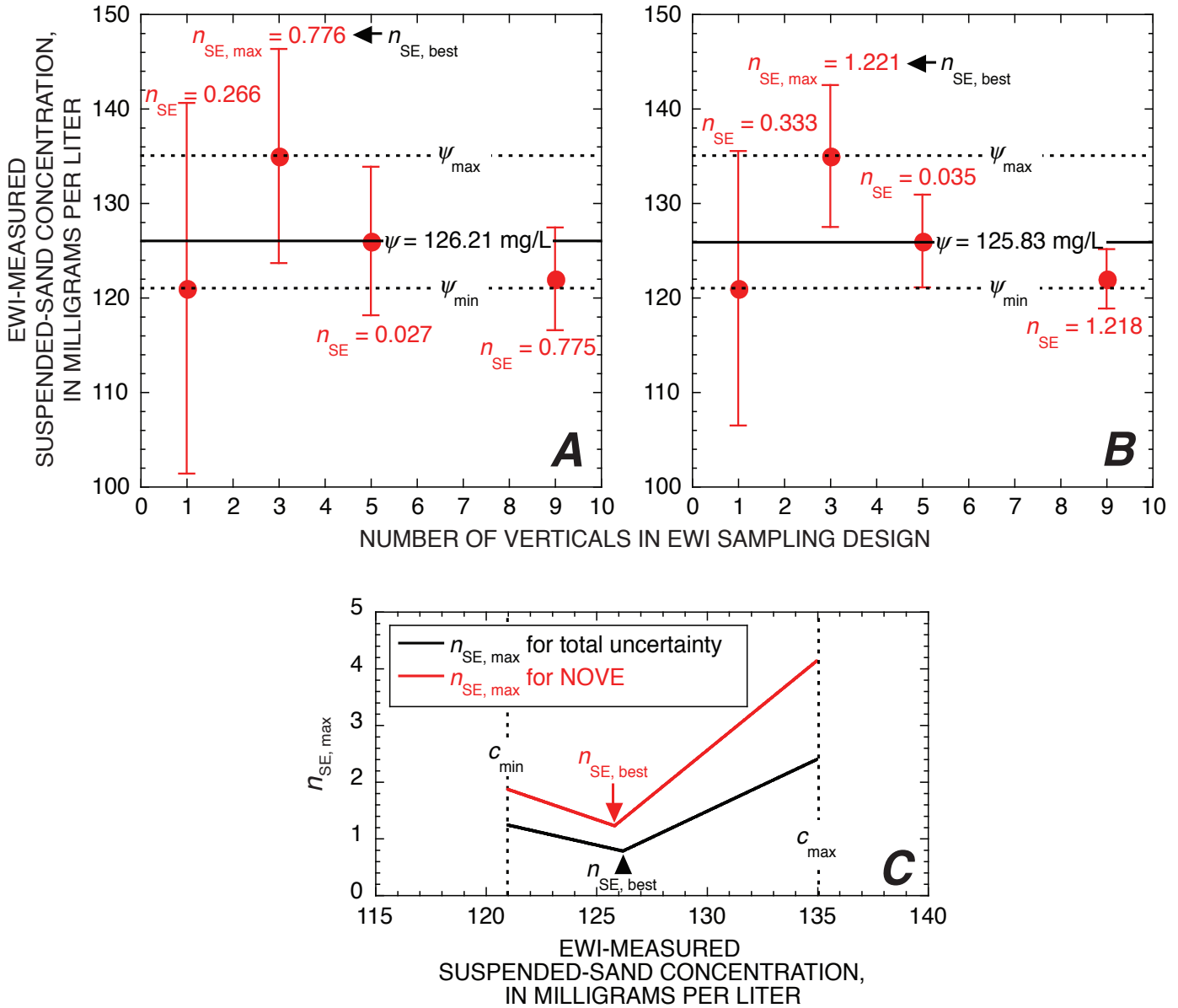


Figure 16. Examples of equal-width-increment (EWI)-measured suspended-sand concentrations, with error bars, for four different EWI sampling designs, showing key steps in analysis of behaviors of total uncertainty and number-of-verticals error (NOVE). Data points were calculated by using noncomposed nine-vertical measurement made along cross section B at the River-mile 30 sediment station between 8:03 and 8:37 a.m. on August 25, 2007. *A*, Error bars calculated for a total-uncertainty interval of $n_{SE}=1$, using equation 27. *B*, Error bars calculated for a NOVE interval of $n_{SE}=1$, using equation 17. In figures 16A and 16B, dashed horizontal lines indicate the bounds of the search domain for ψ defined by the minimum (ψ_{min}) and maximum (ψ_{max}) concentrations calculated among the four EWI sampling designs. Thick, solid horizontal lines indicate “optimal concentration of agreement” ψ value determined in this analysis. Values of n_{SE} in red indicate the required value of n_{SE} for each EWI sampling design to result in agreement in concentration among all four EWI sampling designs. Maximum of these n_{SE} values, $n_{SE,max}$ is value minimized over search domain between ψ_{min} and ψ_{max} to solve for ψ . *C*, Values of $n_{SE,max}$ among four EWI sampling designs over search domain between ψ_{min} and ψ_{max} . Minimum $n_{SE,max}$ values are $n_{SE,best}$ values (indicated in figures 16A and 16B) used to solve for ψ in figures 16A and 16B.

appendixes A, B). As shown in figure 17B, the agreement between the empirical cumulative probability associated with the TU in suspended-silt-and-clay concentration and the theoretical cumulative probability expected by equation 31 is poor in comparison with the good agreement between the empirical and theoretical cumulative probabilities in figure 17A for suspended-sand concentration. This relatively poor agreement is the result of the behavior of the TU at low suspended-silt-and-clay concentrations. In contrast to the results for the TU in suspended-sand concentration, analysis of variance using a standard F -test indicates that at the $p=0.05$ level of significance, the values of $n_{SE, best}$ depend significantly on suspended-silt-and-clay concentration (fig. 18B). Removal of the cases from the analysis with suspended-silt-and-clay concentrations <50 mg/L results in a much better agreement between the empirical and theoretical cumulative probabilities associated with the TU in suspended-silt-and-clay concentration (fig. 17A) and removes the significant dependence of the $n_{SE, best}$ values associated with the TU on suspended-silt-and-clay concentration (fig. 18B). Importantly, the $MNOTE_{SE}$ used to calculate the TU in suspended-silt-and-clay concentration was partly derived using data collected at the River-mile 30 sediment station when the suspended-silt-and-clay concentration was

<50 mg/L. Therefore, the relatively poor characterization of error by the TU (equation 30) at low suspended-silt-and-clay concentrations likely results from incorrect parameterization of the NOVE and not the $MNOTE_{SE}$ at low suspended-silt-and-clay concentrations. Again, because stable cross-stream structures in suspended-silt-and-clay concentration have been observed to persist between measurements spaced hours apart, laboratory-processing errors cannot be used to entirely explain this behavior. These observations together suggest that at least at lower suspended-silt-and-clay concentrations, the NOVE should likely be a small positive number, not zero as assumed by P.R. Jordan.

In summary, results from this final analysis of error behavior indicate that (1) the TU is a much better estimator than is the NOVE of the error in an EWI measurement of the time-averaged velocity-weighted suspended-sand concentration in a cross section, (2) because P.R. Jordan's parameterization of the NOVE is incapable of describing error in suspended-silt-and-clay concentration, the TU is also a much better estimator than is the NOVE of the error in an EWI measurement of the time-averaged velocity-weighted suspended-silt-and-clay in a cross section, and (3) at lower suspended-silt-and-clay concentrations (that is, less than about 50 mg/L), the NOVE of zero derived by P.R. Jordan may

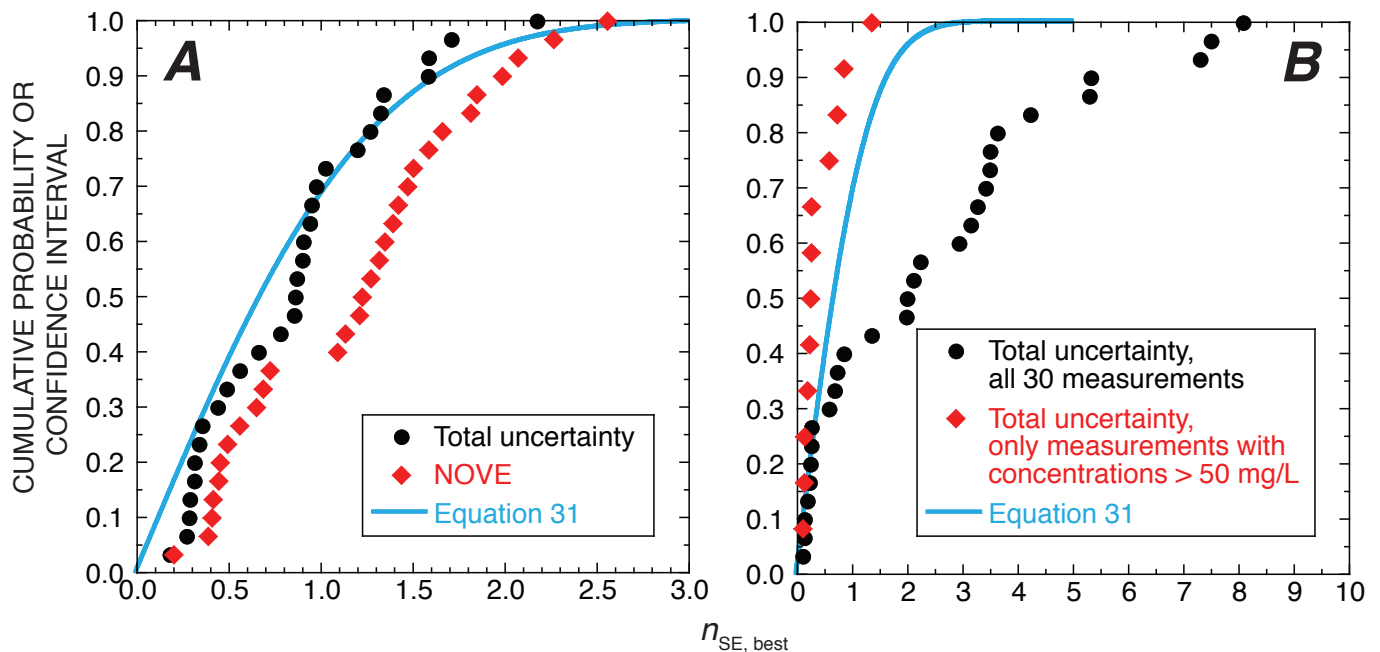


Figure 17. Comparison of empirical and theoretical relations between $n_{SE, best}$ and cumulative probability, or confidence interval, for total uncertainty (TU) and number-of-verticals error (NOVE). A, Cumulative probability plotted as a function of $n_{SE, best}$ for TU and NOVE in time-averaged velocity-weighted suspended-sand concentration in a cross section compared with the theoretical relation between n_{SE} and cumulative probability (equation 31). B, Cumulative probability plotted as a function of $n_{SE, best}$ for TU in time-averaged velocity-weighted suspended-silt-and-clay concentration in a cross section compared with the theoretical relation between n_{SE} and cumulative probability (equation 31). Shown are the empirical relations calculated for all 30 noncomposed nine-vertical measurements and for only those measurements with an "optimal concentration of agreement" >50 mg/L.

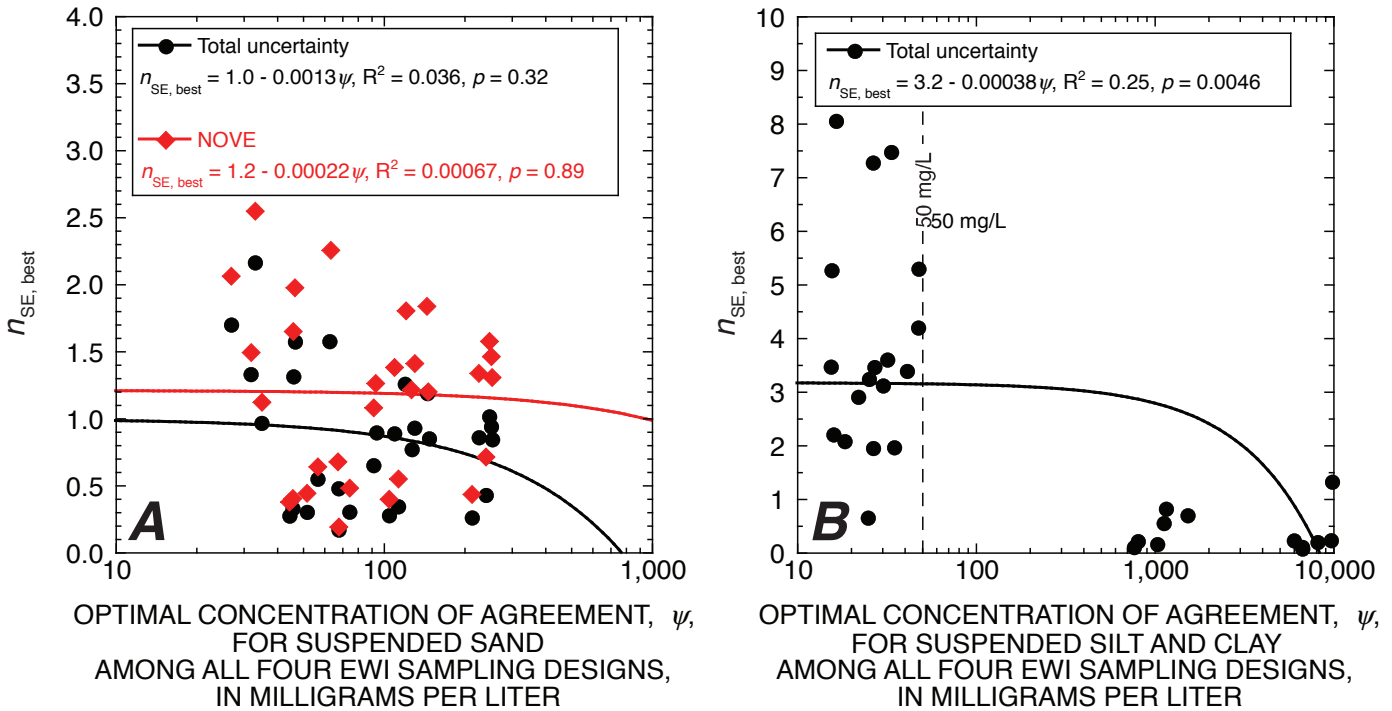


Figure 18. Evaluation of the dependence of $n_{SE, best}$ associated with total uncertainty (TU) and number-of-verticals error (NOVE) on the “optimal concentration of agreement” (ψ). Values of $n_{SE, best}$ plotted as a function of ψ for suspended sand (A) and suspended silt and clay (B) in the 30 noncomposited nine-vertical depth-integrated measurements. A, Values of $n_{SE, best}$ associated with TU and NOVE, with best-fit linear regressions, plotted as a function of ψ for suspended sand. Both regressions are insignificant at the $p=0.05$ level, indicating no significant dependence of $n_{SE, best}$ on suspended-sand concentration for either the TU or NOVE. B, Values of $n_{SE, best}$ associated with TU, with best-fit linear regression, plotted as a function of ψ for suspended silt and clay. Removal of cases with suspended-silt-and-clay concentrations < 50 mg/L (indicated by vertical dashed line) results in an increase in the level of significance of this regression from $p=0.0046$ to $p=0.77$.

be incorrect. Although this analysis was conducted for EWI measurements, there is no physical reason why the results from this analysis should not also apply to EDI measurements.

Conclusions

When depth-integrating samplers are properly used in the field, the two most common sources of error are (1) inadequate sampling of the cross-stream spatial structure in suspended-sediment concentration and (2) the inability of these samplers to collect adequate time-averaged data during standard operation, when only two transits are collected at each vertical in a cross section. Both of these errors must be included in an estimate of the TU in an EDI or EWI measurement. Though outside the scope of this study, laboratory-processing errors must also be included in a completely comprehensive estimate of the TU in an EDI or EWI measurement. The error arising from inadequate time averaging (1) is positively correlated with grain size, (2) does not depend on elevation above the

bed for any given size class of sediment, and (3) does not largely depend on flow conditions. An average of 1 minute is the likely minimum duration of time averaging required to result in substantial decreases in this error. As the number of transits is doubled at an individual vertical, this error is reduced by ~30 percent in each size class of sediment. For a given size class of sediment, the error arising from inadequate sampling of the cross-stream spatial structure in suspended-sediment concentration depends only on the number of verticals collected, whereas the error arising from inadequate time averaging depends on both the number of verticals collected and the number of transits collected at each vertical.

Exclusive of laboratory-processing errors (which are typically small), the TU in suspended-sand and suspended-silt-and-clay concentrations is dominated by the random error arising from inadequate time averaging. When two transits are collected at five verticals in a simple trapezoidal channel, the TU in the EDI- or EWI-measured suspended-sand concentration calculated by using both the errors arising from (1) inadequate sampling of the cross-stream spatial structure

in suspended-sand concentration and from (2) inadequate time averaging at each vertical is ~6.3 percent (expressed as a relative SE). For comparison, the error arising only from inadequate sampling of the cross-stream spatial structure in suspended-sand concentration for this case is ~3.9 percent, and the error arising only from inadequate time averaging at each vertical in this case is ~4.9 percent. When two transits are collected at five verticals in a simple trapezoidal channel, the TU in the EDI- or EWI-measured suspended-silt-and-clay concentration results almost entirely from inadequate time averaging at each vertical and is ~2.7 percent (at least at suspended-silt-and-clay concentrations in excess of about 50 mg/L). Therefore, the error arising from inadequate time averaging will likely be the dominant error introduced during the calibration of other approaches to measuring suspended-sediment concentration (for example, automatic pump samplers, optical backscatter, laser diffraction, or acoustic attenuation and backscatter) if too few EDI or EWI measurements are used in these calibrations.

Although adding verticals to an EDI or EWI measurement is slightly more effective in reducing the TU than is only adding transits at each vertical (because additional verticals reduce both spatial and temporal errors), adding a combination of verticals and transits is likely a more practical approach to reducing the TU in real field situations. In many field situations, it may be easier to add transits than to add verticals because it typically takes much less time to collect depth-integrated samples at additional transits at a vertical than to collect depth-integrated samples at additional verticals in a cross section. However, because the reduction in the TU decreases progressively less rapidly as the number of transits increases, it does not usually make sense to collect more than four transits at each vertical. Therefore, the best EDI or EWI sampling design to minimize the TU in the time-averaged velocity-weighted suspended-sediment concentration is to double the number of transits collected during standard two-way depth integration and to collect four transits at as many verticals as is practical for a given field situation.

References Cited

- Allen, P.B., and Petersen, D.V., 1981, A study of the variability of suspended sediment measurements, *in* Erosion and sediment transport measurement; Proceedings of the Florence Symposium, June 1981: International Association of Hydrological Sciences publication 133, p. 203–211.
- Best, J., 2005, The fluid mechanics of river dunes; a review and some future research directions: *Journal of Geophysical Research*, v. 110, F04S02, 21 p., doi:10.1029/2004JF000218 [http://www.agu.org/journals/jf/jf0504/2004JF000218/2004JF000218.pdf].
- Bevington, P., and Robinson, D.K., 2003, *Data reduction and error analysis for the physical sciences* (3d ed.): New York, McGraw-Hill, 320 p.
- Colby, B.R., 1963, *Fluvial sediments—a summary of source, transportation, deposition, and measurement of sediment discharge*: U.S. Geological Survey Bulletin 1181-A, 47 p. [http://pubs.er.usgs.gov/usgspubs/b/b1181A].
- Colby, B.R., 1964, *Discharge of sands and mean-velocity relationships in sand-bed streams*: U.S. Geological Survey Professional Paper 462-A, 47 p. [http://pubs.er.usgs.gov/usgspubs/pp/pp462A].
- Davis, J.C., 1986, *Statistics and data analysis in geology* (2d ed.): New York, John Wiley and Sons, 646 p.
- Dietrich, W.E., 1982, Settling velocity of natural particles: *Water Resources Research*, v. 18, p. 1615–1626 [http://www.agu.org/journals/wr/v018/i006/WR018i006p01615/WR018i006p01615.pdf].
- Dinehart, R.L., 1998, *Sediment transport at gaging stations near Mount St. Helens, Washington, 1980–90; data collection and analysis*: U.S. Geological Survey Professional Paper 1573, 105 p. [http://pubs.er.usgs.gov/usgspubs/pp/pp1573].
- Dunlop, D.D., 1994, Regression for longitudinal data; a bridge from least squares regression: *American Statistician*, v. 48, p. 299–303.
- Edwards, T.K., and Glysson, G.D., 1999, *Field methods for measurement of fluvial sediment: Techniques of Water-Resources Investigations of the U.S. Geological Survey*, book 3, chap. C2, 89 p. [http://pubs.usgs.gov/twri/twri3-c2/].
- Federal Interagency Sedimentation Project, 1941, Report 5, *Laboratory investigation of suspended sediment samplers; a study of methods used in measurement and analysis of sediment loads in streams*: Iowa City, University of Iowa, St. Paul U.S. Engineer District Sub-Office Hydraulic Laboratory, 99 p. [http://water.usgs.gov/fisp/docs/Report_5.pdf].
- Federal Interagency Sedimentation Project, 1952, Report 6, *The design of improved types of suspended sediment samplers; a study of methods used in measurement and analysis of sediment loads in streams*: Minneapolis, Minn., St. Anthony Falls Hydraulic Laboratory, 103 p. [http://water.usgs.gov/fisp/docs/Report_6.pdf].
- Federal Interagency Sedimentation Project, 1957, Report 11, *The development and calibration of the visual-accumulation tube; a study of methods used in measurement and analysis of sediment loads in streams*: Minneapolis, Minn., St. Anthony Falls Hydraulic Laboratory, 109 p. [http://water.usgs.gov/fisp/docs/Report_11.pdf].

- Federal Interagency Sedimentation Project, 1958, Report K, Operator's manual on the visual-accumulation tube method for sedimentation analysis of sands; a study of methods used in measurement and analysis of sediment loads in streams: Minneapolis, Minn. St. Anthony Falls Hydraulic Laboratory, 29 p. [http://water.usgs.gov/fisp/docs/Report_K.pdf].
- Federal Interagency Sedimentation Project, 2003, Report PP, The US D-96; an isokinetic suspended-sediment/water quality collapsible bag sampler, addendum II—The US D-96-A1; a lightweight version of the US-96: Vicksburg, Miss., 4 p. [http://water.usgs.gov/fisp/docs/Report_PP-Addendum_II,_US_D-96_030507_.pdf].
- Gordon, J.D., Newland, C.A., and Gray, J.R., 2001, Sediment laboratory quality-assurance project; studies of methods and materials: Federal Interagency Sedimentation Conference, 7th, Reno, Nev., 2001, Proceedings, v. 2, p. VI-41 to VI-48 [http://pubs.usgs.gov/misc/FISC_1947-2006/].
- Guy, H.P., 1969, Laboratory theory and methods for sediment analysis; U.S. Geological Survey Techniques of Water-Resources Investigations, book 5, chapter C1, 58 p. [<http://pubs.usgs.gov/twri/twri5c1/>].
- Guy, H.P., 1970, Fluvial sediment concepts: U.S. Geological Survey Techniques of Water-Resources Investigations, book 3, chapter C1, 55 p. [<http://pubs.usgs.gov/twri/twri3-c1/>].
- Guy, H.P., and Norman, V.W., 1970, Field methods for measurement of fluvial sediment: U.S. Geological Survey Techniques of Water-Resources Investigations, book 3, chapter C2, 59 p. [Superseded by Edwards and Glysson, 1999.].
- Heidel, S.G., 1956, The progressive lag of sediment concentration with flood waves: Transactions, American Geophysical Union, v. 37, no. 1, p. 56–66.
- Hubbell, D.W., and others, 1956, Progress report number 1, Investigations of some sedimentation characteristics of a sand-bed stream: U.S. Geological Survey Open-File Report, 78 p.
- Knott, J.M., Sholar, C.J., and Matthes, W.J., 1992, Quality assurance guidelines for the analysis of sediment concentration by U.S. Geological Survey sediment laboratories: U.S. Geological Survey Open-File Report 92-33, 22 p. [<http://pubs.er.usgs.gov/publication/ofr9233>].
- Knott, J.M., Glysson, G.D., Malo, B.A., and Shroder, L.J., 1993, Quality assurance plan for the collection and processing of sediment data by the U.S. Geological Survey, Water Resources Division: U.S. Geological Survey Open-File Report 92-499, 18 p. [<http://pubs.er.usgs.gov/usgspubs/ofr/ofr92499>].
- Long, C.E., Wiberg, P.L., and Nowell, A.R.M., 1993, Evaluation of von Karman's constant from integral flow parameters: Journal of Hydraulic Engineering, v. 119, p. 1182–1190 [[http://dx.doi.org/10.1061/\(ASCE\)0733-9429\(1993\)119:10\(1182\)](http://dx.doi.org/10.1061/(ASCE)0733-9429(1993)119:10(1182))].
- McLean, S.R., 1992, On the calculation of suspended load for noncohesive sediments: Journal of Geophysical Research, v. 97, p. 5759–5770 [<http://www.agu.org/journals/jc/v097/iC04/91JC02933/91JC02933.pdf>].
- Melis, T.S., Topping, D.J., and Rubin, D.M., 2003, Testing laser-based sensors for continuous *in situ* monitoring of suspended sediment in the Colorado River, Arizona, in Bogen, J., Fergus, T., and Walling, D.E., eds., Erosion and sediment transport measurement in rivers; technological and methodological advances: Wallingford, U.K., IAHS Press, International Association of Hydrological Sciences Publication 283, p. 21–27 [http://www.gemrc.gov/library/reports/physical/Fine_Sed/Melis2003.pdf].
- Nolan, K.M., Gray, J.R., and Glysson, G.D., 2005, Introduction to suspended-sediment sampling: U.S. Geological Survey Scientific Investigations Report 2005-5077, CD-ROM [<http://pubs.usgs.gov/sir/2005/5077/>].
- Porterfield, G., 1972, Computation of fluvial sediment discharge: U.S. Geological Survey Techniques of Water-Resources Investigations, book 3, chapter C3, 66 p. [<http://pubs.usgs.gov/twri/twri3-c3/>].
- Press, W.H., Flannery, B.P., Teukolsky, S.A., and Vetterling, W.T., 1992, Evaluation of functions by path integration, chap. 5.14, in Numerical recipes in FORTRAN; the art of scientific computing (2d ed.): Cambridge, U.K., Cambridge University Press, p. 201–204.
- Quinn, G.P., and Keough, M.J., 2003, Experimental design and data analysis for biologists: New York, Cambridge University Press, 537 p.
- Rantz, S.E., and others, 1982, Measurement and computation of streamflow—volume 1, Measurement of stage and discharge: U.S. Geological Survey Water-Supply Paper 2175, 284 p. [<http://pubs.usgs.gov/wsp/wsp2175/>].
- Rattray, M., Jr., and Mitsuda, E., 1974, Theoretical analysis of conditions in a salt wedge: Estuarine Coastal Marine Science, v. 2, p. 373–394.
- Rubin, D.M., and Topping, D.J., 2001, Quantifying the relative importance of flow regulation and grain size regulation of suspended-sediment transport α and tracking changes in bed-sediment grain size β : Water Resources Research, v. 37, p. 133–146 [<http://www.agu.org/journals/wr/v037/i001/2000WR900250/2000WR900250.pdf>].

- Rubin, D.M., and Topping, D.J., 2008, Correction to “Quantifying the relative importance of flow regulation and grain size regulation of suspended sediment transport α and tracking changes in grain size of bed sediment β ”: *Water Resources Research*, v. 44, p. W09701, doi:10.1029/2008WR006819 [http://www.agu.org/journals/wr/wr0809/2008WR006819/2008WR006819.pdf].
- Rubin, D.M., Tate, G.M., Topping, D.J., and Anima, R.A., 2001, Use of rotating side-scan sonar to measure bedload: Federal Interagency Sedimentation Conference, 7th, Reno, Nev., 2001, Proceedings, v. 1, p. III-139 to III-143 [http://pubs.usgs.gov/misc/FISC_1947-2006/pdf/1st-7thFISCs-CD/7thFISC/7Fisc-V1/7FISC1-3.pdf].
- Rubin, D.M., Tate, G.M., and Anima, R.A., 2006, Special features, app. 2 of *Sonar movies, Colorado River, Little Colorado, part C of: Rubin, D.M., and Carter, C.L., eds., 2006, Bedforms and cross-bedding in animation: Tulsa, Okla., SEPM (Society for Sedimentary Geology), Atlas Series 2, DVD.*
- Sabol, T.A., Topping, D.J., and Griffiths, R.E., 2010, Field evaluation of sediment-concentration errors arising from non-isokinetic intake efficiency in depth-integrating suspended-sediment bag samplers: Joint Federal Interagency Conference on Sedimentation and Hydrologic Modeling, Las Vegas, Nev., 2010, Proceedings.
- Schmeeckle, M.W., Shimizu, Y., Hoshi, K., Baba, H., and Ikezaki, S. 1999, Turbulent structures and suspended sediment over two-dimensional dunes, *in River, Coastal and Estuarine Morphodynamics: New York, Springer-Verlag, International Association for Hydraulic Research Symposium, Genova, Italy, 1999, Proceedings*, p. 261–270.
- Schoellhamer, D.H., 2001, Continuous monitoring of suspended sediment in rivers by use of optical sensors: Federal Interagency Sedimentation Conference, 7th, Reno, NV, 2001, Proceedings, v. 1, p. III-160 through III-167. [http://pubs.usgs.gov/misc/FISC_1947-2006/pdf/1st-7thFISCs-CD/7thFISC/7Fisc-V1/7FISC1-3.pdf].
- Smith, W.O., Vetter, C.P., Cummings, G.B., and others, 1960, Comprehensive survey of sedimentation in Lake Mead, 1948–49: U.S. Geological Survey Professional Paper 295, 254 p. [http://pubs.er.usgs.gov/usgpsubs/pp/pp295].
- Szalona, J.J., 1982, Report Y, Development of a bag-type suspended-sediment sampler; a study of methods used in measurement and analysis of sediment loads in streams: Minneapolis, Minn., Federal Interagency Sedimentation Project, St. Anthony Falls Hydraulic Laboratory, 32 p. [http://water.usgs.gov/fisp/docs/Report_Y.pdf].
- Taylor, J.R., 1997, An introduction to error analysis; the study of uncertainties in physical measurements (2nd ed.): Sausalito, Calif., University Science Books, 327 p.
- Tennekes, H., and Lumley, J.L., 1972, *A first course in turbulence: Cambridge, Mass., MIT Press*, 300 p.
- Topping, D.J., 1997, *Physics of flow, sediment transport, hydraulic geometry, and channel geomorphic adjustment during flash floods in an ephemeral river, the Paria River, Utah and Arizona: Seattle, University of Washington, Ph.D. dissertation*, 405 p.
- Topping, D.J., Rubin, D.M., Nelson, J.M., Kinzel, P.J., III, and Corson, I.C., 2000a, Colorado River sediment transport 2. Systematic bed-elevation and grain-size effects of sand supply limitation: *Water Resources Research*, v. 36, p. 543–570 [http://www.agu.org/journals/wr/v036/i002/1999WR900286/1999WR900286.pdf].
- Topping, D.J., Rubin, D.M., and Vierra, L.E., Jr., 2000b, Colorado River sediment transport 1. Natural sediment supply limitation and the influence of Glen Canyon Dam: *Water Resources Research*, v. 36, p. 515–542 [http://www.agu.org/journals/wr/v036/i002/1999WR900285/1999WR900285.pdf].
- Topping, D.J., Melis, T.S., Rubin, D.M., and Wright, S.A., 2004, High-resolution monitoring of suspended-sediment concentration and grain size in the Colorado River in Grand Canyon using a laser-acoustic system, *in Hu, C., and Tan, Y., eds., International Symposium on River Sedimentation, 9th, Yichang, People’s Republic of China, 2004, Proceedings*, p. 2507–2514 [http://www.gcmrc.gov/library/reports/Physical/Fine_Sed/Topping2004.pdf].
- Topping, D.J., Wright, S.A., Melis, T.S., and Rubin, D.M., 2006, High-resolution monitoring of suspended-sediment concentration and grain size in the Colorado River using laser-diffraction instruments and a three-frequency acoustic system: CD-ROM Proceedings of the 8th Federal Interagency Sedimentation Conference, Reno, Nevada, April 2–6, 2006, ISBN 0-9779007-1-1 [http://pubs.usgs.gov/misc/FISC_1947-2006/pdf/1st-7thFISCs-CD/8thFISC/Session%206C-3_Topping.pdf].
- Topping, D.J., Wright, S.A., Melis, T.S., and Rubin, D.M., 2007a, High-resolution measurements of suspended-sediment concentration and grain size in the Colorado River in Grand Canyon using a multi-frequency acoustic system: Tenth International Symposium on River Sedimentation, Moscow, Russia, August 1–4, 2007, Proceedings, p. 330–339, ISBN 978-5-89575-124-4, 978-5-89575-127-5 [http://www.gcmrc.gov/library/reports/physical/Fine_Sed/Topping2007b.pdf].
- Topping, D.J., Rubin, D.M., and Melis, T.S., 2007b, Coupled changes in sand grain size and sand transport driven by changes in the upstream supply of sand in the Colorado River: relative importance of changes in bed-sand grain size and bed-sand area: *Sedimentary Geology*, v. 202, p. 538–561, doi: 10.1016/j.sedgeo.2007.03.016 [http://www.sciencedirect.com/science/article/pii/S0037073807001492].

Wall, G.R., Nystrom, E.A., and Litten, S., 2006, Use of an ADCP to compute suspended-sediment discharge in the tidal Hudson River, New York: U.S. Geological Survey Scientific Investigations Report 2006-5055, 26 p. [<http://pubs.usgs.gov/sir/2006/5055/>].

Webster, M.D., Anderson, S.W., Rockwell, G.L., Smithson, J.R., and Friebel, M.F., 2000, Water resources data, California, water year 1999: U.S. Geological Survey Water-Data Report CA-99-4, v. 4. <http://ca.water.usgs.gov/data/water-data/99/volume4.pdf>].

Weisstein, E.W., 2004, Path integral: MathWorld—a Wolfram Web resource [<http://mathworld.wolfram.com/PathIntegral.html>].

Zelen, M., and Severo, N.C., 1964, Probability functions, chap. 26 of Abramowitz, M., and Stegun, I.A., eds., Handbook of mathematical functions with formulas, graphs, and mathematical tables: National Bureau of Standards Applied Mathematics Series, n. 55, p. 925–964.

Appendix A. Suspended-Sediment Data

P-61 suspended-sediment samples collected at the Cisco gaging station on May 12, 1995; vertical located at the station 340 ft from the left-bank bridge abutment																											
Time (MST)	Sample type	Water depth (m)	Sample elevation above bed (m)	Sample collection time (s)	Point intake velocity (m/s)	Silt and clay conc. (mg/L)	Sand conc. (mg/L)	Grain-size analysis of sand (0.0625-2.0 mm) fraction																			
								% sand < 0.074 mm	% sand < 0.088 mm	% sand < 0.105 mm	% sand < 0.125 mm	% sand < 0.149 mm	% sand < 0.177 mm	% sand < 0.210 mm	% sand < 0.250 mm	% sand < 0.297 mm	% sand < 0.354 mm	% sand < 0.420 mm	% sand < 0.500 mm	% sand < 0.595 mm	% sand < 0.707 mm	% sand < 0.841 mm	% sand < 1.00 mm	% sand < 1.19 mm	% sand < 1.41 mm	% sand < 1.68 mm	% sand < 2.00 mm
12:39	Point	5.03	0.11	20.00	0.531	502	1,730	0.8	1.4	2.2	2.9	5.8	9.9	15.8	28.0	45.6	72.0	94.5	98.2	100.0	100.0	100.0	100.0	100.0	100.0	100.0	100.0
12:42	Point	5.03	0.11	20.00	0.388	541	2,450	0.3	1.2	2.2	4.5	6.5	10.3	15.3	22.7	40.1	74.6	95.1	100.0	100.0	100.0	100.0	100.0	100.0	100.0	100.0	100.0
12:45	Point	5.03	0.11	20.00	0.373	470	2,130	1.0	2.5	4.1	6.7	9.3	12.9	18.1	25.6	44.3	77.2	94.8	99.3	100.0	100.0	100.0	100.0	100.0	100.0	100.0	100.0
12:48	Point	5.03	0.11	20.00	0.324	457	2,900	0.2	1.8	2.3	4.5	7.3	10.8	16.5	26.9	44.1	75.1	95.6	99.2	100.0	100.0	100.0	100.0	100.0	100.0	100.0	100.0
12:52	Point	5.03	0.11	20.00	0.440	474	1,980	1.3	1.9	3.8	5.1	7.7	11.5	18.8	27.0	43.0	71.2	93.7	98.3	100.0	100.0	100.0	100.0	100.0	100.0	100.0	100.0
12:54	Point	5.03	0.26	20.00	0.531	504	1,740	0.2	1.9	3.3	4.8	7.4	11.4	18.8	30.0	54.1	82.9	95.8	100.0	100.0	100.0	100.0	100.0	100.0	100.0	100.0	100.0
12:57	Point	5.03	0.26	20.00	0.414	451	1,320	2.1	4.6	8.1	10.3	15.4	20.9	29.1	41.0	56.9	80.9	92.8	99.8	100.0	100.0	100.0	100.0	100.0	100.0	100.0	100.0
13:01	Point	5.03	0.26	20.00	0.541	454	1,860	1.9	3.6	4.3	6.7	9.9	13.9	20.9	32.2	47.3	78.6	97.4	98.8	99.9	100.0	100.0	100.0	100.0	100.0	100.0	100.0
13:04	Point	5.03	0.26	20.00	0.592	445	1,730	1.5	1.9	3.7	6.2	8.6	11.8	19.9	35.3	53.4	75.9	96.2	99.7	100.0	100.0	100.0	100.0	100.0	100.0	100.0	100.0
13:07	Point	5.03	0.26	20.00	0.683	457	1,590	0.8	3.0	4.2	6.6	9.1	13.6	20.7	32.6	48.1	79.4	95.8	99.9	100.0	100.0	100.0	100.0	100.0	100.0	100.0	100.0
13:09	Point	5.03	0.57	20.00	1.008	472	464	2.8	6.8	12.0	18.1	22.7	29.1	45.9	58.2	79.1	88.7	97.7	100.0	100.0	100.0	100.0	100.0	100.0	100.0	100.0	100.0
13:12	Point	5.03	0.57	20.00	1.098	452	506	3.2	6.3	10.7	16.7	21.7	27.2	36.5	48.1	67.0	84.4	93.7	98.3	99.9	100.0	100.0	100.0	100.0	100.0	100.0	100.0
13:15	Point	5.03	0.57	20.00	1.117	442	643	2.6	5.2	7.9	9.9	12.9	23.0	32.7	48.2	68.6	86.8	97.4	100.0	100.0	100.0	100.0	100.0	100.0	100.0	100.0	100.0
13:18	Point	5.03	0.57	20.00	0.913	458	564	2.0	6.5	9.7	15.4	20.3	26.2	40.6	54.6	77.0	89.3	96.5	100.0	100.0	100.0	100.0	100.0	100.0	100.0	100.0	100.0
13:20	Point	5.03	0.57	20.00	1.081	483	454	4.0	8.2	11.5	13.6	24.8	33.0	45.0	61.0	81.9	92.0	95.9	97.2	100.0	100.0	100.0	100.0	100.0	100.0	100.0	100.0
13:23	Point	5.03	1.18	20.00	1.244	485	303	1.4	6.9	12.5	20.7	29.4	37.3	49.5	59.0	73.0	84.6	92.8	98.4	100.0	100.0	100.0	100.0	100.0	100.0	100.0	100.0
13:26	Point	5.03	1.18	16.00	1.525	527	402	1.8	7.9	10.4	15.0	20.0	26.0	32.7	47.0	60.4	83.1	90.7	96.0	100.0	100.0	100.0	100.0	100.0	100.0	100.0	100.0
13:29	Point	5.03	1.18	20.00	1.214	493	408	2.2	5.8	12.4	16.3	22.1	27.8	39.9	54.5	72.8	88.2	96.2	100.0	100.0	100.0	100.0	100.0	100.0	100.0	100.0	100.0
13:32	Point	5.03	1.18	12.00	1.333	536	337	6.9	8.0	15.2	22.7	28.0	34.7	43.7	57.9	73.9	87.2	96.2	100.0	100.0	100.0	100.0	100.0	100.0	100.0	100.0	100.0
13:35	Point	5.03	1.18	12.00	1.131	521	565	1.3	5.8	9.8	12.9	17.0	23.6	31.2	47.2	60.4	79.2	90.4	97.8	100.0	100.0	100.0	100.0	100.0	100.0	100.0	100.0
13:38	Point	5.03	1.18	12.00	1.302	525	311	4.8	9.4	14.4	20.6	28.2	38.4	50.8	67.6	80.2	91.6	99.3	100.0	100.0	100.0	100.0	100.0	100.0	100.0	100.0	100.0
13:41	Point	5.03	1.18	12.00	1.114	569	363	2.0	6.3	10.5	13.4	18.1	23.3	33.2	42.9	60.5	84.9	96.6	99.6	100.0	100.0	100.0	100.0	100.0	100.0	100.0	100.0
13:44	Point	5.03	1.18	12.00	1.131	569	545	3.4	6.6	11.7	16.5	18.1	29.1	37.7	47.9	62.3	83.7	95.6	100.0	100.0	100.0	100.0	100.0	100.0	100.0	100.0	100.0
13:47	Point	5.03	2.70	12.00	1.227	543	160	3.4	11.9	21.2	32.2	43.0	56.0	73.7	85.6	91.9	97.2	98.6	100.0	100.0	100.0	100.0	100.0	100.0	100.0	100.0	100.0
13:49	Point	5.03	2.70	12.00	1.215	579	169	5.5	15.8	27.1	36.2	47.4	60.5	70.9	81.4	89.2	97.3	99.8	100.0	100.0	100.0	100.0	100.0	100.0	100.0	100.0	100.0
13:51	Point	5.03	2.70	12.00	1.273	565	203	6.2	12.8	18.5	26.1	33.0	45.3	61.3	77.8	87.0	93.0	98.6	100.0	100.0	100.0	100.0	100.0	100.0	100.0	100.0	100.0
13:53	Point	5.03	2.70	12.00	1.281	521	194	6.1	15.3	24.8	36.2	46.5	59.6	71.7	81.0	90.2	94.3	98.8	100.0	100.0	100.0	100.0	100.0	100.0	100.0	100.0	100.0
13:56	Point	5.03	2.70	12.00	1.216	565	193	5.8	10.8	18.1	25.7	31.0	45.1	61.1	75.5	85.6	92.5	97.9	99.5	100.0	100.0	100.0	100.0	100.0	100.0	100.0	100.0
13:58	Point	5.03	4.53	12.00	1.252	536	98.0	4.9	17.4	31.1	42.1	53.5	71.0	78.3	85.6	93.2	97.5	100.0	100.0	100.0	100.0	100.0	100.0	100.0	100.0	100.0	100.0
14:00	Point	5.03	4.53	12.00	1.178	536	69.8	5.7	21.5	35.5	46.2	62.1	75.1	83.8	93.4	98.8	100.0	100.0	100.0	100.0	100.0	100.0	100.0	100.0	100.0	100.0	100.0
14:01	Point	5.03	4.53	12.00	1.318	512	89.7	10.4	20.7	32.2	42.9	54.2	67.9	75.0	81.2	87.0	94.7	99.4	100.0	100.0	100.0	100.0	100.0	100.0	100.0	100.0	100.0
14:03	Point	5.03	4.53	12.00	1.388	505	109	6.8	16.7	28.2	41.8	55.5	65.1	76.9	86.1	92.8	96.9	99.2	100.0	100.0	100.0	100.0	100.0	100.0	100.0	100.0	100.0
14:05	Point	5.03	4.53	12.00	1.269	531	184	9.3	21.2	35.3	43.7	53.8	64.6	73.3	81.1	88.6	95.5	98.6	100.0	100.0	100.0	100.0	100.0	100.0	100.0	100.0	100.0

Notes: Water depths associated with the point samples are the mean water depths at this vertical during the collection of the 18 point samples; point-sample elevations are relative to the mean bed elevation associated with this mean water depth.

P-61 suspended-sediment samples collected at the Cisco gaging station on May 13, 1995; vertical located at the station 340 ft from the left-bank bridge abutment																										
Time (MST)	Sample type	Water depth (m)	Sample elevation above bed (m)	Sample collection time (s)	DI intake velocity (m/s)	Silt and clay conc. (mg/L)	Sand conc. (mg/L)	Grain-size analysis of sand (0.0625-2.0 mm) fraction																		
								% sand < 0.074 mm	% sand < 0.088 mm	% sand < 0.105 mm	% sand < 0.125 mm	% sand < 0.149 mm	% sand < 0.177 mm	% sand < 0.210 mm	% sand < 0.250 mm	% sand < 0.297 mm	% sand < 0.354 mm	% sand < 0.420 mm	% sand < 0.500 mm	% sand < 0.595 mm	% sand < 0.707 mm	% sand < 0.841 mm	% sand < 1.00 mm	% sand < 1.19 mm	% sand < 1.41 mm	% sand < 1.68 mm
10:34	Up DI	5.09	n/a	9.80	1.211	1,480	512	8.1	18.2	27.8	35.1	42.9	51.1	60.3	68.6	78.1	89.5	95.0	99.2	100.0	100.0	100.0	100.0	100.0	100.0	100.0
10:36	Up DI	5.09	n/a	11.60	0.934	1,500	631	5.0	10.9	18.2	25.5	33.1	43.3	54.6	65.4	77.0	89.9	96.5	99.8	100.0	100.0	100.0	100.0	100.0	100.0	100.0
10:38	Up DI	5.09	n/a	12.10	1.301	1,500	704	5.3	11.9	17.6	23.1	30.4	37.9	45.5	55.5	67.4	80.3	93.8	97.9	98.4	99.5	100.0	100.0	100.0	100.0	100.0
10:40	Up DI	5.09	n/a	13.00	1.208	1,470	544	6.3	15.3	24.8	33.6	44.5	54.5	65.3	76.6	86.0	93.9	97.5	99.3	100.0	100.0	100.0	100.0	100.0	100.0	100.0
10:41	Up DI	5.09	n/a	12.10	1.208	1,440	733	5.2	13.2	21.5	29.6	36.7	43.8	53.6	65.5	79.4	91.2	98.7	99.8	100.0	100.0	100.0	100.0	100.0	100.0	100.0
12:42	Up DI	5.55	n/a	11.40	1.195	1,400	604	6.8	14.8	21.5	28.1	34.9	41.1	48.7	58.9	72.9	87.0	96.4	98.8	100.0	100.0	100.0	100.0	100.0	100.0	100.0
12:44	Up DI	5.55	n/a	11.40	1.300	1,380	509	6.0	13.0	19.3	25.9	34.7	42.1	50.1	57.7	69.1	81.7	93.5	95.8	97.7	100.0	100.0	100.0	100.0	100.0	100.0
12:46	Up DI	5.55	n/a	11.10	1.432	1,380	508	6.6	14.0	21.2	29.3	36.8	46.0	58.5	69.6	78.7	87.4	95.1	98.3	100.0	100.0	100.0	100.0	100.0	100.0	100.0
12:48	Up DI	5.55	n/a	11.70	1.359	1,450	651	6.7	14.6	22.1	27.5	33.0	39.1	47.4	57.5	70.1	86.2	96.1	99.1	100.0	100.0	100.0	100.0	100.0	100.0	100.0
12:50	Up DI	5.55	n/a	11.40	1.342	1,390	626	6.2	13.8	21.5	29.0	36.2	45.2	55.7	70.5	84.2	94.4	99.3	100.0	100.0	100.0	100.0	100.0	100.0	100.0	100.0
13:54	Up DI	6.04	n/a	12.80	1.142	1,610	1,080	6.5	9.9	12.4	14.9	19.0	23.3	29.7	36.1	48.8	74.6	90.0	95.9	100.0	100.0	100.0	100.0	100.0	100.0	100.0
13:56	Up DI	6.04	n/a	13.10	1.175	1,590	978	4.3	10.3	16.6	21.9	27.9	33.8	40.7	49.3	61.0	78.9	94.0	98.6	99.8	100.0	100.0	100.0	100.0	100.0	100.0
13:58	Up DI	6.04	n/a	13.20	1.278	1,470	329	9.4	20.7	33.5	48.0	61.2	70.1	78.2	84.4	88.7	93.3	96.1	96.7	99.9	100.0	100.0	100.0	100.0	100.0	100.0
14:00	Up DI	6.04	n/a	12.60	1.404	1,520	433	8.6	20.9	31.8	43.8	55.1	65.3	73.8	80.4	86.8	92.9	96.6	97.5	98.4	98.7	100.0	100.0	100.0	100.0	100.0
14:02	Up DI	6.04	n/a	13.60	1.286	1,540	493	7.2	15.7	23.4	31.6	40.1	50.2	61.3	72.6	83.5	93.3	97.8	99.0	100.0	100.0	100.0	100.0	100.0	100.0	100.0
15:39	Up DI	5.77	n/a	11.40	1.588	1,680	471	9.9	22.1	33.2	41.6	50.0	56.6	65.7	78.5	88.8	94.7	97.8	99.2	100.0	100.0	100.0	100.0	100.0	100.0	100.0
15:41	Up DI	5.77	n/a	11.70	1.332	1,670	577	8.4	18.5	27.3	34.6	41.9	51.7	63.2	75.8	87.4	94.3	98.5	100.0	100.0	100.0	100.0	100.0	100.0	100.0	100.0
15:43	Up DI	5.77	n/a	11.90	1.536	1,650	575	7.2	14.9	22.4	30.2	39.0	49.1	60.8	75.1	85.6	93.7	97.5	98.9	100.0	100.0	100.0	100.0	100.0	100.0	100.0
15:45	Up DI	5.77	n/a	11.90	1.184	1,670	507	6.3	15.1	23.6	31.1	37.3	45.9	56.4	68.2	78.7	86.6	93.2	97.0	98.5	99.3	100.0	100.0	100.0	100.0	100.0
15:47	Up DI	5.77	n/a	12.30	1.396	1,610	343	10.2	22.9	37.1	45.6	52.9	60.4	73.4	83.5	92.4	97.4	99.0	100.0	100.0	100.0	100.0	100.0	100.0	100.0	100.0

Notes: Up DI = depth-integrated on upward transit (intake closed during downward transit).

P-61 suspended-sediment samples collected at the Cisco gaging station on May 14, 1995; vertical located at the station 403 ft from the left-bank bridge abutment																										
Time (MST)	Sample type	Water depth (m)	Sample elevation above bed (m)	Sample collection time (s)	DI intake velocity (m/s)	Silt and clay conc. (mg/L)	Sand conc. (mg/L)	Grain-size analysis of sand (0.0625-2.0 mm) fraction																		
								% sand < 0.074 mm	% sand < 0.088 mm	% sand < 0.105 mm	% sand < 0.125 mm	% sand < 0.149 mm	% sand < 0.177 mm	% sand < 0.210 mm	% sand < 0.250 mm	% sand < 0.297 mm	% sand < 0.354 mm	% sand < 0.420 mm	% sand < 0.500 mm	% sand < 0.595 mm	% sand < 0.707 mm	% sand < 0.841 mm	% sand < 1.00 mm	% sand < 1.19 mm	% sand < 1.41 mm	% sand < 1.68 mm
10:22	Up DI	7.86	n/a	12.00	1.454	1,360	483	1.5	4.7	9.8	13.9	19.0	23.7	29.0	35.4	43.6	53.9	69.5	83.7	90.6	96.7	100.0	100.0	100.0	100.0	100.0
10:25	Up DI	7.86	n/a	12.90	1.770	1,300	426	2.2	8.1	11.6	14.5	18.0	22.0	28.4	37.3	45.0	55.2	66.0	77.5	86.8	94.2	97.3	100.0	100.0	100.0	100.0
10:27	Up DI	7.86	n/a	11.60	1.586	1,320	407	3.9	11.6	18.4	25.5	33.9	42.5	50.7	59.6	69.2	79.1	89.4	96.5	98.6	100.0	100.0	100.0	100.0	100.0	100.0
10:30	Up DI	7.86	n/a	10.50	1.787	1,280	241	6.0	16.6	29.5	41.8	53.5	64.5	74.0	83.1	90.0	94.9	99.2	100.0	100.0	100.0	100.0	100.0	100.0	100.0	100.0
10:32	Up DI	7.86	n/a	12.00	1.787	1,260	261	5.9	13.4	22.9	29.2	37.1	50.9	64.5	76.9	87.1	95.0	98.1	100.0	100.0	100.0	100.0	100.0	100.0	100.0	100.0
12:00	Up DI	7.72	n/a	11.10	1.349	1,310	294	2.7	9.0	21.4	32.4	44.1	59.7	73.0	82.9	89.5	94.0	99.2	99.4	100.0	100.0	100.0	100.0	100.0	100.0	100.0
12:02	Up DI	7.72	n/a	11.80	1.504	1,270	258	5.0	16.4	25.9	35.3	49.0	63.8	77.6	85.6	92.5	98.3	99.6	100.0	100.0	100.0	100.0	100.0	100.0	100.0	100.0
12:03	Up DI	7.72	n/a	10.90	1.466	1,320	317	5.3	11.3	20.8	28.3	38.8	51.8	64.8	75.0	85.1	93.7	98.1	100.0	100.0	100.0	100.0	100.0	100.0	100.0	100.0
12:05	Up DI	7.72	n/a	11.50	1.632	1,210	278	4.4	13.6	21.0	29.3	36.8	50.7	63.3	74.0	83.8	91.4	98.0	99.2	100.0	100.0	100.0	100.0	100.0	100.0	100.0
12:07	Up DI	7.72	n/a	11.20	1.641	1,200	261	4.8	9.8	16.3	25.9	40.1	49.5	61.6	72.3	81.5	92.1	97.2	98.3	98.9	100.0	100.0	100.0	100.0	100.0	100.0
14:07	Up DI	7.66	n/a	11.00	1.590	1,200	257	7.2	14.4	22.8	30.4	39.7	52.2	63.8	72.7	81.4	89.7	96.2	99.2	100.0	100.0	100.0	100.0	100.0	100.0	100.0
14:10	Up DI	7.66	n/a	10.90	1.730	1,270	292	8.0	17.7	27.4	37.0	47.0	61.2	73.1	83.2	91.9	98.0	99.3	100.0	100.0	100.0	100.0	100.0	100.0	100.0	100.0
14:12	Up DI	7.66	n/a	11.00	1.316	1,210	295	5.7	15.1	22.5	30.4	39.3	51.0	62.8	73.2	81.3	88.6	94.5	97.6	100.0	100.0	100.0	100.0	100.0	100.0	100.0
14:14	Up DI	7.66	n/a	10.00	1.477	1,260	282	4.8	10.5	18.5	28.4	35.9	46.6	58.7	69.5	79.9	88.3	94.5	97.3	98.2	100.0	100.0	100.0	100.0	100.0	100.0
14:16	Up DI	7.66	n/a	10.00	1.369	1,250	331	6.1	15.2	25.3	36.1	44.8	56.0	70.0	81.1	90.0	95.6	98.1	100.0	100.0	100.0	100.0	100.0	100.0	100.0	100.0

Notes: Up DI = depth-integrated on upward transit (intake closed during downward transit).

P-61 suspended-sediment samples collected at River-mile 30 sediment station cross section B on August 7, 2006; vertical located at the station 92 ft from the left-bank end point of the tagline																										
Time (MST)	Sample type	Water depth (m)	Sample elevation above bed (m)	Sample collection time (s)	Point intake velocity (m/s)	Silt and clay conc. (mg/L)	Sand conc. (mg/L)	Grain-size analysis of sand (0.0625-2.0 mm) fraction																		
								% sand < 0.074 mm	% sand < 0.088 mm	% sand < 0.105 mm	% sand < 0.125 mm	% sand < 0.149 mm	% sand < 0.177 mm	% sand < 0.210 mm	% sand < 0.250 mm	% sand < 0.297 mm	% sand < 0.354 mm	% sand < 0.420 mm	% sand < 0.500 mm	% sand < 0.595 mm	% sand < 0.707 mm	% sand < 0.841 mm	% sand < 1.00 mm	% sand < 1.19 mm	% sand < 1.41 mm	% sand < 1.68 mm
10:45	Point	6.86	0.57	42.13	0.613	19.4	34.8	8.4	19.1	35.8	53.4	68.7	80.7	89.3	95.8	98.6	99.2	99.7	100.0	100.0	100.0	100.0	100.0	100.0	100.0	100.0
10:48	Point	6.86	0.57	42.03	0.598	26.1	32.6	9.3	20.0	37.5	55.9	73.4	87.0	95.3	98.9	99.9	100.0	100.0	100.0	100.0	100.0	100.0	100.0	100.0	100.0	100.0
10:53	Point	6.86	0.57	45.59	0.775	15.3	51.7	6.8	15.9	31.0	47.9	63.4	76.9	86.8	94.2	97.7	98.4	99.2	99.7	99.9	100.0	100.0	100.0	100.0	100.0	100.0
10:57	Point	6.86	1.18	40.13	0.606	17.8	31.4	9.4	21.5	40.2	59.5	74.7	85.6	92.1	97.0	99.6	100.0	100.0	100.0	100.0	100.0	100.0	100.0	100.0	100.0	100.0
11:00	Point	6.86	1.18	42.09	0.814	43.3	18.4	9.1	20.3	37.6	54.9	69.3	80.2	87.1	91.8	93.8	94.2	96.4	99.4	99.8	100.0	100.0	100.0	100.0	100.0	100.0
11:06	Point	6.86	1.18	42.18	0.769	11.3	16.5	---	---	---	---	---	---	---	---	---	---	---	---	---	---	---	---	---	---	---
11:10	Point	6.86	2.39	40.25	0.775	14.1	21.3	11.4	25.8	47.5	68.2	82.9	92.1	97.2	99.3	100.0	100.0	100.0	100.0	100.0	100.0	100.0	100.0	100.0	100.0	100.0
11:14	Point	6.86	2.39	40.09	0.832	14.1	16.2	---	---	---	---	---	---	---	---	---	---	---	---	---	---	---	---	---	---	---
11:16	Point	6.86	2.39	39.68	0.813	15.2	20.6	8.7	18.5	33.4	50.1	65.7	79.3	89.3	96.6	99.6	100.0	100.0	100.0	100.0	100.0	100.0	100.0	100.0	100.0	100.0
11:19	Point	6.86	4.53	39.90	0.809	14.1	14.4	---	---	---	---	---	---	---	---	---	---	---	---	---	---	---	---	---	---	---
11:21	Point	6.86	4.53	40.00	0.823	15.1	19.0	7.2	14.7	27.2	42.8	60.0	77.7	90.8	97.8	99.9	100.0	100.0	100.0	100.0	100.0	100.0	100.0	100.0	100.0	100.0
11:23	Point	6.86	4.53	39.93	0.816	15.0	20.9	11.3	23.8	43.8	61.9	77.3	88.6	95.7	99.0	99.9	100.0	100.0	100.0	100.0	100.0	100.0	100.0	100.0	100.0	100.0
11:26	Point	6.86	6.05	40.28	0.793	19.2	16.8	12.2	25.0	43.0	60.1	74.5	85.8	93.4	98.1	99.8	100.0	100.0	100.0	100.0	100.0	100.0	100.0	100.0	100.0	100.0
11:33	Point	6.86	6.05	40.09	0.787	14.6	14.8	---	---	---	---	---	---	---	---	---	---	---	---	---	---	---	---	---	---	---
11:36	Point	6.86	6.05	40.00	0.811	11.9	14.4	---	---	---	---	---	---	---	---	---	---	---	---	---	---	---	---	---	---	---

Notes: Water depths associated with the point samples are the mean water depths at this vertical during the collection of the 18 point samples; point-sample elevations are relative to the mean bed elevation associated with this mean water depth.

P-61 suspended-sediment samples collected at River-mile 30 sediment station cross section B on August 7, 2006; vertical located at the station 188 ft from the left-bank end point of the tagline																										
Time (MST)	Sample type	Water depth (m)	Sample elevation above bed (m)	Sample collection time (s)	Point intake velocity (m/s)	Silt and clay conc. (mg/L)	Sand conc. (mg/L)	Grain-size analysis of sand (0.0625-2.0 mm) fraction																		
								% sand < 0.074 mm	% sand < 0.088 mm	% sand < 0.105 mm	% sand < 0.125 mm	% sand < 0.149 mm	% sand < 0.177 mm	% sand < 0.210 mm	% sand < 0.250 mm	% sand < 0.297 mm	% sand < 0.354 mm	% sand < 0.420 mm	% sand < 0.500 mm	% sand < 0.595 mm	% sand < 0.707 mm	% sand < 0.841 mm	% sand < 1.00 mm	% sand < 1.19 mm	% sand < 1.41 mm	% sand < 1.68 mm
11:41	Point	6.55	0.87	39.78	0.698	20.9	28.2	7.1	16.8	33.5	50.7	65.2	77.5	85.8	91.8	94.7	97.3	99.5	99.9	100.0	100.0	100.0	100.0	100.0	100.0	100.0
11:43	Point	6.55	0.87	39.83	0.593	22.2	26.8	11.1	24.3	45.0	64.8	79.9	89.9	96.0	98.9	99.9	100.0	100.0	100.0	100.0	100.0	100.0	100.0	100.0	100.0	100.0
11:46	Point	6.55	0.87	39.91	0.598	18.8	32.2	10.0	22.4	41.2	60.6	76.2	86.8	93.4	97.9	99.8	100.0	100.0	100.0	100.0	100.0	100.0	100.0	100.0	100.0	100.0
11:51	Point	6.55	1.63	40.00	0.722	18.4	22.8	12.3	25.1	44.5	64.2	80.6	91.5	96.9	99.3	99.9	100.0	100.0	100.0	100.0	100.0	100.0	100.0	100.0	100.0	100.0
11:54	Point	6.55	1.63	43.00	0.734	16.7	23.2	9.0	19.5	35.6	52.3	66.6	78.7	86.8	92.4	95.2	97.1	99.3	99.9	100.0	100.0	100.0	100.0	100.0	100.0	100.0
11:57	Point	6.55	1.63	40.06	0.703	17.8	19.3	10.4	23.1	42.8	61.7	76.7	87.2	94.5	98.4	99.9	100.0	100.0	100.0	100.0	100.0	100.0	100.0	100.0	100.0	100.0
12:03	Point	6.55	3.61	40.03	0.797	16.4	17.2	18.9	37.7	67.3	89.1	98.6	100.0	100.0	100.0	100.0	100.0	100.0	100.0	100.0	100.0	100.0	100.0	100.0	100.0	100.0
12:07	Point	6.55	3.61	39.97	0.746	12.5	20.4	9.9	20.9	37.5	53.3	64.8	71.7	76.1	78.9	80.2	82.5	88.8	93.3	98.3	99.2	100.0	100.0	100.0	100.0	100.0
12:11	Point	6.55	3.61	40.06	0.686	15.9	25.3	---	---	---	---	---	---	---	---	---	---	---	---	---	---	---	---	---	---	---
12:14	Point	6.55	5.14	40.16	0.730	15.0	22.5	9.6	20.1	37.2	55.2	72.0	83.7	90.6	95.1	97.0	97.6	99.3	99.9	100.0	100.0	100.0	100.0	100.0	100.0	100.0
12:17	Point	6.55	5.14	40.25	0.734	16.3	19.1	10.4	23.9	45.5	66.8	84.9	95.5	99.4	100.0	100.0	100.0	100.0	100.0	100.0	100.0	100.0	100.0	100.0	100.0	100.0
12:21	Point	6.55	5.14	40.10	0.784	13.2	16.2	---	---	---	---	---	---	---	---	---	---	---	---	---	---	---	---	---	---	---
12:26	Point	6.55	5.75	39.91	0.750	12.6	12.9	---	---	---	---	---	---	---	---	---	---	---	---	---	---	---	---	---	---	---
12:30	Point	6.55	5.75	39.90	0.797	18.2	12.5	---	---	---	---	---	---	---	---	---	---	---	---	---	---	---	---	---	---	---
12:34	Point	6.55	5.75	39.94	0.770	12.8	12.2	---	---	---	---	---	---	---	---	---	---	---	---	---	---	---	---	---	---	---

Notes: Water depths associated with the point samples are the mean water depths at this vertical during the collection of the 18 point samples; point-sample elevations are relative to the mean bed elevation associated with this mean water depth.

D-77-bag-type noncomposited multivertical suspended-sediment samples collected at River-mile 30 sediment station cross section A on February 24, 2007;
 verticals 1 through 9 located respectively at stations 46, 67, 88, 109, 130, 151, 172, 193, and 214 ft from the left-bank end point of the tagline, left and right edges of water are respectively at 25 and 235 fet from the left-bank end point of the tagline

Time (MST)	Sample type	Water depth (m)	Sample elevation above bed (m)	Sample collection time (s)	DI intake velocity (m/s)	Silt and clay conc. (mg/L)	Sand conc. (mg/L)	Grain-size analysis of sand (0.0625-2.0 mm) fraction																			
								% sand < 0.074 mm	% sand < 0.088 mm	% sand < 0.105 mm	% sand < 0.125 mm	% sand < 0.149 mm	% sand < 0.177 mm	% sand < 0.210 mm	% sand < 0.250 mm	% sand < 0.297 mm	% sand < 0.354 mm	% sand < 0.420 mm	% sand < 0.500 mm	% sand < 0.595 mm	% sand < 0.707 mm	% sand < 0.841 mm	% sand < 1.00 mm	% sand < 1.19 mm	% sand < 1.41 mm	% sand < 1.68 mm	% sand < 2.00 mm
11:33-12:43	EWI-5v	n/a	n/a	665	n/a	16.6	57.7	10.0	21.6	39.2	56.6	69.7	79.3	85.2	89.9	94.0	96.7	97.7	98.1	98.4	99.3	99.7	100.0	100.0	100.0	100.0	100.0
11:40-12:37	EWI-3v	n/a	n/a	456	n/a	14.1	54.3	9.6	21.5	39.7	57.7	71.1	80.9	87.0	91.6	95.3	97.6	98.3	98.6	98.6	99.4	99.7	100.0	100.0	100.0	100.0	100.0
11:33-12:43	EWI-9v	n/a	n/a	1300	n/a	15.4	56.9	9.4	21.0	39.1	57.1	70.6	80.4	86.5	91.2	94.9	97.3	98.4	98.9	99.1	99.6	99.8	100.0	100.0	100.0	100.0	100.0
12:39	v1 8DI	2.74	n/a	82	0.225	24.2	42.1	9.6	22.0	41.9	61.5	75.9	85.5	90.4	93.6	95.6	96.7	97.6	98.1	98.6	99.4	99.8	100.0	100.0	100.0	100.0	100.0
12:33	v2 8DI	6.71	n/a	168	0.377	11.7	51.0	9.8	21.8	40.3	58.2	71.5	80.7	86.9	92.1	95.7	98.2	99.7	100.0	100.0	100.0	100.0	100.0	100.0	100.0	100.0	100.0
12:22	v3 8DI	7.92	n/a	202	0.426	8.58	51.2	11.9	24.0	42.0	59.5	72.3	80.8	85.5	89.1	92.5	95.0	96.4	97.0	97.8	99.0	99.6	100.0	100.0	100.0	100.0	100.0
12:12	v4 8DI	7.62	n/a	195	0.513	12.6	57.1	8.9	20.4	38.7	56.8	70.5	80.4	86.6	91.6	95.5	97.9	99.5	99.9	100.0	100.0	100.0	100.0	100.0	100.0	100.0	100.0
12:02	v5 8DI	6.86	n/a	175	0.622	15.2	55.0	10.1	22.1	39.9	57.3	70.3	79.9	86.0	90.4	94.4	97.0	97.2	97.3	97.3	98.8	99.5	100.0	100.0	100.0	100.0	100.0
11:55	v6 8DI	6.40	n/a	159	0.477	18.5	58.4	7.9	19.3	38.4	57.7	72.2	82.9	88.9	93.1	95.7	97.4	98.6	99.3	99.5	99.8	99.9	100.0	100.0	100.0	100.0	100.0
11:46	v7 8DI	6.10	n/a	152	0.415	27.0	78.4	8.3	18.7	34.9	51.4	64.4	74.7	82.0	88.2	93.6	97.3	99.1	99.6	99.9	99.9	100.0	100.0	100.0	100.0	100.0	100.0
11:40	v8 8DI	4.57	n/a	113	0.402	14.7	57.3	8.1	19.6	38.7	58.0	72.5	83.4	89.7	93.8	96.6	98.3	99.2	99.8	100.0	100.0	100.0	100.0	100.0	100.0	100.0	100.0
11:33	v9 8DI	2.29	n/a	54	0.295	18.4	46.3	9.9	23.2	44.2	64.6	79.3	89.0	94.4	98.1	99.7	100.0	100.0	100.0	100.0	100.0	100.0	100.0	100.0	100.0	100.0	100.0

Notes: EW1-5v = 5-vertical EW1 measurement mathematically composited using raw laboratory data from verticals 1, 3, 5, 7, and 9; EW1-3v = 3-vertical quasi-EW1 measurement mathematically composited using raw laboratory data from verticals 2, 5, and 8; EW1-9v = 9-vertical quasi-EW1 measurement mathematically composited using raw laboratory data from all 9 verticals; DI = depth-integrated (nozzle open during downward and upward transits); v1 through v9 refer to verticals 1 through 9; number preceding DI indicates the number of transits at each vertical.

D-77-bag-type noncomposited multivertical suspended-sediment samples collected at River-mile 30 sediment station cross section B on February 24, 2007;
 verticals 1 through 9 located respectively at stations 44, 68, 91, 115, 138, 162, 185, 209, and 232 ft from the left-bank end point of the tagline, left and right edges of water are respectively at 21 and 256 ft from the left-bank end point of the tagline

Time (MST)	Sample type	Water depth (m)	Sample elevation above bed (m)	Sample collection time (s)	DI intake velocity (m/s)	Silt and clay conc. (mg/L)	Sand conc. (mg/L)	Grain-size analysis of sand (0.0625-2.0 mm) fraction																			
								% sand < 0.074 mm	% sand < 0.088 mm	% sand < 0.105 mm	% sand < 0.125 mm	% sand < 0.149 mm	% sand < 0.177 mm	% sand < 0.210 mm	% sand < 0.250 mm	% sand < 0.297 mm	% sand < 0.354 mm	% sand < 0.420 mm	% sand < 0.500 mm	% sand < 0.595 mm	% sand < 0.707 mm	% sand < 0.841 mm	% sand < 1.00 mm	% sand < 1.19 mm	% sand < 1.41 mm	% sand < 1.68 mm	% sand < 2.00 mm
12:55-13:55	EWI-5v	n/a	n/a	532	n/a	15.6	45.8	10.2	23.1	43.4	63.1	77.1	86.6	91.4	94.2	95.7	96.7	97.8	98.5	98.9	99.5	99.8	100.0	100.0	100.0	100.0	100.0
13:03-13:52	EWI-3v	n/a	n/a	337	n/a	15.1	44.4	10.6	24.2	45.7	66.1	80.4	89.5	93.8	95.9	97.0	97.9	98.7	99.2	99.4	99.8	99.9	100.0	100.0	100.0	100.0	100.0
12:55-13:55	EWI-9v	n/a	n/a	998	n/a	16.2	45.9	9.9	22.9	43.7	63.7	78.0	87.6	92.5	95.3	96.7	97.5	98.4	99.0	99.3	99.7	99.9	100.0	100.0	100.0	100.0	100.0
13:53	v1 6DI	2.13	n/a	51	0.369	25.0	36.5	11.1	23.5	42.2	59.6	71.5	79.1	83.4	86.6	88.8	90.3	92.2	93.9	95.7	98.2	99.4	100.0	100.0	100.0	100.0	100.0
13:49	v2 6DI	3.96	n/a	87	0.452	15.1	38.9	10.9	25.5	48.5	69.8	84.1	93.2	97.4	99.4	100.0	100.0	100.0	100.0	100.0	100.0	100.0	100.0	100.0	100.0	100.0	100.0
13:43	v3 6DI	6.10	n/a	140	0.480	9.88	41.1	11.0	24.9	45.9	65.5	79.2	88.3	92.8	95.2	96.3	97.1	97.8	98.5	98.9	99.5	99.8	100.0	100.0	100.0	100.0	100.0
13:35	v4 6DI	5.94	n/a	130	0.451	14.0	45.5	9.7	22.9	43.9	64.1	78.3	87.9	92.9	95.6	96.9	97.6	98.5	99.1	99.4	99.7	99.9	100.0	100.0	100.0	100.0	100.0
13:24	v5 6DI	5.79	n/a	126	0.458	16.0	45.2	11.0	24.5	45.3	65.2	78.9	87.5	91.3	93.2	94.5	95.9	97.3	98.2	98.6	99.5	99.8	100.0	100.0	100.0	100.0	100.0
13:15	v6 6DI	5.79	n/a	125	0.397	24.0	50.3	8.6	20.8	41.0	61.2	76.1	86.6	92.1	95.3	97.1	98.1	99.0	99.4	99.6	99.8	99.9	100.0	100.0	100.0	100.0	100.0
13:09	v7 6DI	5.79	n/a	124	0.346	12.3	62.1	8.4	20.2	39.6	59.4	74.6	85.8	92.0	95.5	97.5	98.4	99.1	99.5	99.7	99.8	99.9	100.0	100.0	100.0	100.0	100.0
13:03	v8 6DI	5.85	n/a	124	0.339	13.7	48.5	9.7	22.7	43.9	64.6	79.4	89.4	94.3	96.8	97.9	98.7	99.6	99.9	100.0	100.0	100.0	100.0	100.0	100.0	100.0	100.0
12:55	v9 6DI	4.27	n/a	91	0.293	27.9	38.8	9.9	22.5	42.8	62.9	77.2	86.8	91.9	95.3	96.9	97.9	99.4	99.9	100.0	100.0	100.0	100.0	100.0	100.0	100.0	100.0

Notes: EW1-5v = 5-vertical EW1 measurement mathematically composited using raw laboratory data from verticals 1, 3, 5, 7, and 9; EW1-3v = 3-vertical quasi-EW1 measurement mathematically composited using raw laboratory data from verticals 2, 5, and 8; EW1-9v = 9-vertical quasi-EW1 measurement mathematically composited using raw laboratory data from all 9 verticals; DI = depth-integrated (nozzle open during downward and upward transits); v1 through v9 refer to verticals 1 through 9; number preceding DI indicates the number of transits at each vertical.

D-96-A1 noncomposited multivertical suspended-sediment samples collected at River mile 30 sediment station cross section A on February 24, 2007;																										
verticals 1 through 9 located respectively at stations 46, 67, 88, 109, 130, 151, 172, 193, and 214 ft from the left-bank end point of the tagline, left and right edges of water are respectively at 25 and 235 ft from the left-bank end point of the tagline																										
Time (MST)	Sample type	Water depth (m)	Sample elevation above bed (m)	Sample collection time (s)	DI intake velocity (m/s)	Silt and clay conc. (mg/L)	Sand conc. (mg/L)	Grain-size analysis of sand (0.0625-2.0 mm) fraction																		
								% sand < 0.074 mm	% sand < 0.088 mm	% sand < 0.105 mm	% sand < 0.125 mm	% sand < 0.149 mm	% sand < 0.177 mm	% sand < 0.210 mm	% sand < 0.250 mm	% sand < 0.297 mm	% sand < 0.354 mm	% sand < 0.420 mm	% sand < 0.500 mm	% sand < 0.595 mm	% sand < 0.707 mm	% sand < 0.841 mm	% sand < 1.00 mm	% sand < 1.19 mm	% sand < 1.41 mm	% sand < 1.68 mm
17:10-18:41	EWI-5v	n/a	n/a	639	n/a	14.7	67.0	9.5	22.0	41.9	61.4	75.5	85.2	90.6	94.2	96.6	98.3	99.4	99.8	99.9	100.0	100.0	100.0	100.0	100.0	100.0
17:16-18:36	EWI-3v	n/a	n/a	447	n/a	19.0	67.4	9.0	21.2	40.7	59.6	73.3	82.9	88.6	92.9	96.0	98.4	99.7	99.9	100.0	100.0	100.0	100.0	100.0	100.0	100.0
17:10-18:41	EWI-9v	n/a	n/a	1280	n/a	16.1	67.7	9.3	21.6	41.2	60.3	74.2	83.8	89.3	93.3	96.1	98.2	99.5	99.9	100.0	100.0	100.0	100.0	100.0	100.0	100.0
18:39	v1 8DI	2.74	n/a	60	0.302	25.1	66.2	8.6	20.1	39.9	60.6	75.9	86.2	91.4	94.6	96.6	97.7	99.0	99.8	100.0	100.0	100.0	100.0	100.0	100.0	100.0
18:28	v2 8DI	6.71	n/a	164	0.482	17.3	63.6	8.3	20.1	39.5	58.6	72.6	82.0	87.6	92.0	95.4	98.2	99.7	100.0	100.0	100.0	100.0	100.0	100.0	100.0	100.0
18:13	v3 8DI	7.92	n/a	210	0.638	14.3	66.0	9.6	22.0	41.7	61.0	74.9	84.5	89.8	93.6	96.3	98.3	99.6	99.9	100.0	100.0	100.0	100.0	100.0	100.0	100.0
18:00	v4 8DI	7.62	n/a	198	0.820	15.0	68.5	9.7	22.5	42.6	62.0	76.0	85.5	90.7	94.2	96.7	98.4	99.5	99.9	100.0	100.0	100.0	100.0	100.0	100.0	100.0
17:45	v5 8DI	6.86	n/a	165	0.883	17.4	65.8	9.9	22.9	43.1	62.5	76.3	85.7	91.1	94.7	96.8	98.5	99.6	99.9	100.0	100.0	100.0	100.0	100.0	100.0	100.0
17:37	v6 8DI	6.40	n/a	161	0.692	16.5	67.3	9.3	21.2	40.0	58.4	71.7	81.2	87.0	91.5	95.1	97.9	99.4	99.9	100.0	100.0	100.0	100.0	100.0	100.0	100.0
17:23	v7 8DI	6.10	n/a	152	0.483	7.01	67.4	8.6	20.8	40.6	60.2	74.5	84.6	90.0	93.5	95.9	97.6	98.8	99.5	99.7	99.8	99.9	100.0	100.0	100.0	100.0
17:16	v8 8DI	4.57	n/a	118	0.536	24.9	76.0	7.9	19.2	37.1	54.7	68.3	78.2	84.6	90.2	94.9	98.4	99.7	100.0	100.0	100.0	100.0	100.0	100.0	100.0	100.0
17:10	v9 8DI	2.29	n/a	52	0.432	17.4	79.7	9.3	21.7	41.9	61.9	76.5	86.9	92.7	96.4	98.3	99.1	99.8	100.0	100.0	100.0	100.0	100.0	100.0	100.0	100.0

Notes: EWI-5v = 5-vertical EWI measurement mathematically composited using raw laboratory data from verticals 1, 3, 5, 7, and 9; EWI-3v = 3-vertical quasi-EWI measurement mathematically composited using raw laboratory data from verticals 2, 5, and 8; EWI-9v = 9-vertical quasi-EWI measurement mathematically composited using raw laboratory data from all 9 verticals; DI = depth-integrated (nozzle open during downward and upward transits); v1 through v9 refer to verticals 1 through 9; number preceding DI indicates the number of transits at each vertical.

D-96-A1 noncomposited multivertical suspended-sediment samples collected at River mile 30 sediment station cross section B on February 25, 2007;																										
verticals 1 through 9 located respectively at stations 44, 68, 91, 115, 138, 162, 185, 209, and 232 ft from the left-bank end point of the tagline, left and right edges of water are respectively at 21 and 256 ft from the left-bank end point of the tagline																										
Time (MST)	Sample type	Water depth (m)	Sample elevation above bed (m)	Sample collection time (s)	DI intake velocity (m/s)	Silt and clay conc. (mg/L)	Sand conc. (mg/L)	Grain-size analysis of sand (0.0625-2.0 mm) fraction																		
								% sand < 0.074 mm	% sand < 0.088 mm	% sand < 0.105 mm	% sand < 0.125 mm	% sand < 0.149 mm	% sand < 0.177 mm	% sand < 0.210 mm	% sand < 0.250 mm	% sand < 0.297 mm	% sand < 0.354 mm	% sand < 0.420 mm	% sand < 0.500 mm	% sand < 0.595 mm	% sand < 0.707 mm	% sand < 0.841 mm	% sand < 1.00 mm	% sand < 1.19 mm	% sand < 1.41 mm	% sand < 1.68 mm
9:27-10:06	EWI-5v	n/a	n/a	332	n/a	14.3	44.8	8.4	20.0	39.7	60.0	75.4	86.3	92.0	95.1	96.5	97.1	97.8	98.2	98.5	99.4	99.7	100.0	100.0	100.0	100.0
9:31-10:02	EWI-3v	n/a	n/a	225	n/a	16.7	43.5	8.1	18.9	37.5	57.0	72.2	83.4	89.6	93.5	95.6	96.9	98.0	98.7	99.2	99.6	99.9	100.0	100.0	100.0	100.0
9:27-10:06	EWI-9v	n/a	n/a	642	n/a	15.0	43.7	8.1	19.4	38.9	59.4	75.1	86.2	92.0	95.2	96.7	97.6	98.4	98.8	99.1	99.6	99.8	100.0	100.0	100.0	100.0
9:27	v1 4DI	2.43	n/a	31	0.468	21.2	53.7	7.7	18.3	36.5	55.8	70.9	81.7	87.8	91.4	92.7	92.9	92.9	93.1	97.0	98.7	100.0	100.0	100.0	100.0	
9:31	v2 4DI	4.27	n/a	53	0.622	18.8	40.4	8.3	19.2	38.0	58.1	73.7	84.9	91.1	94.9	96.9	97.8	98.8	99.6	99.8	99.9	100.0	100.0	100.0	100.0	
9:34	v3 4DI	6.40	n/a	81	0.608	11.3	52.0	8.0	19.4	39.2	59.9	75.9	87.5	93.5	96.6	97.9	98.5	99.4	99.8	100.0	100.0	100.0	100.0	100.0	100.0	
9:40	v4 4DI	6.25	n/a	89	0.597	12.1	44.4	7.0	17.8	37.5	58.9	75.7	87.7	93.7	96.8	98.2	99.0	99.8	100.0	100.0	100.0	100.0	100.0	100.0	100.0	
9:45	v5 4DI	6.10	n/a	88	0.545	13.8	45.3	7.4	18.1	36.6	56.0	71.3	82.8	89.5	93.7	96.0	97.4	98.3	99.0	99.3	99.7	99.9	100.0	100.0	100.0	
9:52	v6 4DI	6.10	n/a	84	0.603	15.5	41.2	7.3	18.6	38.7	59.9	76.2	87.6	93.4	96.4	97.9	98.9	99.7	100.0	100.0	100.0	100.0	100.0	100.0	100.0	
9:56	v7 4DI	6.10	n/a	78	0.515	13.4	33.9	10.6	24.8	47.7	69.8	85.1	94.4	98.2	99.6	100.0	100.0	100.0	100.0	100.0	100.0	100.0	100.0	100.0	100.0	
10:00	v8 4DI	6.16	n/a	84	0.421	18.7	43.9	8.8	19.9	38.3	57.5	72.2	82.8	88.6	92.0	94.0	95.3	96.8	97.7	98.4	99.3	99.8	100.0	100.0	100.0	
10:05	v9 4DI	15.0	n/a	54	0.405	19.7	41.4	9.3	20.8	39.6	58.9	73.2	83.1	88.1	90.7	91.5	92.0	93.1	93.7	94.9	97.8	99.1	100.0	100.0	100.0	

Notes: EWI-5v = 5-vertical EWI measurement mathematically composited using raw laboratory data from verticals 1, 3, 5, 7, and 9; EWI-3v = 3-vertical quasi-EWI measurement mathematically composited using raw laboratory data from verticals 2, 5, and 8; EWI-9v = 9-vertical quasi-EWI measurement mathematically composited using raw laboratory data from all 9 verticals; DI = depth-integrated (nozzle open during downward and upward transits); v1 through v9 refer to verticals 1 through 9; number preceding DI indicates the number of transits at each vertical.

D-96-A1 noncomposited multivertical suspended-sediment samples collected at River-mile 30 sediment station cross section A on August 24, 2007;																											
verticals 1 through 9 located respectively at stations 78, 100, 122, 144, 165, 187, 209, 231, and 252 ft from the left-bank end point of the tagline, left and right edges of water are respectively at 56 and 274 ft from the left-bank end point of the tagline, left-bank end point of tagline is approximately 30 ft farther from the river than the end point used in February 2007																											
Time (MST)	Sample type	Water depth (m)	Sample elevation above bed (m)	Sample collection time (s)	DI intake velocity (m/s)	Silt and clay conc. (mg/L)	Sand conc. (mg/L)	Grain-size analysis of sand (0.0625-2.0 mm) fraction																			
								% sand < 0.074 mm	% sand < 0.088 mm	% sand < 0.105 mm	% sand < 0.125 mm	% sand < 0.149 mm	% sand < 0.177 mm	% sand < 0.210 mm	% sand < 0.250 mm	% sand < 0.297 mm	% sand < 0.354 mm	% sand < 0.420 mm	% sand < 0.500 mm	% sand < 0.595 mm	% sand < 0.707 mm	% sand < 0.841 mm	% sand < 1.00 mm	% sand < 1.19 mm	% sand < 1.41 mm	% sand < 1.68 mm	% sand < 2.00 mm
14:02-14:37	EWI-5v	n/a	n/a	320	n/a	28.7	65.2	8.2	19.0	36.3	54.3	68.9	80.6	88.0	93.1	96.3	97.9	98.8	99.3	99.5	99.8	99.9	100.0	100.0	100.0	100.0	100.0
14:07-14:33	EWI-3v	n/a	n/a	218	n/a	25.6	66.7	7.6	17.8	34.5	52.0	66.5	78.5	86.5	92.2	95.9	97.8	98.7	99.1	99.4	99.7	99.9	100.0	100.0	100.0	100.0	100.0
14:02-14:37	EWI-9v	n/a	n/a	634	n/a	28.8	66.8	7.7	18.0	34.9	52.5	67.0	78.9	86.6	92.2	95.8	97.8	98.8	99.4	99.6	99.8	99.9	100.0	100.0	100.0	100.0	100.0
14:35	v1 4DI	4.11	n/a	99	0.268	30.7	49.2	8.4	19.8	38.1	57.1	72.2	83.7	91.1	96.3	98.5	98.9	98.9	98.9	99.5	99.8	100.0	100.0	100.0	100.0	100.0	
14:32	v2 2DI	7.01	n/a	88	0.569	27.8	57.9	7.7	18.3	35.7	53.9	68.7	80.9	88.9	94.6	98.1	99.6	99.9	100.0	100.0	100.0	100.0	100.0	100.0	100.0	100.0	
14:27	v3 2DI	8.08	n/a	101	0.754	29.6	62.5	8.2	19.1	36.9	55.0	69.7	81.7	89.2	94.4	97.5	98.9	99.6	99.9	100.0	100.0	100.0	100.0	100.0	100.0	100.0	
14:21	v4 2DI	7.77	n/a	98	0.789	29.6	62.3	7.6	18.3	36.0	54.2	69.0	80.7	87.9	92.7	95.7	97.4	98.6	99.5	99.8	99.9	100.0	100.0	100.0	100.0	100.0	
14:19	v5 2DI	6.71	n/a	83	0.846	22.1	72.9	7.7	17.7	33.7	50.6	64.8	76.6	84.5	90.4	94.4	96.6	97.8	98.5	98.9	99.5	99.8	100.0	100.0	100.0	100.0	
14:15	v6 2DI	6.55	n/a	81	0.742	27.8	85.8	6.4	15.2	29.7	45.4	59.0	71.3	80.3	87.7	93.2	96.4	97.9	98.9	99.4	99.7	99.9	100.0	100.0	100.0	100.0	
14:12	v7 2DI	5.49	n/a	67	0.632	35.9	62.4	9.0	20.9	39.8	58.9	73.9	85.0	91.2	94.8	96.8	98.3	99.3	99.9	100.0	100.0	100.0	100.0	100.0	100.0		
14:07	v8 4DI	3.96	n/a	93	0.363	33.2	66.8	7.1	17.3	34.7	53.3	68.6	81.0	88.7	94.0	97.0	98.4	99.5	99.9	100.0	100.0	100.0	100.0	100.0	100.0	100.0	
14:02	v9 6DI	1.83	n/a	59	0.213	44.3	61.1	8.1	19.5	38.6	58.4	73.8	85.1	92.3	97.2	99.6	100.0	100.0	100.0	100.0	100.0	100.0	100.0	100.0	100.0	100.0	

Notes: EW1-5v = 5-vertical EW1 measurement mathematically composited using raw laboratory data from verticals 1, 3, 5, 7, and 9; EW1-3v = 3-vertical quasi-EW1 measurement mathematically composited using raw laboratory data from verticals 2, 5, and 8; EW1-9v = 9-vertical quasi-EW1 measurement mathematically composited using raw laboratory data from all 9 verticals; DI = depth-integrated (nozzle open during downward and upward transits); v1 through v9 refer to verticals 1 through 9; number preceding DI indicates the number of transits at each vertical.

D-96-A1 noncomposited multivertical suspended-sediment samples collected at River-mile 30 sediment station cross section B on August 24, 2007;																											
verticals 1 through 9 located respectively at stations 44, 67, 91, 114, 138, 161, 185, 208, and 232 ft from the left-bank end point of the tagline, left and right edges of water are respectively at 20 and 255 ft from the left-bank end point of the tagline																											
Time (MST)	Sample type	Water depth (m)	Sample elevation above bed (m)	Sample collection time (s)	DI intake velocity (m/s)	Silt and clay conc. (mg/L)	Sand conc. (mg/L)	Grain-size analysis of sand (0.0625-2.0 mm) fraction																			
								% sand < 0.074 mm	% sand < 0.088 mm	% sand < 0.105 mm	% sand < 0.125 mm	% sand < 0.149 mm	% sand < 0.177 mm	% sand < 0.210 mm	% sand < 0.250 mm	% sand < 0.297 mm	% sand < 0.354 mm	% sand < 0.420 mm	% sand < 0.500 mm	% sand < 0.595 mm	% sand < 0.707 mm	% sand < 0.841 mm	% sand < 1.00 mm	% sand < 1.19 mm	% sand < 1.41 mm	% sand < 1.68 mm	% sand < 2.00 mm
14:48-15:25	EWI-5v	n/a	n/a	312	n/a	30.9	51.5	9.6	22.1	41.8	61.3	76.2	86.9	92.7	96.0	97.5	98.3	99.3	99.6	99.8	99.9	100.0	100.0	100.0	100.0	100.0	100.0
14:52-15:20	EWI-3v	n/a	n/a	236	n/a	30.9	52.6	9.8	22.4	42.0	61.5	76.1	86.7	92.4	95.6	97.1	98.0	98.8	99.3	99.5	99.8	99.9	100.0	100.0	100.0	100.0	100.0
14:48-15:25	EWI-9v	n/a	n/a	625	n/a	31.9	50.7	9.8	22.6	42.7	62.4	77.2	87.8	93.6	96.8	98.2	98.8	99.4	99.7	99.8	99.9	100.0	100.0	100.0	100.0	100.0	100.0
15:22	v1 4DI	2.59	n/a	68	0.541	39.1	51.0	11.2	24.4	44.4	63.7	78.2	88.3	93.7	96.6	97.8	98.6	99.6	99.9	100.0	100.0	100.0	100.0	100.0	100.0	100.0	
15:18	v2 2DI	7.32	n/a	93	0.496	30.1	50.7	8.9	20.9	40.1	59.5	74.2	84.9	90.7	94.1	95.8	96.9	98.2	99.0	99.4	99.8	99.9	100.0	100.0	100.0	100.0	
15:14	v3 2DI	6.71	n/a	84	0.550	31.8	53.1	8.9	20.7	39.8	59.2	74.3	85.6	92.2	96.3	98.1	98.9	99.7	99.9	100.0	100.0	100.0	100.0	100.0	100.0	100.0	
15:10	v4 2DI	6.10	n/a	77	0.716	33.9	43.8	10.5	24.1	44.9	64.8	79.3	89.7	95.7	98.8	99.9	100.0	100.0	100.0	100.0	100.0	100.0	100.0	100.0	100.0	100.0	
15:05	v5 2DI	5.64	n/a	71	0.753	25.1	48.8	10.0	22.3	41.6	60.7	75.4	86.0	91.3	94.2	96.0	97.2	98.2	98.9	99.2	99.7	99.9	100.0	100.0	100.0	100.0	
15:01	v6 2DI	5.79	n/a	71	0.687	28.5	48.2	10.1	23.7	44.9	65.4	80.4	90.9	96.4	99.1	99.9	100.0	100.0	100.0	100.0	100.0	100.0	100.0	100.0	100.0	100.0	
14:56	v7 2DI	5.94	n/a	75	0.707	31.7	53.0	9.3	22.1	42.3	62.1	77.0	87.9	93.7	96.9	98.0	98.6	99.6	99.9	100.0	100.0	100.0	100.0	100.0	100.0	100.0	
14:52	v8 2DI	5.79	n/a	72	0.524	40.2	60.1	10.6	23.9	44.5	64.4	78.9	89.4	95.4	98.8	99.9	100.0	100.0	100.0	100.0	100.0	100.0	100.0	100.0	100.0	100.0	
14:48	v9 4DI	3.96	n/a	95	0.401	35.0	51.2	9.8	22.9	43.6	63.7	78.4	88.4	93.7	96.8	98.2	98.8	99.7	99.9	100.0	100.0	100.0	100.0	100.0	100.0	100.0	

Notes: EW1-5v = 5-vertical EW1 measurement mathematically composited using raw laboratory data from verticals 1, 3, 5, 7, and 9; EW1-3v = 3-vertical quasi-EW1 measurement mathematically composited using raw laboratory data from verticals 2, 5, and 8; EW1-9v = 9-vertical quasi-EW1 measurement mathematically composited using raw laboratory data from all 9 verticals; DI = depth-integrated (nozzle open during downward and upward transits); v1 through v9 refer to verticals 1 through 9; number preceding DI indicates the number of transits at each vertical.

D-77-bag-type noncomposited multivertical suspended-sediment samples collected at River-mile 30 sediment station cross section A on August 24, 2007;
 verticals 1 through 9 located respectively at stations 78, 100, 122, 144, 165, 187, 209, 231, and 252 ft from the left-bank end point of the tagline, left and right edges of water are respectively at 56 and 274 ft from the left-bank end point of the tagline,
 left-bank end point of tagline is approximately 30 ft farther from the river than the end point used in February 2007

Time (MST)	Sample type	Water depth (m)	Sample elevation above bed (m)	Sample collection time (s)	DI intake velocity (m/s)	Silt and clay conc. (mg/L)	Sand conc. (mg/L)	Grain-size analysis of sand (0.0625-2.0 mm) fraction																			
								% sand < 0.074 mm	% sand < 0.088 mm	% sand < 0.105 mm	% sand < 0.125 mm	% sand < 0.149 mm	% sand < 0.177 mm	% sand < 0.210 mm	% sand < 0.250 mm	% sand < 0.297 mm	% sand < 0.354 mm	% sand < 0.420 mm	% sand < 0.500 mm	% sand < 0.595 mm	% sand < 0.707 mm	% sand < 0.841 mm	% sand < 1.00 mm	% sand < 1.19 mm	% sand < 1.41 mm	% sand < 1.68 mm	% sand < 2.00 mm
15:44-16:18	EWI-5v	n/a	n/a	321	n/a	28.7	89.3	6.8	15.9	31.3	47.8	61.9	74.0	82.7	89.4	93.8	96.5	98.2	99.2	99.5	99.8	99.9	100.0	100.0	100.0	100.0	100.0
15:48-16:13	EWI-3v	n/a	n/a	219	n/a	36.1	98.3	6.6	15.6	30.7	46.9	60.9	73.1	82.0	89.1	94.0	96.9	98.8	99.8	100.0	100.0	100.0	100.0	100.0	100.0	100.0	100.0
15:44-16:18	EWI-9v	n/a	n/a	619	n/a	31.9	89.5	6.6	15.7	31.2	48.0	62.3	74.5	83.0	89.5	94.0	96.6	98.3	99.2	99.5	99.8	99.9	100.0	100.0	100.0	100.0	100.0
15:44	v1 4DI	4.11	n/a	83	0.300	35.1	72.6	7.8	17.9	34.2	51.8	66.5	78.4	85.7	90.7	93.7	95.4	96.6	96.9	97.5	98.9	99.6	100.0	100.0	100.0	100.0	100.0
15:48	v2 2DI	7.01	n/a	87	0.284	44.6	84.4	7.1	17.2	34.0	51.9	66.5	78.4	86.2	92.0	95.6	97.5	99.2	99.9	100.0	100.0	100.0	100.0	100.0	100.0	100.0	100.0
15:52	v3 2DI	8.08	n/a	104	0.488	24.2	76.9	7.4	17.5	34.1	51.6	66.0	77.9	85.9	91.7	95.3	97.4	98.9	99.8	99.9	100.0	100.0	100.0	100.0	100.0	100.0	100.0
15:55	v4 2DI	7.77	n/a	84	0.463	35.0	80.5	7.0	17.0	34.1	52.7	68.3	80.8	88.2	93.0	96.1	97.9	99.2	99.8	100.0	100.0	100.0	100.0	100.0	100.0	100.0	100.0
16:00	v5 2DI	6.71	n/a	85	0.465	29.3	109	6.2	14.3	28.1	43.1	56.6	69.0	78.8	87.0	92.9	96.4	98.5	99.7	99.9	100.0	100.0	100.0	100.0	100.0	100.0	100.0
16:04	v6 2DI	6.55	n/a	81	0.569	29.0	100	5.5	13.4	27.0	42.3	55.9	68.4	77.8	85.6	91.8	95.5	97.4	98.6	99.2	99.7	99.9	100.0	100.0	100.0	100.0	100.0
16:07	v7 2DI	5.49	n/a	68	0.359	33.4	91.2	6.2	15.1	30.5	47.4	61.6	73.8	82.6	89.1	92.9	95.1	96.9	98.1	98.6	99.4	99.7	100.0	100.0	100.0	100.0	100.0
16:11	v8 4DI	3.96	n/a	93	0.197	42.3	88.1	7.7	18.3	35.8	54.4	69.6	81.4	88.6	93.4	96.2	97.9	99.4	99.9	100.0	100.0	100.0	100.0	100.0	100.0	100.0	100.0
16:15	v9 8DI	1.83	n/a	88	0.071	39.2	88.7	9.0	22.1	43.5	68.2	87.5	97.3	99.9	100.0	100.0	100.0	100.0	100.0	100.0	100.0	100.0	100.0	100.0	100.0	100.0	100.0

Notes: EW1-5v = 5-vertical EWI measurement mathematically composited using raw laboratory data from verticals 1, 3, 5, 7, and 9; EW1-3v = 3-vertical quasi-EWI measurement mathematically composited using raw laboratory data from verticals 2, 5, and 8; EW1-9v = 9-vertical quasi-EWI measurement mathematically composited using raw laboratory data from all 9 verticals; DI = depth-integrated (nozzle open during downward and upward transits); v1 through v9 refer to verticals 1 through 9; number preceding DI indicates the number of transits at each vertical.

D-77-bag-type noncomposited multivertical suspended-sediment samples collected at River-mile 30 sediment station cross section B on August 24, 2007;
 verticals 1 through 9 located respectively at stations 44, 67, 91, 114, 138, 161, 185, 208, and 232 ft from the left-bank end point of the tagline, left and right edges of water are respectively at 20 and 255 ft from the left-bank end point of the tagline

Time (MST)	Sample type	Water depth (m)	Sample elevation above bed (m)	Sample collection time (s)	DI intake velocity (m/s)	Silt and clay conc. (mg/L)	Sand conc. (mg/L)	Grain-size analysis of sand (0.0625-2.0 mm) fraction																			
								% sand < 0.074 mm	% sand < 0.088 mm	% sand < 0.105 mm	% sand < 0.125 mm	% sand < 0.149 mm	% sand < 0.177 mm	% sand < 0.210 mm	% sand < 0.250 mm	% sand < 0.297 mm	% sand < 0.354 mm	% sand < 0.420 mm	% sand < 0.500 mm	% sand < 0.595 mm	% sand < 0.707 mm	% sand < 0.841 mm	% sand < 1.00 mm	% sand < 1.19 mm	% sand < 1.41 mm	% sand < 1.68 mm	% sand < 2.00 mm
16:23-16:55	EWI-5v	n/a	n/a	308	n/a	36.5	87.2	7.5	17.7	35.0	53.7	69.1	81.5	89.1	93.9	96.5	97.7	98.6	99.0	99.2	99.7	99.9	100.0	100.0	100.0	100.0	100.0
16:26-16:51	EWI-3v	n/a	n/a	234	n/a	33.4	93.0	7.2	17.3	34.7	54.0	70.3	83.2	90.6	95.2	97.6	98.7	99.5	99.9	100.0	100.0	100.0	100.0	100.0	100.0	100.0	100.0
16:23-16:55	EWI-9v	n/a	n/a	620	n/a	33.2	93.5	7.5	17.8	35.3	54.0	69.5	82.0	89.6	94.4	96.9	98.1	99.0	99.4	99.6	99.8	99.9	100.0	100.0	100.0	100.0	100.0
16:23	v1 4DI	2.44	n/a	59	0.318	31.5	87.3	7.6	17.5	34.3	53.0	68.8	81.3	88.9	93.7	96.2	97.7	99.4	99.9	100.0	100.0	100.0	100.0	100.0	100.0	100.0	100.0
16:26	v2 2DI	7.32	n/a	93	0.336	30.6	70.5	7.9	19.1	38.1	58.4	74.5	86.2	92.3	95.7	97.2	98.2	99.3	99.9	100.0	100.0	100.0	100.0	100.0	100.0	100.0	100.0
16:30	v3 2DI	6.71	n/a	84	0.350	40.9	91.2	7.3	17.1	33.3	51.0	66.1	78.8	87.2	92.9	96.0	97.5	98.6	99.1	99.3	99.7	99.9	100.0	100.0	100.0	100.0	100.0
16:34	v4 2DI	6.10	n/a	77	0.452	31.3	65.7	8.1	20.0	40.3	61.1	76.9	88.8	95.7	99.0	99.9	100.0	100.0	100.0	100.0	100.0	100.0	100.0	100.0	100.0	100.0	100.0
16:38	v5 2DI	5.64	n/a	70	0.332	35.5	91.0	7.6	18.1	36.1	55.8	72.5	85.5	92.6	96.9	99.2	99.9	100.0	100.0	100.0	100.0	100.0	100.0	100.0	100.0	100.0	100.0
16:41	v6 2DI	5.79	n/a	71	0.460	25.1	144	7.7	17.9	34.6	52.2	66.8	79.3	87.4	93.0	96.2	97.9	98.9	99.7	99.9	100.0	100.0	100.0	100.0	100.0	100.0	100.0
16:45	v7 2DI	5.94	n/a	77	0.434	33.1	83.7	6.9	16.8	33.7	52.0	67.2	79.5	87.0	91.8	94.5	95.9	96.9	97.4	97.9	99.1	99.7	100.0	100.0	100.0	100.0	100.0
16:49	v8 2DI	5.79	n/a	71	0.381	34.7	121	6.6	15.6	31.6	49.9	66.1	79.7	88.2	93.7	96.7	98.2	99.2	99.8	100.0	100.0	100.0	100.0	100.0	100.0	100.0	100.0
16:53	v9 4DI	3.96	n/a	95	0.319	40.0	81.0	8.9	21.0	40.5	59.9	74.5	85.4	91.9	95.9	97.4	98.1	99.3	99.9	100.0	100.0	100.0	100.0	100.0	100.0	100.0	100.0

Notes: EW1-5v = 5-vertical EWI measurement mathematically composited using raw laboratory data from verticals 1, 3, 5, 7, and 9; EW1-3v = 3-vertical quasi-EWI measurement mathematically composited using raw laboratory data from verticals 2, 5, and 8; EW1-9v = 9-vertical quasi-EWI measurement mathematically composited using raw laboratory data from all 9 verticals; DI = depth-integrated (nozzle open during downward and upward transits); v1 through v9 refer to verticals 1 through 9; number preceding DI indicates the number of transits at each vertical.

D-96-A1 noncomposited multivertical suspended-sediment samples collected at River-mile 30 sediment station cross section A on August 25, 2007; verticals 1 through 9 located respectively at stations 78, 100, 122, 144, 165, 187, 209, 231, and 252 ft from the left-bank end point of the tagline, left and right edges of water are respectively at 56 and 274 ft from the left-bank end point of the tagline, left-bank end point of tagline is approximately 30 ft farther from the river than the end point used in February 2007																											
Time (MST)	Sample type	Water depth (m)	Sample elevation above bed (m)	Sample collection time (s)	DI intake velocity (m/s)	Silt and clay conc. (mg/L)	Sand conc. (mg/L)	Gran-size analysis of sand (0.0625-2.0 mm) fraction																			
								% sand < 0.074 mm	% sand < 0.088 mm	% sand < 0.105 mm	% sand < 0.125 mm	% sand < 0.149 mm	% sand < 0.177 mm	% sand < 0.210 mm	% sand < 0.250 mm	% sand < 0.297 mm	% sand < 0.354 mm	% sand < 0.420 mm	% sand < 0.500 mm	% sand < 0.595 mm	% sand < 0.707 mm	% sand < 0.841 mm	% sand < 1.00 mm	% sand < 1.19 mm	% sand < 1.41 mm	% sand < 1.68 mm	% sand < 2.00 mm
10:27-11:06	EWI-5v	n/a	n/a	323	n/a	24.3	73.3	7.6	17.3	33.1	50.1	64.7	77.4	86.0	92.2	96.2	98.3	99.3	99.9	100.0	100.0	100.0	100.0	100.0	100.0	100.0	100.0
10:30-11:02	EWI-3v	n/a	n/a	226	n/a	24.0	72.0	7.9	17.9	34.1	51.2	65.8	78.3	86.6	92.6	96.3	98.1	99.2	99.8	99.9	100.0	100.0	100.0	100.0	100.0	100.0	100.0
10:27-11:06	EWI-9v	n/a	n/a	648	n/a	24.9	74.9	7.6	17.5	33.7	51.0	65.7	78.3	86.6	92.5	96.2	98.1	99.2	99.8	99.9	100.0	100.0	100.0	100.0	100.0	100.0	100.0
10:27	v1 2DI	3.75	n/a	48	0.540	24.9	67.3	7.2	17.2	33.9	52.4	68.3	81.5	90.2	96.0	99.1	99.9	100.0	100.0	100.0	100.0	100.0	100.0	100.0	100.0	100.0	100.0
10:30	v2 2DI	7.16	n/a	91	0.722	22.5	73.2	8.1	18.2	34.2	51.2	65.8	78.3	86.8	92.7	96.4	98.1	99.1	99.7	99.9	99.9	100.0	100.0	100.0	100.0	100.0	100.0
10:34	v3 2DI	8.23	n/a	104	0.717	23.4	76.2	7.7	17.3	32.6	49.0	63.4	76.0	84.6	91.0	95.4	98.0	99.2	99.8	100.0	100.0	100.0	100.0	100.0	100.0	100.0	100.0
10:39	v4 2DI	7.92	n/a	100	0.803	28.0	84.9	7.1	16.8	33.1	50.5	65.4	78.1	86.4	92.3	95.8	97.7	98.9	99.6	99.8	99.9	100.0	100.0	100.0	100.0	100.0	100.0
10:44	v5 2DI	6.86	n/a	85	0.617	24.7	73.1	7.6	17.5	33.5	50.6	65.0	77.5	86.0	92.2	96.2	98.2	99.3	99.9	100.0	100.0	100.0	100.0	100.0	100.0	100.0	100.0
10:49	v6 2DI	6.71	n/a	84	0.651	24.5	70.9	7.9	18.4	35.6	53.7	68.7	80.9	88.5	93.4	96.2	97.9	99.1	99.8	100.0	100.0	100.0	100.0	100.0	100.0	100.0	100.0
10:54	v7 4DI	5.64	n/a	140	0.310	22.6	78.4	7.5	17.0	33.0	50.2	65.0	77.8	86.4	92.4	95.8	97.5	99.0	99.8	100.0	100.0	100.0	100.0	100.0	100.0	100.0	100.0
11:00	v8 4DI	4.11	n/a	99	0.276	28.5	62.1	8.3	19.0	36.0	54.2	69.3	81.4	89.0	93.9	96.6	98.1	99.2	99.8	100.0	100.0	100.0	100.0	100.0	100.0	100.0	100.0
11:05	v9 4DI	1.98	n/a	32	0.186	49.9	19.6	---	---	---	---	---	---	---	---	---	---	---	---	---	---	---	---	---	---	---	---

Notes: EWI-5v = 5-vertical EWI measurement mathematically composited using raw laboratory data from verticals 1, 3, 5, 7, and 9; EWI-3v = 3-vertical quasi-EWI measurement mathematically composited using raw laboratory data from verticals 2, 5, and 8; EWI-9v = 9-vertical quasi-EWI measurement mathematically composited using raw laboratory data from all 9 verticals; DI = depth-integrated (nozzle open during downward and upward transits); v1 through v9 refer to verticals 1 through 9; number preceding DI indicates the number of transits at each vertical.

P-61 suspended-sediment samples collected at Lower Marble Canyon gaging station cross section C on August 11, 2006; vertical located at the station 295 ft from the former right-bank end point of the cableway																											
Time (MST)	Sample type	Water depth (m)	Sample elevation above bed (m)	Sample collection time (s)	Point intake velocity (m/s)	Silt and clay conc. (mg/L)	Sand conc. (mg/L)	Grain-size analysis of sand (0.0625-2.0 mm) fraction																			
								% sand < 0.074 mm	% sand < 0.088 mm	% sand < 0.105 mm	% sand < 0.125 mm	% sand < 0.149 mm	% sand < 0.177 mm	% sand < 0.210 mm	% sand < 0.250 mm	% sand < 0.297 mm	% sand < 0.354 mm	% sand < 0.420 mm	% sand < 0.500 mm	% sand < 0.595 mm	% sand < 0.707 mm	% sand < 0.841 mm	% sand < 1.00 mm	% sand < 1.19 mm	% sand < 1.41 mm	% sand < 1.68 mm	% sand < 2.00 mm
10:56	Point	4.33	0.47	30.10	0.844	60.2	170	8.3	18.8	35.1	51.9	65.8	77.5	85.6	91.5	95.2	97.0	98.4	99.3	99.8	99.9	100.0	100.0	100.0	100.0	100.0	100.0
10:59	Point	4.33	0.47	30.40	0.893	55.8	148	9.9	21.7	39.1	56.2	69.7	80.7	88.0	93.2	96.2	97.6	98.7	99.7	99.9	100.0	100.0	100.0	100.0	100.0	100.0	100.0
11:01	Point	4.33	0.47	30.30	0.845	54.7	135	8.7	19.5	36.1	52.9	66.7	78.2	86.2	91.9	95.1	96.8	98.6	99.7	99.9	100.0	100.0	100.0	100.0	100.0	100.0	100.0
11:05	Point	4.33	1.18	30.40	0.990	51.1	103	11.0	24.2	43.5	61.9	76.0	86.8	93.6	97.9	99.7	100.0	100.0	100.0	100.0	100.0	100.0	100.0	100.0	100.0	100.0	100.0
11:07	Point	4.33	1.18	30.20	1.037	49.4	102	10.1	22.4	40.7	58.0	71.3	81.7	88.4	93.2	95.9	97.5	99.1	99.8	100.0	100.0	100.0	100.0	100.0	100.0	100.0	100.0
11:10	Point	4.33	1.18	25.00	1.109	44.4	103	10.7	23.0	40.7	57.4	70.4	80.8	87.6	92.6	95.7	97.6	99.3	99.9	100.0	100.0	100.0	100.0	100.0	100.0	100.0	100.0
11:13	Point	4.33	1.69	25.20	1.148	47.4	80.1	13.2	28.1	48.6	66.6	79.2	87.8	92.6	95.7	97.3	98.3	99.5	99.9	100.0	100.0	100.0	100.0	100.0	100.0	100.0	100.0
11:16	Point	4.33	1.69	25.30	1.217	44.9	81.9	13.3	27.9	47.5	64.4	76.1	83.9	88.4	91.3	92.6	93.1	94.1	94.3	95.5	98.0	99.3	100.0	100.0	100.0	100.0	100.0
11:18	Point	4.33	1.69	23.20	1.199	44.1	79.4	12.9	27.6	47.9	66.3	80.3	90.2	95.8	98.8	99.9	100.0	100.0	100.0	100.0	100.0	100.0	100.0	100.0	100.0	100.0	100.0
11:20	Point	4.33	2.15	19.70	1.024	43.3	62.2	10.5	23.9	43.9	61.8	74.5	83.4	88.8	92.4	93.8	94.8	97.3	99.0	99.7	99.9	100.0	100.0	100.0	100.0	100.0	100.0
11:22	Point	4.33	2.15	23.00	1.127	44.7	82.3	11.3	24.9	44.5	62.4	75.7	85.4	91.3	95.2	97.1	98.1	99.5	99.9	100.0	100.0	100.0	100.0	100.0	100.0	100.0	100.0
11:24	Point	4.33	2.15	23.00	1.172	40.0	54.5	11.8	26.4	47.3	66.3	80.4	89.7	95.1	98.5	99.8	100.0	100.0	100.0	100.0	100.0	100.0	100.0	100.0	100.0	100.0	100.0
11:27	Point	4.33	3.22	23.20	1.031	36.2	53.0	12.1	27.5	50.0	70.1	83.9	92.8	97.3	99.3	100.0	100.0	100.0	100.0	100.0	100.0	100.0	100.0	100.0	100.0	100.0	100.0
11:29	Point	4.33	3.22	22.90	1.177	52.7	58.3	15.0	31.5	53.7	72.5	85.1	93.1	97.2	99.2	99.9	100.0	100.0	100.0	100.0	100.0	100.0	100.0	100.0	100.0	100.0	100.0
11:31	Point	4.33	3.22	30.00	1.024	49.0	62.1	14.9	31.6	53.9	72.8	85.6	93.5	97.3	99.2	99.9	100.0	100.0	100.0	100.0	100.0	100.0	100.0	100.0	100.0	100.0	100.0

Notes: Water depths associated with the point samples are the mean water depths at this vertical during the collection of the 18 point samples; point-sample elevations are relative to the mean bed elevation associated with this mean water depth.

P-61 suspended-sediment samples collected at Lower Marble Canyon gaging station cross section C on August 11, 2006; vertical located at the station 165 ft from the former right-bank end point of the cableway																											
Time (MST)	Sample type	Water depth (m)	Sample elevation above bed (m)	Sample collection time (s)	Point intake velocity (m/s)	Silt and clay conc. (mg/L)	Sand conc. (mg/L)	Grain-size analysis of sand (0.0625-2.0 mm) fraction																			
								% sand < 0.074 mm	% sand < 0.088 mm	% sand < 0.105 mm	% sand < 0.125 mm	% sand < 0.149 mm	% sand < 0.177 mm	% sand < 0.210 mm	% sand < 0.250 mm	% sand < 0.297 mm	% sand < 0.354 mm	% sand < 0.420 mm	% sand < 0.500 mm	% sand < 0.595 mm	% sand < 0.707 mm	% sand < 0.841 mm	% sand < 1.00 mm	% sand < 1.19 mm	% sand < 1.41 mm	% sand < 1.68 mm	% sand < 2.00 mm
11:35	Point	4.97	0.81	29.50	0.912	51.0	174	6.4	15.5	30.8	47.1	61.3	73.7	82.6	89.5	94.3	97.0	98.5	99.6	99.8	99.9	100.0	100.0	100.0	100.0	100.0	100.0
11:37	Point	4.97	0.81	29.70	1.116	50.7	146	7.9	17.3	31.4	46.1	58.7	70.2	79.2	86.9	92.8	96.6	98.7	99.7	99.9	100.0	100.0	100.0	100.0	100.0	100.0	100.0
11:40	Point	4.97	0.81	27.10	0.976	52.4	171	6.6	15.4	29.4	44.5	58.1	70.5	79.8	87.6	93.1	96.3	98.0	98.9	99.3	99.7	99.9	100.0	100.0	100.0	100.0	100.0
11:43	Point	4.97	1.36	28.20	0.940	65.7	130	8.4	19.3	36.0	53.0	67.1	78.7	86.7	92.7	96.4	98.2	99.5	99.9	100.0	100.0	100.0	100.0	100.0	100.0	100.0	100.0
11:45	Point	4.97	1.36	25.90	0.927	53.9	159	7.6	17.7	33.7	50.2	64.4	76.6	85.3	91.8	95.9	98.0	99.5	99.9	100.0	100.0	100.0	100.0	100.0	100.0	100.0	100.0
11:47	Point	4.97	1.36	26.40	1.152	52.1	116	8.9	20.1	37.4	54.7	68.7	80.2	88.0	93.6	96.9	98.2	99.3	99.9	100.0	100.0	100.0	100.0	100.0	100.0	100.0	100.0
11:50	Point	4.97	1.88	24.90	1.228	36.0	76.7	10.2	23.1	42.5	61.2	75.5	86.5	93.3	97.9	99.7	100.0	100.0	100.0	100.0	100.0	100.0	100.0	100.0	100.0	100.0	100.0
11:52	Point	4.97	1.88	23.00	1.286	44.1	95.8	11.4	24.7	43.6	60.9	73.9	83.8	90.1	94.4	96.5	97.8	99.4	99.9	100.0	100.0	100.0	100.0	100.0	100.0	100.0	100.0
11:54	Point	4.97	1.88	24.00	1.059	51.0	107	8.2	18.7	34.9	51.3	64.8	76.6	85.4	92.3	96.2	98.1	99.6	99.9	100.0	100.0	100.0	100.0	100.0	100.0	100.0	100.0
11:57	Point	4.97	2.82	22.80	1.385	54.3	52.3	12.2	27.0	48.7	68.3	82.0	90.9	95.7	98.8	99.9	100.0	100.0	100.0	100.0	100.0	100.0	100.0	100.0	100.0	100.0	100.0
11:59	Point	4.97	2.82	19.70	1.201	44.4	81.5	10.4	23.5	43.2	61.9	76.1	86.6	93.4	97.9	99.8	100.0	100.0	100.0	100.0	100.0	100.0	100.0	100.0	100.0	100.0	100.0
12:01	Point	4.97	2.82	20.70	1.198	55.4	92.3	9.5	21.2	39.4	57.5	72.2	84.1	92.0	97.4	99.7	100.0	100.0	100.0	100.0	100.0	100.0	100.0	100.0	100.0	100.0	100.0
12:03	Point	4.97	3.86	24.70	1.212	42.2	43.0	15.3	32.2	54.8	73.8	86.1	93.4	97.0	99.1	99.9	100.0	100.0	100.0	100.0	100.0	100.0	100.0	100.0	100.0	100.0	100.0
12:05	Point	4.97	3.86	22.30	1.397	49.6	50.6	11.8	27.0	48.7	68.2	82.1	91.3	96.6	99.1	99.9	100.0	100.0	100.0	100.0	100.0	100.0	100.0	100.0	100.0	100.0	100.0
12:08	Point	4.97	3.86	22.10	1.248	54.5	60.8	11.1	24.4	44.1	62.6	76.9	87.6	94.0	98.2	99.8	100.0	100.0	100.0	100.0	100.0	100.0	100.0	100.0	100.0	100.0	100.0

Notes: Water depths associated with the point samples are the mean water depths at this vertical during the collection of the 18 point samples; point-sample elevations are relative to the mean bed elevation associated with this mean water depth.

D-96-A1 noncomposited multivertical suspended-sediment samples collected at Lower Marble Canyon gaging station cross section C on February 27, 2007; verticals 1 through 9 located respectively at stations 84, 118, 151, 185, 219, 253, 287, 321, and 354 ft from the left-bank end point of the tagline, left and right edges of water are respectively at 50 and 388 ft from the left-bank end point of the tagline																										
Time (MST)	Sample type	Water depth (m)	Sample elevation above bed (m)	Sample collection time (s)	DI intake velocity (m/s)	Silt and clay conc. (mg/L)	Sand conc. (mg/L)	Grain-size analysis of sand (0.0625-2.0 mm) fraction																		
								% sand < 0.074 mm	% sand < 0.088 mm	% sand < 0.105 mm	% sand < 0.125 mm	% sand < 0.149 mm	% sand < 0.177 mm	% sand < 0.210 mm	% sand < 0.250 mm	% sand < 0.297 mm	% sand < 0.354 mm	% sand < 0.420 mm	% sand < 0.500 mm	% sand < 0.595 mm	% sand < 0.707 mm	% sand < 0.841 mm	% sand < 1.00 mm	% sand < 1.19 mm	% sand < 1.41 mm	% sand < 1.68 mm
17:21-18:55	EWI-5v	n/a	n/a	840	n/a	49.9	34.9	20.8	40.7	62.5	77.1	85.0	89.3	91.7	93.7	95.7	97.5	99.0	99.5	99.7	99.9	99.9	100.0	100.0	100.0	100.0
17:28-18:49	EWI-3v	n/a	n/a	602	n/a	43.8	28.8	21.1	41.1	63.0	77.3	84.9	88.8	90.9	92.8	95.0	97.0	98.6	99.3	99.6	99.8	99.9	100.0	100.0	100.0	100.0
17:21-18:55	EWI-9v	n/a	n/a	1660	n/a	47.5	35.2	21.7	41.5	63.0	77.3	85.2	89.5	91.8	93.8	95.7	97.5	99.0	99.5	99.7	99.9	100.0	100.0	100.0	100.0	100.0
17:21	v1 8DI	1.89	n/a	84	0.189	50.4	34.6	23.6	44.8	67.6	82.8	91.4	95.9	98.0	99.3	99.9	100.0	100.0	100.0	100.0	100.0	100.0	100.0	100.0	100.0	100.0
17:28	v2 8DI	3.20	n/a	149	0.434	42.9	41.1	18.3	39.1	64.0	81.0	89.7	93.8	95.4	96.4	96.8	97.1	97.7	98.3	98.8	99.5	99.8	100.0	100.0	100.0	100.0
17:36	v3 8DI	3.35	n/a	172	0.598	53.6	43.1	22.1	41.5	62.0	75.8	83.6	87.7	89.9	92.3	94.7	97.1	99.3	99.9	100.0	100.0	100.0	100.0	100.0	100.0	100.0
17:44	v4 8DI	4.08	n/a	206	0.583	53.1	38.0	18.6	38.0	59.5	74.3	83.0	87.8	90.3	92.6	95.0	97.3	99.2	99.9	100.0	100.0	100.0	100.0	100.0	100.0	100.0
17:56	v5 8DI	4.48	n/a	209	0.891	50.4	29.0	21.1	41.5	63.3	77.3	84.8	88.6	90.8	93.0	95.5	97.7	99.4	99.9	100.0	100.0	100.0	100.0	100.0	100.0	100.0
18:09	v6 8DI	4.42	n/a	221	0.777	49.2	42.0	25.9	46.1	66.5	79.7	87.0	91.2	93.9	95.9	97.2	98.6	99.7	99.9	100.0	100.0	100.0	100.0	100.0	100.0	100.0
18:29	v7 8DI	4.27	n/a	219	0.544	49.8	40.7	18.5	37.7	60.0	75.6	84.3	89.6	92.4	94.4	95.8	96.9	98.1	98.6	99.0	99.5	99.8	100.0	100.0	100.0	100.0
18:40	v8 8DI	4.72	n/a	244	0.594	35.7	23.0	23.1	42.0	61.7	74.5	81.2	85.1	87.4	89.7	92.7	95.9	97.9	99.1	99.7	99.8	100.0	100.0	100.0	100.0	100.0
18:50	v9 8DI	3.35	n/a	156	0.199	34.6	20.7	24.7	48.4	73.6	89.6	96.9	99.6	100.0	100.0	100.0	100.0	100.0	100.0	100.0	100.0	100.0	100.0	100.0	100.0	100.0

Notes: EWI-5v = 5-vertical EWI measurement mathematically composited using raw laboratory data from verticals 1, 3, 5, 7, and 9; EWI-3v = 3-vertical quasi-EWI measurement mathematically composited using raw laboratory data from verticals 2, 5, and 8; EWI-9v = 9-vertical quasi-EWI measurement mathematically composited using raw laboratory data from all 9 verticals; DI = depth-integrated (nozzle open during downward and upward transits); v1 through v9 refer to verticals 1 through 9; number preceding DI indicates the number of transits at each vertical.

D-77-bag-type noncomposited multivertical suspended-sediment samples collected at Lower Marble Canyon gaging station cross section A on February 28, 2007; verticals 1 through 9 located respectively at stations 64, 88, 112, 136, 160, 184, 208, 232, and 256 ft from the left-bank end point of the tagline, left and right edges of water are respectively at 40 and 280 ft from the left-bank end point of the tagline																											
Time (MST)	Sample type	Water depth (m)	Sample elevation above bed (m)	Sample collection time (s)	DI intake velocity (m/s)	Silt and clay conc. (mg/L)	Sand conc. (mg/L)	Grain-size analysis of sand (0.0625-2.0 mm) fraction																			
								% sand < 0.074 mm	% sand < 0.088 mm	% sand < 0.105 mm	% sand < 0.125 mm	% sand < 0.149 mm	% sand < 0.177 mm	% sand < 0.210 mm	% sand < 0.250 mm	% sand < 0.297 mm	% sand < 0.354 mm	% sand < 0.420 mm	% sand < 0.500 mm	% sand < 0.595 mm	% sand < 0.707 mm	% sand < 0.841 mm	% sand < 1.00 mm	% sand < 1.19 mm	% sand < 1.41 mm	% sand < 1.68 mm	% sand < 2.00 mm
11:12-12:03	EWI-5v	n/a	n/a	343	n/a	28.3	50.1	10.8	23.7	41.5	57.7	69.9	79.1	85.0	89.8	93.9	97.2	99.3	99.9	100.0	100.0	100.0	100.0	100.0	100.0	100.0	100.0
11:15-11:56	EWI-3v	n/a	n/a	239	n/a	24.7	42.5	13.1	27.4	46.0	61.9	73.7	81.6	86.4	90.3	94.0	97.4	99.5	99.9	100.0	100.0	100.0	100.0	100.0	100.0	100.0	100.0
11:12-12:03	EWI-9v	n/a	n/a	670	n/a	24.2	44.0	12.0	25.3	43.2	58.8	70.6	79.1	84.6	89.1	93.3	96.9	99.2	99.9	100.0	100.0	100.0	100.0	100.0	100.0	100.0	100.0
11:12	v1 6DI	1.98	n/a	36	0.377	21.7	28.5	11.0	26.1	48.9	70.4	84.4	94.1	98.2	99.8	100.0	100.0	100.0	100.0	100.0	100.0	100.0	100.0	100.0	100.0	100.0	
11:15	v2 6DI	3.05	n/a	49	0.743	21.1	31.0	14.7	30.8	52.4	71.0	83.7	92.1	96.5	99.0	99.9	100.0	100.0	100.0	100.0	100.0	100.0	100.0	100.0	100.0	100.0	
11:20	v3 6DI	3.05	n/a	52	0.804	17.9	34.3	12.0	27.0	48.2	66.6	79.4	88.3	93.3	96.5	98.0	98.8	99.7	99.9	100.0	100.0	100.0	100.0	100.0	100.0	100.0	
11:24	v4 6DI	4.27	n/a	75	0.713	22.3	41.8	12.6	25.6	42.0	55.9	66.7	74.2	79.3	84.2	89.8	95.8	99.0	99.9	100.0	100.0	100.0	100.0	100.0	100.0	100.0	
11:31	v5 6DI	5.36	n/a	87	0.507	35.3	56.5	12.4	26.1	43.9	59.2	71.0	78.9	83.6	87.7	92.2	96.8	99.4	99.9	100.0	100.0	100.0	100.0	100.0	100.0	100.0	
11:39	v6 6DI	6.10	n/a	100	0.904	20.4	40.4	13.0	26.5	43.8	58.5	69.4	77.2	82.4	87.1	91.5	95.6	98.7	99.8	100.0	100.0	100.0	100.0	100.0	100.0	100.0	
11:47	v7 6DI	6.31	n/a	107	0.605	32.2	69.2	9.7	20.7	35.9	50.0	61.6	71.2	78.4	85.0	90.9	95.8	98.8	99.8	100.0	100.0	100.0	100.0	100.0	100.0	100.0	
11:54	v8 6DI	6.25	n/a	103	0.762	20.4	39.9	13.1	27.2	45.3	60.8	72.2	80.1	85.0	89.3	93.3	97.0	99.3	99.9	100.0	100.0	100.0	100.0	100.0	100.0	100.0	
12:02	v9 6DI	3.81	n/a	61	0.675	27.3	36.3	10.6	24.8	46.2	66.2	80.4	90.5	95.9	98.9	99.9	100.0	100.0	100.0	100.0	100.0	100.0	100.0	100.0	100.0	100.0	

Notes: EWI-5v = 5-vertical EWI measurement mathematically composited using raw laboratory data from verticals 1, 3, 5, 7, and 9; EWI-3v = 3-vertical quasi-EWI measurement mathematically composited using raw laboratory data from verticals 2, 5, and 8; EWI-9v = 9-vertical quasi-EWI measurement mathematically composited using raw laboratory data from all 9 verticals; DI = depth-integrated (nozzle open during downward and upward transits); v1 through v9 refer to verticals 1 through 9; number preceding DI indicates the number of transits at each vertical.

D-77-bag-type noncomposited multivertical suspended-sediment samples collected at Lower Marble Canyon gaging station cross section B on February 28, 2007;																											
verticals 1 through 9 located respectively at stations 97, 130, 165, 196, 229, 262, 295, 328, and 361 ft from the left-bank end point of the tagline, left and right edges of water are respectively at 64 and 396 ft from the left-bank end point of the tagline									Grain-size analysis of sand (0.0625-2.0 mm) fraction																		
Time (MST)	Sample type	Water depth (m)	Sample elevation above bed (m)	Sample collection time (s)	DI intake velocity (m/s)	Silt and clay conc. (mg/L)	Sand conc. (mg/L)	% sand < 0.074 mm	% sand < 0.088 mm	% sand < 0.105 mm	% sand < 0.125 mm	% sand < 0.149 mm	% sand < 0.177 mm	% sand < 0.210 mm	% sand < 0.250 mm	% sand < 0.297 mm	% sand < 0.354 mm	% sand < 0.420 mm	% sand < 0.500 mm	% sand < 0.595 mm	% sand < 0.707 mm	% sand < 0.841 mm	% sand < 1.00 mm	% sand < 1.19 mm	% sand < 1.41 mm	% sand < 1.68 mm	% sand < 2.00 mm
12:48-13:26	EWI-5v	n/a	n/a	245	n/a	21.5	48.7	12.3	25.9	44.4	60.6	72.4	81.0	86.6	90.8	93.8	96.2	98.2	99.1	99.5	99.8	99.9	100.0	100.0	100.0	100.0	100.0
12:55-13:23	EWI-3v	n/a	n/a	135	n/a	21.9	43.4	15.1	30.8	50.6	66.6	77.4	84.6	89.0	92.1	94.8	97.6	98.7	99.1	99.4	99.7	99.9	100.0	100.0	100.0	100.0	100.0
12:48-13:26	EWI-9v	n/a	n/a	424	n/a	21.0	43.7	13.0	27.4	46.7	63.3	74.9	83.1	88.3	92.0	94.7	97.2	98.8	99.4	99.7	99.9	99.9	100.0	100.0	100.0	100.0	100.0
12:48	v1 6DI	4.42	n/a	78	0.746	19.1	48.4	13.2	26.2	42.7	56.8	67.4	75.6	81.8	86.9	91.4	95.7	98.8	99.8	100.0	100.0	100.0	100.0	100.0	100.0	100.0	100.0
12:55	v2 6DI	3.05	n/a	51	0.862	20.7	42.2	16.1	31.2	49.3	63.8	73.8	80.5	85.2	88.9	93.0	98.2	99.7	100.0	100.0	100.0	100.0	100.0	100.0	100.0	100.0	100.0
13:00	v3 6DI	2.59	n/a	44	0.866	21.7	51.8	10.7	23.5	42.1	59.1	71.5	80.6	86.1	90.1	93.0	95.2	97.1	98.4	99.0	99.6	99.9	100.0	100.0	100.0	100.0	100.0
13:06	v4 6DI	2.83	n/a	45	0.680	18.9	30.7	11.5	26.7	48.2	67.1	79.8	88.0	92.5	95.3	96.7	98.1	99.6	99.9	100.0	100.0	100.0	100.0	100.0	100.0	100.0	100.0
13:09	v5 6DI	2.99	n/a	48	0.638	24.2	48.3	14.4	29.6	49.5	65.9	77.1	84.8	89.3	92.3	94.0	95.4	96.8	97.6	98.4	99.3	99.8	100.0	100.0	100.0	100.0	100.0
13:14	v6 6DI	2.93	n/a	47	0.575	21.1	33.6	13.1	29.5	52.5	71.9	84.6	92.7	96.9	99.1	99.9	100.0	100.0	100.0	100.0	100.0	100.0	100.0	100.0	100.0	100.0	100.0
13:17	v7 6DI	2.77	n/a	45	0.515	20.2	48.4	9.7	22.4	41.5	59.7	73.4	83.9	90.6	95.1	97.2	98.1	99.4	99.9	100.0	100.0	100.0	100.0	100.0	100.0	100.0	100.0
13:21	v8 6DI	2.26	n/a	36	0.589	20.8	38.7	14.2	31.9	55.4	74.3	86.2	93.5	97.1	99.2	99.9	100.0	100.0	100.0	100.0	100.0	100.0	100.0	100.0	100.0	100.0	100.0
13:25	v9 6DI	2.04	n/a	30	0.510	26.8	43.8	13.3	29.7	52.3	71.2	83.8	91.8	96.1	98.9	99.9	100.0	100.0	100.0	100.0	100.0	100.0	100.0	100.0	100.0	100.0	100.0

Notes: EWI-5v = 5-vertical EWI measurement mathematically composited using raw laboratory data from verticals 1, 3, 5, 7, and 9; EWI-3v = 3-vertical quasi-EWI measurement mathematically composited using raw laboratory data from verticals 2, 5, and 8; EWI-9v = 9-vertical quasi-EWI measurement mathematically composited using raw laboratory data from all 9 verticals; DI = depth-integrated (nozzle open during downward and upward transits); v1 through v9 refer to verticals 1 through 9; number preceding DI indicates the number of transits at each vertical.

D-77-bag-type noncomposited multivertical suspended-sediment samples collected at Lower Marble Canyon gaging station cross section C on February 28, 2007;																											
verticals 1 through 9 located respectively at stations 84, 118, 151, 185, 219, 253, 287, 321, and 354 ft from the left-bank end point of the tagline, left and right edges of water are respectively at 50 and 388 ft from the left-bank end point of the tagline									Grain-size analysis of sand (0.0625-2.0 mm) fraction																		
Time (MST)	Sample type	Water depth (m)	Sample elevation above bed (m)	Sample collection time (s)	DI intake velocity (m/s)	Silt and clay conc. (mg/L)	Sand conc. (mg/L)	% sand < 0.074 mm	% sand < 0.088 mm	% sand < 0.105 mm	% sand < 0.125 mm	% sand < 0.149 mm	% sand < 0.177 mm	% sand < 0.210 mm	% sand < 0.250 mm	% sand < 0.297 mm	% sand < 0.354 mm	% sand < 0.420 mm	% sand < 0.500 mm	% sand < 0.595 mm	% sand < 0.707 mm	% sand < 0.841 mm	% sand < 1.00 mm	% sand < 1.19 mm	% sand < 1.41 mm	% sand < 1.68 mm	% sand < 2.00 mm
13:33-14:14	EWI-5v	n/a	n/a	291	n/a	26.3	34.2	12.6	28.3	50.4	69.6	82.7	91.4	95.9	98.0	99.0	99.4	99.8	100.0	100.0	100.0	100.0	100.0	100.0	100.0	100.0	100.0
13:36-14:10	EWI-3v	n/a	n/a	204	n/a	23.8	36.6	12.9	27.8	48.3	66.1	78.4	87.0	92.0	95.2	96.8	97.7	98.7	99.2	99.3	99.7	99.9	100.0	100.0	100.0	100.0	100.0
13:33-14:14	EWI-9v	n/a	n/a	559	n/a	25.4	35.9	13.1	28.6	49.7	68.0	80.6	89.1	93.8	96.4	97.6	98.2	98.9	99.3	99.5	99.8	99.9	100.0	100.0	100.0	100.0	100.0
13:33	v1 6DI	1.89	n/a	33	0.236	65.3	35.2	13.6	28.3	48.1	66.3	80.6	91.7	97.3	99.6	100.0	100.0	100.0	100.0	100.0	100.0	100.0	100.0	100.0	100.0	100.0	100.0
13:36	v2 6DI	3.20	n/a	51	0.324	29.5	39.1	17.0	34.1	56.1	74.2	85.9	93.4	97.4	99.3	100.0	100.0	100.0	100.0	100.0	100.0	100.0	100.0	100.0	100.0	100.0	100.0
13:40	v3 6DI	3.35	n/a	57	0.536	26.7	33.8	13.5	30.8	54.6	74.5	87.2	94.8	98.2	99.6	100.0	100.0	100.0	100.0	100.0	100.0	100.0	100.0	100.0	100.0	100.0	100.0
13:44	v4 6DI	4.08	n/a	65	0.632	27.4	34.4	13.3	29.0	49.9	67.3	79.1	87.3	91.8	94.6	96.2	97.1	98.4	99.2	99.4	99.8	99.9	100.0	100.0	100.0	100.0	100.0
13:47	v5 6DI	4.48	n/a	75	0.789	22.4	30.7	12.4	27.4	48.4	66.4	78.7	87.1	92.1	95.3	97.2	98.3	99.5	99.9	100.0	100.0	100.0	100.0	100.0	100.0	100.0	100.0
13:57	v6 6DI	4.42	n/a	74	0.723	21.4	34.7	14.0	29.4	49.7	66.7	78.5	86.8	91.6	94.6	96.2	97.0	97.9	98.4	98.8	99.5	99.8	100.0	100.0	100.0	100.0	100.0
14:02	v7 6DI	4.27	n/a	72	0.527	24.8	38.3	10.8	25.6	47.8	68.5	83.1	93.0	97.7	99.5	100.0	100.0	100.0	100.0	100.0	100.0	100.0	100.0	100.0	100.0	100.0	100.0
14:08	v8 6DI	4.72	n/a	78	0.438	23.4	45.7	34.5	60.4	86.6	97.9	100.0	100.0	100.0	100.0	100.0	100.0	100.0	100.0	100.0	100.0	100.0	100.0	100.0	100.0	100.0	100.0
14:12	v9 6DI	3.35	n/a	54	0.238	24.3	39.1	20.7	38.6	57.4	70.2	77.4	81.2	83.9	86.7	90.1	95.9	98.8	99.8	100.0	100.0	100.0	100.0	100.0	100.0	100.0	100.0

Notes: EWI-5v = 5-vertical EWI measurement mathematically composited using raw laboratory data from verticals 1, 3, 5, 7, and 9; EWI-3v = 3-vertical quasi-EWI measurement mathematically composited using raw laboratory data from verticals 2, 5, and 8; EWI-9v = 9-vertical quasi-EWI measurement mathematically composited using raw laboratory data from all 9 verticals; DI = depth-integrated (nozzle open during downward and upward transits); v1 through v9 refer to verticals 1 through 9; number preceding DI indicates the number of transits at each vertical.

D-96-A1 noncomposited multivertical suspended-sediment samples collected at Lower Marble Canyon gaging station cross section B on August 28, 2007;																											
verticals 1 through 9 located respectively at stations 103, 136, 169, 202, 235, 268, 301, 334, and 367 ft from the left-bank end point of the tagline, left and right edges of water are respectively at 70 and 400 ft from the left-bank end point of the tagline																											
Time (MST)	Sample type	Water depth (m)	Sample elevation above bed (m)	Sample collection time (s)	DI intake velocity (m/s)	Silt and clay conc. (mg/L)	Sand conc. (mg/L)	Grain-size analysis of sand (0.0625-2.0 mm) fraction																			
								% sand < 0.074 mm	% sand < 0.088 mm	% sand < 0.105 mm	% sand < 0.125 mm	% sand < 0.149 mm	% sand < 0.177 mm	% sand < 0.210 mm	% sand < 0.250 mm	% sand < 0.297 mm	% sand < 0.354 mm	% sand < 0.420 mm	% sand < 0.500 mm	% sand < 0.595 mm	% sand < 0.707 mm	% sand < 0.841 mm	% sand < 1.00 mm	% sand < 1.19 mm	% sand < 1.41 mm	% sand < 1.68 mm	% sand < 2.00 mm
14:18-14:42	EWI-5v	n/a	n/a	92.9	n/a	1130	128	10.1	22.4	40.3	57.3	70.8	81.6	88.4	93.1	95.9	97.4	98.5	99.3	99.6	99.8	100.0	100.0	100.0	100.0	100.0	
14:20-14:39	EWI-3v	n/a	n/a	53.0	n/a	1110	127	10.2	22.5	40.3	57.4	70.9	81.6	88.5	93.1	95.8	97.2	98.3	99.1	99.4	99.8	99.9	100.0	100.0	100.0	100.0	
14:18-14:42	EWI-9v	n/a	n/a	163.8	n/a	1100	126	10.3	22.7	40.8	58.0	71.4	82.1	88.9	93.5	96.0	97.4	98.6	99.3	99.7	99.9	100.0	100.0	100.0	100.0	100.0	
14:42	v1 2DI	4.72	n/a	28.2	1.464	1130	115	9.8	22.1	40.6	58.5	72.5	83.6	90.3	94.4	96.7	97.9	98.7	99.3	99.6	99.8	99.9	100.0	100.0	100.0	100.0	
14:39	v2 2DI	3.35	n/a	19.4	1.510	1070	158	9.8	21.6	38.9	56.1	70.2	81.7	89.0	93.7	96.3	97.5	98.3	99.0	99.3	99.7	99.9	100.0	100.0	100.0	100.0	
14:37	v3 2DI	3.20	n/a	17.7	1.468	1100	178	7.8	18.0	33.7	49.8	63.5	75.6	84.4	91.0	94.9	96.9	98.5	99.5	99.9	100.0	100.0	100.0	100.0	100.0	100.0	
14:35	v4 2DI	3.20	n/a	18.2	1.429	1060	104	11.1	24.3	43.1	60.3	73.2	83.3	89.6	93.7	95.5	96.6	98.2	99.4	99.9	100.0	100.0	100.0	100.0	100.0	100.0	
14:32	v5 2DI	3.20	n/a	18.8	1.378	1140	98.7	10.4	23.1	41.2	57.8	70.3	80.0	86.2	90.8	94.1	96.2	97.6	98.5	99.1	99.6	99.9	100.0	100.0	100.0	100.0	
14:26	v6 2DI	3.20	n/a	18.5	1.364	1010	105	11.1	24.4	43.4	61.1	74.2	84.0	90.1	94.3	96.8	98.3	99.5	99.9	100.0	100.0	100.0	100.0	100.0	100.0	100.0	
14:23	v7 2DI	2.90	n/a	16.3	1.232	1130	121	12.6	25.7	43.3	59.3	71.8	81.8	88.1	92.5	95.1	96.7	98.1	99.0	99.4	99.7	99.9	100.0	100.0	100.0	100.0	
14:20	v8 2DI	2.59	n/a	14.8	1.145	1120	116	10.7	23.6	42.3	59.9	73.3	83.6	90.2	94.6	96.6	97.8	98.3	99.9	100.0	100.0	100.0	100.0	100.0	100.0	100.0	
14:18	v9 2DI	2.13	n/a	11.9	0.986	1200	141	13.1	29.3	51.7	71.4	85.2	94.4	98.3	99.7	100.0	100.0	100.0	100.0	100.0	100.0	100.0	100.0	100.0	100.0	100.0	

Notes: EWI-5v = 5-vertical EWI measurement mathematically composited using raw laboratory data from verticals 1, 3, 5, 7, and 9; EWI-3v = 3-vertical quasi-EWI measurement mathematically composited using raw laboratory data from verticals 2, 5, and 8; EWI-9v = 9-vertical quasi-EWI measurement mathematically composited using raw laboratory data from all 9 verticals; DI = depth-integrated (nozzle open during downward and upward transits); v1 through v9 refer to verticals 1 through 9; number preceding DI indicates the number of transits at each vertical.

D-77-bag-type noncomposited multivertical suspended-sediment samples collected at Lower Marble Canyon gaging station cross section C on August 28, 2007;																											
verticals 1 through 9 located respectively at stations 114, 148, 182, 216, 250, 284, 318, 352, and 386 ft from the left-bank end point of the tagline, left and right edges of water are respectively at 80 and 420 ft from the left-bank end point of the tagline, left-bank end point of tagline is approximately 30 ft farther from the river than the end point used in February 2007																											
Time (MST)	Sample type	Water depth (m)	Sample elevation above bed (m)	Sample collection time (s)	DI intake velocity (m/s)	Silt and clay conc. (mg/L)	Sand conc. (mg/L)	Grain-size analysis of sand (0.0625-2.0 mm) fraction																			
								% sand < 0.074 mm	% sand < 0.088 mm	% sand < 0.105 mm	% sand < 0.125 mm	% sand < 0.149 mm	% sand < 0.177 mm	% sand < 0.210 mm	% sand < 0.250 mm	% sand < 0.297 mm	% sand < 0.354 mm	% sand < 0.420 mm	% sand < 0.500 mm	% sand < 0.595 mm	% sand < 0.707 mm	% sand < 0.841 mm	% sand < 1.00 mm	% sand < 1.19 mm	% sand < 1.41 mm	% sand < 1.68 mm	% sand < 2.00 mm
14:56-15:32	EWI-5v	n/a	n/a	232.6	n/a	1020	139	10.6	23.6	42.7	60.6	74.2	84.4	90.4	94.3	96.5	97.8	98.6	99.2	99.5	99.8	99.9	100.0	100.0	100.0	100.0	
15:01-15:28	EWI-3v	n/a	n/a	155.6	n/a	1030	152	9.2	21.0	39.0	56.5	70.3	81.2	87.8	92.4	95.2	97.0	98.4	99.2	99.5	99.8	99.9	100.0	100.0	100.0	100.0	
14:56-15:32	EWI-9v	n/a	n/a	437.1	n/a	1020	141	10.4	23.2	42.1	59.9	73.4	83.5	89.5	93.4	95.7	97.1	98.3	99.0	99.4	99.8	99.9	100.0	100.0	100.0	100.0	
14:56	v1 2DI	2.13	n/a	23.8	0.304	1070	155	12.1	27.3	49.1	68.7	82.1	90.8	95.8	98.8	99.9	100.0	100.0	100.0	100.0	100.0	100.0	100.0	100.0	100.0	100.0	
15:01	v2 2DI	3.05	n/a	39.2	0.449	1050	101	11.9	26.2	46.0	63.4	75.6	84.1	88.9	92.2	94.1	95.5	97.5	98.7	99.2	99.7	99.9	100.0	100.0	100.0	100.0	
15:04	v3 2DI	3.81	n/a	46.9	0.597	1050	99.6	14.5	30.7	52.3	70.6	83.1	91.8	96.4	99.0	99.9	100.0	100.0	100.0	100.0	100.0	100.0	100.0	100.0	100.0	100.0	
15:08	v4 2DI	4.27	n/a	51.4	0.647	1040	125	9.4	21.5	39.6	56.6	69.4	79.3	85.7	90.2	93.2	95.3	97.1	98.6	99.3	99.7	99.9	100.0	100.0	100.0	100.0	
15:12	v5 2DI	4.72	n/a	59.6	0.664	1030	170	8.1	18.6	35.2	52.0	65.9	77.6	85.2	90.7	94.5	96.8	98.2	99.0	99.4	99.7	99.9	100.0	100.0	100.0	100.0	
15:18	v6 2DI	4.57	n/a	57.1	0.602	1010	170	10.1	22.3	40.6	58.1	71.6	81.9	88.2	92.4	94.8	96.4	97.6	98.6	99.1	99.6	99.9	100.0	100.0	100.0	100.0	
15:22	v7 2DI	4.57	n/a	56.0	0.650	983	134	11.2	24.7	44.3	62.5	75.9	85.6	90.8	93.9	95.6	96.9	97.8	98.6	99.1	99.7	99.9	100.0	100.0	100.0	100.0	
15:27	v8 2DI	4.72	n/a	56.8	0.368	1020	160	10.1	23.1	42.9	62.0	76.3	86.8	92.6	95.9	97.3	98.2	99.2	99.9	100.0	100.0	100.0	100.0	100.0	100.0	100.0	
15:31	v9 2DI	3.66	n/a	46.3	0.225	950	132	11.5	26.5	49.0	69.7	84.1	93.3	97.5	99.4	99.9	100.0	100.0	100.0	100.0	100.0	100.0	100.0	100.0	100.0	100.0	

Notes: EWI-5v = 5-vertical EWI measurement mathematically composited using raw laboratory data from verticals 1, 3, 5, 7, and 9; EWI-3v = 3-vertical quasi-EWI measurement mathematically composited using raw laboratory data from verticals 2, 5, and 8; EWI-9v = 9-vertical quasi-EWI measurement mathematically composited using raw laboratory data from all 9 verticals; DI = depth-integrated (nozzle open during downward and upward transits); v1 through v9 refer to verticals 1 through 9; number preceding DI indicates the number of transits at each vertical.

D-77-bag-type noncomposited multivertical suspended-sediment samples collected at Lower Marble Canyon gaging station cross section B on August 29, 2007;																											
verticals 1 through 9 located respectively at stations 103, 136, 169, 202, 235, 268, 301, 334, and 367 ft from the left-bank end point of the tagline, left and right edges of water are respectively at 70 and 400 ft from the left-bank end point of the tagline																											
Time (MST)	Sample type	Water depth (m)	Sample elevation above bed (m)	Sample collection time (s)	DI intake velocity (m/s)	Silt and clay conc. (mg/L)	Sand conc. (mg/L)	Grain-size analysis of sand (0.0625-2.0 mm) fraction																			
								% sand < 0.074 mm	% sand < 0.088 mm	% sand < 0.105 mm	% sand < 0.125 mm	% sand < 0.149 mm	% sand < 0.177 mm	% sand < 0.210 mm	% sand < 0.250 mm	% sand < 0.297 mm	% sand < 0.354 mm	% sand < 0.420 mm	% sand < 0.500 mm	% sand < 0.595 mm	% sand < 0.707 mm	% sand < 0.841 mm	% sand < 1.00 mm	% sand < 1.19 mm	% sand < 1.41 mm	% sand < 1.68 mm	% sand < 2.00 mm
8:04-8:21	EWI-5v	n/a	n/a	91	n/a	5980	239	9.2	20.7	37.8	54.6	68.1	79.2	86.5	91.8	95.2	97.0	98.1	98.9	99.3	99.7	99.9	100.0	100.0	100.0	100.0	100.0
8:06-8:19	EWI-3v	n/a	n/a	52	n/a	5890	271	11.5	23.9	41.3	57.6	70.3	80.6	87.5	92.5	95.6	97.2	98.3	99.0	99.5	99.8	99.9	100.0	100.0	100.0	100.0	100.0
8:04-8:21	EWI-9v	n/a	n/a	162	n/a	5940	252	9.7	21.2	38.0	54.3	67.5	78.4	85.7	91.1	94.5	96.5	97.8	98.8	99.3	99.7	99.9	100.0	100.0	100.0	100.0	100.0
8:04	v1 2DI	4.88	n/a	26	0.907	5930	232	9.4	21.3	39.4	57.3	71.4	82.7	89.5	93.9	96.3	97.5	98.3	99.0	99.3	99.7	99.9	100.0	100.0	100.0	100.0	100.0
8:06	v2 2DI	3.51	n/a	18	1.037	5820	286	14.1	27.0	44.0	59.3	70.8	79.9	86.1	90.5	93.3	95.2	96.8	98.1	99.0	99.6	99.9	100.0	100.0	100.0	100.0	100.0
8:08	v3 2DI	3.35	n/a	18	0.994	6020	274	9.6	20.7	36.5	51.5	63.7	74.0	81.1	86.5	90.4	93.1	95.1	96.9	98.2	99.3	99.8	100.0	100.0	100.0	100.0	100.0
8:12	v4 2DI	3.35	n/a	19	0.903	5890	285	7.6	17.6	33.3	49.3	62.9	74.8	83.1	89.5	93.8	96.4	97.8	98.9	99.5	99.8	99.9	100.0	100.0	100.0	100.0	100.0
8:13	v5 2DI	3.35	n/a	18	0.880	5990	224	9.6	22.1	40.5	58.2	72.1	83.2	90.4	95.5	98.7	99.7	99.9	100.0	100.0	100.0	100.0	100.0	100.0	100.0	100.0	100.0
8:15	v6 2DI	3.35	n/a	18	0.834	5970	200	9.4	21.1	38.0	53.9	66.5	76.9	84.0	89.3	92.9	95.2	97.1	98.3	98.9	99.5	99.8	100.0	100.0	100.0	100.0	100.0
8:17	v7 2DI	3.05	n/a	17	0.847	5930	245	7.3	17.2	32.6	48.6	62.6	75.0	84.0	90.9	95.6	98.0	99.3	99.9	100.0	100.0	100.0	100.0	100.0	100.0	100.0	100.0
8:18	v8 2DI	2.74	n/a	16	0.351	5890	354	8.3	18.9	35.2	51.9	65.9	77.8	86.0	92.2	96.1	98.1	99.3	99.9	100.0	100.0	100.0	100.0	100.0	100.0	100.0	100.0
8:20	v9 4DI	2.29	n/a	24	0.545	6120	194	10.3	23.7	43.2	61.1	74.3	84.3	90.6	95.1	97.8	99.0	99.8	100.0	100.0	100.0	100.0	100.0	100.0	100.0	100.0	100.0

Notes: EWI-5v = 5-vertical EWI measurement mathematically composited using raw laboratory data from verticals 1, 3, 5, 7, and 9; EWI-3v = 3-vertical quasi-EWI measurement mathematically composited using raw laboratory data from verticals 2, 5, and 8; EWI-9v = 9-vertical quasi-EWI measurement mathematically composited using raw laboratory data from all 9 verticals; DI = depth-integrated (nozzle open during downward and upward transits); v1 through v9 refer to verticals 1 through 9; number preceding DI indicates the number of transits at each vertical.

D-77-bag-type noncomposited multivertical suspended-sediment samples collected at Lower Marble Canyon gaging station cross section A on August 29, 2007;																											
verticals 1 through 9 located respectively at stations 90, 112, 133, 156, 176, 200, 219, 244, and 262 ft from the left-bank end point of the tagline, left and right edges of water are respectively at 68 and 284 ft from the left-bank end point of the tagline																											
Time (MST)	Sample type	Water depth (m)	Sample elevation above bed (m)	Sample collection time (s)	DI intake velocity (m/s)	Silt and clay conc. (mg/L)	Sand conc. (mg/L)	Grain-size analysis of sand (0.0625-2.0 mm) fraction																			
								% sand < 0.074 mm	% sand < 0.088 mm	% sand < 0.105 mm	% sand < 0.125 mm	% sand < 0.149 mm	% sand < 0.177 mm	% sand < 0.210 mm	% sand < 0.250 mm	% sand < 0.297 mm	% sand < 0.354 mm	% sand < 0.420 mm	% sand < 0.500 mm	% sand < 0.595 mm	% sand < 0.707 mm	% sand < 0.841 mm	% sand < 1.00 mm	% sand < 1.19 mm	% sand < 1.41 mm	% sand < 1.68 mm	% sand < 2.00 mm
8:26-8:46	EWI-5v	n/a	n/a	141	n/a	6610	262	10.6	23.3	41.3	57.9	70.4	80.3	86.8	91.5	94.9	97.0	98.3	99.0	99.4	99.7	99.9	100.0	100.0	100.0	100.0	100.0
8:28-8:44	EWI-3v	n/a	n/a	91	n/a	6620	226	9.3	21.2	39.0	55.9	69.0	79.4	86.1	90.9	94.3	96.4	97.8	98.7	99.1	99.6	99.9	100.0	100.0	100.0	100.0	100.0
8:26-8:46	EWI-9v	n/a	n/a	287	n/a	6610	255	10.1	22.4	40.1	56.5	69.1	79.2	85.9	90.8	94.4	96.6	98.0	98.9	99.4	99.8	99.9	100.0	100.0	100.0	100.0	100.0
8:26	v1 2DI	3.51	n/a	19	0.770	6370	200	11.5	25.6	45.5	63.8	77.1	86.9	92.4	95.9	97.8	98.8	99.7	99.9	100.0	100.0	100.0	100.0	100.0	100.0	100.0	100.0
8:28	v2 2DI	3.51	n/a	19	1.015	6430	187	10.0	23.0	41.9	59.7	73.2	83.4	89.5	93.6	96.1	97.8	99.0	99.7	99.9	99.9	100.0	100.0	100.0	100.0	100.0	100.0
8:29	v3 2DI	4.42	n/a	24	0.983	6480	292	10.4	22.3	39.0	54.7	67.0	77.3	84.4	89.9	94.1	96.7	98.3	99.4	99.8	99.9	100.0	100.0	100.0	100.0	100.0	100.0
8:32	v4 2DI	5.79	n/a	35	0.819	6570	243	9.5	21.3	38.5	54.7	67.4	77.7	84.8	90.2	94.2	96.7	98.2	99.2	99.7	99.9	100.0	100.0	100.0	100.0	100.0	100.0
8:35	v5 2DI	7.01	n/a	39	0.853	6660	249	9.4	21.3	38.6	54.7	67.2	77.2	83.8	88.7	92.6	95.2	96.9	98.0	98.6	99.4	99.8	100.0	100.0	100.0	100.0	100.0
8:38	v6 2DI	7.01	n/a	40	0.933	6680	295	10.1	21.8	38.3	53.6	65.4	75.2	82.1	87.6	91.9	94.8	96.7	98.1	99.0	99.6	99.9	100.0	100.0	100.0	100.0	100.0
8:41	v7 2DI	7.01	n/a	40	0.880	6750	308	11.2	24.6	43.2	60.0	72.4	82.2	88.5	93.1	96.1	97.9	98.7	99.2	99.4	99.8	99.9	100.0	100.0	100.0	100.0	100.0
8:43	v8 2DI	5.94	n/a	33	0.711	6720	225	8.5	19.9	37.8	55.2	69.1	80.3	87.4	92.4	95.6	97.5	98.5	99.1	99.3	99.7	99.9	100.0	100.0	100.0	100.0	100.0
8:44	v9 4DI	3.28	n/a	38	0.458	6630	153	11.6	26.1	46.3	64.0	76.5	85.7	91.2	95.1	97.2	98.4	99.5	99.9	100.0	100.0	100.0	100.0	100.0	100.0	100.0	100.0

Notes: EWI-5v = 5-vertical EWI measurement mathematically composited using raw laboratory data from verticals 1, 3, 5, 7, and 9; EWI-3v = 3-vertical quasi-EWI measurement mathematically composited using raw laboratory data from verticals 2, 5, and 8; EWI-9v = 9-vertical quasi-EWI measurement mathematically composited using raw laboratory data from all 9 verticals; DI = depth-integrated (nozzle open during downward and upward transits); v1 through v9 refer to verticals 1 through 9; number preceding DI indicates the number of transits at each vertical.

D-77-bag-type noncomposited multivertical suspended-sediment samples collected at Lower Marble Canyon gaging station cross section C on August 29, 2007; verticals 1 through 9 located respectively at stations 114, 148, 182, 216, 250, 284, 318, 352, and 386 ft from the left-bank end point of the tagline, left and right edges of water are respectively at 80 and 420 ft from the left-bank end point of the tagline, left-bank end point of tagline is approximately 30 ft farther from the river than the end point used in February 2007																										
Time (MST)	Sample type	Water depth (m)	Sample elevation above bed (m)	Sample collection time (s)	DI intake velocity (m/s)	Silt and clay conc. (mg/L)	Sand conc. (mg/L)	Grain-size analysis of sand (0.0625-2.0 mm) fraction																		
								% sand < 0.074 mm	% sand < 0.088 mm	% sand < 0.105 mm	% sand < 0.125 mm	% sand < 0.149 mm	% sand < 0.177 mm	% sand < 0.210 mm	% sand < 0.250 mm	% sand < 0.297 mm	% sand < 0.354 mm	% sand < 0.420 mm	% sand < 0.500 mm	% sand < 0.595 mm	% sand < 0.707 mm	% sand < 0.841 mm	% sand < 1.00 mm	% sand < 1.19 mm	% sand < 1.41 mm	% sand < 1.68 mm
8:56-9:17	EWI-5v	n/a	n/a	142	n/a	6590	232	9.9	21.8	39.0	55.2	67.9	78.5	85.7	91.1	94.8	96.9	98.2	99.1	99.6	99.8	99.9	100.0	100.0	100.0	100.0
8:59-9:14	EWI-3v	n/a	n/a	96	n/a	6640	239	9.3	20.9	38.0	54.3	67.3	78.0	85.4	90.8	94.5	96.5	97.8	98.8	99.3	99.7	99.9	100.0	100.0	100.0	100.0
8:56-9:17	EWI-9v	n/a	n/a	269	n/a	6610	243	10.5	22.6	39.9	56.2	69.0	79.5	86.5	91.6	95.0	97.1	98.3	99.2	99.5	99.8	99.9	100.0	100.0	100.0	100.0
8:56-9:17	v1 4DI	2.44	n/a	32	0.330	6230	214	9.8	22.5	41.8	60.6	74.8	85.9	92.9	97.6	99.7	100.0	100.0	100.0	100.0	100.0	100.0	100.0	100.0	100.0	100.0
8:59-9:14	v2 2DI	3.66	n/a	25	0.531	6400	190	10.6	23.7	42.5	59.9	72.9	82.7	88.5	92.4	94.7	96.1	97.6	98.5	99.0	99.6	99.8	100.0	100.0	100.0	100.0
9:02-9:14	v3 2DI	4.11	n/a	28	0.741	6530	204	10.4	23.1	41.2	58.2	71.5	82.2	89.0	93.7	96.4	98.0	99.1	99.8	100.0	100.0	100.0	100.0	100.0	100.0	100.0
9:04-9:14	v4 2DI	4.57	n/a	32	0.460	6520	303	13.4	26.0	42.8	58.0	69.8	79.6	86.2	91.2	95.0	97.3	98.6	99.5	99.7	99.9	100.0	100.0	100.0	100.0	100.0
9:06-9:14	v5 2DI	5.03	n/a	36	0.818	6640	247	8.9	19.9	36.2	51.8	64.5	75.5	83.4	89.7	94.0	96.5	97.8	98.8	99.4	99.7	99.9	100.0	100.0	100.0	100.0
9:08-9:14	v6 2DI	4.88	n/a	35	0.852	6700	243	10.1	22.4	40.2	57.2	70.6	81.4	88.3	93.0	96.0	97.7	98.8	99.5	99.6	99.8	99.9	100.0	100.0	100.0	100.0
9:11-9:14	v7 2DI	4.88	n/a	34	0.803	6670	228	10.5	22.6	39.5	55.1	67.3	77.2	83.9	89.1	93.2	96.0	97.7	98.8	99.4	99.7	99.9	100.0	100.0	100.0	100.0
9:13-9:14	v8 2DI	5.03	n/a	35	0.573	6810	259	9.2	20.9	38.3	55.1	68.4	79.3	86.6	91.7	95.0	96.8	98.0	98.8	99.4	99.7	99.9	100.0	100.0	100.0	100.0
9:16-9:14	v9 4DI	3.96	n/a	55	0.304	6570	274	10.6	23.0	40.8	57.4	70.4	81.0	88.1	93.1	95.9	97.3	98.4	99.3	99.7	99.9	100.0	100.0	100.0	100.0	100.0

Notes: EWI-5v = 5-vertical EWI measurement mathematically composited using raw laboratory data from verticals 1, 3, 5, 7, and 9; EWI-3v = 3-vertical quasi-EWI measurement mathematically composited using raw laboratory data from verticals 2, 5, and 8; EWI-9v = 9-vertical quasi-EWI measurement mathematically composited using raw laboratory data from all 9 verticals; DI = depth-integrated (nozzle open during downward and upward transits); v1 through v9 refer to verticals 1 through 9; number preceding DI indicates the number of transits at each vertical.

D-96-A1 noncomposited multivertical suspended-sediment samples collected at Lower Marble Canyon gaging station cross section B on August 29, 2007; verticals 1 through 9 located respectively at stations 103, 136, 169, 202, 235, 268, 301, 334, and 367 ft from the left-bank end point of the tagline, left and right edges of water are respectively at 70 and 400 ft from the left-bank end point of the tagline																										
Time (MST)	Sample type	Water depth (m)	Sample elevation above bed (m)	Sample collection time (s)	DI intake velocity (m/s)	Silt and clay conc. (mg/L)	Sand conc. (mg/L)	Grain-size analysis of sand (0.0625-2.0 mm) fraction																		
								% sand < 0.074 mm	% sand < 0.088 mm	% sand < 0.105 mm	% sand < 0.125 mm	% sand < 0.149 mm	% sand < 0.177 mm	% sand < 0.210 mm	% sand < 0.250 mm	% sand < 0.297 mm	% sand < 0.354 mm	% sand < 0.420 mm	% sand < 0.500 mm	% sand < 0.595 mm	% sand < 0.707 mm	% sand < 0.841 mm	% sand < 1.00 mm	% sand < 1.19 mm	% sand < 1.41 mm	% sand < 1.68 mm
9:41-9:59	EWI-5v	n/a	n/a	118	n/a	8040	265	11.7	24.5	42.0	58.0	70.6	80.9	87.8	92.7	95.7	97.3	98.4	99.1	99.5	99.8	99.9	100.0	100.0	100.0	100.0
9:43-9:57	EWI-3v	n/a	n/a	65	n/a	8120	231	14.0	28.4	46.9	62.8	74.4	83.5	89.2	93.2	95.8	97.2	98.3	99.0	99.4	99.8	99.9	100.0	100.0	100.0	100.0
9:41-9:59	EWI-9v	n/a	n/a	205	n/a	8030	244	12.6	26.0	43.9	59.9	72.0	81.9	88.4	93.0	95.8	97.4	98.4	99.2	99.5	99.8	99.9	100.0	100.0	100.0	100.0
9:41-9:59	v1 2DI	4.88	n/a	37	1.471	7760	298	11.2	23.4	40.7	57.1	70.3	81.5	88.8	93.8	96.4	97.6	98.4	99.1	99.4	99.8	99.9	100.0	100.0	100.0	100.0
9:43-9:59	v2 2DI	3.51	n/a	24	1.421	7900	231	15.5	30.9	50.3	66.3	77.7	86.2	91.4	94.9	96.9	98.0	98.8	99.5	99.6	99.8	99.9	100.0	100.0	100.0	100.0
9:46-9:59	v3 2DI	3.35	n/a	22	1.494	8030	324	9.8	21.0	37.0	52.6	65.4	76.5	84.4	90.5	94.6	97.1	98.4	99.2	99.5	99.8	99.9	100.0	100.0	100.0	100.0
9:47-9:59	v4 2DI	3.35	n/a	22	1.359	8010	237	12.7	26.2	44.0	59.6	71.2	80.3	86.5	91.0	94.0	96.1	97.7	98.9	99.5	99.8	99.9	100.0	100.0	100.0	100.0
9:50-9:59	v5 2DI	3.35	n/a	23	1.568	8170	235	13.9	28.1	46.5	62.6	74.5	83.5	89.0	92.7	95.2	96.7	97.9	98.6	99.2	99.7	99.9	100.0	100.0	100.0	100.0
9:52-9:59	v6 2DI	3.35	n/a	23	1.307	7910	168	16.0	32.2	52.4	68.8	80.0	88.1	93.2	96.6	98.5	99.3	99.8	100.0	100.0	100.0	100.0	100.0	100.0	100.0	100.0
9:54-9:59	v7 2DI	2.74	n/a	21	1.316	8260	202	13.0	27.2	45.6	61.1	72.5	81.8	88.2	92.9	96.0	97.7	98.9	99.8	99.9	100.0	100.0	100.0	100.0	100.0	100.0
9:56-9:59	v8 2DI	2.44	n/a	18	1.257	8360	222	11.9	25.0	42.4	57.6	69.2	79.1	86.2	91.6	95.1	96.8	98.1	99.0	99.5	99.8	99.9	100.0	100.0	100.0	100.0
9:58-9:59	v9 4DI	2.29	n/a	29	0.948	8410	202	13.1	27.9	47.6	64.4	76.2	85.1	90.6	94.4	96.6	97.7	98.5	99.4	99.8	99.9	100.0	100.0	100.0	100.0	100.0

Notes: EWI-5v = 5-vertical EWI measurement mathematically composited using raw laboratory data from verticals 1, 3, 5, 7, and 9; EWI-3v = 3-vertical quasi-EWI measurement mathematically composited using raw laboratory data from verticals 2, 5, and 8; EWI-9v = 9-vertical quasi-EWI measurement mathematically composited using raw laboratory data from all 9 verticals; DI = depth-integrated (nozzle open during downward and upward transits); v1 through v9 refer to verticals 1 through 9; number preceding DI indicates the number of transits at each vertical.

D-96-A1 noncomposited multivertical suspended-sediment samples collected at Lower Marble Canyon gaging station cross section A on August 29, 2007;																										
verticals 1 through 9 located respectively at stations 90, 112, 133, 156, 176, 200, 219, 244, and 262 ft from the left-bank end point of the tagline, left and right edges of water are respectively at 68 and 284 ft from the left-bank end point of the tagline																										
Time (MST)	Sample type	Water depth (m)	Sample elevation above bed (m)	Sample collection time (s)	DI intake velocity (m/s)	Silt and clay conc. (mg/L)	Sand conc. (mg/L)	Grain-size analysis of sand (0.0625-2.0 mm) fraction																		
								% sand < 0.074 mm	% sand < 0.088 mm	% sand < 0.105 mm	% sand < 0.125 mm	% sand < 0.149 mm	% sand < 0.177 mm	% sand < 0.210 mm	% sand < 0.250 mm	% sand < 0.297 mm	% sand < 0.354 mm	% sand < 0.420 mm	% sand < 0.500 mm	% sand < 0.595 mm	% sand < 0.707 mm	% sand < 0.841 mm	% sand < 1.00 mm	% sand < 1.19 mm	% sand < 1.41 mm	% sand < 1.68 mm
10-03-10:23	EWI-5v	n/a	n/a	181	n/a	9380	237	14.1	28.6	47.3	63.2	74.6	83.3	88.7	92.6	95.3	97.1	98.3	99.1	99.5	99.8	99.9	100.0	100.0	100.0	100.0
10-05-10:20	EWI-3v	n/a	n/a	115	n/a	10200	209	14.0	29.1	48.6	64.9	76.3	84.7	89.8	93.5	95.9	97.5	98.6	99.4	99.7	99.9	100.0	100.0	100.0	100.0	100.0
10-03-10:23	EWI-9v	n/a	n/a	338	n/a	9710	227	13.7	28.1	46.9	62.7	74.1	82.6	88.0	92.0	94.9	96.8	98.2	99.1	99.5	99.8	99.9	100.0	100.0	100.0	100.0
10-03	v1 2DI	3.51	n/a	24	1.398	9180	210	14.8	30.8	51.4	68.5	80.2	88.5	93.0	95.7	97.4	98.3	98.9	99.2	99.4	99.8	99.9	100.0	100.0	100.0	100.0
10-05	v2 2DI	3.51	n/a	24	1.630	9200	190	12.6	27.7	48.3	65.9	77.9	86.5	91.4	94.7	96.8	98.0	98.9	99.5	99.7	99.9	100.0	100.0	100.0	100.0	100.0
10-07	v3 2DI	4.42	n/a	31	1.499	9440	233	13.0	27.4	46.3	62.5	74.2	82.8	88.3	92.1	94.8	96.7	98.0	99.0	99.5	99.8	99.9	100.0	100.0	100.0	100.0
10-09	v4 2DI	5.94	n/a	42	1.327	9500	250	12.8	26.9	45.4	61.6	73.5	82.5	88.2	92.4	95.2	97.1	98.3	99.0	99.3	99.7	99.9	100.0	100.0	100.0	100.0
10-12	v5 2DI	7.01	n/a	49	1.335	9530	251	13.2	27.3	45.9	61.9	73.4	82.3	87.8	92.0	95.0	97.0	98.4	99.3	99.7	99.9	100.0	100.0	100.0	100.0	100.0
10-14	v6 2DI	7.01	n/a	49	1.435	9700	240	11.9	25.0	42.4	57.2	67.9	76.3	82.1	87.0	91.4	94.9	97.1	98.6	99.2	99.7	99.9	100.0	100.0	100.0	100.0
10-17	v7 2DI	7.01	n/a	50	1.241	9200	254	15.3	29.3	46.6	61.4	72.3	81.1	87.0	91.4	94.6	96.5	97.8	98.7	99.3	99.7	99.9	100.0	100.0	100.0	100.0
10-19	v8 2DI	5.94	n/a	42	1.119	11900	166	17.2	34.1	54.6	70.5	80.9	88.2	92.5	95.3	96.9	98.0	98.8	99.5	99.7	99.9	100.0	100.0	100.0	100.0	100.0
10-22	v9 2DI	3.81	n/a	27	0.565	9760	171	15.0	32.0	53.9	71.7	83.2	90.7	94.7	97.2	98.4	98.9	99.7	99.9	100.0	100.0	100.0	100.0	100.0	100.0	100.0

Notes: EWI-5v = 5-vertical EWI measurement mathematically composited using raw laboratory data from verticals 1, 3, 5, 7, and 9; EWI-3v = 3-vertical quasi-EWI measurement mathematically composited using raw laboratory data from verticals 2, 5, and 8; EWI-9v = 9-vertical quasi-EWI measurement mathematically composited using raw laboratory data from all 9 verticals; DI = depth-integrated (nozzle open during downward and upward transits); v1 through v9 refer to verticals 1 through 9; number preceding DI indicates the number of transits at each vertical.

D-96-A1 noncomposited multivertical suspended-sediment samples collected at Lower Marble Canyon gaging station cross section C on August 29, 2007;																										
verticals 1 through 9 located respectively at stations 114, 148, 182, 216, 250, 284, 318, 352, and 386 ft from the left-bank end point of the tagline, left and right edges of water are respectively at 80 and 420 ft from the left-bank end point of the tagline, left-bank end point of tagline is approximately 30 ft farther from the river than the end point used in February 2007																										
Time (MST)	Sample type	Water depth (m)	Sample elevation above bed (m)	Sample collection time (s)	DI intake velocity (m/s)	Silt and clay conc. (mg/L)	Sand conc. (mg/L)	Grain-size analysis of sand (0.0625-2.0 mm) fraction																		
								% sand < 0.074 mm	% sand < 0.088 mm	% sand < 0.105 mm	% sand < 0.125 mm	% sand < 0.149 mm	% sand < 0.177 mm	% sand < 0.210 mm	% sand < 0.250 mm	% sand < 0.297 mm	% sand < 0.354 mm	% sand < 0.420 mm	% sand < 0.500 mm	% sand < 0.595 mm	% sand < 0.707 mm	% sand < 0.841 mm	% sand < 1.00 mm	% sand < 1.19 mm	% sand < 1.41 mm	% sand < 1.68 mm
10-31-10:52	EWI-5v	n/a	n/a	141	n/a	9640	208	14.0	28.8	48.0	64.2	75.7	84.1	89.2	92.7	95.2	96.9	98.1	98.9	99.3	99.7	99.9	100.0	100.0	100.0	100.0
10-33-10:48	EWI-3v	n/a	n/a	61	n/a	9500	210	12.5	26.6	45.5	62.1	74.1	83.3	89.1	93.1	95.6	97.2	98.4	99.2	99.6	99.8	99.9	100.0	100.0	100.0	100.0
10-31-10:52	EWI-9v	n/a	n/a	268	n/a	9630	214	14.1	28.7	47.4	63.2	74.5	83.0	88.3	92.2	94.9	96.8	98.1	98.9	99.4	99.7	99.9	100.0	100.0	100.0	100.0
10-31	v1 4DI	2.44	n/a	32	0.418	8750	153	13.8	30.7	53.7	73.4	86.3	94.2	97.9	99.5	100.0	100.0	100.0	100.0	100.0	100.0	100.0	100.0	100.0	100.0	100.0
10-33	v2 2DI	3.66	n/a	25	0.721	9020	203	12.6	27.0	46.6	63.7	75.9	84.9	90.2	93.7	95.9	97.4	98.6	99.3	99.5	99.8	99.9	100.0	100.0	100.0	100.0
10-35	v3 2DI	4.11	n/a	29	1.119	9270	192	15.3	30.4	49.3	65.0	75.9	83.8	88.5	91.7	94.2	96.0	97.2	98.0	98.6	99.4	99.8	100.0	100.0	100.0	100.0
10-38	v4 2DI	4.57	n/a	32	1.287	9460	238	14.8	28.3	45.0	58.8	68.9	76.9	82.4	86.9	90.8	93.9	96.1	97.6	98.5	99.4	99.8	100.0	100.0	100.0	100.0
10-40	v5 2DI	5.03	n/a	35	1.241	9530	208	12.5	26.3	44.6	60.5	72.1	81.1	87.0	91.3	94.2	96.1	97.5	98.6	99.2	99.7	99.9	100.0	100.0	100.0	100.0
10-43	v6 2DI	4.88	n/a	34	1.441	9890	213	15.3	30.5	49.2	64.4	75.2	83.5	89.0	93.2	96.1	97.7	98.7	99.5	99.7	99.9	100.0	100.0	100.0	100.0	100.0
10-45	v7 2DI	4.88	n/a	34	1.250	9780	215	15.2	30.8	50.8	67.2	78.6	86.7	91.3	94.5	96.7	98.2	99.2	99.8	100.0	100.0	100.0	100.0	100.0	100.0	100.0
10-47	v8 2DI	5.03	n/a	36	0.943	9740	215	12.5	26.8	46.2	63.2	75.7	85.3	91.2	95.0	97.1	98.5	99.4	99.9	100.0	100.0	100.0	100.0	100.0	100.0	100.0
10-51	v9 4DI	3.96	n/a	54	0.413	11200	265	12.4	26.2	44.9	61.3	73.3	82.4	87.7	91.4	94.0	96.0	97.4	98.4	99.1	99.6	99.9	100.0	100.0	100.0	100.0

Notes: EWI-5v = 5-vertical EWI measurement mathematically composited using raw laboratory data from verticals 1, 3, 5, 7, and 9; EWI-3v = 3-vertical quasi-EWI measurement mathematically composited using raw laboratory data from verticals 2, 5, and 8; EWI-9v = 9-vertical quasi-EWI measurement mathematically composited using raw laboratory data from all 9 verticals; DI = depth-integrated (nozzle open during downward and upward transits); v1 through v9 refer to verticals 1 through 9; number preceding DI indicates the number of transits at each vertical.

Single-vertical D-96-A1 suspended-sediment samples collected at Lower Marble Canyon gaging station cross section C on August 30, 2007; vertical located at the station 230 ft from the former right-bank end point of the cableway																											
Time (MST)	Sample type	Water depth (m)	Sample elevation above bed (m)	Sample collection time (s)	DI intake velocity (m/s)	Silt and clay conc. (mg/L)	Sand conc. (mg/L)	Grain-size analysis of sand (0.0625-2.0 mm) fraction																			
								% sand < 0.074 mm	% sand < 0.088 mm	% sand < 0.105 mm	% sand < 0.125 mm	% sand < 0.149 mm	% sand < 0.177 mm	% sand < 0.210 mm	% sand < 0.250 mm	% sand < 0.297 mm	% sand < 0.354 mm	% sand < 0.420 mm	% sand < 0.500 mm	% sand < 0.595 mm	% sand < 0.707 mm	% sand < 0.841 mm	% sand < 1.00 mm	% sand < 1.19 mm	% sand < 1.41 mm	% sand < 1.68 mm	% sand < 2.00 mm
6:26	DI	4.97	n/a	34.26	1.372	1,570	265	14.2	30.8	52.2	69.4	80.6	88.1	92.4	95.1	96.9	97.9	98.8	99.3	99.5	99.8	99.9	100.0	100.0	100.0	100.0	100.0
6:29	DI	4.97	n/a	33.79	1.353	1,490	186	11.4	25.4	45.0	62.4	75.1	84.6	90.4	94.3	96.7	98.3	99.2	99.8	100.0	100.0	100.0	100.0	100.0	100.0	100.0	100.0
6:32	DI	4.97	n/a	34.97	1.366	1,550	291	13.8	29.5	49.7	66.2	77.3	85.4	90.2	93.7	96.1	97.5	98.6	99.2	99.4	99.8	99.9	100.0	100.0	100.0	100.0	100.0
6:35	DI	4.97	n/a	33.30	1.459	1,560	300	14.8	31.3	52.3	69.0	79.9	87.3	91.6	94.4	96.4	97.7	98.6	99.2	99.4	99.8	99.9	100.0	100.0	100.0	100.0	100.0
6:38	DI	4.97	n/a	33.50	1.499	1,540	281	14.4	30.9	52.1	69.0	80.1	87.7	92.0	94.8	96.8	98.0	98.8	99.4	99.6	99.8	99.9	100.0	100.0	100.0	100.0	100.0
6:41	DI	4.97	n/a	33.79	1.513	1,500	236	15.5	32.5	53.9	70.6	81.3	88.4	92.1	94.7	96.6	97.8	98.7	99.3	99.5	99.8	99.9	100.0	100.0	100.0	100.0	100.0
6:44	DI	4.97	n/a	33.99	1.360	1,530	304	13.8	29.6	50.0	66.8	78.1	86.1	90.7	93.9	96.2	97.7	98.8	99.4	99.6	99.8	99.9	100.0	100.0	100.0	100.0	100.0
6:47	DI	4.97	n/a	34.87	1.245	1,520	310	12.6	27.7	47.9	65.0	76.6	85.1	90.3	94.0	96.4	97.9	98.7	99.3	99.5	99.8	99.9	100.0	100.0	100.0	100.0	100.0
6:50	DI	4.97	n/a	34.58	1.371	1,490	296	15.2	31.5	52.0	68.4	79.1	86.5	90.8	93.9	96.0	97.3	98.5	99.1	99.4	99.8	99.9	100.0	100.0	100.0	100.0	100.0
6:53	DI	4.97	n/a	34.97	1.380	1,490	211	16.7	34.6	56.2	72.6	82.7	89.4	93.1	95.5	97.0	98.0	98.7	99.3	99.5	99.8	99.9	100.0	100.0	100.0	100.0	100.0
6:56	DI	4.97	n/a	33.30	1.406	1,510	279	14.2	30.5	51.3	67.9	78.9	86.4	90.9	93.9	95.8	97.2	98.3	99.0	99.4	99.8	99.9	100.0	100.0	100.0	100.0	100.0
6:59	DI	4.97	n/a	34.09	1.471	1,520	266	15.0	31.6	52.7	69.3	80.0	87.4	91.5	94.4	96.3	97.5	98.5	99.1	99.3	99.7	99.9	100.0	100.0	100.0	100.0	100.0
7:02	DI	4.97	n/a	34.09	1.341	1,480	423	15.2	31.5	51.7	67.5	77.9	85.3	89.9	93.3	95.7	97.1	98.2	98.8	99.2	99.7	99.9	100.0	100.0	100.0	100.0	100.0
7:05	DI	4.97	n/a	33.60	1.389	1,490	276	14.2	30.2	50.6	66.9	77.6	85.5	90.2	93.7	96.0	97.4	98.5	99.2	99.5	99.8	99.9	100.0	100.0	100.0	100.0	100.0
7:08	DI	4.97	n/a	33.40	1.382	1,470	303	14.2	30.6	51.7	68.8	80.0	87.8	92.3	95.3	97.0	98.1	98.9	99.5	99.6	99.8	99.9	100.0	100.0	100.0	100.0	100.0

Notes: DI = depth-integrated (nozzle open during downward and upward transits).

P-61 suspended-sediment samples collected at the Grand Canyon gaging station on March 31, 1996; vertical located at the station 190 ft from the right-bank end point of the cableway																									
Time (MST)	Sample type	Water depth (m)	Sample elevation above bed (m)	Sample collection time (s)	DI intake velocity (m/s)	Silt and clay conc. (mg/L)	Sand conc. (mg/L)	Grain-size analysis of sand (0.0625-2.0 mm) fraction																	
								% sand < 0.074 mm	% sand < 0.088 mm	% sand < 0.105 mm	% sand < 0.125 mm	% sand < 0.149 mm	% sand < 0.177 mm	% sand < 0.210 mm	% sand < 0.250 mm	% sand < 0.297 mm	% sand < 0.354 mm	% sand < 0.420 mm	% sand < 0.500 mm	% sand < 0.595 mm	% sand < 0.707 mm	% sand < 0.841 mm	% sand < 1.00 mm	% sand < 1.19 mm	% sand < 1.41 mm
14:11	Up DI	6.81	n/a	5.88	2.810	149	1,040	3.3	8.2	15.3	22.1	32.5	42.7	55.2	67.3	79.4	87.7	94.9	97.2	100.0	100.0	100.0	100.0	100.0	100.0
14:14	Up DI	6.90	n/a	5.68	3.093	131	1,320	3.2	7.0	13.8	21.1	29.3	39.5	50.4	63.1	76.7	89.4	96.6	97.9	100.0	100.0	100.0	100.0	100.0	100.0
15:28	Up DI	7.88	n/a	6.50	2.676	162	1,410	2.7	6.2	13.0	19.9	26.5	34.9	44.6	55.6	66.7	78.5	91.6	97.8	100.0	100.0	100.0	100.0	100.0	100.0
15:31	Up DI	7.85	n/a	6.41	2.602	141	1,230	3.2	6.9	12.6	20.8	28.9	37.5	45.9	56.2	67.9	79.4	90.5	96.8	98.3	100.0	100.0	100.0	100.0	100.0

Notes: Up DI = depth-integrated on upward transit (intake closed during downward transit).

P-61 suspended-sediment samples collected at the Grand Canyon gaging station on March 31, 1996; vertical located at the station 290 ft from the right-bank end point of the cableway																									
Time (MST)	Sample type	Water depth (m)	Sample elevation above bed (m)	Sample collection time (s)	DI intake velocity (m/s)	Silt and clay conc. (mg/L)	Sand conc. (mg/L)	Grain-size analysis of sand (0.0625-2.0 mm) fraction																	
								% sand < 0.074 mm	% sand < 0.088 mm	% sand < 0.105 mm	% sand < 0.125 mm	% sand < 0.149 mm	% sand < 0.177 mm	% sand < 0.210 mm	% sand < 0.250 mm	% sand < 0.297 mm	% sand < 0.354 mm	% sand < 0.420 mm	% sand < 0.500 mm	% sand < 0.595 mm	% sand < 0.707 mm	% sand < 0.841 mm	% sand < 1.00 mm	% sand < 1.19 mm	% sand < 1.41 mm
15:36	Up DI	6.48	n/a	5.40	2.472	166	1,190	3.9	8.2	13.5	21.1	30.4	40.5	49.2	58.5	69.5	84.0	92.1	96.1	99.1	100.0	100.0	100.0	100.0	100.0
15:39	Up DI	6.54	n/a	5.40	2.546	173	1,190	1.7	6.4	13.0	21.0	28.4	37.0	48.2	59.5	74.1	86.9	93.3	95.9	97.8	100.0	100.0	100.0	100.0	100.0
16:45	Up DI	6.45	n/a	5.53	2.435	177	1,620	3.1	7.8	12.5	19.6	27.1	34.9	43.9	54.2	65.3	80.2	91.9	96.3	97.7	100.0	100.0	100.0	100.0	100.0
16:48	Up DI	6.57	n/a	5.28	2.736	193	1,810	2.6	6.6	12.8	19.8	26.9	32.5	42.3	51.9	63.4	79.1	91.8	96.1	98.5	100.0	100.0	100.0	100.0	100.0

Notes: Up DI = depth-integrated on upward transit (intake closed during downward transit).

P-61 suspended-sediment samples collected at the Grand Canyon gaging station on April 1, 1996; vertical located at the station 190 ft from the right-bank end point of the cableway																									
Time (MST)	Sample type	Water depth (m)	Sample elevation above bed (m)	Sample collection time (s)	DI intake velocity (m/s)	Silt and clay conc. (mg/L)	Sand conc. (mg/L)	Grain-size analysis of sand (0.0625-2.0 mm) fraction																	
								% sand < 0.074 mm	% sand < 0.088 mm	% sand < 0.105 mm	% sand < 0.125 mm	% sand < 0.149 mm	% sand < 0.177 mm	% sand < 0.210 mm	% sand < 0.250 mm	% sand < 0.297 mm	% sand < 0.354 mm	% sand < 0.420 mm	% sand < 0.500 mm	% sand < 0.595 mm	% sand < 0.707 mm	% sand < 0.841 mm	% sand < 1.00 mm	% sand < 1.19 mm	% sand < 1.41 mm
9:53	Up DI	6.78	n/a	6.22	3.156	123	1,150	3.2	7.4	13.7	21.9	29.7	37.1	46.2	56.7	68.6	79.9	90.5	97.6	98.8	100.0	100.0	100.0	100.0	100.0
9:56	Up DI	6.45	n/a	5.91	2.772	137	1,720	2.5	6.2	9.9	15.6	23.1	30.5	38.5	46.9	58.2	72.4	87.2	96.5	98.5	100.0	100.0	100.0	100.0	100.0
11:32	Up DI	7.36	n/a	6.43	3.007	134	1,080	3.9	9.2	17.3	25.8	34.1	43.5	54.7	68.7	83.7	92.7	96.9	98.8	100.0	100.0	100.0	100.0	100.0	100.0
11:35	Up DI	7.45	n/a	6.44	2.903	159	957	2.6	5.9	13.3	20.9	30.4	39.9	50.7	64.4	77.4	88.4	93.2	95.1	96.2	99.4	100.0	100.0	100.0	100.0

Notes: Up DI = depth-integrated on upward transit (intake closed during downward transit).

P-61 suspended-sediment samples collected at the Grand Canyon gaging station on April 1, 1996; vertical located at the station 290 ft from the right-bank end point of the cableway																									
Time (MST)	Sample type	Water depth (m)	Sample elevation above bed (m)	Sample collection time (s)	DI intake velocity (m/s)	Silt and clay conc. (mg/L)	Sand conc. (mg/L)	Grain-size analysis of sand (0.0625-2.0 mm) fraction																	
								% sand < 0.074 mm	% sand < 0.088 mm	% sand < 0.105 mm	% sand < 0.125 mm	% sand < 0.149 mm	% sand < 0.177 mm	% sand < 0.210 mm	% sand < 0.250 mm	% sand < 0.297 mm	% sand < 0.354 mm	% sand < 0.420 mm	% sand < 0.500 mm	% sand < 0.595 mm	% sand < 0.707 mm	% sand < 0.841 mm	% sand < 1.00 mm	% sand < 1.19 mm	% sand < 1.41 mm
11:40	Up DI	8.04	n/a	6.65	2.046	150	1,450	1.8	5.4	11.8	19.9	30.8	42.2	55.7	70.6	83.9	95.1	98.2	99.0	100.0	100.0	100.0	100.0	100.0	100.0
11:44	Up DI	7.79	n/a	6.56	2.315	160	1,650	1.6	4.9	11.2	17.0	26.4	36.3	47.5	61.6	77.8	92.8	95.8	97.8	100.0	100.0	100.0	100.0	100.0	100.0
12:59	Up DI	6.63	n/a	5.50	2.742	173	1,400	2.4	7.6	14.2	21.0	28.7	37.4	46.8	57.2	72.6	86.0	93.3	97.2	98.3	100.0	100.0	100.0	100.0	100.0
13:05	Up DI	6.60	n/a	5.78	2.613	155	1,330	3.1	7.4	12.7	18.6	25.5	34.9	45.1	57.8	71.4	85.5	93.6	96.2	97.2	97.9	100.0	100.0	100.0	100.0

Notes: Up DI = depth-integrated on upward transit (intake closed during downward transit).

P-61 suspended-sediment samples collected at the Grand Canyon gaging station on April 3, 1996; vertical located at the station 190 ft from the right-bank end point of the cableway																									
Time (MST)	Sample type	Water depth (m)	Sample elevation above bed (m)	Sample collection time (s)	DI intake velocity (m/s)	Silt and clay conc. (mg/L)	Sand conc. (mg/L)	Grain-size analysis of sand (0.0625-2.0 mm) fraction																	
								% sand < 0.074 mm	% sand < 0.088 mm	% sand < 0.105 mm	% sand < 0.125 mm	% sand < 0.149 mm	% sand < 0.177 mm	% sand < 0.210 mm	% sand < 0.250 mm	% sand < 0.297 mm	% sand < 0.354 mm	% sand < 0.420 mm	% sand < 0.500 mm	% sand < 0.595 mm	% sand < 0.707 mm	% sand < 0.841 mm	% sand < 1.00 mm	% sand < 1.19 mm	% sand < 1.41 mm
11:00	Up DI	6.49	n/a	9.38	1.827	131	1,070	3.8	10.4	19.6	29.4	41.1	53.2	62.9	74.0	86.4	92.0	98.1	98.8	100.0	100.0	100.0	100.0	100.0	100.0
12:11	Up DI	6.52	n/a	8.83	2.052	142	1,260	4.1	9.7	17.4	27.2	36.2	44.9	53.5	60.5	66.8	74.1	86.4	93.8	96.2	98.9	100.0	100.0	100.0	100.0
12:15	Up DI	6.58	n/a	8.50	1.671	167	1,030	3.6	11.1	20.8	29.3	41.4	50.8	64.3	77.0	83.9	90.3	94.1	95.9	100.0	100.0	100.0	100.0	100.0	100.0

Notes: Up DI = depth-integrated on upward transit (intake closed during downward transit).

P-61 suspended-sediment samples collected at the Grand Canyon gaging station on April 3, 1996; vertical located at the station 290 ft from the right-bank end point of the cableway																									
Time (MST)	Sample type	Water depth (m)	Sample elevation above bed (m)	Sample collection time (s)	DI intake velocity (m/s)	Silt and clay conc. (mg/L)	Sand conc. (mg/L)	Grain-size analysis of sand (0.0625-2.0 mm) fraction																	
								% sand < 0.074 mm	% sand < 0.088 mm	% sand < 0.105 mm	% sand < 0.125 mm	% sand < 0.149 mm	% sand < 0.177 mm	% sand < 0.210 mm	% sand < 0.250 mm	% sand < 0.297 mm	% sand < 0.354 mm	% sand < 0.420 mm	% sand < 0.500 mm	% sand < 0.595 mm	% sand < 0.707 mm	% sand < 0.841 mm	% sand < 1.00 mm	% sand < 1.19 mm	% sand < 1.41 mm
12:21	Up DI	6.07	n/a	8.78	1.781	172	1,220	2.5	7.6	16.5	28.2	37.9	48.7	59.8	68.6	80.4	91.5	96.1	98.5	100.0	100.0	100.0	100.0	100.0	100.0
12:24	Up DI	5.92	n/a	8.22	1.914	154	846	4.0	10.7	21.4	33.9	46.0	55.8	71.0	86.0	89.4	92.7	95.8	98.1	100.0	100.0	100.0	100.0	100.0	100.0
13:34	Up DI	5.76	n/a	8.30	1.759	161	1,050	3.3	10.0	20.0	32.6	45.1	57.5	71.7	80.5	88.2	93.9	97.4	97.7	99.1	100.0	100.0	100.0	100.0	100.0
13:38	Up DI	5.76	n/a	8.31	1.696	144	1,130	4.5	10.4	19.3	31.1	41.7	53.2	64.6	76.9	87.9	94.4	97.5	100.0	100.0	100.0	100.0	100.0	100.0	100.0

Notes: Up DI = depth-integrated on upward transit (intake closed during downward transit).

P-61 suspended-sediment samples collected at the Grand Canyon gaging station on September 26, 1998; vertical located at the station 290 ft from the right-bank end point of the cableway																									
Time (MST)	Sample type	Water depth (m)	Sample elevation above bed (m)	Sample collection time (s)	Point or DI intake velocity (m/s)	Silt and clay conc. (mg/L)	Sand conc. (mg/L)	Grain-size analysis of sand (0.0625-2.0 mm) fraction																	
								% sand < 0.074 mm	% sand < 0.088 mm	% sand < 0.105 mm	% sand < 0.125 mm	% sand < 0.149 mm	% sand < 0.177 mm	% sand < 0.210 mm	% sand < 0.250 mm	% sand < 0.297 mm	% sand < 0.354 mm	% sand < 0.420 mm	% sand < 0.500 mm	% sand < 0.595 mm	% sand < 0.707 mm	% sand < 0.841 mm	% sand < 1.00 mm	% sand < 1.19 mm	% sand < 1.41 mm
10:22	Up DI	6.26	n/a	10.29	1.008	171	133	8.9	20.4	35.4	48.0	58.1	69.8	77.8	79.7	89.9	97.2	100.0	100.0	100.0	100.0	100.0	100.0	100.0	100.0
10:27	Point	6.36	0.28	20.00	0.805	206	428	6.6	13.4	20.5	29.9	42.8	52.5	68.7	82.6	91.4	95.9	97.8	99.4	100.0	100.0	100.0	100.0	100.0	100.0
10:30	Point	6.36	0.28	20.00	0.819	216	528	4.0	9.9	16.7	23.1	33.0	46.3	59.5	76.4	89.0	95.2	98.6	100.0	100.0	100.0	100.0	100.0	100.0	100.0
10:34	Point	6.36	0.28	20.00	0.881	191	430	4.7	9.9	16.8	25.4	35.6	46.6	62.1	78.3	88.1	94.6	99.0	99.7	100.0	100.0	100.0	100.0	100.0	100.0
10:37	Point	6.36	0.56	15.00	0.985	199	361	7.3	14.8	23.4	33.3	47.3	60.4	75.1	83.7	92.5	98.5	99.3	100.0	100.0	100.0	100.0	100.0	100.0	100.0
10:40	Point	6.36	0.56	15.00	0.913	196	397	4.6	11.2	18.3	28.1	39.6	56.0	73.3	83.4	92.6	97.6	98.9	99.2	100.0	100.0	100.0	100.0	100.0	100.0
10:43	Point	6.36	0.56	15.00	0.762	224	390	6.1	14.3	21.2	33.2	45.0	57.9	71.8	83.3	90.8	97.1	99.2	100.0	100.0	100.0	100.0	100.0	100.0	100.0
10:51	Point	6.36	1.17	12.00	0.997	176	331	5.5	11.5	20.0	30.8	50.0	67.5	79.2	87.3	93.3	98.8	99.9	100.0	100.0	100.0	100.0	100.0	100.0	100.0
10:57	Point	6.36	1.17	14.00	0.924	198	325	5.9	13.7	22.6	35.2	49.3	63.9	78.3	88.9	94.9	99.1	100.0	100.0	100.0	100.0	100.0	100.0	100.0	100.0
11:01	Point	6.36	1.17	14.00	0.802	198	385	6.7	13.9	23.1	33.7	45.8	58.4	70.5	84.2	92.8	96.7	99.0	100.0	100.0	100.0	100.0	100.0	100.0	100.0
11:06	Point	6.36	2.22	12.00	1.214	165	201	5.3	16.5	30.1	44.9	61.3	74.0	83.5	91.1	96.4	98.4	100.0	100.0	100.0	100.0	100.0	100.0	100.0	100.0
11:08	Point	6.36	2.22	13.00	1.100	169	293	3.3	9.7	17.8	30.6	48.3	68.6	79.7	88.4	93.4	97.5	98.9	99.4	100.0	100.0	100.0	100.0	100.0	100.0
11:10	Point	6.36	2.22	13.00	0.958	208	291	8.2	16.3	23.9	34.9	49.5	67.9	82.3	90.0	93.4	99.0	100.0	100.0	100.0	100.0	100.0	100.0	100.0	100.0
11:13	Point	6.36	3.75	13.00	1.285	198	282	9.2	23.9	33.9	49.1	69.4	79.0	90.1	95.5	99.4	99.9	100.0	100.0	100.0	100.0	100.0	100.0	100.0	100.0
11:16	Point	6.36	3.75	13.00	1.400	161	146	6.4	20.4	40.1	64.6	76.6	84.3	92.7	97.7	99.5	99.8	100.0	100.0	100.0	100.0	100.0	100.0	100.0	100.0
11:18	Point	6.36	3.73	13.00	1.309	171	155	12.3	27.4	38.6	55.0	68.3	78.5	87.1	91.8	94.2	98.6	100.0	100.0	100.0	100.0	100.0	100.0	100.0	100.0
11:21	Point	6.36	6.01	10.00	1.320	161	80.5	19.9	46.2	63.5	83.4	87.2	92.8	93.5	97.9	99.4	100.0	100.0	100.0	100.0	100.0	100.0	100.0	100.0	100.0
11:24	Point	6.36	6.01	12.00	1.408	163	101	17.1	37.3	57.3	72.7	87.2	92.4	98.7	99.4	100.0	100.0	100.0	100.0	100.0	100.0	100.0	100.0	100.0	100.0
11:26	Point	6.36	6.01	12.00	1.319	152	50.9	12.3	31.5	56.7	79.8	92.1	94.5	94.5	97.8	99.1	100.0	100.0	100.0	100.0	100.0	100.0	100.0	100.0	100.0
11:34	Up DI	6.47	n/a	14.43	0.892	176	189	13.7	26.6	42.4	58.9	71.4	81.0	88.7	95.8	98.0	98.9	100.0	100.0	100.0	100.0	100.0	100.0	100.0	100.0

Notes: Up DI = depth-integrated on upward transit (intake closed during downward transit); Water depths associated with the point samples are the mean water depths at this vertical during the collection of the 18 point samples; point-sample elevations are relative to the mean bed elevation associated with this mean water depth.

Appendix B. Cross-Stream Spatial Structures in Depth-Integrated Suspended-Sediment Concentration in Noncomposited Nine-Vertical Measurements at the River-mile 30 Sediment Station and Lower Marble Canyon Gaging Station

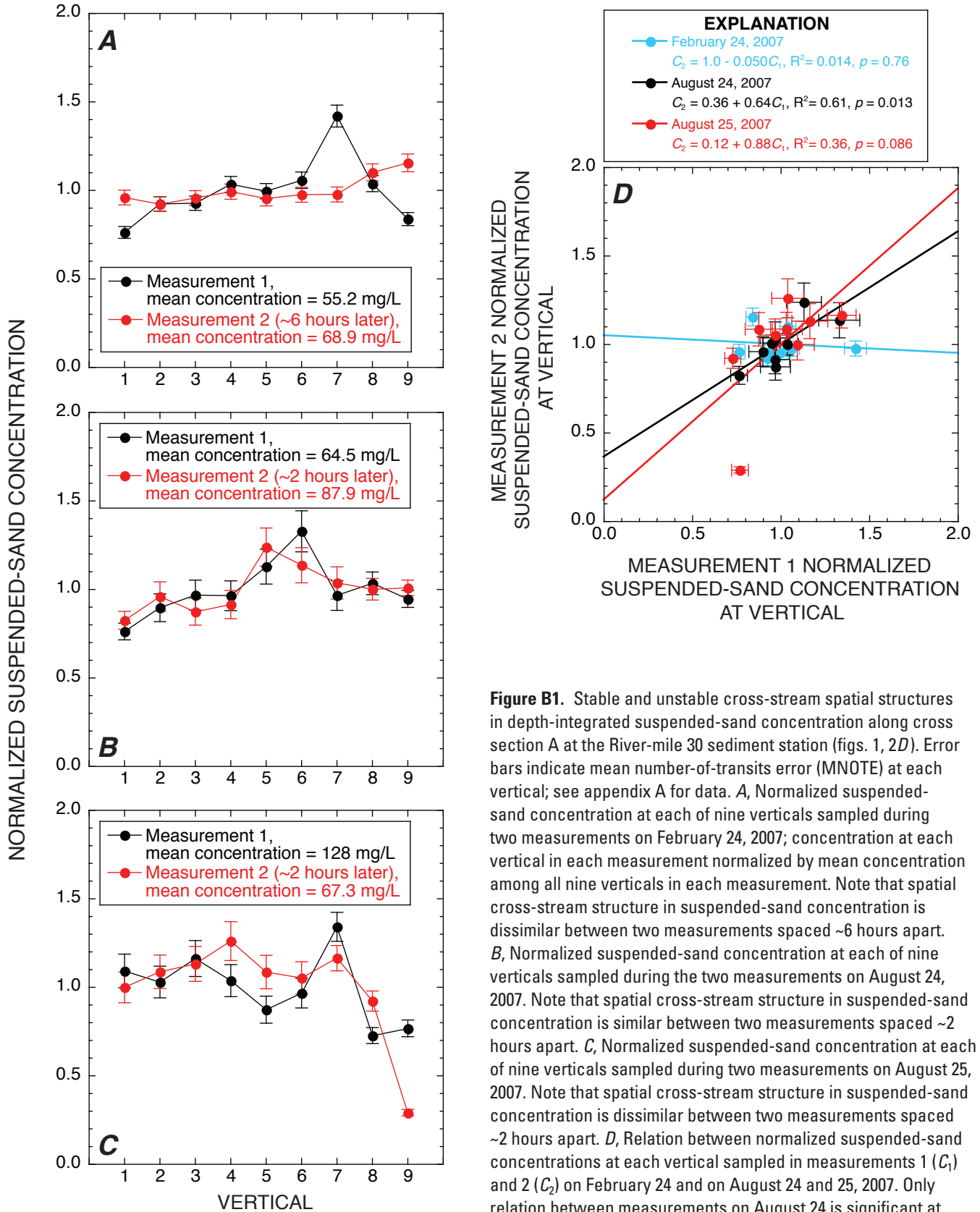


Figure B1. Stable and unstable cross-stream spatial structures in depth-integrated suspended-sand concentration along cross section A at the River-mile 30 sediment station (figs. 1, 2D). Error bars indicate mean number-of-transits error (MNOTE) at each vertical; see appendix A for data. *A*, Normalized suspended-sand concentration at each of nine verticals sampled during two measurements on February 24, 2007; concentration at each vertical in each measurement normalized by mean concentration among all nine verticals in each measurement. Note that spatial cross-stream structure in suspended-sand concentration is dissimilar between two measurements spaced ~6 hours apart. *B*, Normalized suspended-sand concentration at each of nine verticals sampled during the two measurements on August 24, 2007. Note that spatial cross-stream structure in suspended-sand concentration is similar between two measurements spaced ~2 hours apart. *C*, Normalized suspended-sand concentration at each of nine verticals sampled during two measurements on August 25, 2007. Note that spatial cross-stream structure in suspended-sand concentration is dissimilar between two measurements spaced ~2 hours apart. *D*, Relation between normalized suspended-sand concentrations at each vertical sampled in measurements 1 (C_1) and 2 (C_2) on February 24 and on August 24 and 25, 2007. Only relation between measurements on August 24 is significant at $p=0.05$ level.

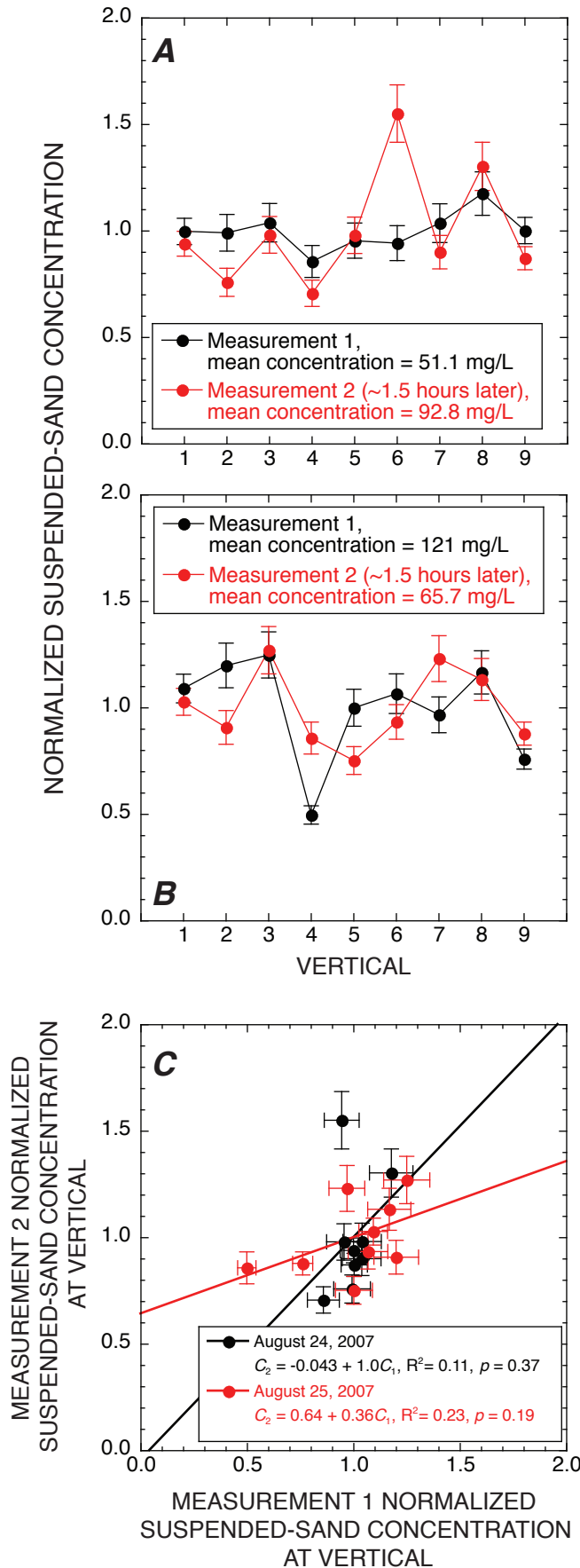


Figure B2. Unstable cross-stream spatial structures in depth-integrated suspended-sand concentration along cross section B at the River-mile 30 sediment station (figs. 1, 2D). Error bars indicate mean number-of-transits error (MNOTE) at each vertical; see appendix A for data. *A*, Normalized suspended-sand concentration at each of nine verticals sampled during two measurements on August 24, 2007; concentration at each vertical in each measurement normalized by mean concentration among all nine verticals in each measurement. Note that spatial cross-stream structure in suspended-sand concentration is dissimilar between two measurements spaced ~1.5 hours apart. *B*, Normalized suspended-sand concentration at each of nine verticals sampled during two measurements on August 25, 2007. Note that spatial cross-stream structure in suspended-sand concentration is dissimilar between the two measurements spaced ~1.5 hours apart and that both cross-stream spatial structures appear to differ from those observed on previous day. *C*, Relation between normalized suspended-sand concentrations at each vertical sampled in measurements 1 (C_1) and 2 (C_2) on August 24 and 25, 2007. Relations are not significant at $p=0.05$ level, indicating no significant temporal correlation in suspended-sand concentration at each vertical over time scales of hours.

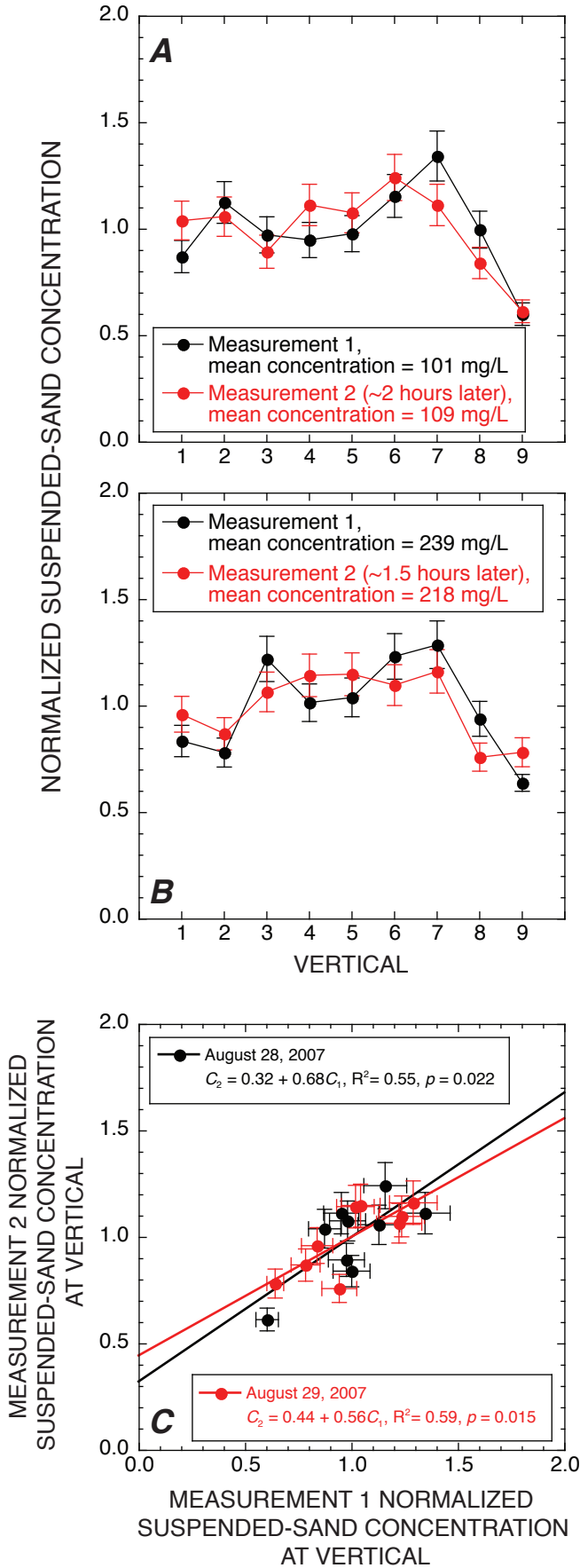


Figure B3. Stable cross-stream spatial structures in depth-integrated suspended-sand concentration along cross section A at the Lower Marble Canyon gaging station (fig. 1, 2C). Error bars indicate mean number-of-transits error (MNOTE) at each vertical; see appendix A for data. *A*, Normalized suspended-sand concentration at each of nine verticals sampled during two measurements on August 28, 2007; concentration at each vertical in each measurement normalized by mean concentration among all nine verticals in each measurement. Note that cross-stream spatial structure in suspended-sand concentration appears to be similar between two measurements spaced ~2 hours apart. *B*, Normalized suspended-sand concentration at each of nine verticals sampled during two measurements on August 29, 2007. Note that cross-stream spatial structure in suspended-sand concentration appears to be similar between two measurements spaced ~1.5 hours apart. *C*, Relations between normalized suspended-sand concentrations at each vertical sampled in measurements 1 (C_1) and 2 (C_2) on August 28 and 29, 2007. Relations are significant at $p=0.05$ level, indicating significant temporal correlation in suspended-sand concentration at each vertical over time scales of hours on each day. Note similarity of relations on both days, identical to behavior observed along cross section C (fig. 13C).

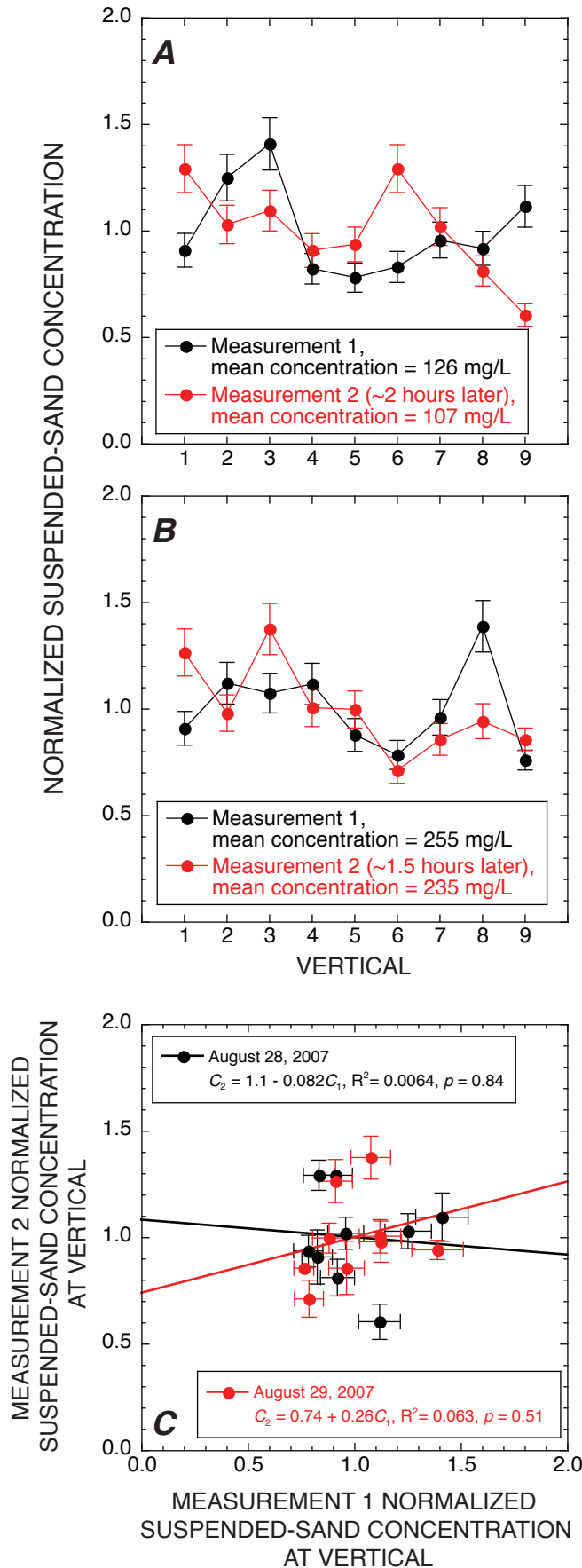


Figure B4. Unstable cross-stream spatial structures in depth-integrated suspended-sand concentration along cross section B at the Lower Marble Canyon gaging station (figs. 1, 2C). Error bars indicate mean number-of-transits error (MNOTE) at each vertical; see appendix A for data. *A*, Normalized suspended-sand concentration at each of nine verticals sampled during two measurements on August 28, 2007; concentration at each vertical in each measurement normalized by mean concentration among all nine verticals in each measurement. Note that cross-stream spatial structure in suspended-sand concentration is dissimilar between two measurements spaced ~2 hours apart. *B*, Normalized suspended-sand concentration at each of nine verticals sampled during two measurements on August 29, 2007. Note that cross-stream spatial structure in suspended-sand concentration is dissimilar between two measurements spaced ~1.5 hours apart and that both cross-stream spatial structures appear to differ from those observed on previous day. *C*, Relations between normalized suspended-sand concentrations at each vertical sampled in measurements 1 (C_1) and 2 (C_2) on August 28 and 29, 2007. Relations are not significant at $p=0.05$ level, indicating no significant temporal correlation in suspended-sand concentration at each vertical over time scales of hours.

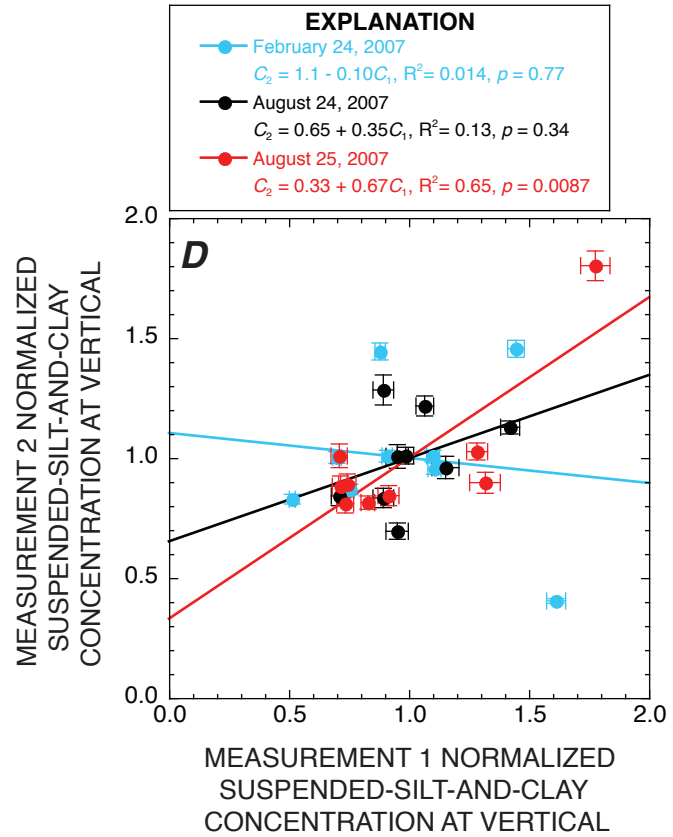
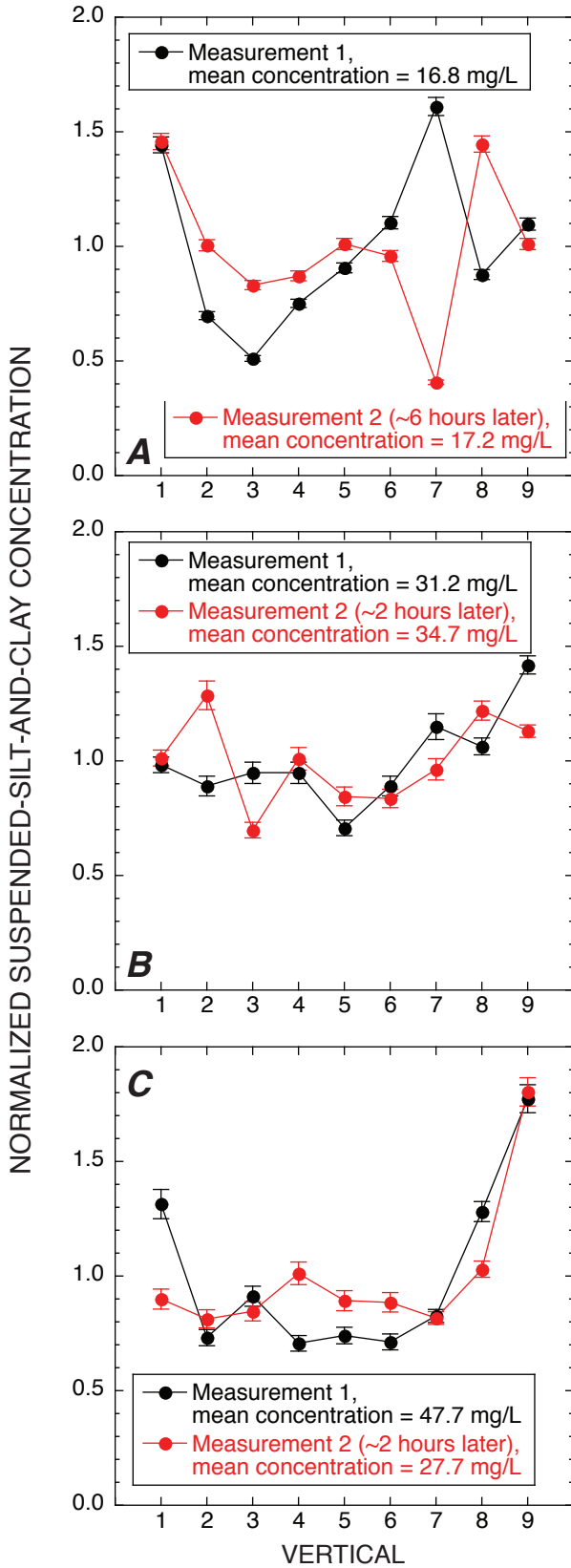


Figure B5. Stable and unstable cross-stream spatial structures in depth-integrated suspended-silt-and-clay concentration along cross section A at the River-mile 30 sediment station (figs. 1, 2D). Error bars indicate mean number-of-transits-error (MNOTE) at each vertical; see appendix A for data. *A*, Normalized suspended-silt-and-clay concentration at each of nine verticals sampled during two measurements on February 24, 2007; concentration at each vertical in each measurement normalized by mean concentration among all nine verticals in each measurement. Note that cross-stream spatial structure in suspended-silt-and-clay concentration is dissimilar between two measurements spaced ~6 hours apart. *B*, Normalized suspended-silt-and-clay concentration at each of nine verticals sampled during two measurements on August 24, 2007. Note that cross-stream spatial structure in suspended-silt-and-clay concentration is dissimilar between two measurements spaced ~2 hours apart. *C*, Normalized suspended-silt-and-clay concentration at each of nine verticals sampled during two measurements on August 25, 2007. Note that spatial cross-stream structure in suspended-silt-and-clay concentration is similar between two measurements spaced ~2 hours apart. *D*, Relations between normalized suspended-silt-and-clay concentrations at each vertical sampled in measurements 1 (C_1) and 2 (C_2) on February 24 and on August 24 and 25, 2007. Only relation between measurements on August 25 is significant at $p=0.05$ level.

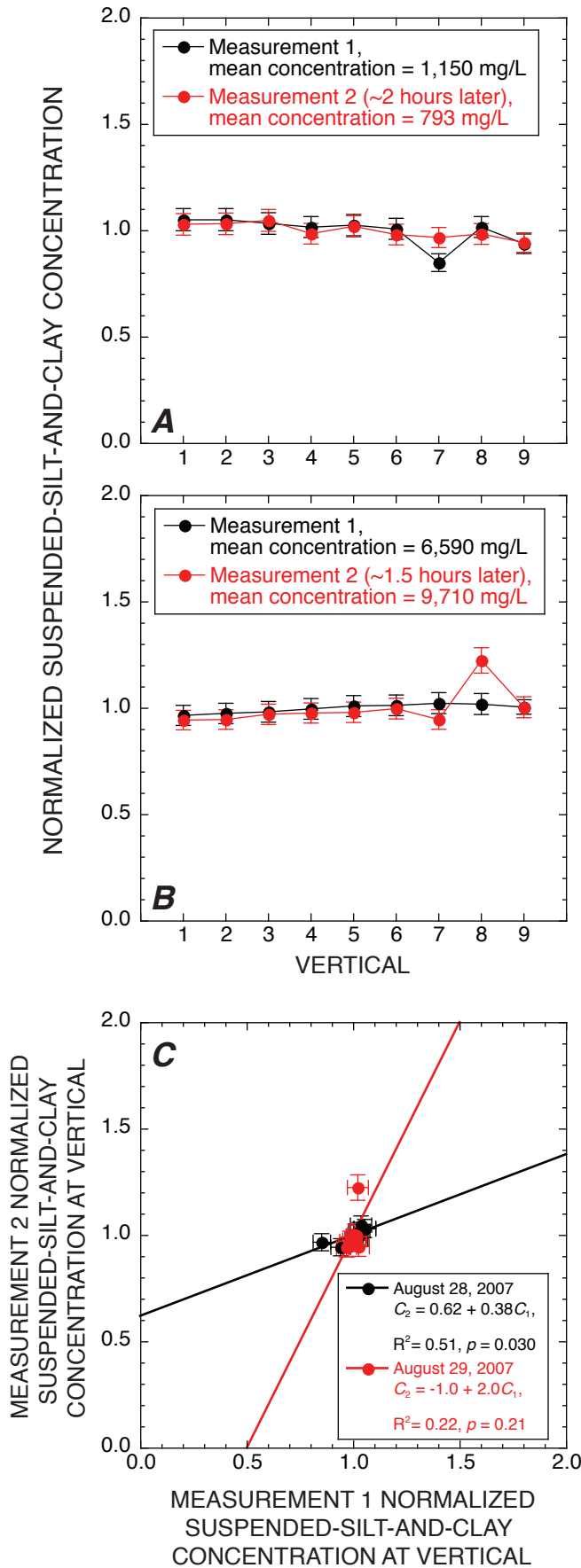


Figure B6. Stable and unstable cross-stream spatial structures in depth-integrated suspended-silt-and-clay concentration along cross section A at the Lower Marble Canyon gaging station (figs. 1, 2C). Error bars indicate mean number-of-transit error (MNOTE) at each vertical; see appendix A for data. *A*, Normalized suspended-silt-and-clay concentration at each of nine verticals sampled during two measurements on August 28, 2007; concentration at each vertical in each measurement normalized by mean concentration among all nine verticals in each measurement. Note that cross-stream spatial structure in suspended-silt-and-clay concentration is similar between two measurements spaced ~2 hours apart. *B*, Normalized suspended-silt-and-clay concentration at each of nine verticals sampled during two measurements on August 29, 2007. Note that although cross-stream spatial structure in suspended-silt-and-clay concentration is somewhat similar between two measurements spaced ~1.5 hours apart, suspended-silt-and-clay concentrations differ widely between two measurements at vertical 8. *C*, Relations between normalized suspended-silt-and-clay concentrations at each vertical sampled in measurements 1 (C_1) and 2 (C_2) on August 28 and 29, 2007. Relation between measurements on August 28 is significant at $p=0.05$ level, whereas that between measurements on August 29 is not.

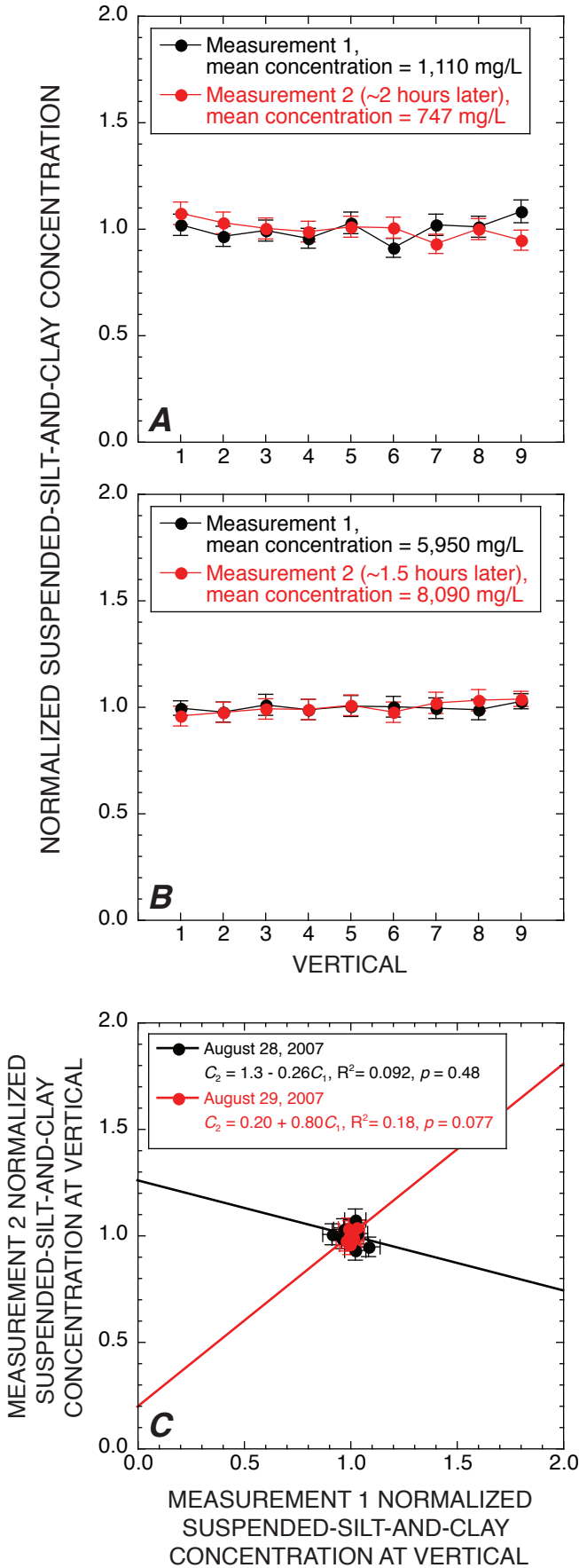


Figure B7. Unstable cross-stream spatial structures in depth-integrated suspended-silt-and-clay concentration along cross section B at the Lower Marble Canyon gaging station (figs. 1, 2C). Error bars indicate mean number-of-transits error (MNOTE) at each vertical; see appendix A for data. *A*, Normalized suspended-silt-and-clay concentration at each of nine verticals sampled during two measurements on August 28, 2007; concentration at each vertical in each measurement normalized by mean concentration among all nine verticals in each measurement. Note that cross-stream spatial structure in suspended-silt-and-clay concentration is dissimilar between two measurements spaced ~2 hours apart (mostly at verticals 6, 7, and 9). *B*, Normalized suspended-silt-and-clay concentration at each of nine verticals sampled during two measurements on August 29, 2007. Note that suspended-silt-and-clay concentration is basically uniform across entire cross section in both measurements. *C*, Relations between normalized suspended-silt-and-clay concentrations at each vertical sampled in measurements 1 (C_1) and 2 (C_2) on August 28 and 29, 2007. Neither relation is significant at $p=0.05$ level; however, note that analysis is hampered by uniform distribution of suspended silt and clay across cross section.

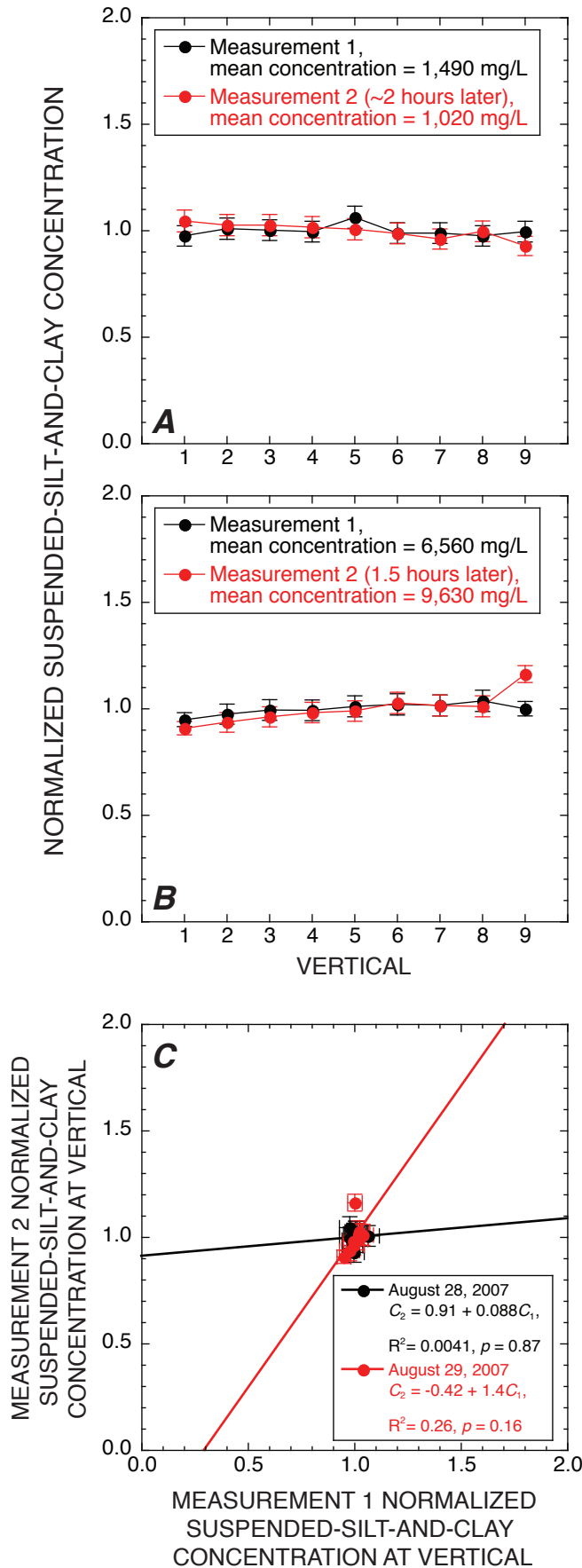


Figure B8. Unstable cross-stream spatial structures in depth-integrated suspended-silt-and-clay concentration along cross section C at the Lower Marble Canyon gaging station (figs. 1, 2C). Error bars indicate mean number-of-transits error (MNOTE) at each vertical; see appendix A for data. *A*, Normalized suspended-silt-and-clay concentration at each of nine verticals sampled during two measurements on August 28, 2007; concentration at each vertical in each measurement normalized by mean concentration among all nine verticals in each measurement. Note that cross-stream spatial structure in suspended-silt-and-clay concentration is dissimilar between two measurements spaced ~2 hours apart (mostly at verticals 1, 5, and 9). *B*, Normalized suspended-silt-and-clay concentration at each of nine verticals sampled during two measurements on August 29, 2007. Note that although cross-stream spatial structure in suspended-silt-and-clay concentration is somewhat similar between two measurements spaced ~1.5 hours apart, suspended-silt-and-clay concentrations differ widely between two measurements at vertical 9. *C*, Relations between normalized suspended-silt-and-clay concentrations at each vertical sampled in measurements 1 (C_1) and 2 (C_2) on August 28 and 29, 2007. Neither relation is significant at $p=0.05$ level.

